ER to Golgi Transport During Apoptosis

Annemieke Walker

A thesis submitted for the degree of Doctor of Philosophy

University of Edinburgh, 2002
Edinburgh University Medical School

DECLARATION

Solely the author carried out the work presented in this thesis, entitled 'ER to Golgi Transport During Apoptosis' unless otherwise stated.

Annemieke Walker

ACKNOWLEDGEMENTS

Many people have contributed to this work and it is wonderful to finally thank them in writing. I would like to thank Dr James G Pryde and Prof. Chris Haslett for their supervision during the course of this project. Many thanks must go to Carol Ward for her friendship and support during my time in the Rayne Lab. Lorna Murray for her help with flow cytometry. Drs Adriano Rossi and Ian Dransfield for all their help. Also, to Mark Marsden, Yatish and Tiina during my molecular biology stint in their lab. Tara, for all her help in the lab and friendship. Linda Sharp for all her help with confocal microscopy and her company. Thanks must also go to John Lucocq for the EM work

My fellow PhD students, many of whom started their PhD at the same time as me, in particular Julie, Sarah, Kath and Aziz – thanks for your friendship and quality company.

Grigori for scanning and general computer support! Katerina for the many tea breaks over the last few months!!!

My brothers: Andrew who bailed me out on many an occasion (thanks!!) and Johnnie for providing the Johnnie Walker. My mother for being tirelessly and endlessly supportive.

George who is definitely a saint.

DEDICATION

This Thesis is Dedicated to my Mother and Grandmother

CONTENTS

ABBREVIATIONS

AIF	Apoptosis Inducing Factor
ANT	Adenine Nucleotide Translocator
ARDS	Adult Respiratory Distress Syndrome
Apaf-1	Apoptotic Protease Activating Factor-1
ATF	Activating Transcription Factor
ATP	Adenosine 5'-triphosphate
ADP	Adenosine 5'-diphosphate
BAD	Bcl- X_L / Bcl-2-Associated Death Promoter
BAX	Bcl-2 -associated x protein
BAK	Bcl-2 Homologous Antagonist/ Killer
Bcl-2	B-cell Lymphoma-2
Bcl-X_L	B cell leukaemia-x long
Bcl-X_s	B cell leukaemia-x short
BH	Bcl-2 homology
BID	BH3 Interacting Domain Death Agonist
BIM	Bcl-2 Interacting Mediator of Cell Death
BiP	B Cell Immunoglobulin Binding Protein
CARD	Caspase Recruitment Domain
CDK	Cyclin Dependent Kinase
CED	Cell Death Defective
CHOP	CCAAT/enhancer-binding protein beta homologous protein
CHX	Cycloheximide
COP	Coatomer
DcR	Decoy Receptor
DD	Death Domain
DED	Death Effector Domain
DIABLO	Direct Inhibitor of Apoptosis Binding Protein with Low pI
DISC	Death Inducing Signalling Complex
DMEM	Dulbecco's Modified Eagle's Medium
DTT	Dithiothreitol
EM	Electron Microscope/ Microscopy
eIF2α	Eukaryotic Translation Initiation Factor 2α
Endo-H	Endoglycosidase-H
ER	Endoplasmic Reticulum
ERSE	Endoplasmic Reticulum Stress Element
FADH	Flavin Adenine Dinucleotide

FADD	Fas-Associated Death Domain
FasR	Fas Receptor
FITC	
fMLP	N-formylmethionylleucyl phenylalanine
Gal	Galactose
GalNAc	N-acetylgalactosamine
GADD	Growth Arrest and DNA Damage Inducible
GAP	GTPase-activating Protein
G-CSF	Granulocyte Colony Stimulating Factor
GM-CSF	Granulocyte Macrophage Colony Stimulating Factor
GDP	Guanosine 5'-diphosphate
GEF	Guanine Nucleotide Exchange Factor
GM	Golgi Matrix
GRASP	Golgi Reassembly Stacking Protein
GRP	Glucose Response Protein
GTP	Guanosine 5'-triphosphate
GTPase	Guanosine Triphosphatase
HAC1	Homologous to Activating Transcription Factor/ cyclic 3',5'-Adenosine Monophosphate Response Element Binding Protein 1
HEK	Human Embryonic Kidney
IFN	Interferon
IC	Intermediate Compartment
ICAD	Inhibitor of Caspase-activated Deoxyribonuclease
IGF	Insulin-like Growth Factor
I-kB	Inhibitor of kB
IKK	Inhibitor of kB Kinase
IL	Interleukin
IRE	Inositol Requiring
JNK	c-Jun N-terminal kinase
Mcl-1	Myeloid Cell Leukaemia-1
MEM	Minimal Essential Medium
MPO	Myeloperoxidase
mtHSP	Mitochondrial Heat Shock Protein
NADH	Nicotinamide Adenine Dinucleotide
NF-kB	Nuclear Factor-kB
NGF	Nerve Growth Factor
NIK	Nuclear Factor-kB Inducing Kinase
NRK	Normal Rat Kidney cells
NSF	*N*-ethyl-maleimide-Sensitive-Fusion Protein

PARP	Poly(ADP)Ribose-Polymerase
PBS	Phosphate Buffered Saline
PDI	Protein Disulphide Isomerase
PERK	Protein Kinase R-like ER Kinase
PFA	Para-formaldehyde
PI3-Kinase	Phosphoinositide 3-Kinase
PKA	Protein Kinase A
Plk	Polo-like Kinase
PS	Phosphatidylserine
PTP	Permeability Transition Pore
Rab	Ras-like Protein from Rat Brain
Rb	Retinoblastoma
RIP	Receptor Interacting Protein
S1P or S2P	Site-1 Protease or Site-2 Protease
SNAP	Soluble NSF Attachment Protein
SNARE	SNAP Receptor
SSP	Staurosporine
TEMED	N,N,N',N-Tetramethylenediamine
TNF	Tumour Necrosis Factor
TNFR	Tumour Necrosis Factor Receptor
TRADD	TNFR-assiated Death Domain
TRAF2	TNFR-Associated Death Domain
Tris	Tris[Hydroxymethyl]aminomethane
UPR	Unfolded Protein Response
UPRE	Unfolded Protein Response Element
VAMP	Vesicle Associated Membrane Protein
VDAC	Voltage Dependent Anion Channel
VSV	Vesicular Stomatitis Virus
VSVG	Vesicular Stomatitis Virus Glycoprotein
X-IAP	X-Chromosome Linked Inhibitor of Apoptosis
z-VAD-fmk	N-benzyloxycarbonyl-Val-Ala-Asp-fluoromethylketone

ABSTRACT

The Golgi complex, a single-copy organelle, is composed of a ribbon of flattened stacks of cisternae during interphase. However, during apoptosis the Golgi is shown to fragment and disperse throughout the cytoplasm. Immunoelectron microscopy identified these fragments as vesicular-tubular structures that contained the Golgi marker n-acetyl-glucosaminyl-transferase-1. Newly-synthesised proteins translocated to the endoplasmic reticulum also failed to exit from this organelle and reach the Golgi in apoptotic cells.

Induction of apoptosis by Fas receptor ligation led to the caspase-dependent cleavage of GM130, a key Golgi-localised protein involved in tethering incoming secretory vesicles to the *cis*-Golgi. Cleavage of GM130 was prevented by the broad-range protein kinase inhibitor staurosporine, suggesting that phosphorylation played a role in the regulation of GM130 activity during apoptosis. These morphological and functional changes to the early secretory pathway during apoptosis could explain the down-regulation of the exocytic pathway in apoptotic neutrophils, which may prevent the inappropriate release of proinflammatory agents during resolution of inflammation.

CHAPTER 1: INTRODUCTION

1.1 Inflammation & the Neutrophil

Inflammation is the primary response to tissue damage or infection and an essential part of the immune response. Neutrophils are the first cells to be recruited to the inflammatory site where they form a first line of defence against invading bacteria and fungi. They are terminally differentiated and characteristic of neutrophils are the multi-lobed nuclei and dense cytoplasmic granules. During maturation in the bone marrow, they pass through six morphological stages: myeloblast, promyeloblast, myelocyte, metamyelocyte, non-segmented and segmented neutrophil prior to their release into the blood stream (Zajicek *et al.*, 1984). High numbers of neutrophils are present in peripheral blood, despite their short life span (4-6 hours), thus there is constant replacement of cells by the bone marrow which produces 10^{11} neutrophils per day in a normal adult (Cannistra & Griffin, 1988). During an inflammatory response, large numbers of circulating neutrophils are rapidly recruited to the affected site, a process requiring migration across the vascular endothelium. Once at the site of injury or infection, inflammatory mediators act to extend the life-span of the neutrophil (Haslett *et al.*, 1989).

Migration of leukocytes from the blood vessels into the site of inflammation is dependent on the activation of adhesive molecules, on both the circulating cells and the endothelial cells (Wagner & Roth, 2000). Neutrophils bind to the vessel wall transiently, a form of adhesion known as 'rolling' and this is mediated by the reversible binding of selectins to their ligands expressed on both neutrophils and vascular endothelial cells (Crockett-Torabi & Fantone, 1995). Selectins are found on most circulating leukocytes and on endothelial cells lining the blood and lymph vessels (Wagner & Roth, 2000). Rolling adhesion *via* activated endothelial cell selectins allows engagement of neutrophils to integrins, particularly when chemokines are present to facilitate 'firm' adhesion to the endothelial cell and arrest from vascular flow (Williams & Solomkin, 1999). Following adhesion, neutrophils undergo diapedesis and migrate by chemotaxis towards the site of inflammation. At the inflammatory site, neutrophils can then phagocytose and destroy invading microorganisms by releasing proteolytic enzymes, bactericidal proteins and toxic oxygen products into the phagolysosome.

Necrotic cell death or the inappropriate release of neutrophil granule contents is thought to be a major contributing factor to tissue damage occurring during inflammatory disease. Oxygen metabolites, produced by neutrophils to exert microbicidal function, can also injure surrounding host tissue. Although tissues contain protective anti-oxidant enzymes e.g. superoxide dismutase and catalase, these enzyme systems may be overwhelmed during intense local production of toxic oxygen metabolites. Neutrophil granules also contain a large family of over 20 enzymes, of which the serine proteases, elastase and the two metalloproteinases collagenase and gelatinase, seem to have the greatest potential to act as mediators of tissue destruction (Borregaard & Cowland, 1997). Disease states in which the inappropriate release of neutrophil granule contents have been implicated, include adult respiratory distress syndrome (ARDS), rheumatoid arthritis, chronic bronchitis, emphysema and glomerulonephritis (Haslett, 1992; Rossi & Haslett, 1998) highlighting the importance of control of secretion.

For resolution of inflammation to occur and the tissues to return to normal, the inflammatory stimulus must be removed, influx of inflammatory cells must cease and inflammatory cells already present at the inflammatory site must also be removed. The removal of neutrophils has been shown to be mediated by apoptosis (Haslett, 1992; Haslett *et al.*, 1989; Haslett *et al.*, 1994; Savill *et al.*, 1993; Savill, 1997; Savill & Haslett, 1995; Savill *et al.*, 1989; Whyte *et al.*, 1997) and their subsequent phagocytosis by macrophages or neighbouring cells, providing a mechanism for the safe removal of 'unwanted' cells without eliciting an inflammatory response (Savill *et al.*, 1993). However, if the inflammatory response becomes overwhelmed and either apoptotic neutrophils become too numerous for quick removal by macrophages or there is a defect in the phagocytic potential of macrophages then apoptotic neutrophils may undergo secondary necrosis and cause tissue damage. This is supported by the observation that apoptotic neutrophils incubated *in vitro* in the absence of macrophages, spontaneously release their granule contents (Meagher *et al.*, 1992). Nevertheless, the control of secretion must be tightly regulated in the neutrophil since there is still a time window for inappropriate granule release between the induction of apoptosis and their eventual removal by phagocytes. The induction of apoptosis in addition to assigning the cell for removal may also have the built-in safety mechanism of inhibiting exocytosis. In support of this, one study has shown that apoptotic neutrophils are unable to respond to inflammatory mediators and are effectively isolated from their external milieu (Whyte *et al.*, 1993). A possible explanation for this could be the shut down of the secretory pathway in the apoptotic

cell rendering it incapable of replenishing its cell surface receptors. It is this potential inhibition of secretion during apoptosis in the neutrophil that may provide new targets for therapeutic manipulation of inflammatory processes. Thus it is essential to understand the mechanisms underlying control of secretion during apoptosis in the neutrophil.

1.2 Apoptosis

Normal cells are thought to survive only in the presence of survival factors and simply withdrawing them is often enough to promote apoptosis. These survival factors include, cytokines and physical factors such as cell-cell contact and adhesion in the case of adherent cells (Raff, 1992). Apoptosis has far reaching implications not only in the process of inflammation but also in development, immune regulation, degenerative disease and cancer to name a few. Regulation of the apoptotic pathways represents a promising new target for control of these processes, either *via* promotion of cell death (e.g. cancer) or inhibition (e.g. Alzheimer's disease). Thus, a detailed understanding of regulatory mechanisms and cell type specific differences is crucial if this phenomenon is to be exploited to maximum potential for therapeutic gain.

1.2.1 Morphological & Molecular Changes During Apoptosis

Some of the characteristic morphological features of apoptosis are chromatin condensation, DNA fragmentation, cytoplasmic shrinkage and membrane blebbing, where the intracellular contents are contained (Kerr *et al.*, 1972; Wyllie *et al.*, 1980). Many of these characteristic features are due to an evolutionary conserved apoptotic death pathway on which many apoptotic stimuli converge. Common to most models of apoptosis is the exposure of phosphatidyl serine (PS) on the outer leaflet of the plasma membrane, activation of the caspases, a specific family of proteases that are responsible for the disassembly of the cell, including control of DNA fragmentation (Strasser *et al.*, 2000).

1.2.2 Caspases

Before the discovery of the cysteinyl aspartate-specific proteinases (caspases), apoptosis was known to be distinct from necrotic forms of cell death; however the underlying molecular mechanisms remained undefined. Whilst a number of genes involved in cell death had been identified in *Caenorhabditis elegans* their precise role in apoptosis had not been elucidated (Thornberry, 1999). The discovery of interleukin-1β converting enzyme (ICE) and its relation to the CED-3 death gene in *C. elegans* by Yuan *et al.* (1993) led to the connection between caspases and apoptosis and the view that the molecular mechanisms of apoptosis were highly conserved.

The caspase family of proteins contain cysteine residues within their active sites and cleave target proteins at aspartic acid residues (Alnemri *et al.*, 1996). Caspases are present in the cytosol as zymogens that contain three domains, which become activated by specific cleavage at aspartic acids between domains, followed by association of the large and small subunits to form a heterodimer (Nicholson, 1999). To date, at least 14 mammalian caspases have been identified that can be broadly divided into 2 groups: those centrally involved in the cell death program (caspases –2, -3, -6, -7, -8, -9, -10, -12, -14) and those involved in cytokine processing (-1, -4, -5, -11, -13) (Nakagawa *et al.*, 2000; Van de *et al.*, 1998; Zimmermann & Green, 2001). Those caspases centrally involved in apoptosis may further be divided in terms of function into 2 categories: initiator caspases and effector caspases. Initiator caspases such as –8 and –10 have long prodomains, containing death effector domains (DED), allowing association with adapter molecules such as Fas-associated death domain (FADD). The long prodomains of initiator caspases also allow oligomerisation, resulting in their activation by autocatalysis by a poorly defined mechanism (Kumar, 1999). The preferred cleavage motif of the initiator caspases is IETD or LETD a tetrapeptide sequence found in most maturation sites of the initiator and effector caspases (Earnshaw *et al.*, 1999). This specificity is consistent with the view that initiator caspases are primarily upstream activators of the effector caspases. Once activated, initiator caspases process the effector caspases –3, -6, -7, whose primary function is thought to be cleavage of cellular proteins to disassemble the cell (Nicholson, 1999). Typically, effector caspases have short prodomains and lack any 'adaptor' domains, suggesting that their activation is dependent on cleavage by initiator caspases (Fig. 1.1). The preferred cleavage motif of the effector caspases is DExD and has been found in many of the proteins cleaved

during apoptosis (Earnshaw *et al.*, 1999). Other caspases such as caspase-2 and caspase-9 contain caspase recruitment domains (CARD) that permit interaction with other procaspases or adaptor proteins such as inhibitor of apoptosis proteins (IAPs) (Kumar, 1999).

Two caspase activation pathways are well established. One is initiated by caspase-8, and -10 upon death receptor ligation, the other is initiated by caspase-9 and is mitochondria-dependent. However, there is overlap between the two pathways depending on the cell type and apoptotic stimulus used and in many cases the two pathways have been shown to converge (see Fig. 1.3) (Kumar, 1999). If the death signal is death-receptor-mediated, then caspase-8 may directly process procaspase-3 initiating the caspase cascade (Stennicke *et al.*, 1998). On the other hand, caspase-9 is central to apoptosis induced by cytotoxic drugs or cellular stress (Slee *et al.*, 1999a). Activation of caspase-9 requires the release of cytochrome c and apoptosis protease-activating factor 1 (Apaf-1) from the inner mitochondrial membrane. Apaf-1 contains multiple WD-40 repeats on its C-terminal domain which negatively regulate the oligomerisation and binding of procaspase-9. This was shown by deletion of the WD-40 region that allowed binding of procaspase-9 in the absence of cytochrome c and dATP (Hu *et al.*, 1999; Srinivasula *et al.*, 1998). Binding of cytochrome c and ATP is thought to cause a conformational change in Apaf-1, which allows procaspase-9 to interact with its CARD. This complex of cytochrome c, ATP and procaspase-9 has been termed the 'apoptosome' and is believed to allow the proximity-induced processing of caspase-9 (Li *et al.*, 1997; Pan *et al.*, 1998b; Saleh *et al.*, 1999). The caspase activation events driven by caspase-9 appear to be the simultaneous activation of caspases –3 and –7 (Pan *et al.*, 1998a; Slee *et al.*, 1999b). Caspase-3 then drives the activation of caspases –2 and –6, followed by the activation of caspases –8 and –10 (Slee *et al.*, 1999b). In a cell-free system, caspase-3 was shown to be the key caspase involved in cleaving cellular proteins. Some of the cellular substrates of caspase-3 are inhibitor of caspase-activated DNase (ICAD), receptor- interacting protein (RIP), X-linked inhibitor of apoptosis protein (X-IAP), topoisomerase I, Rb and lamin B, but not poly (ADP-ribose) polymerase (PARP) or lamin A (Slee *et al.*, 2001). In addition, caspase-3 was also essential for apoptosis-associated chromatin margination, DNA fragmentation, and nuclear collapse in this system. Caspase-6 and -7 however, had little impact on any of the parameters investigated, whether this is also the case in

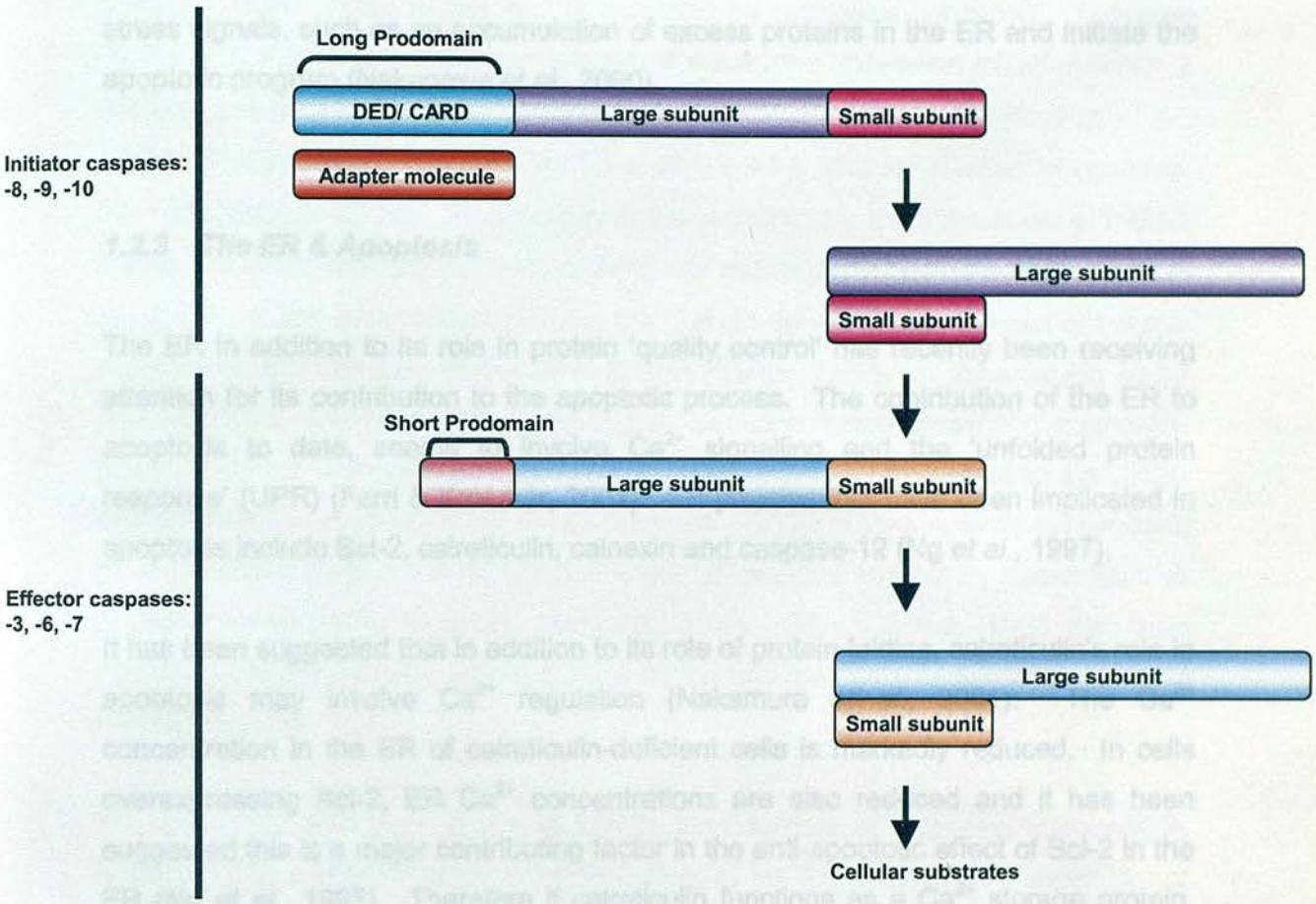

Figure 1.1: Model of caspase structure and function. Caspases are divided into 2 subgroups: initiator caspases and effector caspases. Initiator caspases such as –8 -9 –10 have long prodomains, containing DED or CARD domains, allowing association with adapter molecules. Autocatalytic cleavage of initiator caspases allows the large and small subunit to heterodimerise forming the active caspase. Once activated, they cleave the effector caspases –3, -6, -7, between domains allowing the heterodimerisation of the large and small subunit. Caspases –1, -2, -4, -5 have not been fully characterised.

the whole cell however or whether this is cell type dependent remains to be shown (Slee *et al.*, 2001).

Another pathway resulting in the induction of caspases has recently been discovered. Caspase-12 localised to the ER, appears to act as an initiator caspase, although in terms of structure, it most closely resembles the subfamily of caspases involved in cytokine processing. However, it was shown to be activated in response to ER stress signals, such as an accumulation of excess proteins in the ER and initiate the apoptotic program (Nakagawa *et al.*, 2000).

1.2.3 The ER & Apoptosis

The ER in addition to its role in protein 'quality control' has recently been receiving attention for its contribution to the apoptotic process. The contribution of the ER to apoptosis to date, seems to involve Ca^{2+} signalling and the 'unfolded protein response' (UPR) (Ferri & Kroemer, 2001). ER proteins that have been implicated in apoptosis include Bcl-2, calreticulin, calnexin and caspase-12 (Ng *et al.*, 1997).

It has been suggested that in addition to its role of protein folding, calreticulin's role in apoptosis may involve Ca^{2+} regulation (Nakamura *et al.*, 2001). The Ca^{2+} concentration in the ER of calreticulin-deficient cells is markedly reduced. In cells overexpressing Bcl-2, ER Ca^{2+} concentrations are also reduced and it has been suggested this is a major contributing factor in the anti-apoptotic effect of Bcl-2 in the ER (Ng *et al.*, 1997). Therefore if calreticulin functions as a Ca^{2+} storage protein, calreticulin-deficient cells may be more resistant to apoptosis due to the reduced Ca^{2+} concentration in the ER. Calnexin is also believed to play a role in the UPR, however, Ca^{2+} concentrations in the ER of calnexin-deficient cells are not affected, indicating that the role of calnexin in apoptosis is independent of Ca^{2+} concentrations (Zuppini *et al.*, 2002).

The accumulation of misfolded proteins in the ER leads to the activation of two separate signaling pathways specific to the UPR. Misfolded proteins bind to the ER chaperone BiP, a 70kDa transmembrane heat shock protein and a build-up of misfolded protein can result in the competitive disruption of B Cell Immunoglobulin Binding Protein/ Inositol requiring 1-α (BiP/ Ire1-α) complex and BiP/ Protein Kinase

R-like ER Kinase (PERK) (Urano *et al.*, 2000). Ire-α is a type I transmembrane protein with a ribonuclease (Rnase) domain on its cytoplasmic tail and a serine/ threonine kinase domain that becomes activated upon dimerisation resulting in the autophosphorylation and dimerisation of Ire-α (Harding *et al.*, 1999; Urano *et al.*, 2000). Upon dissociation from BiP, phosphorylated Ire1-α can recruit TRAF2 *via* its cytoplasmic domain and hence activate the c-Jun N-terminal kinase (JNK) pathway, initiating apoptosis (Urano *et al.*, 2000). Upon dissociation of the BiP/ PERK complex, PERK oligomerises and is activated by autophosphorylation. Activated PERK then mediates the phosphorylation of eukaryotic translation initiation factor 2 (eIF2α) and eIF2α subsequently inhibits translation (see Fig. 1.2) (Harding *et al.*, 1999). The cytoplasmic face of the ER is also the intracellular location of caspase-12. Procaspase-12 has been shown to be recruited by Ire-α associated TRAF2 during the UPR, resulting in the processing and activation of caspase-12 (Yoneda *et al.*, 2001). It has been shown in yeast that the dimerised RNase domain of Ire-α is required for the induction of the UPR (Cox & Walter, 1996). A transcription factor was identified, 'homologous to activating transcription factor/ cyclic 3',5'-adenosine monophosphate response element binding protein 1 (HAC1) that binds to the UPRE and induces the transcription of ER chaperones. HAC1 is constitutively synthesised in an unspliced form but is rapidly degraded. Alternative splicing by dimerised and phosphorylated Ire1-α however, generates active HAC1. Active HAC1 can then translocate to the nucleus where it binds to the unfolded protein response element (UPRE) (see Fig. 1.2).

ER stress has also been shown to induce the cleavage of activating transcription factor (ATF)6, a type II transmembrane protein of the ER, although the exact signal for cleavage is unknown. Site-1 protease (S1P) and Site-2 Protease (S2P), involved in sterol regulatory binding proteins, were shown to cleave ATF6 during the UPR (Ye *et al.*, 2000). Cleavage of ATF6, on the cytosolic region, results in the release of a 50kDa fragment (p50ATF6) that translocates to the nucleus where it acts as a transcription factor and activates transcription of ER chaperone genes (Haze *et al.*, 1999; Yoshida *et al.*, 2000). In addition, the ATF6 fragment may activate CCAAT/enhancer-binding protein beta homologous protein/ growth arrest and DNA damage inducible 153 (CHOP/ GADD)153, a transcription factor that decreases the expression of Bcl-2 and may therefore promote apoptosis (see Fig. 1.2) (McCullough *et al.*, 2001).

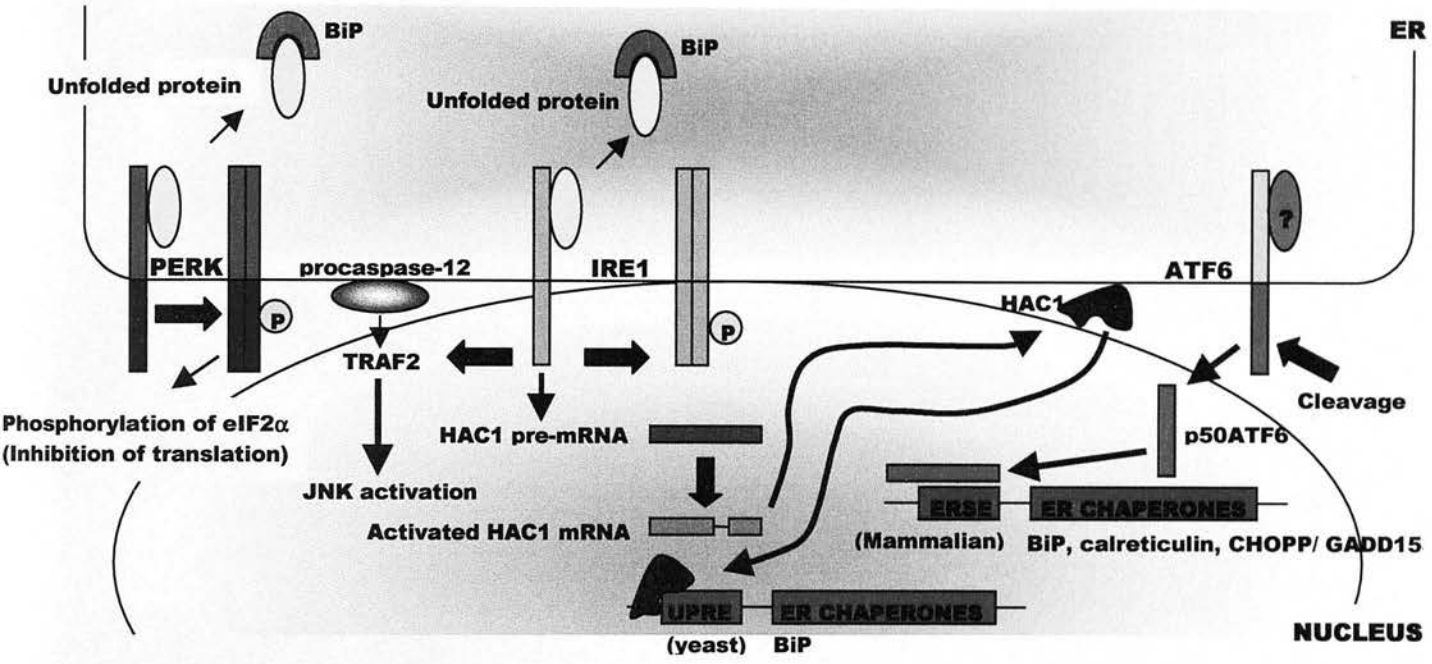

Figure 1.2: Mechanism of ER stress response. Accumulation of misfolded proteins in the ER results in the competitive dissociation of BiP from Ire1. This dissociation leads to the oligomerisation of Ire1, inducing its autophosphorylation and activation of endonuclease domains with a subsequent induction of ER chaperone genes, *via* the cleavage of HAC1 pre-mRNA in yeast. A mammalian homologue of HAC1 has yet to be identified. In addition, oligomerisation of Ire1 may also lead to the activation of JNK pathways, *via* the recruitment of TRAF2, which in turn can recruit caspase-12 leading to apoptosis. ATF6 is also cleaved, although the regulatory ATF6 molecule is unknown and the cytosolic cleavage product is translocated to the nucleus, where it acts as a transcription factor and induces the transcription of ER chaperone genes. UPRE = unfolded protein response element (yeast), ERSE=endoplasmic reticulum stress element (mammalian cells).

1.2.4 Inhibitors of Caspases

The inhibitor of apoptosis (IAP) proteins (X-IAP, C-IAP, C-IAP-2, N-AIP) were initially identified as baculovirus products that could inhibit apoptosis. Later, homologous mammalian proteins X-IAP (MIHA, hILP), c-IAP1 (MIHB), C-IAP-2 (MIHC), N-AIP and Survivin were discovered and found to inhibit caspase-3, caspase-7 and caspase-9 activity (Ekert *et al.*, 1999). Their mode of action appears to be by acting as pseudosubstrates for the caspases, binding to active caspases and neutralising their activity (Srinivasula *et al.*, 2001). However, upon the induction of apoptosis, the inhibitory activity of X-IAP is suppressed by a second mitochondria-derived activator of caspase (Smac/ DIABLO), released from the mitochondrial inner membrane space (Chai *et al.*, 2000; Du *et al.*, 2000). The role of some IAPs in apoptosis remains somewhat controversial however, since C-IAP1 (MIHB), C-IAP-2 (MIHC) and N-AIP only inhibited apoptosis at very high concentrations, which probably do not occur *in vivo* (Roy *et al.*, 1997; Ekert *et al.*, 1999). Although, the role of IAPs remains unclear, X-IAP and Survivin were demonstrated to be potent inhibitors of caspases at more physiological concentrations, thus suggesting that they play a role in regulating the apoptotic machinery (Deveraux *et al.*, 1997; 1998; Li *et al.*, 1998).

1.2.5 Initiation of Apoptosis: Death Receptors

Apoptosis involves an initiation phase where cells receive a signal to die, a commitment phase where pro-apoptotic and anti-apoptotic proteins influence the decision to die and an execution phase where the caspases are mobilised to disassemble the cell architecture. Initiators of the apoptosis machinery can be broadly grouped into two different categories: (1) death receptors (2) stimuli that provoke generalised cellular damage or cellular stress. The commitment phase involves members of the Bcl-2 family, which may be pro- or anti- apoptotic and in many cases act upon the mitochondria.

The death receptors belong to the tumor necrosis factor (TNF) receptor superfamily, with the exception of the nerve growth factor (NGF) receptor (Smith *et al.*, 1994) and by definition contain homologous cytoplasmic regions called death domains (DD) (Tartaglia *et al.*, 1993). Typically, the TNF family death receptors are present on the cell surface as homotrimeric molecules that require three ligands to bind and promote clustering of the cytoplasmic death domain (DD) (Smith *et al.*, 1994). In the case of

the Fas receptor (FasR), clustering of the DD leads to the binding of FADD through its own DD. FADD also contains a region termed the CARD, which recruits procaspase-8 and or procaspase-10, promoting the oligomerisation and cleavage of caspase-8 (Kischkel *et al.*, 2001; Muzio *et al.*, 1998). Following the activation of caspase-8, there are two ways in which the apoptotic machinery can be mobilized depending on the cell type (Scaffidi *et al.*, 1998). Type I cell: caspase-8 directly activates downstream caspases, initiating the caspase cascade. Type II cell: caspase-8 modulates members of the Bcl-2 family of proteins, which influence the mitochondrial pathway of caspase activation (Scaffidi *et al.*, 1998).

In most cell types, TNF binding can result in the activation of three distinct pathways and only results in apoptosis in the presence of protein synthesis inhibitors (Ashkenazi & Dixit, 1998). TNF binding results in trimerisation of the TNF receptors (TNFR), causing association of the cytoplasmic DDs to which TNFR-associated DD (TRADD) then binds through its own DD. TRADD binding results in the recruitment of TNFR-associated factor-2 (TRAF2) and receptor-interacting protein (RIP) (Ashkenazi & Dixit, 1999). TRAF2 and RIP are thought to be involved in activating the NF-κB or JNK/AP-1 pathway, leading to the induction of proinflammatory genes. NF-κB inducing kinase (NIK) is activated by TRAF2 and RIP, subsequently activates inhibitor of κB (I-κB) kinase (IKK) (Ashkenazi & Dixit, 1999). IKK phosphorylates I-κB, targeting I-κB for degradation and allowing NF-κB translocation to the nucleus to initiate transcription. TRADD also binds to FADD and thereby can activate caspase-8 and or -10 and hence apoptosis (Ashkenazi & Dixit, 1998; Kischkel *et al.*, 2001). It has also been suggested that ligation of the TNFR results in the recruitment of caspase-2, *via* the adapter molecule RAIDD which binds to the RIP/ TRAF2 complex (Duan & Dixit, 1997; Chou *et al.*, 1998; Droin *et al.*, 2001) . However, this is disputed since caspase-8 deficient cells are resistant to TNF induced apoptosis (Varfolomeev *et al.*, 1998).

1.2.6 Initiation of Apoptosis: Stress

The second type of death stimulus includes diverse apoptosis-promoting stimuli such as cytotoxic drugs, radiation, heat shock, survival factor deprivation and other cellular stresses. Despite the apparent diversity of these stimuli, all the pathways involved seem to converge on the mitochondria, where modulation of mitochondrial proteins results in the activation of caspases (Strasser *et al.*, 2000).

1.2.7 Mitochondria & Bcl-2 Family Proteins

In addition to the text-book role of mitochondria in cellular respiration, mitochondria have in recent years also taken centre stage for their role in apoptosis. In 1994, Newmeyer *et al.*, demonstrated that mitochondria were required in cytosols to induce nuclear fragmentation characteristic of apoptosis in nuclei isolated from *Xenopus* eggs. Further studies revealed that the release of cytochrome c from mitochondria was required for caspase activation (Desagher & Martinou, 2000). Other mitochondrial proteins involved in the apoptotic programme including procaspases, Smac/ DIABLO and apoptosis inducing factor (AIF) are all released from the intermembrane space of mitochondria where many members of the Bcl-2 family proteins also reside (Zamzami & Kroemer, 2001).

Critical to the release of apoptotic proteins from the mitochondrial intermembrane space is the permeabilisation of the inner and outer mitochondrial membranes by the action of the putative permeability transition pore (PTP). Under normal conditions, the PTP facilitates the release of Ca^{2+} from the mitochondrial matrix, through the action of adenine nucleotide translocator (ANT) on the inner mitochondrial membrane (Li & Weinman, 2002). The voltage-dependent anion channel (VDAC) is located on the outer mitochondrial membrane and allows the free exchange of molecules up to 5kDa, facilitating the exchange of NADH, FADH and ATP/ADP between in the inner mitochondrial membrane and the cytosol. Together the ANT/VDAC in conjunction with other interacting proteins form the PTP (Li & Weinman, 2002). The permanent permeability of the mitochondrial membrane results in the release of cytochrome c and other pro-apoptotic molecules and members of the Bcl-2 protein family are thought to play a key role in regulating the opening of the PTP, but their precise mode of action remains controversial (Susin *et al.*, 1996; Zamzami & Kroemer, 2001).

Bcl-2 family members can be functionally divided into two classes, those that are anti-apoptoptic (e.g. Bcl-2, Bcl-xL, Mcl-1, A-1) and those that promote apoptosis (e.g. Bax, Bak, Bcl-xs, Bad, Bid, Bim) (Kelekar & Thompson, 1998). All Bcl-2 family members share homology in one of four regions: BH1, BH2, BH3 and BH4, where they may share all these domains or are missing one or more domains. However, all Bcl-2 family members possess a BH3 domain, a stretch of 16 amino acids, necessary for interaction with anti-apoptotic members or to promote cell death

(Kelekar & Thompson, 1998). Many of the proteins have a C-terminal region that allows them to interact with the outer mitochondrial membrane and the ER (Kelekar & Thompson, 1998). For example, Bax, Bak, Bad and Bid are normally cytosolic but upon the induction of apoptosis are inserted into the mitochondrial membrane (Kluck *et al.*, 1997; Kluck *et al.*, 1999; Murphy *et al.*, 1999b; Nechushtan *et al.*, 2001; Pryde *et al.*, 2000; Wei *et al.*, 2001; Wolter *et al.*, 1997).

Regulation of Bcl-2 family members may be at the transcriptional level or posttranscriptional level. Both pro- and anti- apoptotic members can heterodimerize with each other which has led to the suggestion that the relative levels of either in a given cell may determine the ease with which a cell will activate the apoptotic program. Posttranslational regulation, in addition to the formation of heterodimers, involves in some cases phosphorylation events. Bcl-2, Bad and Bid have been shown to be regulated by phosphorylation (Desagher *et al.*, 2001; Downward, 1999; Schurmann *et al.*, 2000; Strasser *et al.*, 2000). Phosphorylation of Bcl-2 has been reported to occur *via* several different kinases including PKC, PKA and CDK1. In the majority of studies, Bcl-2 is inhibited by phosphorylation (Adams & Cory, 1998). In the case of Bad, survival signals mediate its phosphorylation *via* protein kinase A (PKA) or protein kinase B (PKB or Akt) which results in its release from Bcl-X_L at the mitochondrion. In type II cells, only the phosphorylated form of Bid is cleaved by caspase-8 to yield the pro-apoptotic truncated Bid (tBid) which is then thought to translocate to mitochondria and trigger cytochrome c release (Desagher *et al.*, 2001). At the transcriptional level, A1 and Mcl-1 expression have both been shown to be induced by GM-CSF and inflammatory cytokines (Chao *et al.*, 1998; Karsan *et al.*, 1996). Therefore, a cell may increase the ratio of anti-apoptotic Bcl-2 proteins to pro-apoptotic in unfavourable environmental circumstances such as inflammation. See Fig. 1.3 for schematic overview of apoptosis.

1.2.8 Neutrophil Apoptosis

Evolutionary conservation of death programmes across a diverse range of species and tissue types means that in many cases the central pathways leading to cellular demise are the same. However, a thorough understanding of the subtle differences in the apoptotic program between cell types may be key for selective drug targeting strategies for the therapeutic manipulation of disease pathogenesis. While the

previous discussion has centred on 'global' apoptotic death programs, this section highlights specific neutrophil apoptotic programs.

Neutrophils undergo constitutive apoptosis during *in vitro* culture, but IL-1β, IL-2, TNF-α, IL-15, INF-γ, G-CSF, GM-CSF, LPS and hypoxic conditions can inhibit this (Akgul *et al.*, 2001; Ward *et al.*, 1999b). It is likely that neutrophils would encounter these stimuli at inflammatory sites *in vivo*, thereby prolonging their life-span and allowing them to fulfil their role in clearance of microbes. In contrast, stimulation of neutrophils with an antibody against the Fas receptor *in vitro* has been proposed to increase their rate of apoptosis (Liles *et al.*, 1996). In addition, agents that inhibit protein synthesis or transcription such as cycloheximide and actinomycin D have been shown to promote neutrophil apoptosis (Ward *et al.*, 1999b). While the inhibition of protein synthesis may not represent a useful target for *in vivo* modulation of neutrophil apoptosis, the observed induction of apoptosis implies that *de novo* synthesis of survival proteins are required for neutrophil survival.

The Bcl-2 family members that have been detected in neutrophils are Bcl-X_L, Mcl-1, A1, Bax, Bad, Bak and Bid (Akgul *et al.*, 2001; Chuang *et al.*, 1998; Pryde *et al.*, 2000). Anti-apoptotic Bcl-2 is not expressed in neutrophils, but Mcl-1 and A1 mRNA levels, which normally have very short half-lives, have been shown to be increased or maintained by inflammatory mediators that inhibit neutrophil apoptosis (Chuang *et al.*, 1998; Moulding *et al.*, 1998). In contrast, the pro-apoptotic Bcl-2 family members, Bax, Bad, Bak and Bid are constitutively expressed in neutrophils and have a long half-life, perhaps explaining why on balance, neutrophils are 'primed' for apoptosis (Moulding *et al.*, 2001). Further, during constitutive neutrophil apoptosis Bax translocates from the cytoplasm to the mitochondria resulting in caspase-3 activation (Pryde *et al.*, 2000). In addition, translocation was not inhibited by z-VAD-fmk, the broad range caspase inhibitor, suggesting that Bax redistribution is caspase-independent, a topic that is examined in Chapter 3 (Maianski *et al.*, 2002).

The execution pathway in neutrophils is also mediated by caspases. Effector caspases that have been identified in neutrophils are –8 and –3 (Daigle & Simon, 2001; Yamashita *et al.*, 1999) and mRNA transcripts have been detected for caspases –7, -9 and –10 (Santos-Beneit & Mollinedo, 2000). Caspase-3 was shown to be critical for the induction of apoptosis in neutrophils, where the active form was detected in both constitutive and Fas-induced apoptosis (Daigle & Simon, 2001).

Caspase-8 has been shown to be active in freshly isolated neutrophils and expression of a FasL/ FasR on the neutrophil cell surface could lead to autocrine/ paracrine induction of apoptosis (Iwai *et al.*, 1994; Kiener *et al.*, 1997). This is thought not to occur. Recently, it has been reported that soluble FasL acts as a chemotactic factor for neutrophils implying that like TNFα, Fas may act to stimulate neutrophil function under certain conditions (Ottonello *et al.*, 1999). The function of caspase-8 activity in freshly isolated neutrophils is not known and further work is necessary to define its role in apoptosis.

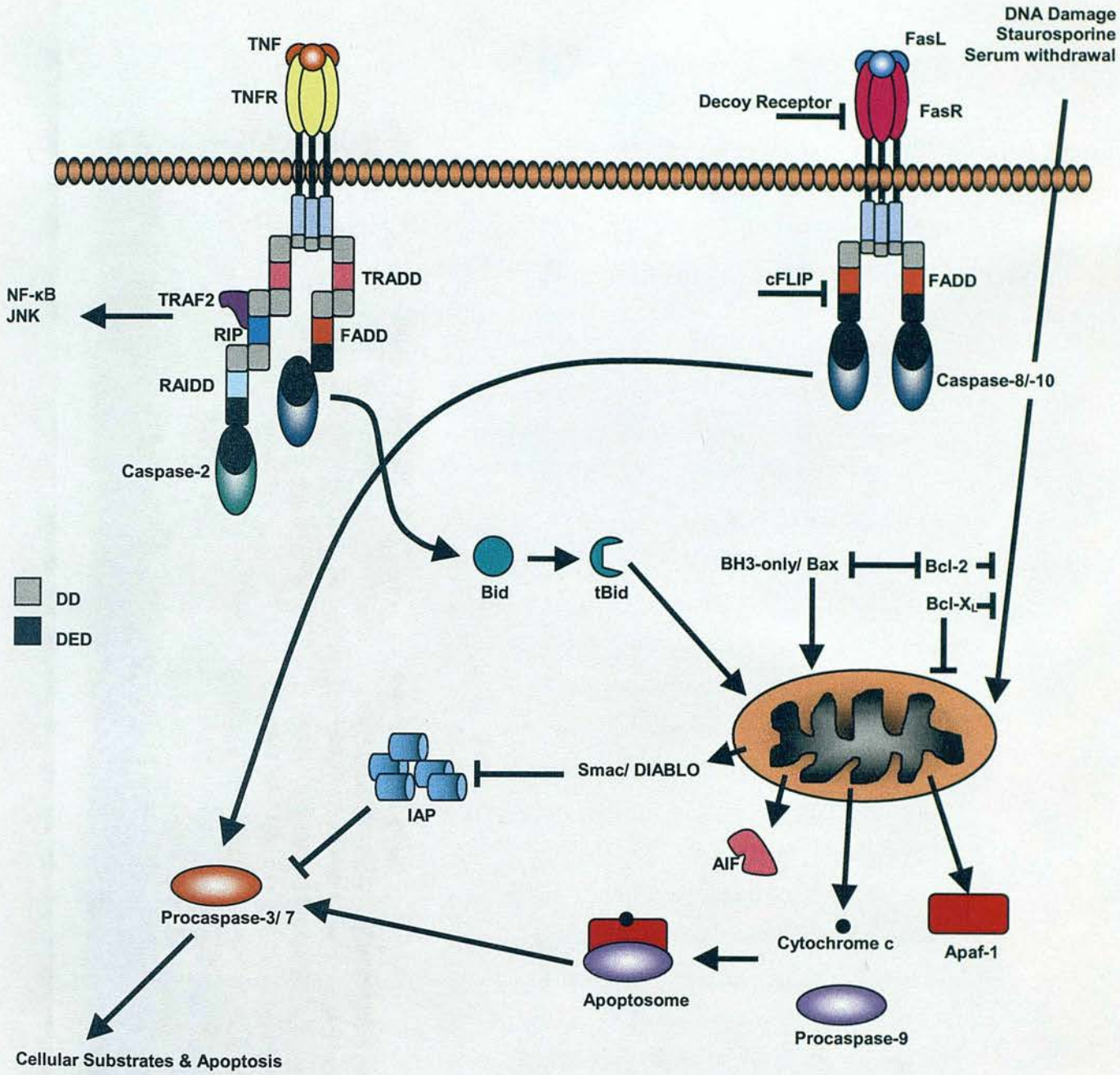

Figure 1.3: Apoptotic signalling pathways. The death receptor pathway may be triggered by binding of Fas ligand (FasL), inducing trimerisation of the Fas receptor (FasR). This results in the recruitment of procaspase-8 *via* the adaptor molecule FADD leading to activation of caspase-8. Caspase-8 (or FLICE) can be blocked by FLIP (FLICE-inhibitory protein) present in several viruses. Death receptor induced apoptosis may also be blocked through decoy receptors (DcR) that lack the death domain and compete for ligand binding without inducing apoptosis. The mitochondrial death pathway is induced by cellular stress which can includes cytotoxic drugs, serum withdrawel or DNA damage. The death receptor and mitochondrial pathways converge at the point of caspase-3 activation, which results in the cleavage of cellular substrates and apoptosis. Crosstalk between the apoptosis-inducing pathways is provided by caspase-8 mediated cleavage of Bid, resulting in truncated Bid (tBid) translocating to the mitochondria where it promotes the release of cytochrome c.

1.3 Neutrophil Granules & Exocytosis

In addition to the unresponsiveness of apoptotic neutrophils to inflammatory stimuli, apoptotic neutrophils have a reduced capacity to degranulate and to bind fMLP to surface receptors, suggesting a loss of fMLP receptors (Whyte *et al.*, 1993). Surprisingly, few studies have attempted to delineate the underlying mechanism for this 'unresponsive state' of the apoptotic neutrophil since it is a key phenomenon that prevents the inappropriate release of histotoxic contents from granules before apoptotic neutrophils are phagocytosed.

1.3.1 Neutrophil Granules

Granules form in the neutrophil during the maturation stage from myeloblast to promyelocyte and continue to form until maturation is complete (Borregaard *et al.*, 1995). Neutrophil granules are divided into myeloperoxidase (MPO) positive and MPO negative (Bainton *et al.*, 1971), where MPO positive granules are further divided into defensin-rich and defensin-poor granules (Rice *et al.*, 1987). MPO negative granules are further divided into 'specific' granules and 'gelatinase' granules, both contain lactoferrin and gelatinase but lactoferrin predominates in specific granules and gelatinase predominates in gelatinase granules (Kjeldsen *et al.*, 1992). Neutrophil storage granules, in addition to containing anti-microbial proteases, contain membrane-bound receptors. Secretory vesicles are classified separately since their only known content is plasma, although their membranes are rich in receptors (see Table 1.1 for known granular content in neutrophils) (Sengelov *et al.*, 1993b; Sengelov *et al.*, 1994). Secretory vesicles appear to be mobilised when neutrophils are activated e.g. by binding to endothelial cells, by inflammatory cytokines or by chemoattractants. (Crockett-Torabi *et al.*, 1995; Crockett-Torabi & Fantone, 1995; Patel *et al.*, 1994). Neutrophil activation commonly involves the expression of the CD18 (CD11b/CD18 integrin), the fMLP receptor and IL-8. During exocytosis, not only are the granule contents released but the neutrophil gains a new repertoire of receptors as the granule membrane fuses with the plasma membrane, enabling the neutrophil to interact in a new way with its environment (Berger *et al.*, 1984; Berger *et al.*, 1991; Kuijpers *et al.*, 1991). Mobilisation of secretory vesicles for example, enables neutrophil phagocytosis of complement opsonised particles (Sengelov *et al.*, 1993b).

1.3.2 Regulated Secretion

Little is known about the sorting of proteins in neutrophils into different granule subsets that renders them distinct from each other. The formation of granules must involve specificity however, in targeting proteins to the granules and not the plasma membrane. Further, specific proteins must be delivered to the different types of granule. The transport vesicles destined for the granules through the regulated secretory pathway must be sorted from the vesicles containing constitutively secreted proteins, destined for the plasma membrane through the constitutive secretory pathway (Sossin *et al.*, 1990). Control of granule exocytosis (regulated exocytosis) however, appears to be regulated by mechanisms that differentiate between azurophilic granules and peroxidase negative granules but not between the subsets of those two classes of granule (Sengelov *et al.*, 1993a; Sengelov *et al.*, 1995). Differential sensitivity to elevated intracellular Ca^{2+} levels has been shown in mobilisation of granules and secretory vesicles (Lew *et al.*, 1986). However, both constitutive and regulated secretion play an important role in furnishing the neutrophil cell surface with receptors that allow interaction with the extracellular milieu. A number of studies have shown that the cell surface receptors are also synthesized *de novo* and therefore by necessity must traffic through the ER to Golgi and from the Golgi to the plasma membrane or to granules (Crepaldi *et al.*, 2001; Girard *et al.*, 1996; Girard *et al.*, 1997; Grenier *et al.*, 1999; Jost *et al.*, 1990; Jost *et al.*, 1991; Zhou *et al.*, 2000).

1.3.3 The SNARE Hypothesis

Only recently has a hypothesis been put forward to explain the precise targeting of vesicles to specific membranes. The SNARE (soluble NSF attachment protein receptor where NSF stands for *N*-ethyl-maleimide-sensitive-fusion protein) family proteins consist of v-SNAREs (vesicle-SNARE) and t-SNAREs (target-SNARE) and are thought to be part of a conserved group of proteins in mammalian cells (Chen & Scheller, 2001). The SNARE hypothesis states that a vesicle contains a membrane bound SNARE protein and a partner molecule on the target membrane (Sollner *et al.*, 1993). Two other known proteins are necessary for vSNARE/ tSNARE mediated membrane fusion, known as NSF and α-SNAP (soluble NSF attachment protein), which are cytosolic proteins (Block *et al.*, 1988; Clary *et al.*, 1990).

Azurophilic Granules

Membrane:
- CD63 (LAMP-1)
- CD68 (scavenger receptor)
- V-type H- -ATPase

Granule Contents:
- Acid b-glycerophosphatase
- Acid mucopolysaccharide
- α1-Antitrypsin
- α-Mannosidase (acid hydrolase)
- Azurocidin/ CAP37/ heparin binding protein
- Bactericidal permeability increasing protein
- β-Glycerophosphatase
- β-Glucuronidase
- Cathepsins (antimicrobial function)
- Defensins (antimicrobial function)
- Elastase
- Lysozyme (antimicrobial function)
- Myeloperoxidase (antimicrobial function)
- N-Acetyl- β-glucosaminidase
- Proteinase-3
- Sialidase
- Ubiquitin-protein

Specific Granules

Membrane:
- CD11b/ CD18 (firm adhesion)
- CD15 antigens (rolling)
- CD66 (rolling)
- CD67 (rolling)
- Cytochrome b558 (NADPH oxidase component)
- fMLP-R (chemotaxis)
- Fibronectin
- G-proteinα -subunit
- Laminin-R
- NB 1 antigen
- 19kD protein
- 155kD protein
- Rap1, Rap2
- SCAMP (membrane fusion)
- Thrombospondin-R (migration)
- TNF-R
- Urokinase-type plasminogen activator-R (migration)
- VAMP-2 (vSNARE)
- Vitronectin-R (migration)

Granule Contents:
- β2-Microglobulin
- Collagenase
- hCAP-18
- Histaminase
- Heparanase
- Lactoferrin (prevents microbial growth)
- Lysozyme (antimicrobial function)
- NGAL
- Urokinase-type plasminogen activator
- Sialidase
- SGP28
- Vitamin B_{12} –binding protein

Gelatinase Granules

Membrane:
- CD11b
- Cytochrome b_{558} (NADPH oxidase component)
- Diacylglycerol-deacylating enzyme
- fMLP-R
- SCAMP
- Urokinase-type plasminogen activator-R
- VAMP-2
- V-type H^+ -ATPase

Granule Contents:
- Acetyltransferase
- β2-Microglobulin
- Gelatinase
- Lysozyme

Secretory Vesicles

Membrane:
- Alkaline phosphatase
- CR1
- Cytochrome b_{558} (NADPH oxidase component)
- CD11b/ CD18 (firm adhesion)
- CD14
- CD16 (Fc receptor)
- fMLP-R
- SCAMP
- Urokinase-type plasminogen activator-R
- V-type H+ -ATPase
- VAMP-2 (vSNARE)
- CD10 (endopeptidase)
- CD13 (aminopeptidase)
- CD45 (phosphatase)
- C1q-receptor
- DAF (complement regulatory protein)

Granule Contents:
- Plasma proteins

Table 1.1: Contents of neutrophil granules and secretory vesicles with some associated functions (Borregaard & Cowland, 1997).

Different subsets of vSNAREs and tSNAREs in many cases, operate between distinct cellular membranes (see Fig. 1.4) (Baumert *et al.*, 1989; Chen & Scheller, 2001; Hay *et al.*, 1996; Hay *et al.*, 1997; Hay *et al.*, 1998; Subramaniam *et al.*, 1996). In addition, vSNAREs and tSNAREs have been identified as part of a complex that mediates fusion between a vesicle and its target membrane in almost all fusion events studied to date (Scales *et al.*, 2000). However, it is unlikely that the SNARE molecules alone are enough to confer specificity, since it was shown that a single vSNARE interacted with two separate tSNAREs on separate membrane compartments (Gotte & von Mollard, 1998; Rothman, 1994; von Mollard *et al.*, 1997). In addition, tetanus toxin exerts its effects by vSNARE proteolysis thereby blocking the assembly of SNARES (Hunt *et al.*, 1994). Thus, if SNAREs alone accounted for the specificity and targeting of vesicles, then in the presence of tetanus toxin there should not be any vesicle association with the target membrane. However, the converse was found to be true, with increased numbers of vesicles associated with the target membrane, suggesting that vesicles were still targeted correctly. It has therefore been proposed that 'tethering factors' are required for correct targeting of the vesicle. Another family of proteins have been implicated in vesicle targeting, adding another layer of specificity to membrane fusion events. The Rab family, belonging to the small G protein superfamily, have been shown to be important for membrane fusion and different Rab proteins have been shown to localise to specific subcellular compartments (see Fig. 1.4) and to control distinct membrane trafficking routes (Novick & Zerial, 1997; Zerial & McBride, 2001). However, SNAREs are essential for membrane fusion since despite vesicle association to the target membrane, no membrane fusion or exocytosis occurred (Hunt *et al.*, 1994).

Several models have been proposed to account for SNARE-mediated membrane fusion (see Hay & Scheller (1997) for review), mainly due to the controversy arising over the timing of NSF/ α-SNAP action. However, the model that is currently gaining favour is described here (see Fig. 1.5). tSNARE availability to bind vSNAREs should be tightly regulated, since not only must vesicle budding from donor organelles be regulated, but also their fusion and hence release of vesicle contents. A tSNARE regulator called n-Sec-1, was shown to bind to the tSNARE syntaxin-1A, present on the plasma membrane, blocking any interaction with its associated vSNARE in neuronal cells (Pevsner *et al.*, 1994). Homologues of n-Sec-1 have been identified which could regulate other t-SNAREs (Pfeffer, 1999).

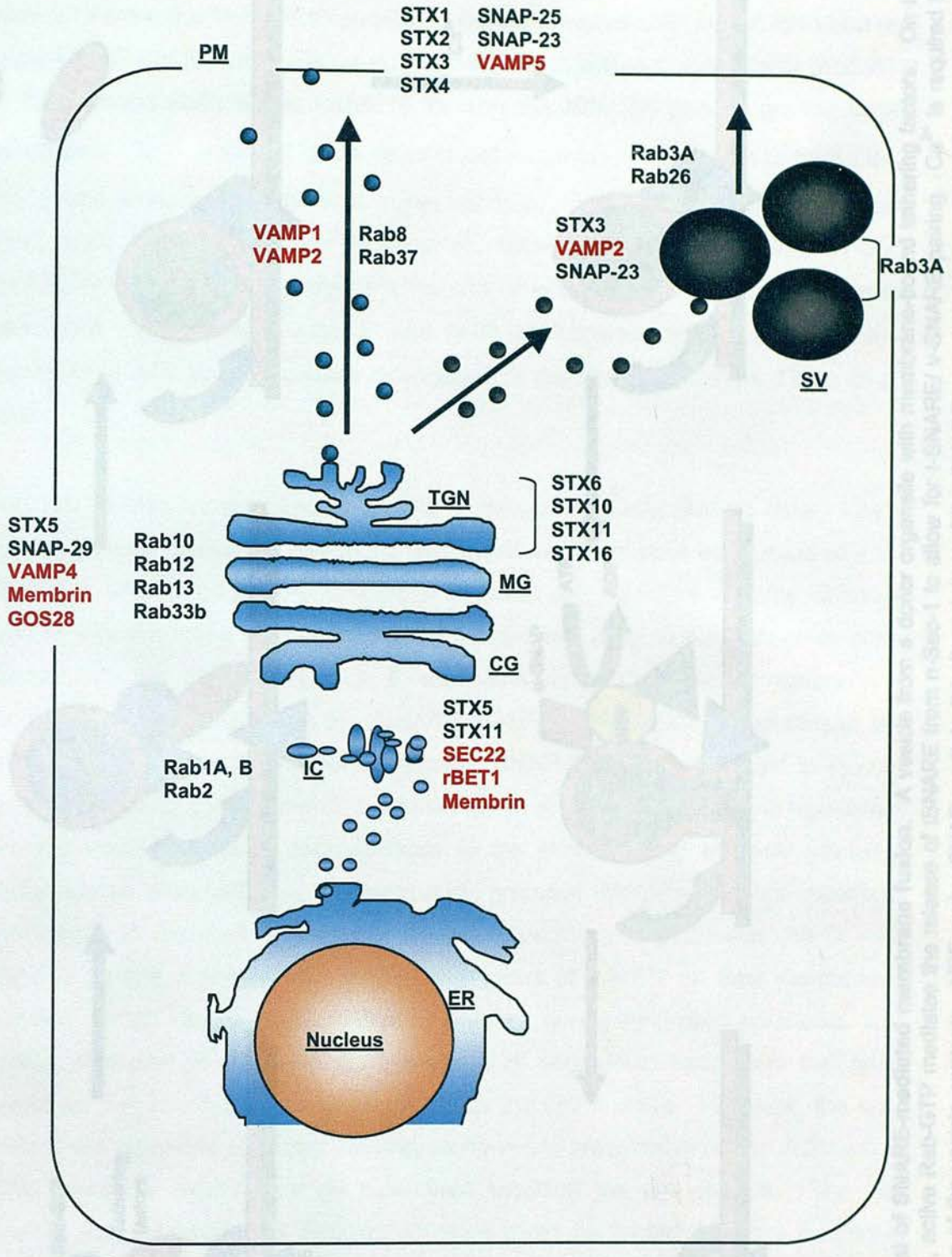

Figure 1.4: Cellular localisation of vSNAREs, tSNAREs and Rab family of small GTPases in the constitutive and regulated secretory pathways. vSNARE family=red text, tSNARE family=black text. TGN=trans Golgi network, MG= medial Golgi, CG= *cis*-Golgi, STX=syntaxin, VAMP=vesicle associated membrane protein, SV= secretory vesicles, ER=endoplasmic reticulum, IC=intermediate compartment, PM= plasma membrane.

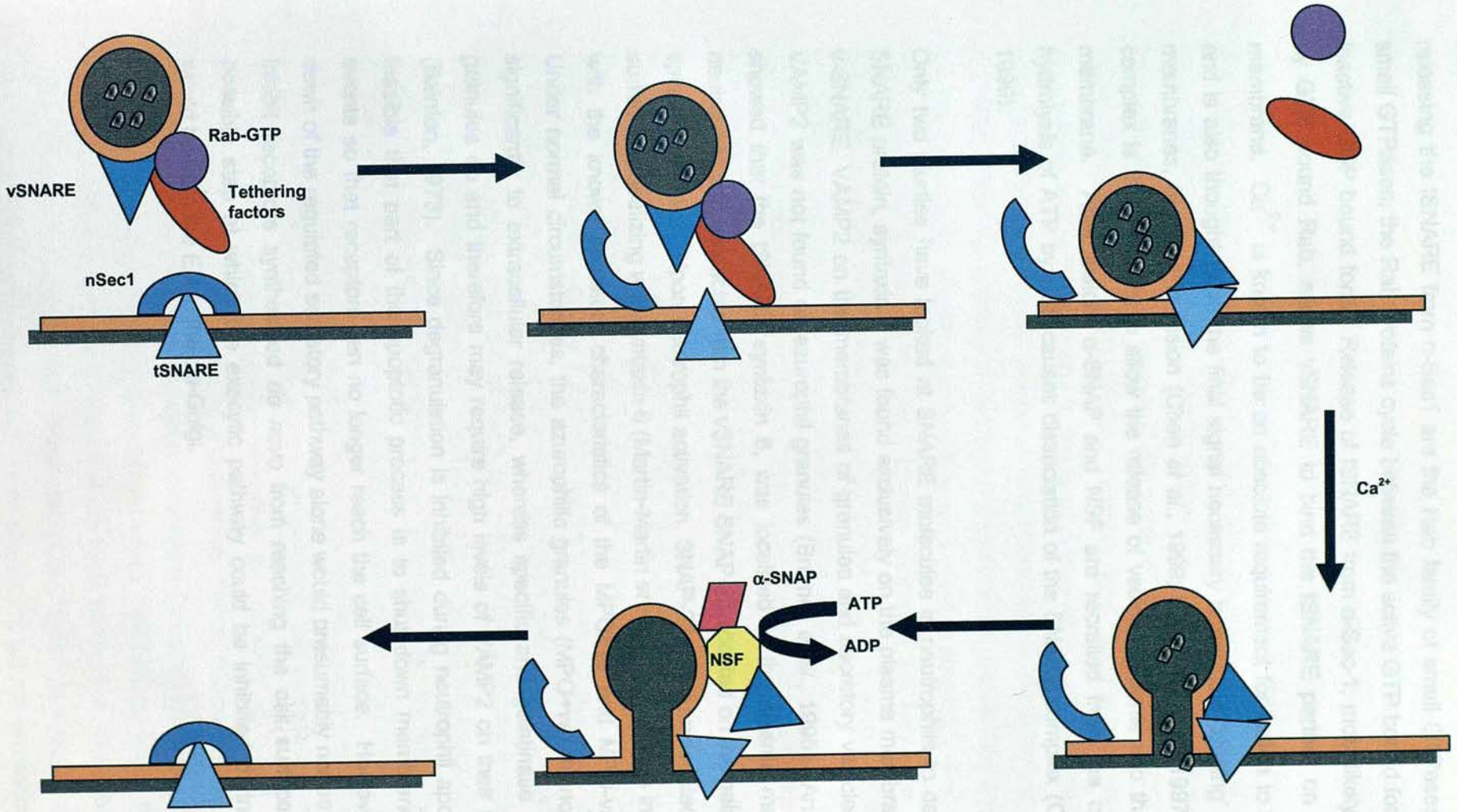

Figure 1.5: Model of SNARE-mediated membrane fusion. A vesicle from a donor organelle with membrane-bound tethering factors. On the target membrane, active Rab-GTP mediates the release of tSNARE from n-Sec-1 to allow for t-SNARE/ v-SNARE pairing. Ca^{2+} is required for fusion and release of the vesicle contents. NSF and α-SNAP mediate the dissociation of the SNARE complex, freeing tSNARE to interact with other incoming vesicles.

However, the tSNARE regulator must also be regulated and possible candidates for releasing the tSNARE from n-Sec1 are the Rab family of small GTPases. Like all small GTPases, the Rab proteins cycle between the active GTP bound form and the inactive GDP bound form. Release of tSNARE from n-Sec-1, most likely mediated by GTP bound Rab, allows vSNARE to bind the tSNARE partner on the target membrane. Ca^{2+} is known to be an absolute requirement for fusion to take place and is also thought to be the final signal necessary to facilitate 'zipping' of the two membranes, resulting in fusion (Chen *et al.*, 1999; Lin & Scheller, 1997). A pore complex is then thought to allow the release of vesicle contents into the acceptor membrane. After fusion, α-SNAP and NSF are recruited from the cytosol and hydrolysis of ATP by NSF causes dissociation of the SNARE complex (Chen *et al.*, 1999).

Only two studies have looked at SNARE molecules in neutrophils to date. The t-SNARE protein, syntaxin-4 was found exclusively on the plasma membrane and the v-SNARE, VAMP2 on the membranes of granules and secretory vesicles, although VAMP2 was not found on azurophil granules (Brumell *et al.*, 1995). Another study showed that the tSNARE syntaxin 6, was localized to the plasma membrane in neutrophils and interacted with the vSNARE SNAP-23, located on the gelatinase and specific granules. Upon neutrophil activation, SNAP-23 was translocated to the cell surface, colocalizing with syntaxin 6 (Martin-Martin *et al.*, 2000). This is in agreement with the known secretory characteristics of the MPO+ve and MPO-ve granules. Under normal circumstances, the azurophilic granules (MPO+ve) do not contribute significantly to extracellular release, whereas specific and gelatinase (MPO –ve) granules do and therefore may require high levels of VAMP2 on their membranes (Bainton, 1973). Since degranulation is inhibited during neutrophil apoptosis, it is feasible that part of the apoptotic process is to shut down membrane trafficking events so that receptors can no longer reach the cell surface. However, the shut down of the regulated secretory pathway alone would presumably not be sufficient to inhibit receptors synthesised *de novo* from reaching the cell surface. The first possible step at which the exocytic pathway could be inhibited during apoptosis would be from the ER to the *cis*-Golgi.

1.3.4 Proteins Involved in ER to Golgi Transport & Tethering Factors

Many of the studies on SNAREs have been performed in neuronal cell lines and tissues. However, the most information available to date on the so-called 'tethering proteins' come from studies of ER to Golgi transport in mammalian cell lines and yeast. In contrast to the well-known clathrin-coated vesicles that are involved in the endocytic pathway, coatomer (COP) coated vesicles shuttle between the ER and the Golgi (COPII) and intra-Golgi (COPI), where COPI is also implicated in retrograde trafficking and recycling of 'escaped' ER proteins (Barlowe *et al.*, 1994). In yeast, COPII subunits Sar1p, Sec23p/24p complex and Sec13p/31p complex bind sequentially to the ER resulting in the construction of a transport vesicle. Sar1p belongs to the Arf small GTPase family and is normally in the cytoplasm (Kuehn *et al.*, 1998). Sec12p, an integral membrane protein of the ER, recruits Sar1p-GDP to the ER membrane. Sec12p also functions as a guanine nucleotide exchange factor (GEF) (Barlowe & Schekman, 1993), thereby facilitating the exchange of GDP for GTP. In contrast, the disassembly, required for fusion, involves GTP hydrolysis activated by Sec23p (a GTPase-activating protein or GAP) (Kaiser & Ferro-Novick, 1998). Since many of the transport processes are highly conserved, a similar system is supposed to operate in the mammalian cell.

In mammalian cells, ER to Golgi SNAREs (rbet1, membrin, syntaxin 5) project into the cytoplasm (Allan *et al.*, 2000). Cytosolic, phosphorylated p115 (Sohda *et al.*, 1998) is complexed with the 3 SNAREs by the transient action of GTP bound Rab1 (Allan *et al.*, 2000). Rab1 is essential for p115 recruitment to budding COPII vesicles. Although, inhibition of Rab1 prevents p115 recruitment it does not inhibit COPII budding but vesicles can no longer fuse with the *cis*-Golgi (Wilson *et al.*, 1994). p115 was originally identified as an essential factor for intra-Golgi transport (Waters *et al.*, 1992) however, it was subsequently shown to be necessary for ER to Golgi transport for tethering vesicles to the Golgi matrix protein GM130 (Sonnichsen *et al.*, 1998). Before vesicles access the *cis*-Golgi, the intermediate compartment (IC) is formed, morphologically described as 'clusters of small vesicles or tubulovesicular elements' (Saraste & Kuismanen, 1984). Although, COPII is required for budding from the ER, it has been shown that during transit to the *cis*-Golgi the COPII vesicles shed their COPII coats and recruit COPI coats, where they undergo homotypic fusion to form the IC (Aridor *et al.*, 1995; Balch *et al.*, 1984; Beckers *et al.*, 1990; Hauri & Schweizer, 1992; Schweizer *et al.*, 1990). In a recent study, the IC was further compartmentalised into three stages: 1) tubular elements marked by

COPII, 2) tubular clusters marked by COPI and 3) tubular cluster marked by COPI juxtaposed to the *cis*-Golgi but containing *cis*-Golgi markers (including the p115 receptor GM130 and GRASP65) but not the *cis*-Golgi marker mannosidase I (Marra *et al.*, 2001). COPI coated vesicles of the middle IC, with giantin and p115 membrane bound, may then tether to the late IC *via* a p115 interaction with the Golgi matrix protein GM130. p115 may act as a 'bridge' between GM130 on the late IC and giantin, present on COPI vesicles (Lesa *et al.*, 2000). GM130 binds GRASP65, a structural *cis*-Golgi membrane protein, *via* it's extreme C-terminus (Barr *et al.*, 1998) and both proteins cycle between the late intermediate compartment and the *cis*-Golgi picking up giantin-p115 vesicles (Marra *et al.*, 2001). Giantin-p115-GM130-GRASP65 vesicles are then tethered to the *cis*-Golgi, in a step preceding SNARE complex formation bringing the appropriate NSF, SNAP, vSNAREs and tSNAREs proteins into close proximity, to promote the formation of the SNARE complex, which then drives membrane fusion (Cao *et al.*, 1998).

In addition to its role in the budding of COPII vesicles, Rab1 GTPase has also been shown to bind to GM130, implicating it in the later vesicle tethering stages of ER to Golgi transport (Weide *et al.*, 2001). However, further work is needed to elucidate the role of Rab1 at this step in ER to Golgi transport.

1.3.5 The Inhibition of ER to Golgi Transport During Mitosis

The Golgi complex is a juxtanuclear reticular structure, which in many cell types can be visualised by immunofluorescence microscopy during interphase. During mitosis however, the Golgi fragments and punctate immunofluorescence staining is seen dispersed throughout the cytoplasm of the dividing cell. During telophase, the Golgi starts to re-assemble and is equally divided between the two daughter cells (Hiller & Weber, 1982). In addition, it was shown that fragmentation of the Golgi complex occurs with a concomitant arrest in ER to Golgi and intra-Golgi transport (Featherstone *et al.*, 1985).

Two thirds of the fragmentation that occurs during mitosis, is thought to be due to what is known as the COPI-dependent pathway. The COPI-mediated fragmentation is linked to the mitotic inhibition of ER to Golgi and intra-Golgi transport (Misteli & Warren, 1995). The current view is that COPI vesicles accumulate in mitosis because they continue to bud, but no longer dock or fuse with their target membrane.

The other pathway, accounting for approximately a third of Golgi fragmentation is the so-called COPI-independent pathway (Misteli & Warren, 1995). Only recently have some of the underlying mechanisms of Golgi fragmentation during mitosis been discovered but the COPI-independent pathway remains poorly defined.

The transition from G2 to M phase is controlled by CDK1, which forms complexes with cyclins of the A and B families (Clarke & Karsenti, 1991). Golgi fragmentation had been thought to be dependent on the activity of CDK1 but identification of CDK1 substrates has only recently been reported (Levine *et al.*, 1996; Mackay *et al.*, 1993; Stuart *et al.*, 1993). Lowe et al. (1998) showed that GM130 a peripheral membrane protein, was phosphorylated during mitosis and this was later confirmed in subsequent studies (Draviam *et al.*, 2001; Lowe *et al.*, 2000). Phosphorylated GM130 was shown to have a reduced affinity for p115, potentially inhibiting docking of transport vesicles and therefore may contribute to Golgi fragmentation (see Fig. 1.6). Nevertheless, other events must also take place because inhibition of the GM130/p115 interaction was not sufficient to cause a complete halt in intracellular transport or total Golgi breakdown. Microinjection of GM130 N-terminal peptide, the p115 binding domain, or over expression of the N-terminal peptide, was shown to cause an increase in the number of COPI vesicles present in the cytoplasm and a reduced rate of intracellular transport. While this study provided support for a model of mitotic Golgi fragmentation in which the tethering complex is disrupted by phosphorylation of GM130, complete Golgi breakdown or complete inhibition of exocytosis did not occur suggesting that other mitotic events were occurring (Seemann *et al.*, 2000). A number of other proteins involved in vesicle trafficking show altered phosphorylation during the cell cycle. p115 was also found to be phosphorylated in a cell cycle-specific manner (Sohda *et al.*, 1998). During interphase, dephosphorylated p115 is Golgi-membrane associated and phosphorylated p115 is present in the cytosol, having been released from membranes by a phosphorylation step involving casein kinase II (CKII) or a CKII-like kinase (Dirac-Svejstrup *et al.*, 2000). However, during mitosis only the dephosphorylated GM130 binding form was present; although this interaction is blocked by GM130 phosphorylation. Further investigation should reveal the significance of cell-cycle dependent regulation of p115 (Sohda *et al.*, 1998). Interestingly, Rab1 was also shown to be phosphorylated during mitosis, however this did not impair the ability to bind GTP (Bailly *et al.*, 1991).

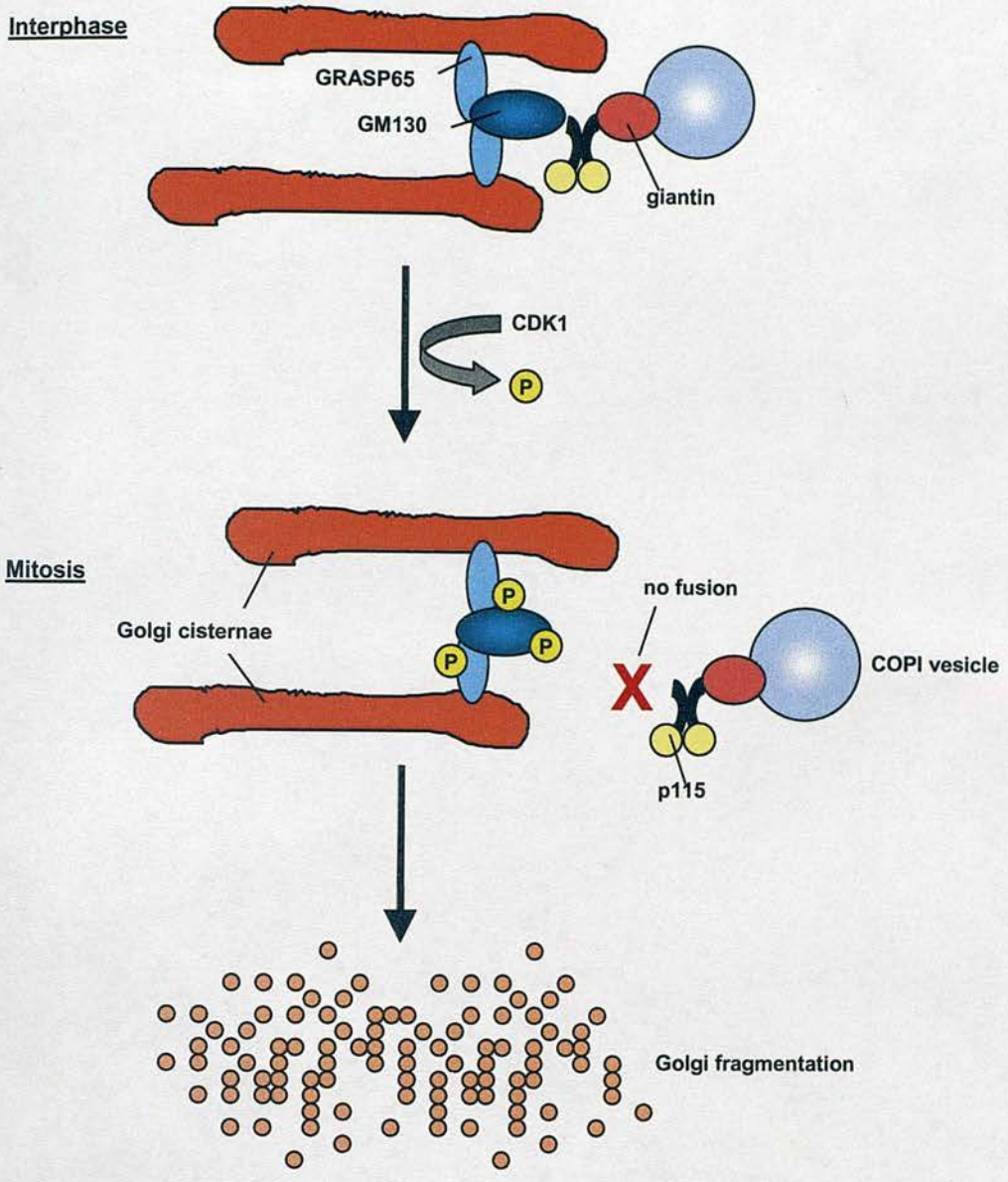

Figure 1.6: Protein interactions involved in tethering COPI vesicles to the *cis*-Golgi. During interphase, COPI coated vesicles move from the intermediate compartment towards the *cis*-Golgi. Giantin on the COPI vesicle, binds cytosolic phosphoryated p115 present as a homodimer. GM130, bound to the peripheral membrane protein GRASP65 acts as a receptor for the p115 molecule bound to the COPI vesicle. During mitosis, GRASP65 and GM130 become phosphorylated rendering GM130 unable to bind p115 and the Golgi fragments.

The GM130 interacting protein, GRASP65 is also phosphorylated during mitosis but can still interact with GM130 (Barr et al., 1997; Barr *et al.*, 1998). Both CDK1 and the mitotic kinase of the polo-like kinase (Plk) family have been implicated in the phosphorylation of GRASP65 although this does not result in the dissociation of the GRASP65-GM130 complex (Lin *et al.*, 2000; Sutterlin *et al.*, 2001). The functional significance of GRASP65 phosphorylation has therefore still to be determined. One possibility is that if multiple kinases and multiple substrates are involved in Golgi structure, the inhibition of any single substrate will not be sufficient to abrogate breakdown.

1.3.6 Mechanism of Golgi Fragmentation During Apoptosis

During mitosis cells fragment their Golgi complex into thousands of 50nm vesicles that are dispersed throughout the cytoplasm and equally divided between the two daughter cells (Lucocq *et al.*, 1988; Lucocq & Warren, 1987; Warren, 1989). Golgi fragmentation has also been shown to occur with a concomitant arrest of ER to Golgi, intra-Golgi and Golgi to plasma membrane protein transport (Barr *et al.*, 1998; Stuart *et al.*, 1993; Warren *et al.*, 1983). In addition to sharing morphological features with mitotic cells such as chromatin condensation, apoptotic cells also have dispersed vesicles throughout the cytoplasm (Chu-Wang I.W., 1978; Philpott *et al.*, 1996; Sheehan *et al.*, 1997; Watt *et al.*, 1994). Until very recently though, whether these vesicles were Golgi derived was not known and hence the question of whether Golgi fragmentation accompanied apoptosis also concomitantly with an arrest of membrane trafficking had not been addressed. Certainly, this would be one possible mechanism to explain the functional down-regulation of apoptotic neutrophils, by their inability to secrete cytokines or an inability to transport receptors to their cell surface.

During the course of this work, studies showing that the Golgi fragments during apoptosis have been published and some of the target membrane transport proteins affected have been identified in several cell types (Lane *et al.*, 2002; Mancini *et al.*, 2000; Sesso *et al.*, 1999). Golgi fragmentation during apoptosis was shown to be morphologically identical to Golgi fragmentation during mitosis by electron microscopy studies. In both cases, 50nm Golgi-associated vesicles are found throughout the cytoplasm (Sesso *et al.*, 1999; Warren *et al.*, 1995). Golgin-160 is a peripheral Golgi membrane-associated autoantigen. Golgin proteins, to which GM130 belongs, are a small group of Golgi associated proteins, which are targets for

autoantibodies in some autoimmune diseases (Eystathioy *et al.*, 2000). Golgin-160 was shown to be cleaved by caspase-2 (Mancini *et al.*, 2000). However, the precise role of Golgin-160 in membrane traffic is unknown and therefore it is difficult to extrapolate the full implications of this cleavage. Intuitively, the fact that Golgin-160 undergoes caspase-mediated proteolysis implies that it is a key protein involved in intra-Golgi trafficking or structure. However, GRASP65 was recently shown to be cleaved by caspase-3 in normal rat kidney (NRK) and HeLa cells during anisomycin and staurosporine induced apoptosis (Lane *et al.*, 2002). GRASP65 was shown to be cleaved once on the C-terminus region, distal from the GM130 binding region on the N-terminus. In cells stably expressing GRASP65, mutated in the caspase-3 cleavage region, Golgi fragmentation was shown to be inhibited, suggesting that GRASP65 plays an important role in maintaining Golgi structure (Lane *et al.*, 2002). GRASP65 is also a mitotic target and is phosphorylated by polo-like kinase and CDK1, therefore GRASP65 is a common target in mitosis as well as in apoptosis (Lin *et al.*, 2000). Further, GM130 was not cleaved and p115, which binds to GM130, were both found to be bound to Golgi membranes in apoptotic cells (Lane *et al.*, 2002).

1.4 Aims of Thesis

The principal aims of this thesis were to assess whether transport through the constitutive secretory pathway was inhibited during neutrophil apoptosis. While neutrophil granules are a major source of cell surface receptors, the constitutive secretory pathway also transports receptors to the cell surface. Therefore, an arrest of ER to Golgi transport during apoptosis would effectively prevent receptors synthesised *de novo* from reaching the cell surface, contributing to the environmental isolation of apoptotic neutrophils. Using the hypothesis that 'the constitutive secretory pathway is inhibited during apoptosis', the key issues to be addressed were:

- To investigate whether ER to Golgi transport is inhibited during apoptosis, using fragmentation of the Golgi complex as an indicator of arrest of membrane trafficking.

- To identify potential mechanisms of inhibition of ER to Golgi transport.

- To assess directly the progress of viral protein through the secretory pathway in apoptotic cells.

CHAPTER 2: MATERIALS & METHODS

2.1 Methods

2.1.1 Isolation of Human Peripheral Blood Neutrophils

Human neutrophils were isolated according to previously described methods (Haslett *et al.*, 1985). Venous blood (36 ml) was collected into 50 ml polypropylene tubes, each containing 4 ml of sterile 3.8% sodium citrate solution to prevent coagulation. Following collection of venous blood, all neutrophil isolation procedures were performed under sterile conditions. The tubes were gently inverted to mix the sodium citrate and blood, before centrifuging the tubes at $350g_{av}$ for 20 min at 20°C. Centrifugation results in two fractions: the upper layer is rich in plasma and platelets whilst the lower layer contains erythrocytes and leukocytes.

The upper platelet-rich plasma layer was removed for preparation of autologous serum and 15 ml mixed with 330 µl of $CaCl_2$ (final concentration 20 µM). The fraction containing erythrocytes and leukocytes suspended in 5 ml of pre-warmed to 37°C 6% dextran (2.5 ml T500 dextran/ 10 ml cells) and the volume adjusted to a total of 50 ml by the addition of 0.9% saline, also pre-warmed to 37°C. After 30 min at 20°C, leukocytes and erythrocytes had sedimented differentially into two layers. The upper layer containing leukocytes and the bottom layer containing erythrocytes.

The leukocyte-rich layer was subsequently removed from the sedimented erythrocytes, centrifuged at $235g_{av}$ for 6 min and then resuspended in 2.5 ml of 55% isotonic Percoll (9:1 v/v Percoll: 10 x PBS) in 1 x PBS without Ca^{2+}/ Mg^{2+}. Discontinuous Percoll gradients were prepared by overlaying 2.5 ml of 70% isotonic Percoll onto 2.5 ml of 81% isotonic Percoll in a 15 ml Falcon tube and the resuspended cell fraction overlayed to form the final layer of the gradient.

These gradients were centrifuged at 720g for 20 min at room temperature. Neutrophils were harvested from the 70%/ 81% interface. Cells were then washed 2 x in 1 x PBS without Ca^{2+}/ Mg^{2+}. Neutrophil yield was assessed by flow cytometry where typically ~98% of cells isolated were neutrophils (see Fig. 3.1).

2.1.2 Cell Culture

2.1.2.1 Neutrophils

Neutrophils were routinely suspended at a density of 2.5 x 10^6 cells/ ml in Iscoves's Dulbecco's Modified Eagle's Medium (DMEM) supplemented with 10% autologous serum and 50 U/ ml penicillin and 50 U/ ml streptomycin. Cells were cultured in flat-bottomed 96-well Falcon Flexiwell plates (Becton-Dickenson, UK) at 37°C in a humidified 5% CO_2 atmosphere.

2.1.2.2 Cell Lines

NRK and HeLa cells were routinely maintained in Minimal Essential Medium (MEM), COS-7 cells in DMEM and J.CaM1.6 cells in RPMI-1640 containing 10% FCS, 100U/ ml of penicillin/streptomycin, 2 mM L-glutamine, and 1% non-essential amino acids. Cells were grown in a 5% CO_2 humidified incubator at 37°C. J.CaM1.6 cells are a mutant derivative of Jurkat Human T cells, which constitutively express FasR.

2.1.2.3 Hybridomas

The hybridoma 1B2, raised against rat liver Golgi membranes (J.Pryde – unpublished results), was maintained in DMEM containing 20% FCS, 100U/ ml of penicillin/streptomycin, 2mM L-glutamine, and 1% non-essential amino acids in a 5% CO_2 humidified incubator at 37°C. Cell density was maintained between 5 x 10^5 and 8 x 10^5 cells/ ml. To harvest the monoclonal anti-Golgi antibody, cell density was allowed to increase to 2 x 10^5 cells/ ml, after which the supernatant was collected.

2.1.3 Induction of Apoptosis

NRK or HeLa cells grown on glass coverslips in a 6-well-plate were incubated in 2 ml serum-free DMEM containing 100U/ ml of penicillin/streptomycin per dish overnight. Apoptosis was induced by the addition of 2 µM staurosporine (SSP) solubilised in dimethyl sulphoxide (DMSO) for various time points and control cells were treated with <1% DMSO.

COS-7 cells were grown on glass coverslips in a 6-well-plate in 2 ml whole DMEM per dish. Cells were incubated overnight with 2-(4-morpholinyl)-S-phenyl-4H-1-benzopynan-4-one (LY294002) and apoptosis was induced by the addition of 2 μM SSP solubilised in DMSO for various time points and control cells were treated with <1% DMSO.

J.CaM1.6 cells were incubated in 96-well-plates at 2.5 x 10^6 cells/ ml in a total volume of 150 μl. Stock SSP (2mM in DMSO) and stock CH11 (5 μg/ ml) were diluted 1/ 100 in complete medium and further diluted 1/ 10 by adding 15 μl into the appropriate wells. Z-VAL-ALA-DL-Asp-fluoromethylketone (z-VAD-fmk, 100 μM) was added to appropriate wells in both SSP and CH11 (monoclonal antibody, 500 ng/ ml) assays and ZB4 (monoclonal antibody, 500 ng/ ml) was added to appropriate wells in CH11 assays.

2.1.4 Assessment of Apoptosis

2.1.4.1 Nuclear Morphology:

Nuclei were stained with Hoechst 33258 and examined by fluorescence microscopy. Apoptotic cells were identified by characteristic fragmented or 'pebbled' nuclei (Wyllie *et al.*, 1980) (Fig. 3.9C). In the case of neutrophils, apoptotic cells were defined as those containing one or more darkly stained pyknotic nuclei (see Fig. 3.4E).

2.1.4.2 Fractional DNA Content

DNA content of cells was assessed by flow cytometry, where cells with fragmented DNA can be identified by their location to the left of the G1 peak representing G1 cells (Bedner *et al.*, 1999). Cells were fixed and permeabilised in ice-cold 70% ethanol over 10 min and pelleted (200 g_{av}, 3 min, 4°C). The cell pellet was then washed 3 x in PBS without Ca^{2+}/ Mg^{2+} and were then incubated with 60 μl of 50 μg/ ml RNase A at 20°C for 30 min. Cells were subsequently stained with 1 mg/ ml propidium iodide (PI) for 25 min and covered in foil. Fractional DNA content was assessed by flow cytometry on a Coulter EPICS (Beckman Coulter (UK) Ltd) and analysed on associated EXPO software. All experiments were assessed in triplicate.

2.1.4.3 Annexin-V Binding

Apoptosis in J.CaM1.6 cells and neutrophils was also assessed by flow cytometry. Externalisation of phosphatidylserine was monitored by FITC-labelled recombinant human Annexin-V binding. Stock Annexin-V-FITC was diluted 1/ 3000 with Annexin-V binding buffer (500 ml Hanks Balanced Salt Solution containing 5 μM $CaCl_2$). 20 μl of cells (5 x 10^6 cells/ ml) were added to 280 μl of the diluted Annexin-V-FITC solution and incubated on ice for 10 min. Annexin-V binding was assessed by flow cytometry on a Coulter EPICS (Beckman Coulter (UK) Ltd) and analysed on associated EXPO software. All experiments were assessed in triplicate.

Alternatively, adherent cell lines grown on glass coverslips, were inverted onto 100 μl of Annexin-V-Alexa 488 (green), diluted 1/ 200 with Annexin-V binding buffer containing 2 μg/ ml Hoechst 33258 to stain the nuclei. Cells were incubated at room temperature for 15 min before samples were fixed with 3% (w/v) PFA in PBS and mounted with Moviol*.

2.1.5 Indirect Immunofluorescence

The indirect immunofluorescence protocol was adapted from the method of (Ash *et al.*, 1977). Cells were grown on 1.5 x 22 x 22-mm glass coverslips in a 6-well Greiner dish or non-adherent cells were cytocentrifuged (300rpm for 3 min) onto 1.5 x 22 x 22-mm glass coverslips and fixed in methanol-free 3% (w/v) PFA/ PBS containing 1mM $CaCl_2$ and 1mM $MgCl_2$ for 20 min at 20°C. All subsequent steps were carried out at room temperature. The aldehyde groups were then quenched with 50 mM NH_4Cl for 10 min. If required, cells were permeabilised with 0.1% (w/v) Triton X-100 and non-specific binding blocked with 10% (v/v) sheep serum (SS) in 0.2% (w/v) fish skin gelatin (FSG). To apply the antibodies to the cells, the coverslips were drained on Whatmann 3mm filter paper and inverted onto a 100 μl drop of antibody diluted in 10% (v/v) SS/ 0.2% (w/v) FSG, placed on a sheet of parafilm. Primary antibodies used were: Rabbit anti-active-caspase-3 rabbit polyclonal antibody 1/ 3000. Mouse anti-rat GM130 monoclonal antibody (stock solution 250 μg/ ml diluted 1/ 200). Mouse anti-rat p115 monoclonal antibody (stock solution 250 μg/ ml diluted 1/ 200).

Rabbit anti-human Bax polyclonal antibody (stock solution 1 mg/ ml diluted 1/ 200). Mouse anti-Bax monoclonal antibody (mouse ascites fluid diluted 1/ 200). Mouse anti-Golgi (1B2) monoclonal antibody neat supernatant from hybridoma culture. Rabbit anti-Golgi (JPR3) polyclonal antibody 1/ 200 (Pryde, 1994). Mouse anti-human MPM2 monoclonal antibody (stock solution 1 mg/ ml diluted 1/ 500). The slides were incubated with the secondary antibodies Alexa™ 488 (green) goat anti-mouse IgG (highly cross-adsorbed) and Alexa™ 568 (red) goat anti-rabbit (highly cross-adsorbed), (stock solutions 2 mg/ ml diluted 1/ 400) for 20 min and washed three times in PBS. Nuclei were stained with 2 µg/ ml Hoechst 33258 for 10 min for fluorescence microscopy or with 1 µM TO-PRO3 for 45 min for confocal microscopy. For confocal microscopy the cells were immediately rinsed in dH_2O following incubation with TO-PRO-3, drained on filter paper and inverted onto a drop of Moviol* on a glass slide. Cells stained with Hoechst 33258 were further washed 3 x in PBS, rinsed in dH_2O and mounted in Moviol*.

*Moviol: 6g of analytical grade glycerol, 2.4g of Moviol 4-88 (Hoechst), add 6 ml of water and leave solution for 2 h at room temperature. Add 12 ml of 0.2 M Tris-HCl pH 8.5 and incubate solution at 50°C for 10 min with occasional stirring to dissolve the Moviol. The mixture is clarified by centrifugation at 5000 g_{av} for 15 min.

2.1.5.1 Immunofluorescence Staining of VSVG

The monoclonal antibody clone 8G5 was shown to only stain the correctly folded VSVGts045. In contrast the monoclonal antibody raised against VSVGts045, clone P5D4 recognised both the misfolded and correctly folded (32°C) VSVGts045 (Fig. 2.1). To ensure that VSVGts045 was labelled a mixture of both antibodies was used in subsequent experiments. Both antibodies were used at a working dilution of 1/200 (P5D4 mouse ascites fluid, 8G5 stock solution 1 mg/ ml).

2.1.6 Microscopy

For fluorescence microscopy, cells were observed using a x63 oil immersion objective lens on a Zeiss Axiovert S100. Images were captured using a colour CoolSNAP camera (Zeiss) and Openlab 3.0 (Zeiss) software. Images were then digitally processed using Adobe Photoshop 5.02 and Paint Shop Pro 5.

For confocal microscopy cells were observed using an x63 oil immersion objective lens on a Leica TCS NT confocal laser scanning microscope system (Heidelberg, GMBH). Single optical sections of the images captured with Leica TCS software were digitally processed using Adobe Photoshop 5.02 and Paint Shop Pro 5.

2.1.7 Statistical Analysis

Results are reported either as pooled data from a series of n separate experiments (mean ± S.E.M) or as individual representative experiments (mean ± S.E.M., each slide counted 3 x/ condition or 3 replicates/ condition). Statistical significance was assessed by one-way analysis of variance with comparisons between groups made using the Tukey procedure.

2.1.8 Preparation of Samples for EM

HeLa cells were treated with 2μM SSP for 5 h in 75cm^2 tissue culture flasks and then fixed in 0.5% (v/v) –glutaraldehyde-200mM PIPES [piperazine-N,N'-bis(2-ethanesulfonic acid)]-KOH, pH 7 for 1 hour and stored in PBS. All subsequent procedures were carried out by J. Lucocq, The University of Dundee, U.K. Cells were then scraped from 75 cm^2 tissue culture flasks and centrifuged at 13,000g_{av} for 15 min. Pellets were cryoprotected by infusion with 2.1M sucrose and frozen in liquid nitrogen and ultrathin cryosections were prepared and immunolabelled with the monoclonal antibody raised against n-acetyl-glucosaminyl-transferase-1, a resident Golgi enzyme, followed by protein-A-gold. For quantitative methods see Pryde *et al.* (1998).

2.1.9 Transport Assay in Transfected COS-7 cells

COS-7 cells (5 x 10^6 cells/ ml) were transiently transfected with the mammalian expression vector JC119/ ts045 by double pulse (750 V, 25 μF and 100V, 1500 μF) on the EasyJect Electroporator (Flowgen, Leicestershire, UK). Following electroporation, cells were immediately transferred to whole DMEM, pre-warmed to 37°C and incubated at 37°C for 12 h to allow the cells to adhere. Cells were then

washed 2 x in PBS without Ca^{2+}/ Mg^{2+} to remove dead cells and trypsinised. The cells were then counted and the % cell survival was typically 40-50%. The remaining cells were subsequently grown on 1.5 x 22 x 22-mm glass coverslips in a 6-well Greiner dish, containing 2 ml of whole DMEM and left overnight. The medium was then replaced with serum-free DMEM containing 100U/ ml of penicillin/streptomycin and 20 μM LY294002 and returned to 37°C. Cells were subsequently shifted to the restrictive temperature (40°C) 12 h prior to the induction of apoptosis to allow an accumulation of VSVGts045 in the ER.

2 μM SSP was added to the appropriate wells and the cells incubated for 8 h at 40°C. 30 min prior to shifting to the permissive temperature of 32°C, 50 μg/ ml CHX was added to halt further translation of VSVG and 100 μM z-VAD-fmk to prevent progression of apoptosis during the transport of VSVGts045 to the cell surface. The cells were then shifted to the permissive temperature (32°C) for 2 h to allow progression of VSVGts045 to the cell surface. Cells were then immediately fixed and immunofluorescently labelled for confocal microscopy as described above.

2.1.10 Western Blotting

2.1.10.1 Western Blotting for GM130

Detection of GM130, a 130kDa peripheral Golgi membrane protein, required that adjustments were made to the standard method of sample preparation to optimise detection by western blotting in J.CaM1.6 cells. Various different lysis buffers were tested:

1) Standard Lysis Buffer: 10 mM Tris-HCl pH 6.8, 1% (w/ v) NP-40, 1% (w/ v) deoxycholate, 1/ 5000 protease inhibitor cocktail (87 mg phenylmethylsufonyl fluoride, 160 mg benzamidine, 10 mg leupeptin and aprotinin, 5 mg of bestatin, antipain, chymostatin and pepstating A solubilised in 1 ml DMSO).

2) Standard Lysis Buffer containing 1% SDS: 10 mM Tris-HCl pH 6.8, 1% (w/ v) NP-40, 1% (w/ v) deoxycholate, 1% (w/ v) SDS, 1/ 5000 protease inhibitor cocktail.

3) Immunoprecipitation buffer: 50 mM Tris-HCl pH 8, 0.4M NaCl, 1% (w/ v) deoxycholate, 1% (w/ v) NP40, 5 mM EDTA, 1/ 5000 protease inhibitor cocktail.

60 µl of lysis buffer was added to the cell pellet (either 2.5 x 10^6 cells or 5 x 10^6 cells), pre-washed in ice-cold PBS containing 1/ 5000 protease inhibitor cocktail and incubated on ice for 10 min. Samples were then centrifuged at 18,000 g_{av} for 3 min and the post-nuclear supernatant added directly to pre-heated (95°C) sample buffer. Figure 2.2 shows the efficiency of GM130 extraction using the different lysis methods. The lysis buffer containing 10 mM Tris-HCl pH 6.8, 1% (w/v) NP-40, 1% (w/ v) deoxycholate, 1% (w/ v) SDS 1/ 5000 protease inhibitor cocktail was the most efficient lysis buffer for the extraction of GM130 from J.CaM1.6 cells and 2.5 x 10^6 cells/ sample were adequate for it's detection (Fig. 2.2, lanes 3 & 4).

2.1.10.2 Sample Preparation

Proteins analysed by western blot were: procaspase-3, GM130, p115 and actin. The standard lysis buffer containing 1% (w/v) SDS was efficient at extracting all proteins of interest and was therefore used as standard in all subsequent experiments.

J.CaM1.6 cells were harvested, put into pre-chilled eppendorfs and pelleted (100 g_{av}, 5 min, 4°C) and washed 1 x in ice-cold PBS without Ca^{2+}/ Mg^{2+} containing a 1/ 5000 dilution of protease inhibitor cocktail and incubated on ice for 30 min. Cells were pelleted again and resuspended in 60µl lysis buffer (10mM Tris-HCl, 1% (w/ v) SDS, 1% (w/ v) NP-40, 1% (w/ v) deoxycholate and incubated on ice for 10 min before being centrifuged (18,000 g_{av}, 3 min, 4°C) to pellet the nuclei. Post-nuclear supernatants were then transferred to eppendorfs containing 2 x pre-heated (95°C) sample buffer (4 x sample buffer is 1 M Tris-HCl pH 6.8, 10% (w/ v) SDS, 40% (w/ v) glycerol, 5µM DTT and 0.01% (w/ v) bromophenol blue) and heated at 95°C for 3 min. Samples were then cooled and 10 mM iodoacetamide added prior to centrifuging (20,000 g_{av}, 1 min, 20°C).

2.1.10.3 Protein Separation By Polyacrylamide Gel Elecrophoresis (PAGE)

Proteins were separated on polyacrylamide gels (Laemmli, 1970) (1 M Tris-HCl pH 8.8, 8% acrylamide) and the stacking gel used was 50 mM Tris-HCl pH 6.8 with 4%

(w/ v) acrylamide. Samples were then resolved on gels, 16 x 20 cm plates, 1 mm thick (Bio-Rad Protean II) overnight at 62V and electrophoreticallly transferred to nitrocellulose at a constant current of 0.85 mA for 90 min at 4°C alongside molecular weight markers. The transfer buffer used was 50 mM Tris-HCl, 0.4 M glycine and 20% (v/v) methanol (Towbin *et al.*, 1979). To check protein transfer the nitrocellulose was stained with Ponceau S. Non-specific protein binding sites on the nitrocellulose membrane were blocked by incubation of the membranes in blocking buffer (Tris Buffered Saline (TBS) is 20 mMTris-HCl pH 7.4, 15 mM NaCl containing 5% (w/ v) casein) for one hour at 37°C. The blots were probed with mouse monoclonal antibodies to procaspase-3 (stock solution 250 mg/ ml diluted 1/ 1000), GM130 (stock solution 250 µg/ ml diluted 1/ 500), p115 (stock solution 250 µg/ ml diluted 1/ 500) and actin (ascites fluid diluted 1/ 5000) for 90 min at 20°C with constant shaking. This was followed by 3 sequential washes (5 min, 20°C) in TBS buffer. Membranes were then incubated with the horse-radish peroxidase (HRP)-conjugated secondary antibody HRP-Goat anti mouse IgG diluted 1/ 10,000 in blocking buffer for one hour at room temperature with gentle shaking. Membranes were washed a further 3 times with Tris Buffered Saline (TBS is 20 mM Tris-HCl pH 7.4, 15 mM NaCl) before 1 min incubation with ECL reagent. The membrane was placed under BioMax MS-1 X-ray sensitive film and processed through an X-ray developer (X-Ograph Imaging Systems, Wilts, U.K.) with a typical exposure time of 5, 10 or 20 min.

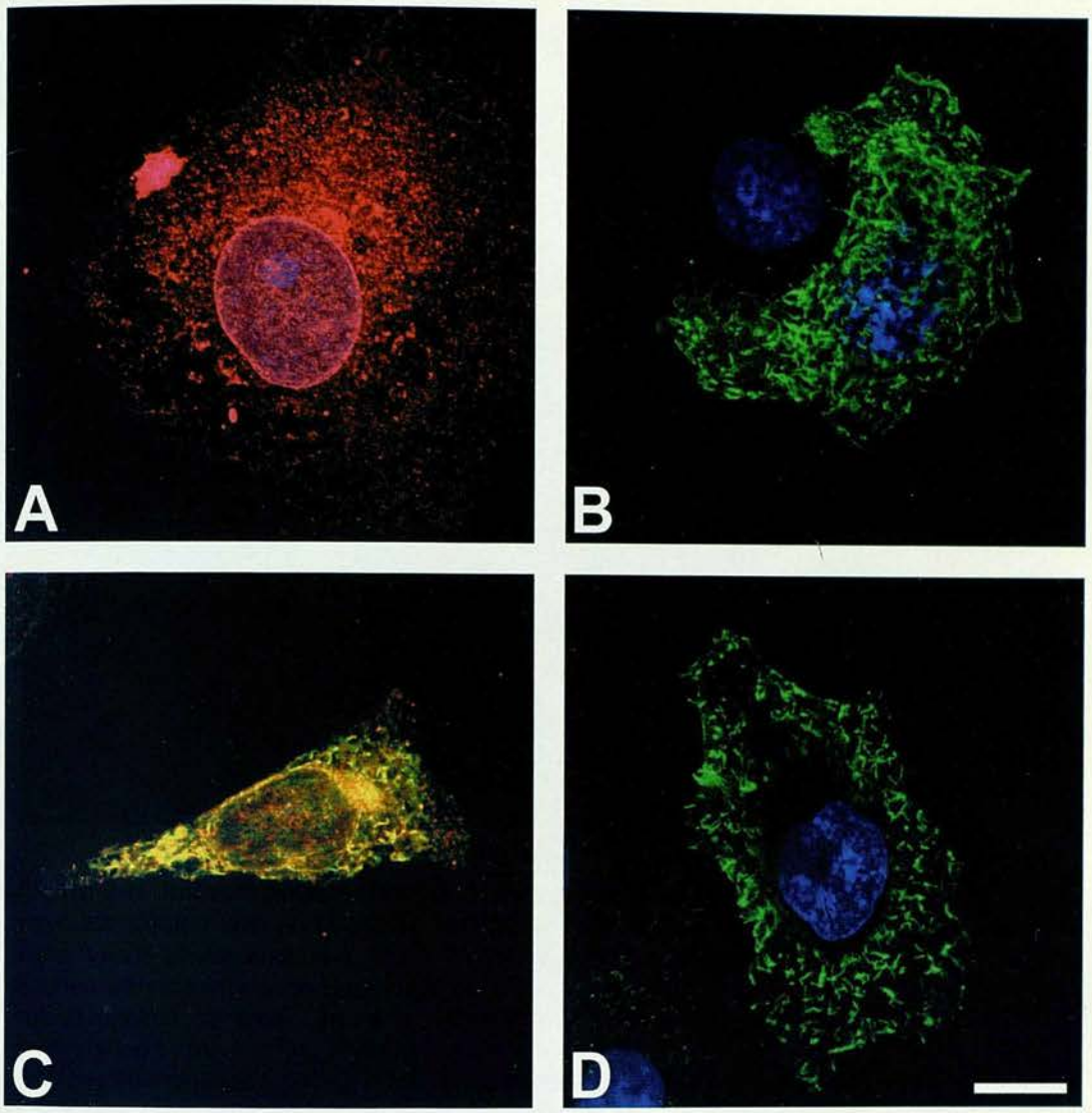

Figure 2.1: Indirect Immunofluorescence staining of VSVGts045 in COS-7 cells. Cells were transfected with JC119/ts045 and held at the restrictive temperature for 12 hours to allow VSVG to accumulate in the ER. (A) cells held at the restrictive temperature (40°C), stained with the monoclonal antibody 8G5. Only the ER (red) was stained with an antibody raised against calnexin. There is no detectable VSVGts045 staining (green). (B) COS-7 cells shifted to the permissive temperature where VSVGts045 is detected on the cell surface with the 8G5 antibody. (C) JC119/ ts045 transfected cell held at the restrictive temperature (40°C), stained with the monoclonal antibody P5D4. VSVGts045 was detected and co-localised (yellow staining) with the ER. In addition, this antibody also detected the properly folded VSVGts045 detected on the cell surface after incubation at the permissive temperature (D). Data are representative of 2 separate experiments. Scalebar represents 10μm.

Lysis Buffer	+ve	1	1	2	2	3	3
GM130 130kDa	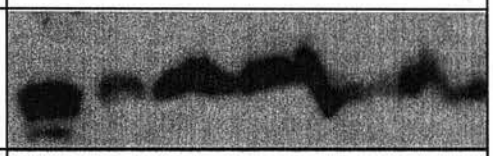						
Lane	1	2	3	4	5	6	7

Figure 2.2: Optimisation of lysis buffer used to extract GM130 from J.CaM1.6 cells for western blotting. Lane 1: positive control. Lane 2: Standard Lysis Buffer, 2.5 x 10^6 cells. Lane 3: Standard Lysis Buffer, 5 x 10^6 cells. Lane 4: Standard Lysis Buffer + 1% SDS, 2.5 x 10^6 cells. Lane 5: Standard Lysis Buffer + 1% SDS, 5 x 10^6 cells. Lane 6: immunoprecipitation buffer, 2.5 x 10^6 cells. Lane 7: immunoprecipitation buffer, 5 x 10^6 cells. Data are representative of 2 experiments.

2.1.11 Molecular Biology Methods

2.1.11.1 Agarose Gels

DNA was typically run on a TBE (90 mM Tris-borate, 2 mM EDTA) agarose gel, with an agarose percentage ranging from 0.7% to 1% (w/ v) depending on the size of DNA fragments to be resolved.

2.1.11.2 Sub-cloning of VSVGts045

pcDNA3 was linearised with the restriction enzyme XhoI in the buffer supplied by the manufacturer (Promega, UK) and run on a 1% (w/ v) agarose gel. Cut pcDNA3 was then gel purified and treated with shrimp alkaline phosphatase (SAP) according to the manufacters instructions to prevent self-ligation of the vector.

JC119/ ts045 was digested with XhoI and the 1.7 Kb insert gel purified using the QIAEX II Kit (Qiagen, UK). Ligation reactions were carried out with various ratios (1:3, 1:5, 1:7, 1:10) of SAP treated pcDNA3 and 1.7 Kb ts045 were then incubated with T4 DNA ligase, in the buffer supplied, at 16°C overnight.

2.1.11.3 Transformation of Competent Bacterial Cells

50 µl of *E.coli* DH5α cells (Gibco, UK) were mixed with 3 µl of ligation reaction in pre-chilled eppendorfs and left on ice for 30 min. The cells were heat-shocked for 35 sec at 45°C and further incubated on ice for 2 min. The cells were then incubated in 400 µl of S.O.C. medium for 60 min at 37°C before being plated onto Lauria Broth (LB) Agar containing 50 µg/ ml ampicillin. The cells were incubated overnight at 37°C.

2.1.11.4 Screening of Transformed Cells for pcDNA3/ VSVGts045

Transformed cells were picked and grown overnight in 5 ml of LB containing 50 µg/ ml ampicillin at 37°C. Plasmid purification was carried out using the Mini-Prep DNA Purification Kit (Promega, UK) and initially, the DNA digested either with XhoI to screen for clones containing the pcDNA3/ ts045 or EcoRV to check the orientation of the 1.7Kb ts045. Subsequent double digests were performed with XbaI and NotI to ensure that the 1.7Kb ts045 had inserted as a single copy into pcDNA3.

2.1.11.5 Transfections

Cells were transiently transfected with VSVGts045 in the expression vectors JC119 or pcDNA3 by electroporation using either single pulse at 400 V, 25 µF or double pulsed at 750 V, 25 µF and 100 V, 1500 µF on the EasyJect Electroporator (Flowgen, Leicestershire, UK) according to the manufacturers instructions. Cells were initially transfected in phosphate buffered sucrose (272 mM sucrose, 7 mM sodium phosphate pH 7.4, 1 mM $MgCl_2$). To optimise transfection efficiencies, the transfection buffer used was 50 mM Glutathione, 200 mM ATP in Hank's Balanced Salt Solution, based on the recommended transfection buffer by the manufacturers: OptiMix™ (Flowgen, Leicestershire, UK).

5 x 10^6 cells were pelleted and resuspended in 800 µl transfection buffer containing 20 µg of expression vector/ VSVGts045 DNA and immediately transferred to GenePulser electroporation cuvettes (0.4 mm gap, Bio-Rad). Cells were then electroporated at the voltages and number of pulses indicated (see Chapter 5) and immediately transferred to a 75 cm^2 tissue culture flask, containing pre-warmed (37°C) whole DMEM. Cells were then left for 12 h before the dead cells were rinsed off with PBS (Ca^{2+}, Mg^{2+} free) and then trypsinised and transferred to 6-well-plates containing glass coverslips. Cells were then left for a further 36 h to allow for maximal protein expression before cells were fixed with 3% (w/ v) PFA in PBS and stained by indirect immunofluorescence.

Transfection efficiency was estimated by counting 100 cells, stained with the monoclonal antibodies P4D5 and 8G5 raised against VSVG protein.

2.2 Materials

Amersham Pharmacia Biotech, UK Ltd (Buckinghamshire, UK): Hybond C nitrocellulose membrane.

Bachem (Saffron Walden, UK): z-Val-Ala-DL-Asp-fluoromethylketone (z-VAD-fmk) dissolved in DMSO and stored at –20°C at a stock concentration of 100mM.

Bender MedSystems, (Vienna, Austria): Fluorescein isothianate (FITC)-labelled recombinant human Annexin-V.

Bio-Rad (UK): GenePulser cuvettes (0.4cm gap).

Boehringer Corporation (UK): Triton X-100.

Calbiochem Novabiochem Ltd (Nottingham, UK): Staurosporine (dissolved in DMSO at 2mM and stored at 4°C).

European Collection of Animal Cell Cultures (Porton Down, UK): COS-7. HEK-293. HeLa. J.CaM1.6. NRK. Spinner HeLa.

Gibco Life Technologies (Paisley, UK): Heat-inactivated Fetal Calf Serum. RPMI-140. L-Glutamine. Penicillin (50 U/ ml). Streptomycin (50 U/ ml). 1M Hepes (tissue culture grade). Non-essential amino acids. Trypsin/EDTA. Competent *Escherichia coli* DH5α.

Hoechst (Frankfurt, Germany): Moviol 4-88.

Invitrogen (UK): Mammalian expression vector pcDNA3.

Molecular Probes (Netherlands): Hoescht 33258. Propidium Iodide. Annexin-V-Alexa 488 (green).

MWG-Biotech AG (UK): Oligonucleotides for sequencing: 5'-TTG TTG ATG AAT ACA CAG GAG A-3', 5'-TTG AGA GGA TCT ATT ATT C-3', 5'-ATC TTC ATC TTA GCT CAA AGG C-3'.

Promega (UK): Restriction enzymes (BamHI, EcoRI, EcoRV, KpnI, HindIII, NotI, SmaI, XbaI, XhoI). T4 DNA Ligase. BenchTop 1kb DNA Ladder. Wizard® *Plus* SV Minipreps DNA Purification System

Qiagen (UK): Endotoxin-Free MaxiPrep. SuperFect™.

Roche (UK): FuGene™6. Shrimp Alkaline Phosphatase (SAP).

Scottish Antibody Production Unit: Sheep serum.

Sigma (UK): Ampicillin. Cycloheximide (dissolved in DMSO at 20mM). Dimethyl sulphoxide (DMSO). Dithiothreitol (DTT). Dulbecco's Phosphate buffered saline (PBS) sterile, endotoxin-free, pH7.4. Dulbecco's Minimal Essential Medium (DMEM). Ethidium bromide. Sodium azide. Kodak BioMax Film. Methanol-free paraformaldehyde. Minimal Essential Medium (MEM).

Sykem (UK): Agarose.

JC119/ ts045 was a kind gift from J.Rose, Yale University.

All other chemicals were of molecular, reagent or cell culture grade and were obtained from **BDH (Leicestershire, UK)**.

2.2.1 Antibodies

Idun Pharmaceuticals (USA):	Rabbit anti-active-caspase-3 polyclonal antibody (clone CM1).
Molecular Probes (Netherlands):	Goat anti-mouse IgG antibodies Alexa™ 488 (Green) (Highly Cross Adsorbed). Goat anti-rabbit IgG antibodies Alexa™ 568 (Red) (Highly Cross Adsorbed).
PharMingen (Europe):	Mouse anti-human procaspase-3 monoclonal antibody (clone 19).
Sigma (UK):	Mouse anti-VSV Glycoprotein (clone P5D4)

	monoclonal antibody.
	Mouse anti-β-actin monoclonal antibody (clone AC-74).
TCS Biologicals (UK):	Mouse anti-human FasR (clone CH11) monoclonal antibody.
	Mouse anti-human FasR (clone ZB4) monoclonal antibody.
	Mouse anti-human MPM-2 monoclonal antibody.
	Mouse mitochondrial heat shock protein 70 (mtHSP70) monoclonal antibody (clone JG1).
	Rabbit anti-human Bax polyclonal antibody.
Transduction Laboratories (San Diego, USA):	Mouse anti-rat GM130 (clone 35) monoclonal antibody.
	Mouse anti-rat p115 (clone 46) monoclonal antibody.
Leo Lefransçois, University of Connecticut Health Center Graduate School, USA.	Hybridoma clone 8G3 (VSVG)
Brian Burke, University of Calgary, Canada.	Polyclonal rabbit calnexin polyclonal antibody
	Mouse VSV Glycoprotein (clone VG1) monoclonal antibody
James G. Pryde, The University of Edinburgh, UK.	Hybridoma clone 1B2 (Golgi)
Herman Schagger, University of Frankfurt-am-Main	Rabbit polyclonal anti-ubiquinol-cytochrome c oxidoreductase (complex III)
Ian Dransfield, The University of Edinburgh, UK.	Monoclonal antibody BOB78

CHAPTER 3: GOLGI MORPHOLOGY DURING APOPTOSIS

3.1 Introduction

Morphologically, the Golgi apparatus is organised juxtanuclearly in a series of stacks of flattened discs linked by filamentous structures in interphase cells. Proteolysis of Golgi stacks in cell-free studies leads to the disorganisation of the flattened discs, giving rise to single cisternae (Cluett & Brown, 1992). This finding suggested that these connecting filamentous structures were proteinaceous and were required for stacking of the Golgi cisternae (Cluett & Brown, 1992), leading to the idea of the intercisternal Golgi matrix; a group of proteins involved in interconnecting the Golgi cisternae. Reassembly of mitotic Golgi membranes in cell-free experiments, required NSF, SNAPs, p115 and p97 to give rise to single cisternae (Rabouille *et al.*, 1995). However, for the stacking of cisternae, GRASP65, GRASP55, giantin and GM130 are required (Barr *et al.*, 1997; Shorter *et al.*, 1999; Shorter & Warren, 1999). Therefore, the main candidates involved primarily in stacking of single Golgi cisternae are GRASP65, GRASP55, giantin and GM130.

During mitosis, the Golgi complex fragments into thousands of ~50nm vesicles dispersed throughout the cytoplasm of the cell with a concomittant inhibition of ER to Golgi transport and intra-Golgi transport (Lucocq *et al.*, 1988; Lucocq & Warren, 1987; Mackay *et al.*, 1993; Stuart *et al.*, 1993; Warren *et al.*, 1983). Golgi fragmentation also occurs when cells are treated with nocodazole, okadaic acid, brefeldin A and ilimaquinone (Lowe *et al.*, 2000). In the case of nocodazole, Golgi fragmentation ocurs without a concomittant arrest of ER to Golgi transport. However, Golgi fragmentation occurred without phosphorylation of GM130 by CDK1 in nocodazole, okadaic acid or ilimaquinone treated cells, as occurs during mitosis (Lowe *et al.*, 2002). Therefore, these models of Golgi fragmentation have no known physiological relevance. Recently, it was shown that the Golgi also fragments during apoptosis, in a manner that is morphologically similar to fragmentation during mitosis (Sesso *et al.*, 1999). It is therefore tempting to hypothesise that the mitotic targets of key Golgi proteins may also be targets during apoptosis.

Golgi fragmentation during mitosis is CDK1 dependent. Interestingly, there have been numerous reports recently showing acitivation of CDKs during apoptosis (Choi

et al., 1999; Hakem *et al.*, 1999; Jin *et al.*, 2000; Kim *et al.*, 2001; Schroter *et al.*, 1996; Shi *et al.*, 1994; Zhou *et al.*, 1998). Inhibitors of CDKs were shown to reduce DNA fragmentation in many models of cell death. Activation of CDK2 during apoptosis was shown to be caspase-dependent in HeLa cells treated with a variety of death inducing stimuli. Inhibition of CDK2 activity was shown to affect chromatin condensation, cell shrinkage and loss of adhesion, features that are also common to mitosis (Harvey *et al.*, 2000). Interestingly, the CDK1 regulatory kinase Wee1 has been shown to be cleaved by caspases –3, -7 and –8 in apoptotic Jurkat cells, while cdc25 was not affected (Zhou *et al.*, 1998). Wee1 phosphorylates threonine 14 and tyrosine 15 on CDK, thereby inhibiting CDK1 activity. Removal of those phosphates by the phosphatase cdc25, results in activation of CDK1 (Obaya & Sedivy, 2002). Also shown in this study was that total CDK1 and CDK2 levels remained constant but there was a dramatic decrease in phosphorylation at tyrosine 15 argueing against the need for *de novo* protein synthesis. However, the MPM-2 antibody, a monoclonal antibody reacting specifically with over 40 mitotic phosphorylated proteins (Westendorf *et al.*, 1994), did not react with apoptotic cells, suggesting that the widespread phosphorylation of mitotic substrates did not occur. Nevertheless, it is possible that potential substrates include those contributing to the morphological similarities between mitosis and apoptosis, one of which may be the fragmentation of the Golgi complex.

Neutrophils have been shown to become environmentally isolated during apoptosis, failing to respond to inflammatory stimuli (Whyte *et al.*, 1993). One mechanism that may account for this environmental isolation is an inhibition of the secretory pathway, where receptors would fail to reach the cell surface. During mitosis, an inhibition of ER to Golgi transport is known to coincide with the fragmentation of the Golgi complex into thousands of ~50nm vesicles dispersed throughout the cytoplasm of the cell (Lucocq *et al.*, 1988). Therefore, Golgi fragmentation during apoptosis may reflect inhibition of the secretory pathway. No studies to date have looked at Golgi morphology in the neutrophil. However, by EM the Golgi can be seen in neutrophils as a relatively small juxtanuclear structure (J.Pryde – unpublished). Golgi morphology may easily be visualised by immunofluorescence and therefore the fate of the Golgi complex was followed during apoptosis using this technique.

3.2 Results

3.2.1 Induction of Neutrophil Apoptosis by the Activity of Anti-FasR (CH11)

Neutrophils were isolated from whole blood and were typically >95% pure as assessed by forward and side scatter flow cytometry profiles (Fig. 3.1). To induce apoptosis, neutrophils were treated with CH11 (500ng/ ml) (Iwai *et al.*, 1994) for 4 h and apoptosis assessed by Annexin-V-FITC binding. Only 1.8% of neutrophils were apoptotic in untreated samples (Fig. 3.2 A&B) compared to 29.9% of CH11 treated cells (Fig. 3.2 C&D). Apoptosis was also assessed by DNA content using PI staining (Bedner *et al.*, 1999). Again, there was a low number (2.9%, Fig. 3.3A&B) of apoptotic cells in untreated samples and 32.3% apoptotic cells (Fig. 3.3C&D) in CH11 treated cells, as is characteristically shown in Fig. 3.3, by the sub-G1 peak to the left of the G1 peak.

3.2.2 Indirect Immunofluorescence Staining of Bax in Neutrophils

In addition to inducing apoptosis in neutrophils by a direct receptor-mediated pathway, neutrophils were also treated with 20μg/ ml cycloheximide (CHX), a protein synthesis inhibitor, to induce apoptosis by the stress-mediated pathway (Ward *et al.*, 1999a). To find a marker of apoptosis by immunofluorescence, neutrophils were stained with a polyclonal antibody raised against Bax. Since Bax has been reported to translocate from the cytoplasm to the mitochondria during apoptosis (Goping *et al.*, 1998; Murphy *et al.*, 1999; Narita *et al.*, 1998; Pryde *et al.*, 2000), mitochondria were stained with a monoclonal antibody raised against the mitochondrial heat shock protein 70 (mtHSP70).

Freshly isolated neutrophils showed little non-specific fluorescence when stained with secondary antibodies only (Fig. 3.4A) or with non-specific mouse and rabbit IgG and followed by secondary antibodies (Fig. 3.4B). Bax and mtHSP70 were not detected in freshly isolated neutrophils (Fig. 3.4C). However, in CHX treated cells with classical apoptotic nuclear morphology, large structures were shown to be aggregated in the cytoplasm in neutrophils stained with antibodies to mitochondria (Fig. 3.4D) and Bax (Fig. 3.4E). When these photomicrographs were merged, many

of these large structures were shown to co-localise (Fig. 3.4F, yellow), but some Bax clusters were present where there was no detectable mitochondrial staining. Clusters of mitochondria and Bax were all closely associated with nuclei (Fig. 3.4D-F) and interestingly, when mitochondrial clustering was inhibited by z-VAD-fmk (Fig. 3.4G), not only did Bax still cluster but translocation was still to the same cellular location, in close association with the nuclei (Fig. 3.4H).

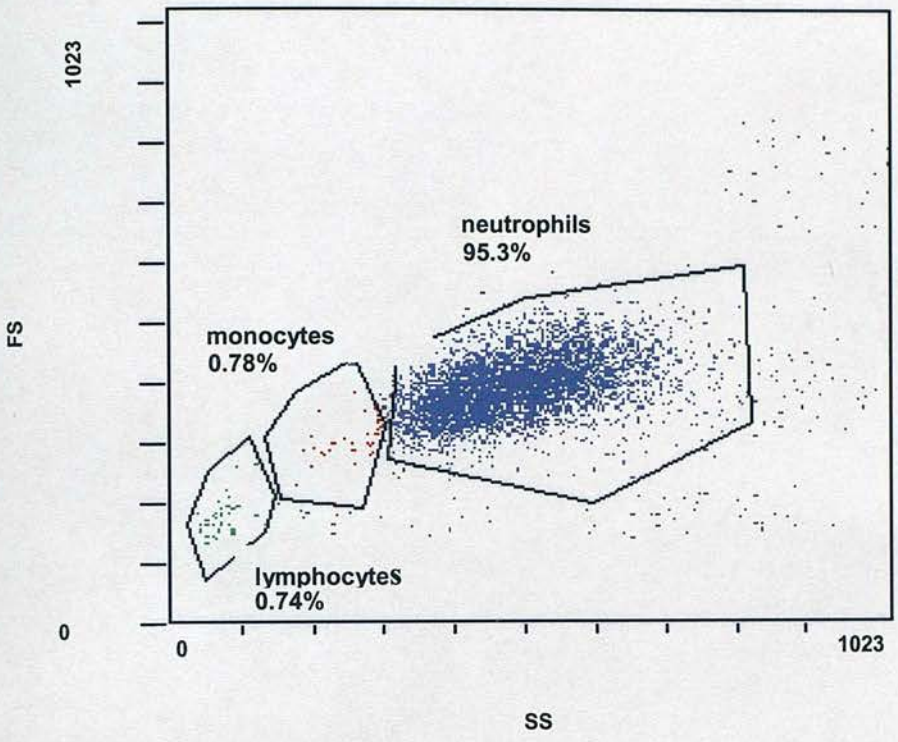

Figure 3.1: Isolated neutrophils from whole blood. Approximately 1.52% of cells were contaminating monocytes and lymphocytes. FS = forward scatter, SS = side scatter. Data are from 1 representative experiment of 2.

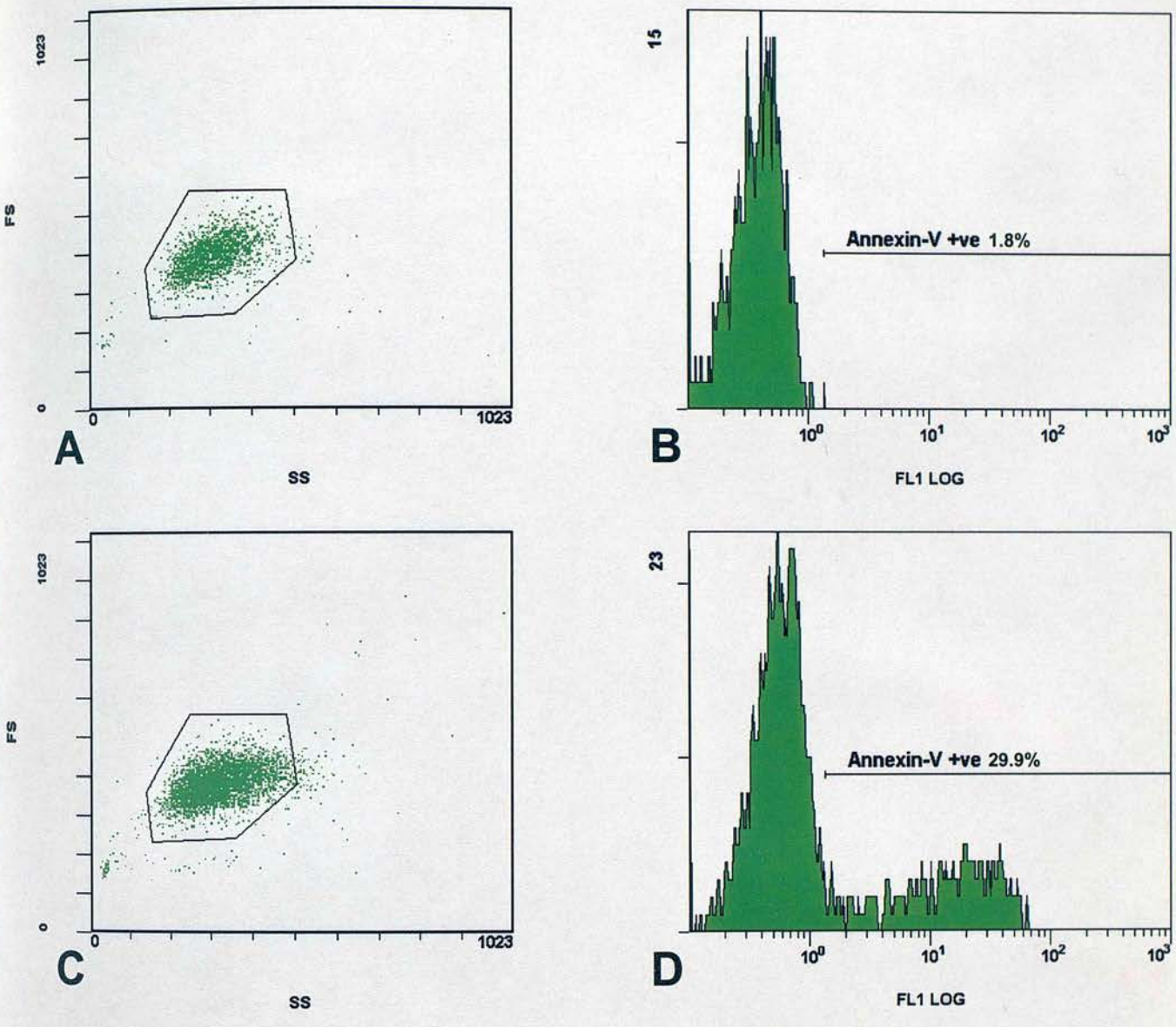

Figure 3.2: Activity of anti-FasR monoclonal antibody (CH11) induces apoptosis, assessed by Annexin-V-FITC binding, in human neutrophils. Human neutrophils (5 x 10^6/ml) were cultured at 37°C in Iscove's DMEM containing 10% autologous serum and treated with or without 500ng/ml anti-FasR (CH11). After 4 hours, cells were incubated with Annexin-V-FITC for 10 min on ice and analysed by flow cytometry. FS = forward scatter, SS = side scatter. Data are from 1 representative experiment of 2.

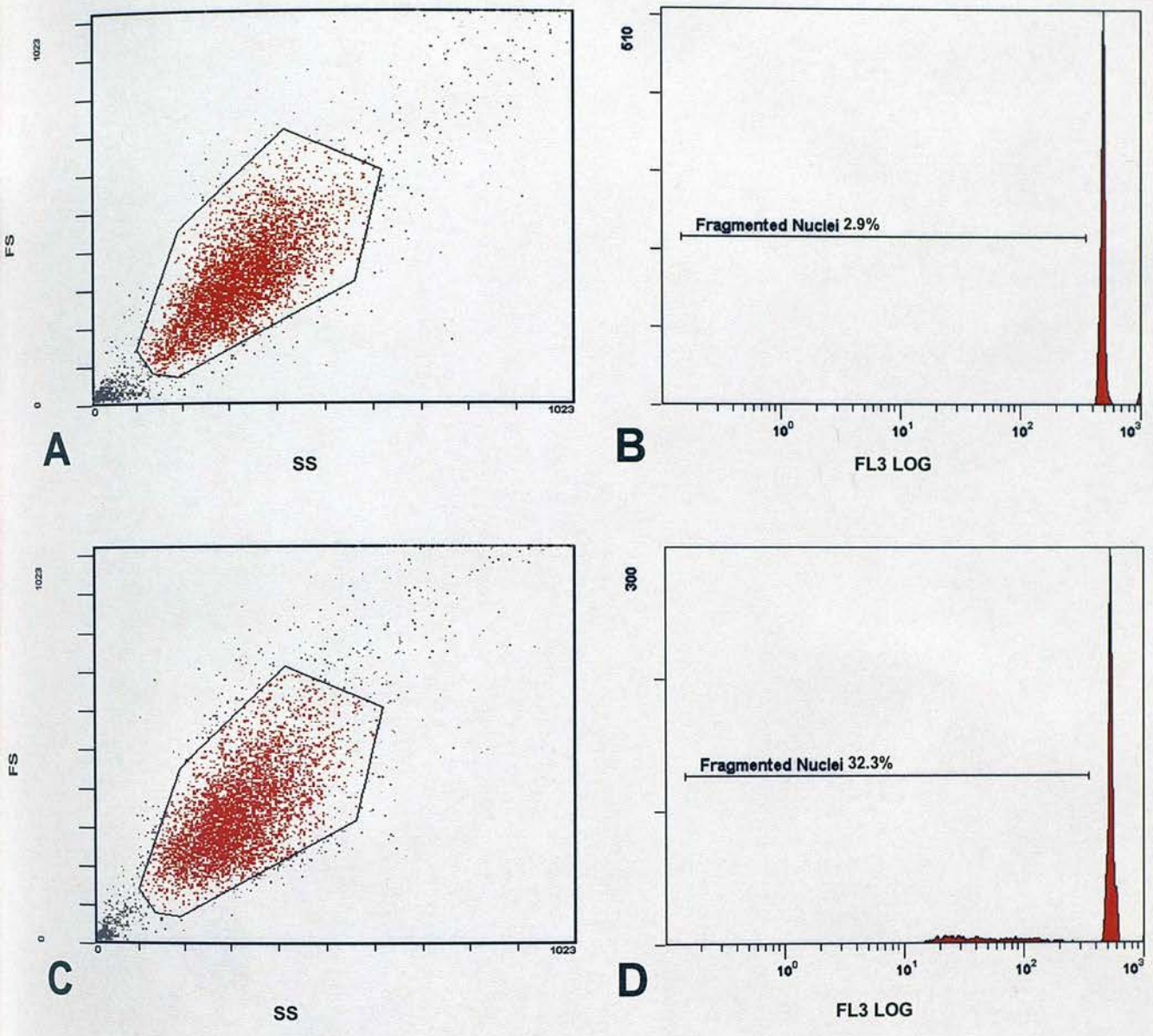

Figure 3.3: Activity of anti-FasR monoclonal antibody (CH11) induces apoptosis, assessed by analysis of DNA content by PI, in human neutrophils. Human neutrophils (5 x 10^6/ ml) were cultured at 37 °C in Iscove's DMEM containing 10% autologous serum and treated with or without 500 ng/ml anti-FasR (CH11). After 4 hours, cells were fixed and permeabilised with ethanol and stained with PI and analysed by flow cytometry. FS = forward scatter, SS = side scatter. Data are from 1 representative experiment of 2.

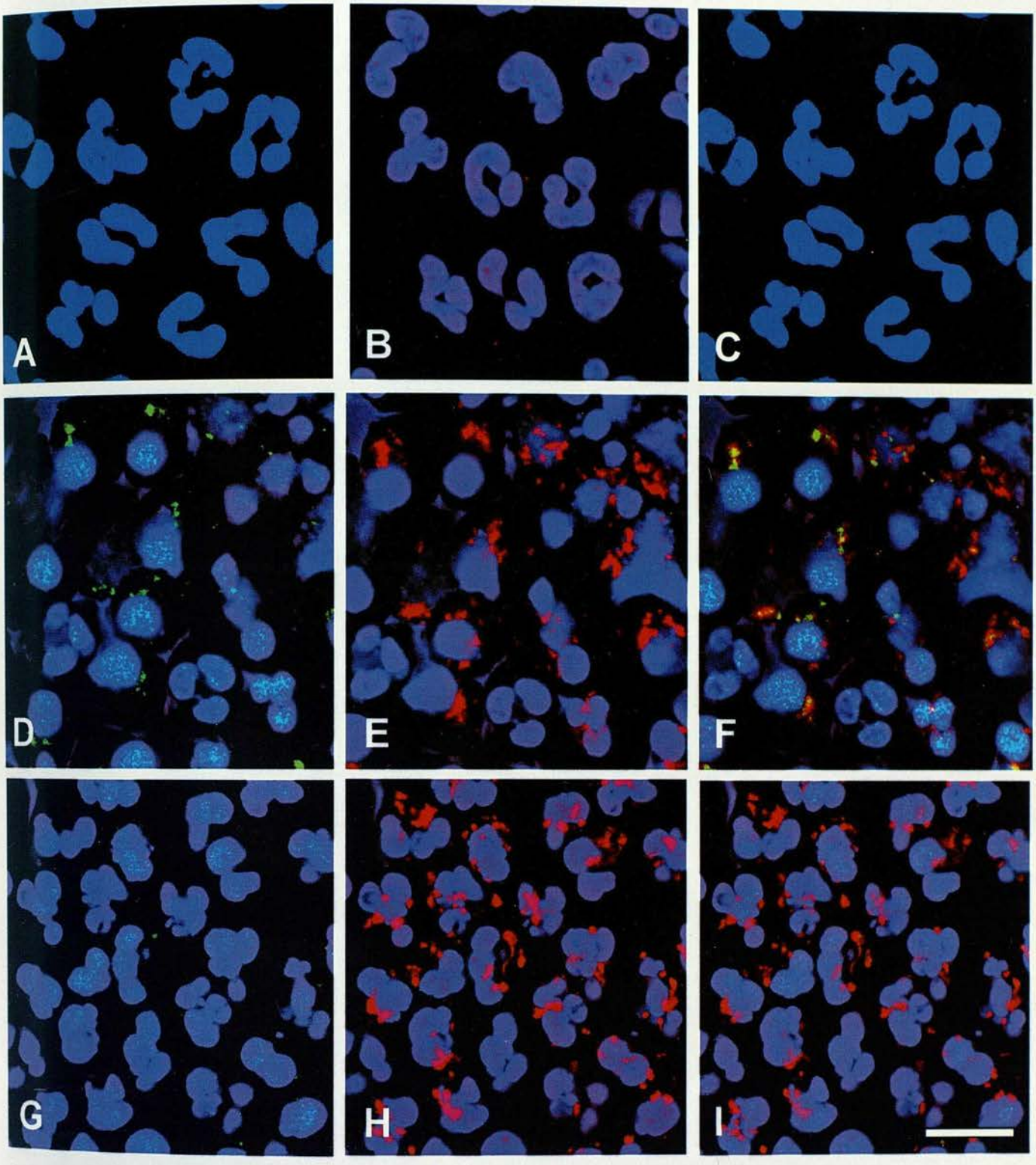

Figure 3.4: Bax aggregates in apoptotic neutrophils by indirect immunofluorescence but aggregation is not inhibited by z-VAD-fmk. Human neutrophils (5 x 10^6/ml) were cultured at 37°C in Iscove's DMEM containing 10% autologous serum and treated with 20μg/ml CHX (D-I). Neutrophils were stained with mouse-anti-mtHSP70 (green), rabbit-anti-bax (red) and the nuclei were stained with TO-PRO-3 (blue). Freshly isolated neutrophils showed minimal non-specific fluorescence when stained with Alexa-488 (green) and Alexa-568 (red) (A) or goat-anti-mouse (green) and goat-anti-rabbit antibodies (red) (B). Bax and mtHSP70 were not detected in freshly isolated neutrophils (C). However, in apoptotic neutrophils stained with mouse-anti-mtHSP70 (D, green) and rabbit-anti-Bax (E, red), large structures were aggregated in the cytoplasm, which co-localised (F, yellow) with many of the clusters revealed my mitochondrial staining. z-VAD-fmk inhibited the aggregation of structures stained with anti-mtHSP70 (G) but did not prevent the aggregation of structures in cells stained with anti-Bax (H), where (I) is the composite photomicrograph. Data are representative of 3 experiments. Scalebar represents 10μm.

3.2.3 *Indirect Immunofluorescence Staining of Golgi in NRK Cells*

To validate immunofluorescence staining of the Golgi apparatus using several antibodies raised against Golgi membranes, we used normal rat kidney (NRK) cells as these cells are known to have large Golgi complexes. There was minimal non-specific staining by cells stained with mouse (Fig. 3.5A) and rabbit IgG (Fig. 3.5B). NRK cells were stained with polyclonal rabbit JPR3 (Fig. 3.5C) raised against rat liver Golgi membranes, mouse monoclonal to mannosidase II 53FC3 (Burke *et al.*, 1982) (Fig. 3.5D), mouse monoclonal 1b2 (Fig. 3.5E), mouse monoclonal GM130 (Fig. 3.5F) and mouse monoclonal p115 (Fig. 3.5G). All antibodies used showed specific juxtanuclear reticular Golgi staining, demonstrating that these antibodies detect the Golgi complex in NRK cells.

3.2.4 *Indirect Immunofluorescence Staining of Golgi in Neutrophils*

Apoptosis in neutrophils may be assessed by morphological criteria such as chromatin condensation, cytoplasmic shrinkage (Savill *et al.*, 1989) and by indirect immunofluorescence, Bax redistribution as a marker of the initiation stages of apoptosis and mitochondrial clustering as a marker of the execution phase (section 3.2.2). In addition, apoptosis could be assessed by Annexin-V-FITC binding and by loss of DNA content as measured by flow cytometry analysis of cells fixed and stained with PI.

To assess the fate of the Golgi complex in models of neutrophil apoptosis, the Golgi complex was stained by indirect immunofluorescence. To optimise Golgi staining, freshly isolated neutrophils were fixed and permeabilised and stained with various antibodies raised against Golgi-membrane proteins. Fig. 3.6A shows neutrophils stained with non-specific rabbit and mouse IgG, followed by Alexa green (goat anti-mouse) and Alexa red (goat anti-rabbit). No non-specific staining was detected. As a positive control, neutrophils were stained with the antibody BOB78 that recognises a 90 kDa antigen localised in intracellular granules (Hart *et al.*, 2000) (Fig. 3.6B). Neutrophils did not show specific staining with the Golgi markers anti-1b2 (Fig. 3.6C), 53FC3 (Fig. 3.6D) and anti-GM130 (Fig. 3.6E), but only diffuse cytoplasmic staining. However, anti-p115 antibody (Fig. 3.6F) showed specific staining of the Golgi (arrows). The Golgi staining shows a distinct aggregate of fluorescence that always stained juxtanuclearly. Serial sections of neutrophils stained with the monoclonal

anti-p115 antibody showed that the fluorescence was through several layers of the cell. As far as is known, the Golgi complex has not been identified by indirect immunofluorescence in neutrophils but has been by EM.

Although, the data demonstrated that the Golgi complex was present in neutrophils, resolution of typical interphase Golgi structures and fragmented Golgi was likely to be difficult in view of the low level of signal seen. Therefore, it was decided to use cell lines to establish whether the Golgi fragments during apoptosis and investigate possible mechanisms of Golgi fragmentation.

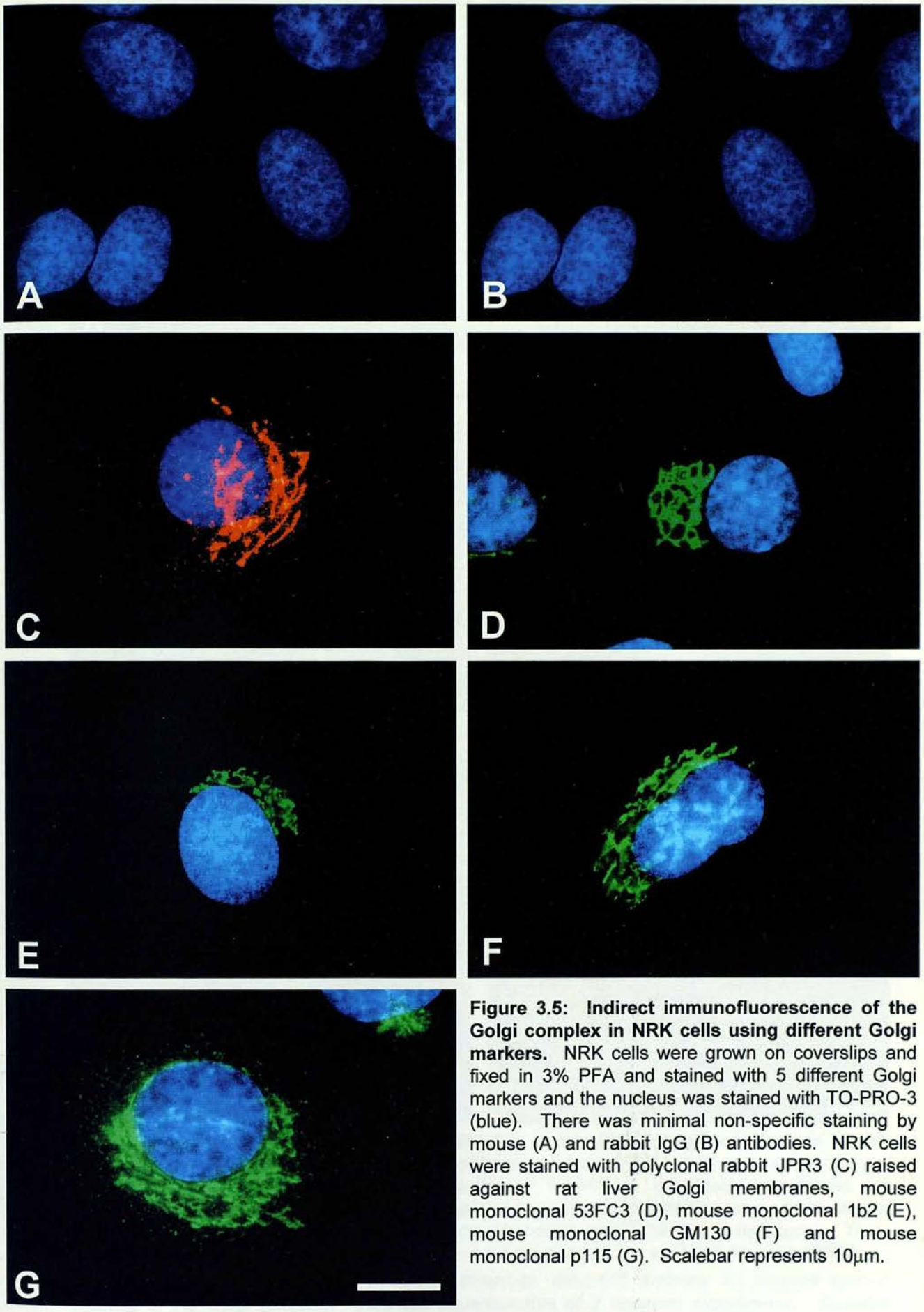

Figure 3.5: Indirect immunofluorescence of the Golgi complex in NRK cells using different Golgi markers. NRK cells were grown on coverslips and fixed in 3% PFA and stained with 5 different Golgi markers and the nucleus was stained with TO-PRO-3 (blue). There was minimal non-specific staining by mouse (A) and rabbit IgG (B) antibodies. NRK cells were stained with polyclonal rabbit JPR3 (C) raised against rat liver Golgi membranes, mouse monoclonal 53FC3 (D), mouse monoclonal 1b2 (E), mouse monoclonal GM130 (F) and mouse monoclonal p115 (G). Scalebar represents 10μm.

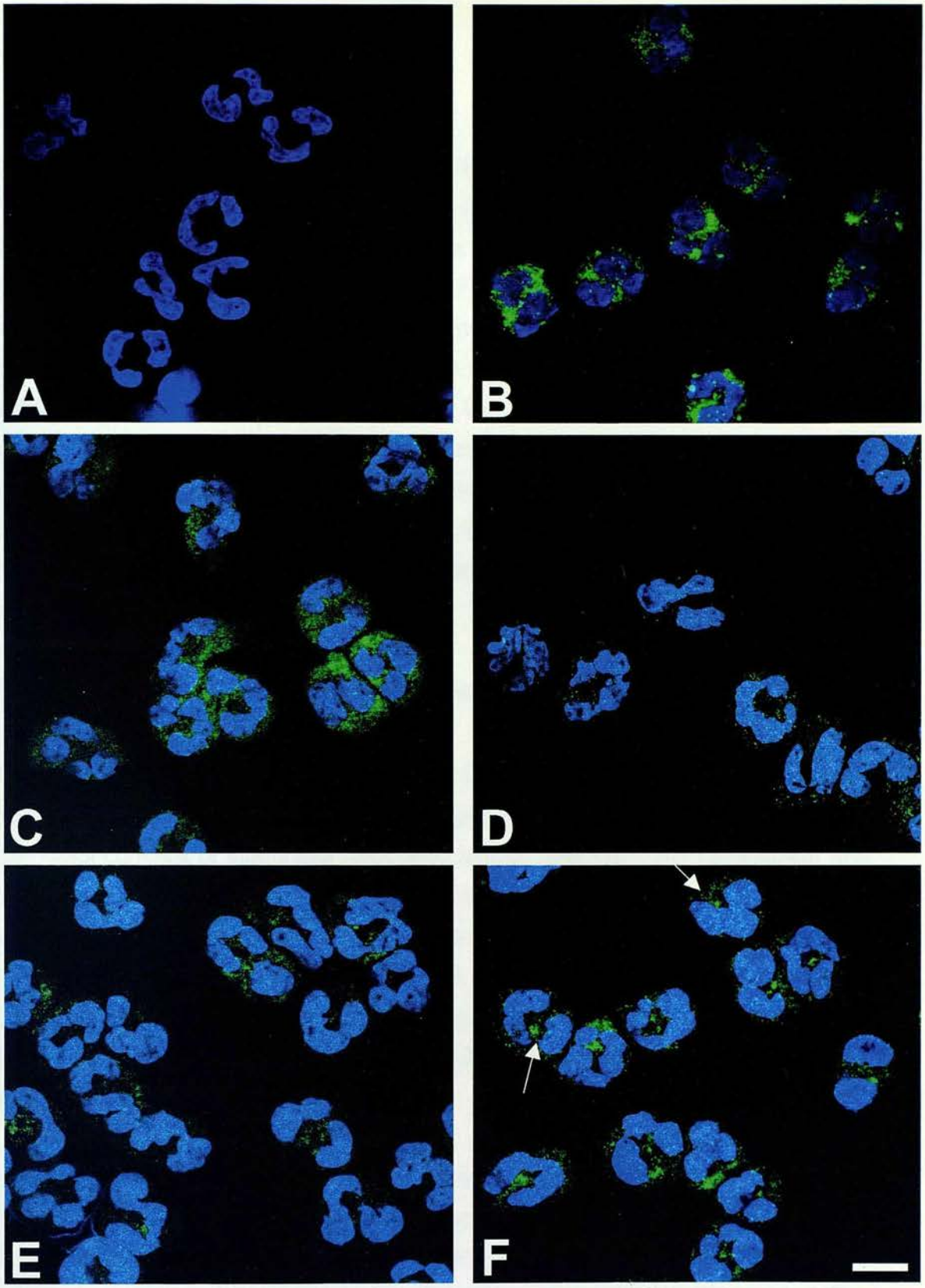

Figure 3.6: Indirect immunofluorescence staining of the Golgi complex (green) in freshly isolated neutrophils. Freshly isolated neutrophils were cytocentrifuged onto glass coverslips and fixed in 3% PFA. The nuclei (blue) were stained with TO-PRO-3. (A) Neutrophils stained with non-specific mouse IgG antibodies showing that non-specific binding was minimal. Cells stained with the granule-specific BOB78 antibody (B), demonstrating specific binding in neutrophils. There was no specific staining when neutrophils were incubated with the anti-1b2 (C), anti-53FC3 (D) and anti-GM130 (E) anti-Golgi antibodies. However, anti-p115 antibody (F) showed specific staining of the Golgi (arrows). Data are representative of 2 separate experiments. Scalebar represents 10μm.

3.2.5 The Golgi Complex During Mitosis in NRK Cells

During mitosis the Golgi complex fragments into thousands of vesicles coinciding with an arrest of intracellular transport. NRK cells were stained with 53FC3, a monoclonal antibody raised against mannosidase II (Burke *et al.*, 1982) and the nuclei stained with Hoechst 33258. The Golgi structure during interphase is juxtanuclear and reticular (Fig. 3.7A). During prometaphase the chromatin condenses and the Golgi starts to lose its reticular structure (Fig. 3.7B). By metaphase (Fig. 3.7C) through to anaphase the Golgi complex is completely fragmented and dispersed throughout the cytoplasm. During telophase (Fig. 3.7D) the Golgi complex is equally divided between the two daughter cells and re-assembles juxtanuclearly.

3.2.6 The Golgi Fragments in SSP Induced Apoptosis in NRK Cells

NRK cells were treated with 2μM SSP over 6 h to induce apoptosis and the nuclei stained with TO-PRO-3 and the Golgi complex with the monoclonal 1B2 antibody. The Golgi complex of interphase NRK cells, stained with 1B2, was juxtanuclear and reticular in structure (Fig. 3.8A). At 6 h, cells that had been incubated with SSP were fixed and permeabilised. In those apoptotic cells that had fragmented or pebbled nuclei, typical of classical apoptosis (Leist & Jaattala, 2001), the Golgi had lost its juxtanuclear reticular structure and had fragmented and dispersed throughout the cytoplasm (Fig. 3.8B). The staining pattern of the apoptotic Golgi morphology was similar to that of mitotic cells (Fig. 3.7C).

However, fragmentation of the Golgi in NRK cells where the nucleus was condensed (Fig. 3.9B) also occurred, compared to interphase nuclei (Fig. 3.9A) but was not fragmented or pebbled (Fig. 3.9C). In addition, for those cells that had 'condensed nuclei', the associated Golgi morphology was not always completely fragmented (Fig. 3.9E) but was not similar to the interphase structure either (Fig. 3.9D). The Golgi appeared to have partially fragmented in these cells but a large aggregate of fluorescence was still visible. This was named 'condensed clustered Golgi' (Fig. 3.9F). It was thought that these different nuclear and Golgi morphologies may represent intermediate stages of apoptosis and Golgi fragmentation and that different nuclear morphologies might be correlated with distinct Golgi morphologies. To

further investigate that these observations were correct, a time-course over 10 h was carried out, with samples taken at 0, 2, 6 and 10 h and the various morphologies counted to follow the kinetics of Golgi fragmentation in NRK cells treated with 2μM SSP.

3.2.7 Kinetics of Golgi Fragmentation in NRK Cells Treated with SSP

Five different Golgi morphologies correlated to nuclear morphology were observed during SSP induced apoptosis in NRK cells: 1) Interphase nucleus & Juxtanuclear Reticular Golgi, 2) Condensed Nucleus & Clustered Golgi Membrane, 3) Condensed Nucleus & Fragmented Golgi, 4) Pebbled Nucleus & Clustered Golgi membrane and 5) Pebbled Nucleus & Fragmented Golgi.

Examination of untreated NRK cells showed that the majority of cells (~90%) had 'Interphase Nuclei & Juxtanuclear Reticular Golgi' (Fig. 3.10). However, after 2 h incubation with 2μM SSP, this morphology was largely replaced by two dominant morphologies: 'Condensed Nuclei & Clustered Golgi Membranes', and 'Condensed Nucleus & Fragmented Golgi', which represented ~50% and ~46% of the total population respectively (Fig. 3.10). The increase in the proportion of cells with 'Condensed Nuclei & Clustered Golgi Membranes' and 'Condensed Nucleus & Fragmented Golgi' compared to control values was statistically significant ($p < 0.001$). These observations raised the possibility that the 'Condensed Nucleus & Clustered Golgi Membrane' morphology was an intermediate morphology during the apoptotic program and that these cells would ultimately progress to the 'Condensed Nucleus & Fragmented Golgi' morphology as apoptosis proceeded.

After 6 h, the 'Condensed Nucleus & Clustered Golgi Membrane' morphology was no longer a dominant morphology (Fig. 3.10). However ~50% of the cell population had 'Condensed Nuclei & Fragmented Golgi' which was not significantly different from the proportion of cells showing this morphology at 2 h ($p > 0.05$). Furthermore, at this time point ~40% of cells had a 'Pebbled Nucleus & Fragmented Golgi' morphology. A significant increase ($p < 0.001$) compared to 0 and 2 h. This confirms that in NRK cells, nuclear condensation occurs prior to pebbling and similarly the Golgi apparatus becomes clustered prior to fragmenting during SSP induced apoptosis. The 'Pebbled Nucleus & Clustered Golgi Membrane' morphology was only observed in a small

proportion of cells, with the highest count at 6 h of just ~5% (Fig. 3.10). Since the nuclei appeared to pebble after condensing and that 'Condensed Nuclei & Fragmented Golgi' were a dominant morphology at 2 and 6 h, it appeared that the Golgi fragmented after nuclear condensation but prior to nuclear pebbling.

At the latest time point of 10 h, ~25% of cells had 'Condensed Nuclei & Fragmented Golgi Membranes' (Fig. 3.10), which was significantly reduced compared to 2 and 6 h ($p<0.001$), whilst ~75% of NRK cells belonged in the 'Pebbled Nucleus & Fragmented Golgi' category confirming that the end-stage of Golgi morphology during SSP induced apoptosis in NRK cells is fragmentation.

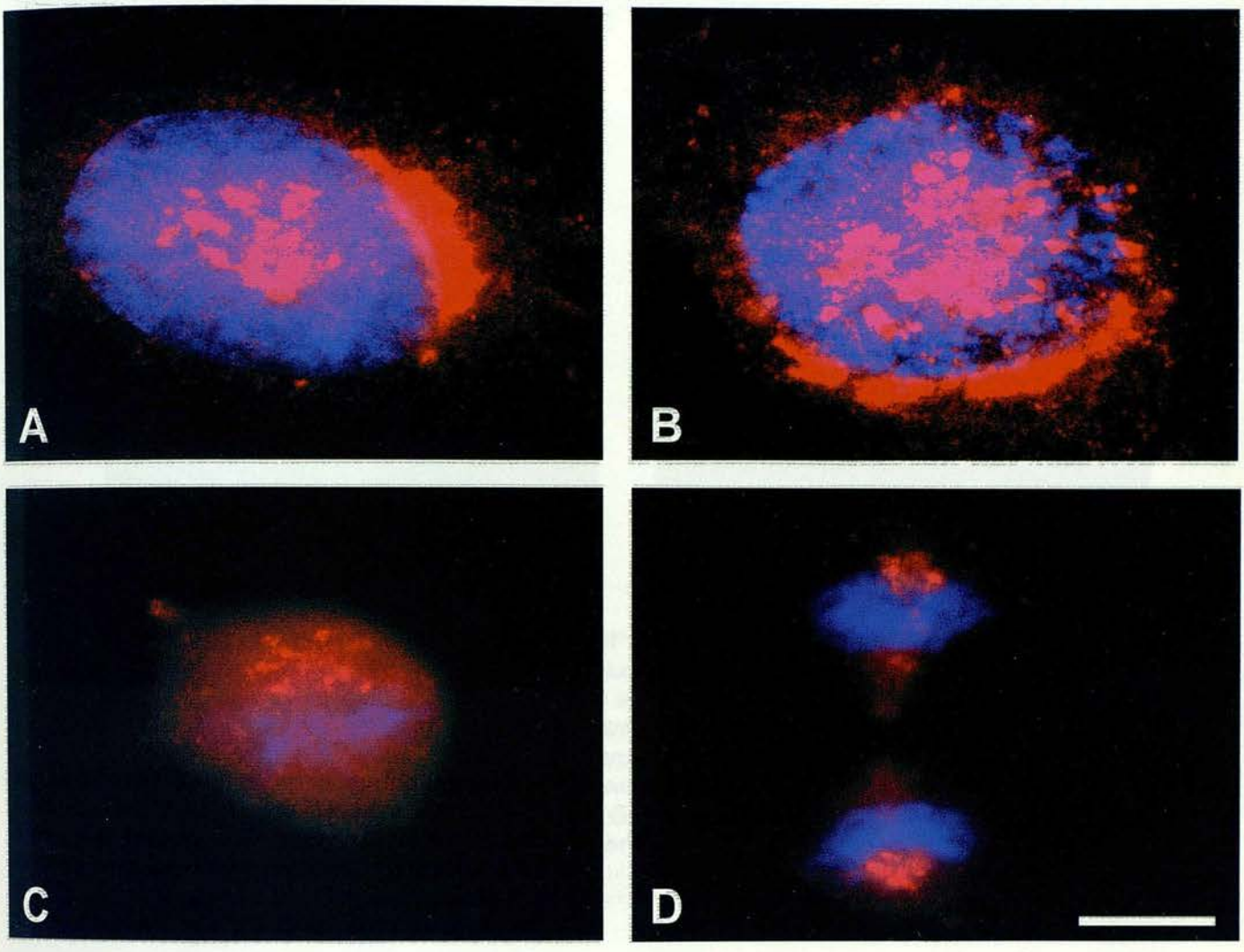

Figure 3.7: The Golgi complex during interphase and mitosis. NRK cells were grown on glass coverslips and fixed with 3% PFA. The nuclei were stained with TO-PRO-3 (blue) and the Golgi complex with the anti-Golgi monoclonal antibody 1B2 (red). (A) Typical nuclear and juxtanuclear reticular Golgi structure during interphase. During prometaphase the chromatin condenses and the Golgi starts to lose its reticular structure (B). By metaphase (C) through to anaphase the Golgi complex is completely fragmented and dispersed throughout the cytoplasm. During telophase (D) the Golgi complex is equally divided between the two daughter cells and re-assembles juxtanuclearly. Scalebar respresents 5μm.

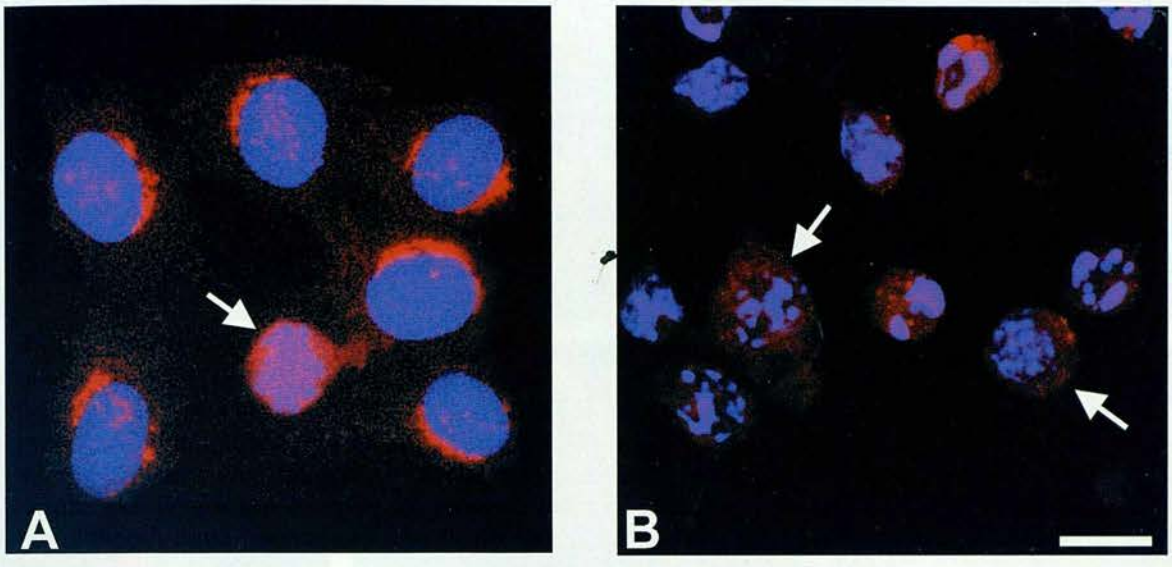

Figure 3.8: The Golgi Fragments During SSP Induced Apoptosis in NRK Cells. NRK were grown on glass coverslips in serum-free medium and treated with or without 2μM SSP over 6 hours. Cells were fixed in 3% PFA. The nuclei are stained with TO-PRO-3 and the Golgi with the monoclonal anti-mouse 1B2 antibody followed by Alexa-568 red (goat anti-mouse). (A) Untreated interphase cells with interphase nuclei and typical interphase juxtanuclear reticular Golgi. A mitotic cell where the Golgi is fragmented (arrow). After 6 hours, apoptotic cells (by nuclear morphology) have fragmented and dispersed Golgi staining (B). Data are representative of at least 5 separate experiments. Scalebar represents 10μm.

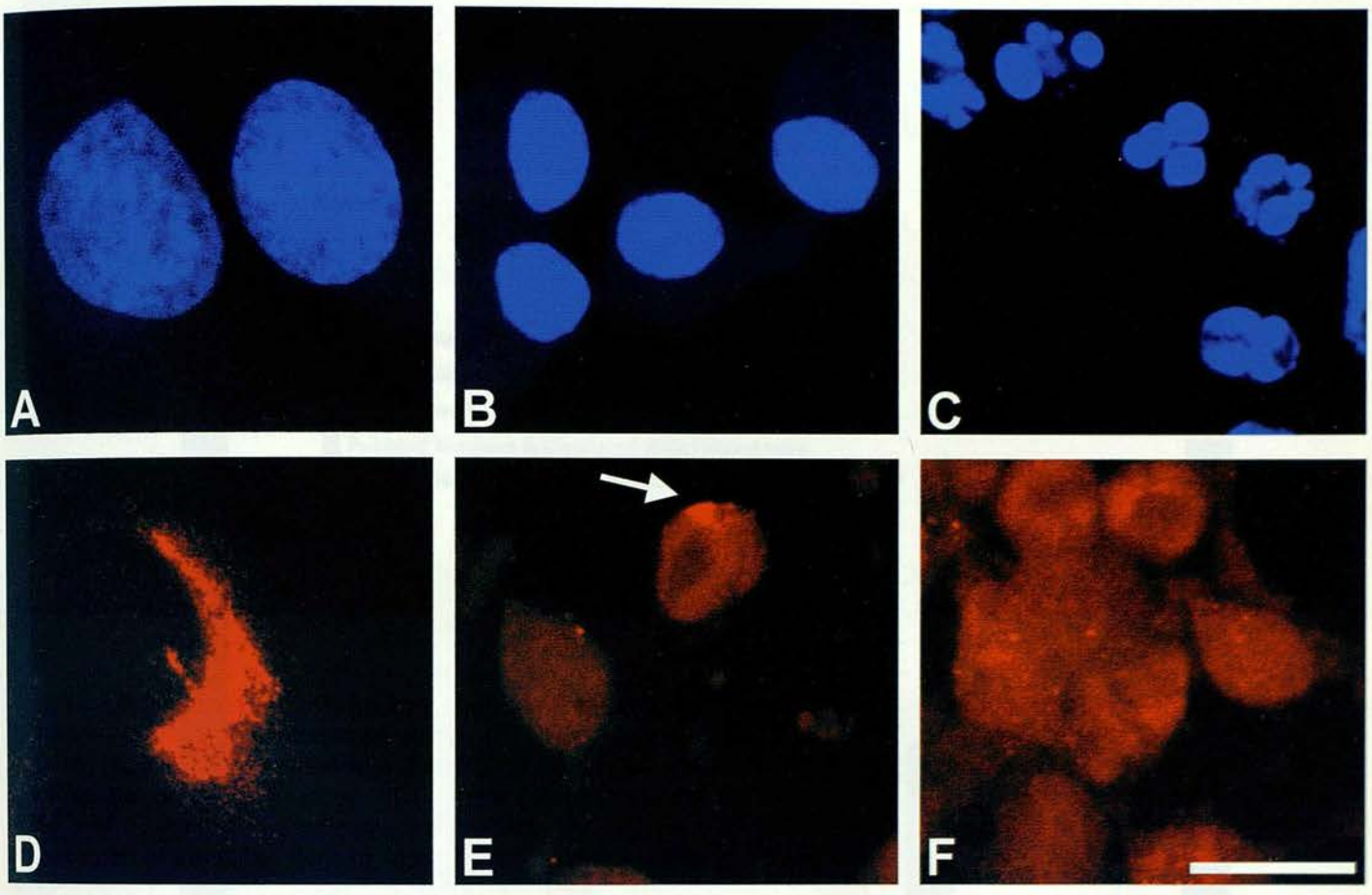

Figure 3.9: Nuclear and Golgi morphologies observed during SSP induced apoptosis in NRK cells. (A) Untreated cells, normal interphase nuclei. (B) NRK cells treated with 2μM SSP over 2 hours. The nuclei are reduced in size. (C) NRK cells treated with 2μM SSP for 6 hours. The nuclei have fragmented resulting in the appearance of pebbles, hence 'pebbled nuclei'. (D) normal interphase juxtanuclear Golgi structure (E) NRK cells treated with 2μM SSP over 2 hours. Arrow indicates a cell where the Golgi has lost its characteristic interphase morphology, however a large part of the Golgi remains intact hence 'clustered Golgi'. (F) NRK cells treated with 2μM SSP over 6 hours. The Golgi is completely fragmented in these cells resulting in a dispersed fluorescence signal distributed throughout the cytoplasm, similar to the fragmentation during mitosis by indirect immunofluorescence. Data are representative of at least 5 separate experiments. Scalebar represents 10μm.

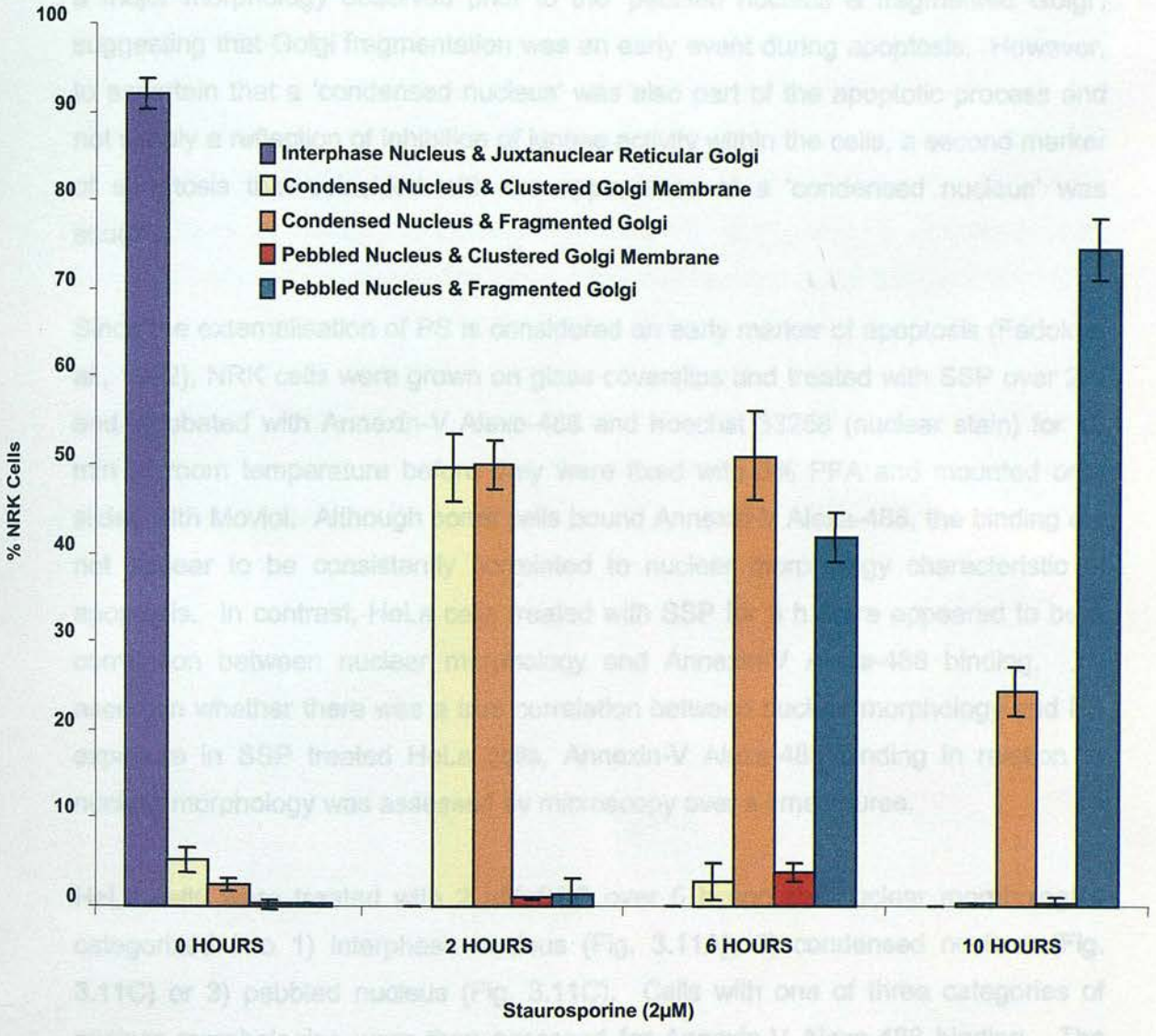

Figure 3.10: Kinetics of Golgi fragmentation in SSP treated NRK cells. NRK cells were treated with 2μM SSP over 10 hours. The nuclei were stained with Hoescht 33258 and the Golgi with the monoclonal anti-mouse 1B2 antibody. Five different morphologies were observed in control cells and SSP treated cells over 10 hours. Data represent the mean ± SEM of a typical experiment, where 500 cells were counted at random 3x/ slide. Data are representative of 2 experiments.

3.2.8 Annexin-V Alexa-488 Binding Correlated to Nuclear Morphology

From kinetic studies of Golgi fragmentation during SSP induced apoptosis in NRK cells it appeared that the Golgi fragmented prior to the classical 'pebbled' morphology of apoptotic nuclei in this system. The 'condensed nucleus & fragmented Golgi' was a major morphology observed prior to the 'pebbled nucleus & fragmented Golgi', suggesting that Golgi fragmentation was an early event during apoptosis. However, to ascertain that a 'condensed nucleus' was also part of the apoptotic process and not simply a reflection of inhibition of kinase activity within the cells, a second marker of apoptosis that coincided with the appearance of a 'condensed nucleus' was sought.

Since the externalisation of PS is considered an early marker of apoptosis (Fadok *et al.*, 1992), NRK cells were grown on glass coverslips and treated with SSP over 2 h and incubated with Annexin-V Alexa-488 and hoechst 33258 (nuclear stain) for 15 min at room temperature before they were fixed with 3% PFA and mounted onto slides with Moviol. Although some cells bound Annexin-V Alexa-488, the binding did not appear to be consistently correlated to nuclear morphology characteristic of apoptosis. In contrast, HeLa cells treated with SSP for 3 h there appeared to be a correlation between nuclear morphology and Annexin-V Alexa-488 binding. To ascertain whether there was a true correlation between nuclear morphology and PS exposure in SSP treated HeLa cells, Annexin-V Alexa-488 binding in relation to nuclear morphology was assessed by microscopy over a time course.

HeLa cells were treated with 2 µM SSP over 5 h and the nuclear morphologies categorized into 1) interphase nucleus (Fig. 3.11A), 2) condensed nucleus (Fig. 3.11C) or 3) pebbled nucleus (Fig. 3.11C). Cells with one of three categories of nuclear morphologies were then assessed for Annexin-V Alexa-488 binding. The majority of untreated cells had interphase nuclei and were Annexin-V Alexa-488 negative (Fig. 3.12A). After 2 h and 3 h, this changed where the dominant nuclear morphology was of the condensed nucleus category. Cells with this morphology did not however expose PS on their cell surface (Fig. 3.12B&C). After 4 h, cells with 'pebbled nuclei' started to appear, of which the majority bound Annexin-V Alexa-488 (Fig. 3.12D). PS exposure did not mark those cells with condensed nuclei as apoptotic. This suggests that PS exposure is a later event than nuclear condensation in the apoptotic process in SSP treated HeLa cells. However, the

question remained whether nuclear condensation represented an event specific to apoptosis or whether it was due to the inhibition of kinase activity in the cells.

3.2.9 Ultrastructure of the Golgi in SSP Treated HeLa Cells

By EM, the cytoplasm of mitotic cells contains thousands of ~50nm vesicles derived from the Golgi complex (Lucocq *et al.*, 1988). To determine if the fragmentation of the Golgi complex during apoptosis also produced similar vesicles at the ultrastructural level, we treated HeLa cells with SSP over 5 h and fixed them with 2% glutaraldehyde. EM was performed by J. Lucocq. HeLa cells were labelled with a Golgi marker, n-acetyl-glucosaminyl-transferase-1 conjugated to Protein-A-Gold. The gold particles can be seen to localise to small vesicles within the cytoplasm (Fig. 3.13, arrows indicate gold labelling) and the vesicles were reported to be ~50nm in size, similar to those observed in mitotic cells (J.Lucocq – personal communication). Quantitation of Golgi cisternae or stacks versus Golgi-derived vesicles in untreated cells and SSP treated cells showed a dramatic loss of Golgi stacks and increase in the presence of vesicles (Fig. 3.14).

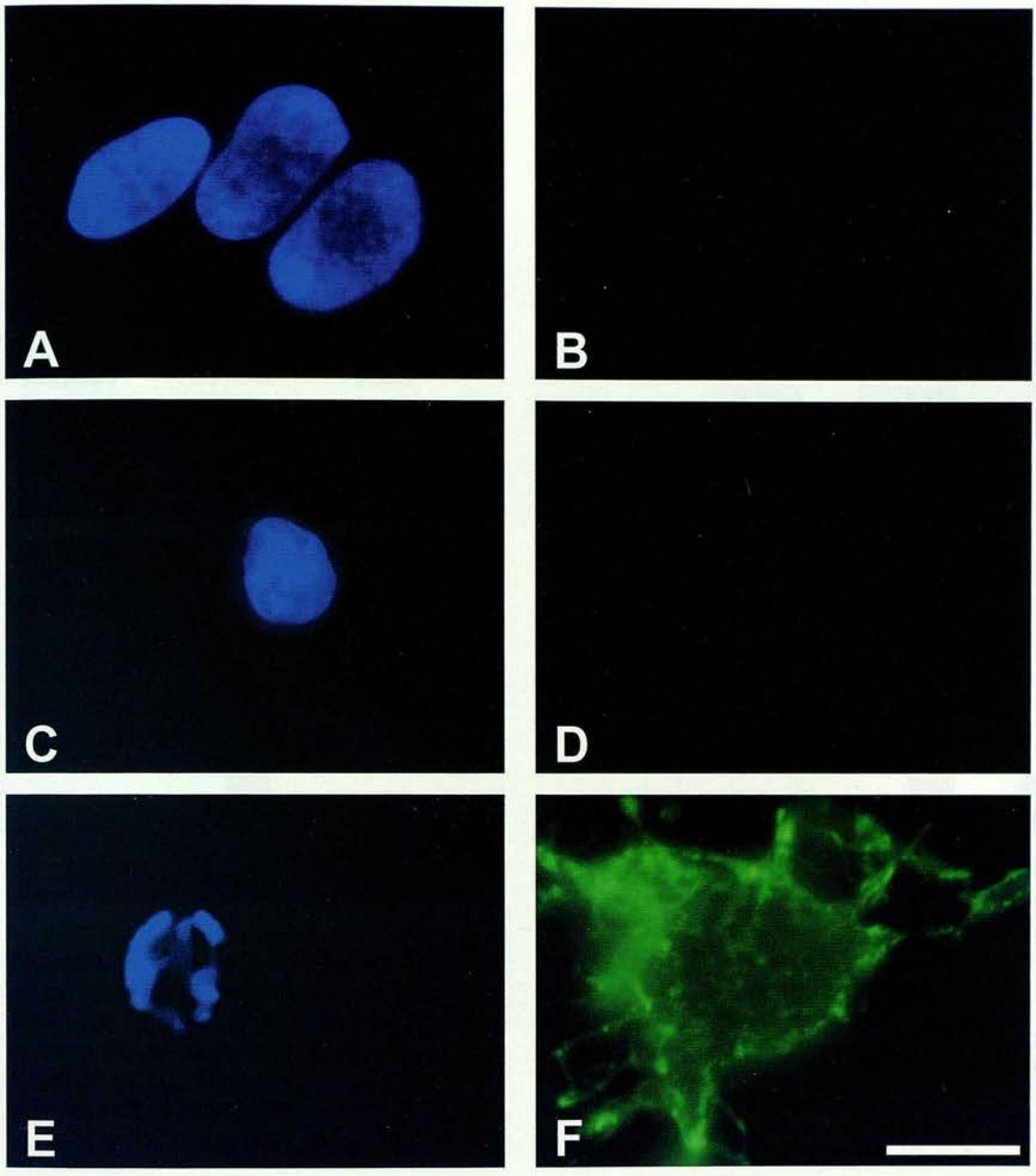

Figure 3.11: Annexin-V binding in SSP treated HeLa cells. HeLa cells were grown on glass coverslips in serum-free medium and were either untreated or incubated with 2 μM SSP over 5 hours. Cells were then stained with annexin-V conjugated to Alexa-488 (green) at room temperature over 15 minutes and fixed in 3% PFA. The nuclei were stained with Hoechst 33258. Non-apoptotic (A) cells did not bind annexin-V (B). HeLa cells treated with SSP over 5 hours that had condensed but not fragmented nuclei (C) also did not bind annexin-V (D). Only the cells which had fragmented nuclei (E) appeared to bind annexin-V (F). Data are representative of at least 5 separate experiments. Scalebar represents 10μm.

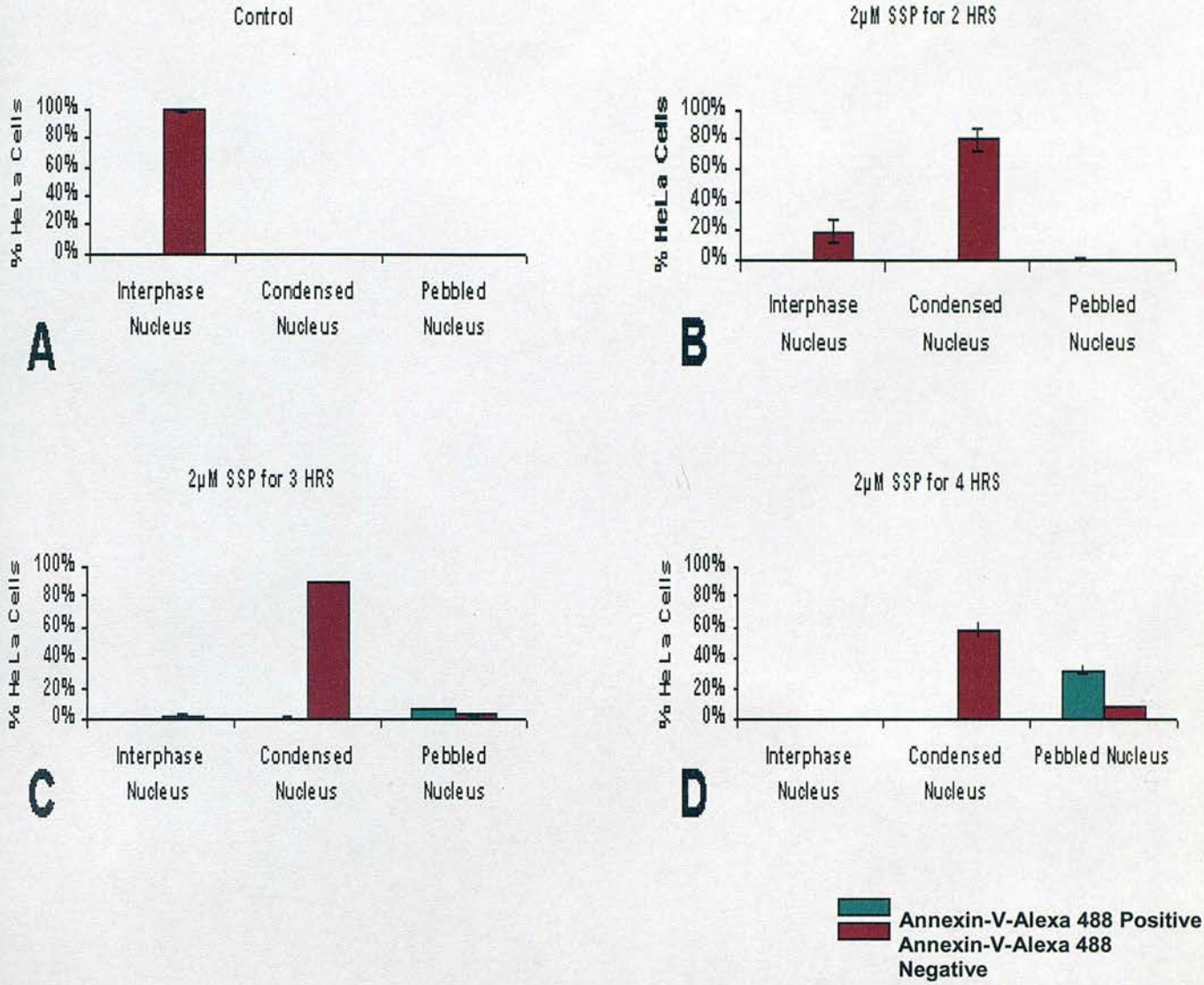

Figure 3.12: % Annexin-V-Alexa 488 binding correlated to nuclear morphology in HeLa cells treated with 2µM SSP over 5 hours. (A) Untreated cells had typical interphase nuclei and did not bind Annexin-V. (B) After 2 hours, the nuclei had mostly condensed but still did not bind Annexin-V (79.8 ± 7.6%SEM). (C) After 3 hours the majority of cells had condensed nuclei and there was a slight increase in cells with pebbled nuclei, the majority of which bound Annexin-V (pebbled nuclei: 6.6% ± 0.6SEM Annexin-V +ve, 2.7% ± 0.3SEM Annexin-V –ve). (D) After 4 hours there was an increase in cells with pebbled nuclei (~41%) of which 32.8% ± 4SEM bound Annexin-V. Cells with condensed nuclei (58.5% ± 5.9SEM) did not bind Annexin-V. (E) the majority of cells had condensed nuclei and there was a slight increase in cells with pebbled nuclei, the majority of which bound Annexin-V (pebbled nuclei: 6.6% ± 0.6SEM Annexin-V +ve, 2.7% ± 0.3% Annexin-V –ve). Data represent the mean ± SEM of a typical experiment, where 500 cells were counted at random 3 x / slide.

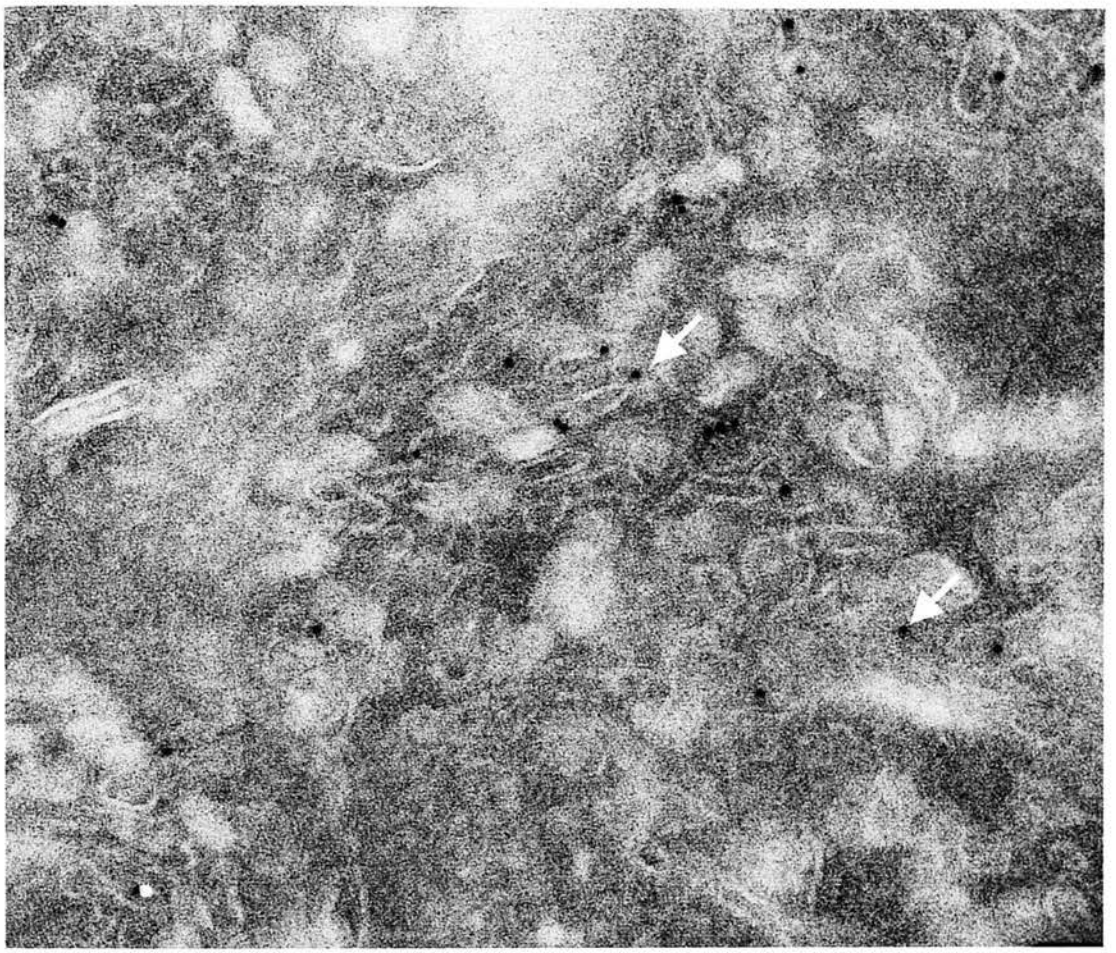

Figure 3.13: Golgi-derived vesicles in apoptotic SSP treated HeLa cells are morphologically similar to mitotic Golgi fragments. Ultrathin frozen sections of HeLa cells treated with 2μM SSP over 5 hours, labelled with n-acetyl-glucosaminyl-transferase-1 conjugated to Protein-A-Gold. An apoptotic cell where the Golgi stack has fragmented into ~50nm vesicles, similar to mitotic vesicles. (Micrograph by J. Lucocq).

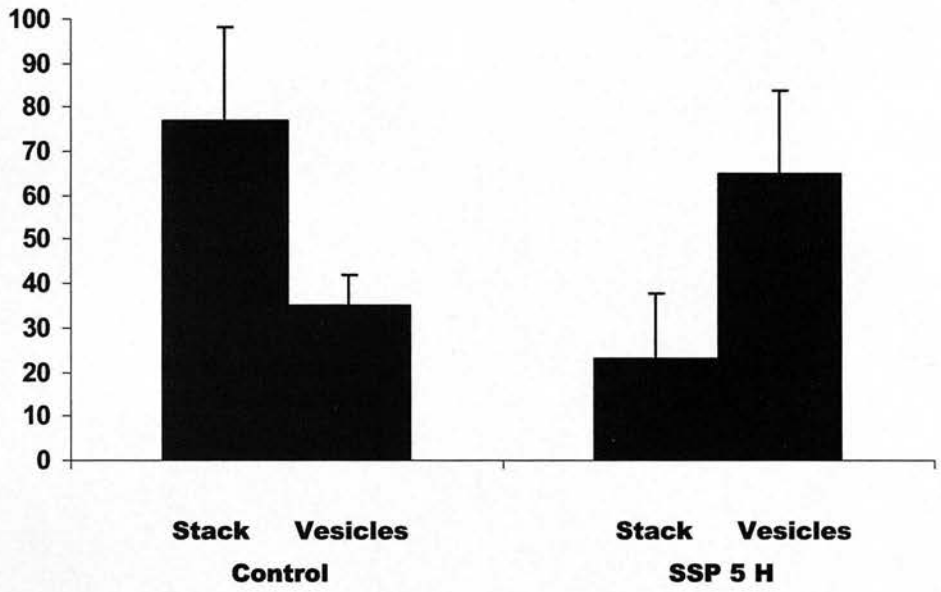

Figure 3.14: Quantitation of Golgi cisternae (stack) versus Golgi vesicles in SSP treated HeLa cells. Bars represent ± SEM. (Data by John Lucocq).

3.2.10 The Golgi Fragments During CHX Induced Apoptosis in NRK Cells

Using SSP to induce apoptosis in NRK and HeLa cells we have shown that in both cell types, the Golgi fragments during SSP induced apoptosis. Inhibition of ER to Golgi transport during apoptosis would render the dying cell environmentally isolated by preventing delivery of cell surface receptors. While Golgi fragmentation during apoptosis is also a strong indicator of the inhibition of ER to Golgi transport during apoptosis, its fragmentation may also serve a physical need. Just like mitotic cells are able to divide the Golgi, which is present as a single-copy organelle, equally between the two daughter cells; an apoptotic cell must surely fragment its Golgi for eventual enclosure into apoptotic bodies.

I therefore investigated whether Golgi fragmentation also occurred with other agents that induce apoptosis. NRK cells were treated with 10μg/ ml CHX, a protein synthesis inhibitor, over 4 h and cells were stained with the anti-GM130 antibody to mark the Golgi complex and an antibody that recognises only the active form of caspase-3. It is important to note that in untreated cells with juxtanuclear reticular Golgi structures and in dividing cells where the Golgi is completely fragmented throughout the cytoplasm, that there is no caspase-3 activity (Fig. 3.14A). However, a very early apoptotic cell was observed where the nucleus had condensed but not yet pebbled and the cell was still adherent (Fig. 3.14B). The caspase-3 activity was present throughout the cytoplasm of the cell and importantly, the Golgi was still intact, raising the possibility that Golgi fragmentation may be downstream of the early execution phase of apoptosis. In addition, at least in the model of CHX induced apoptosis, the morphology of 'condensed nucleus' appears to be specific to the very early stages of apoptosis. After 4 h many of the cells had rounded up and the nuclei become pebbled, characteristic of apoptosis and stained positive for anti-active caspase-3. In these cells the Golgi was completely fragmented and dispersed throughout the cytoplasm (Fig. 3.15C) and the insert in Fig. 3.15C shows apoptotic cells with only Golgi staining to demonstrate the punctate Golgi staining more clearly. Importantly, Golgi fragmentation was completely inhibited by z-VAD-fmk, the broad-range caspase inhibitor (Fig. 3.15D), demonstrating that Golgi fragmentation during apoptosis is caspase-dependent.

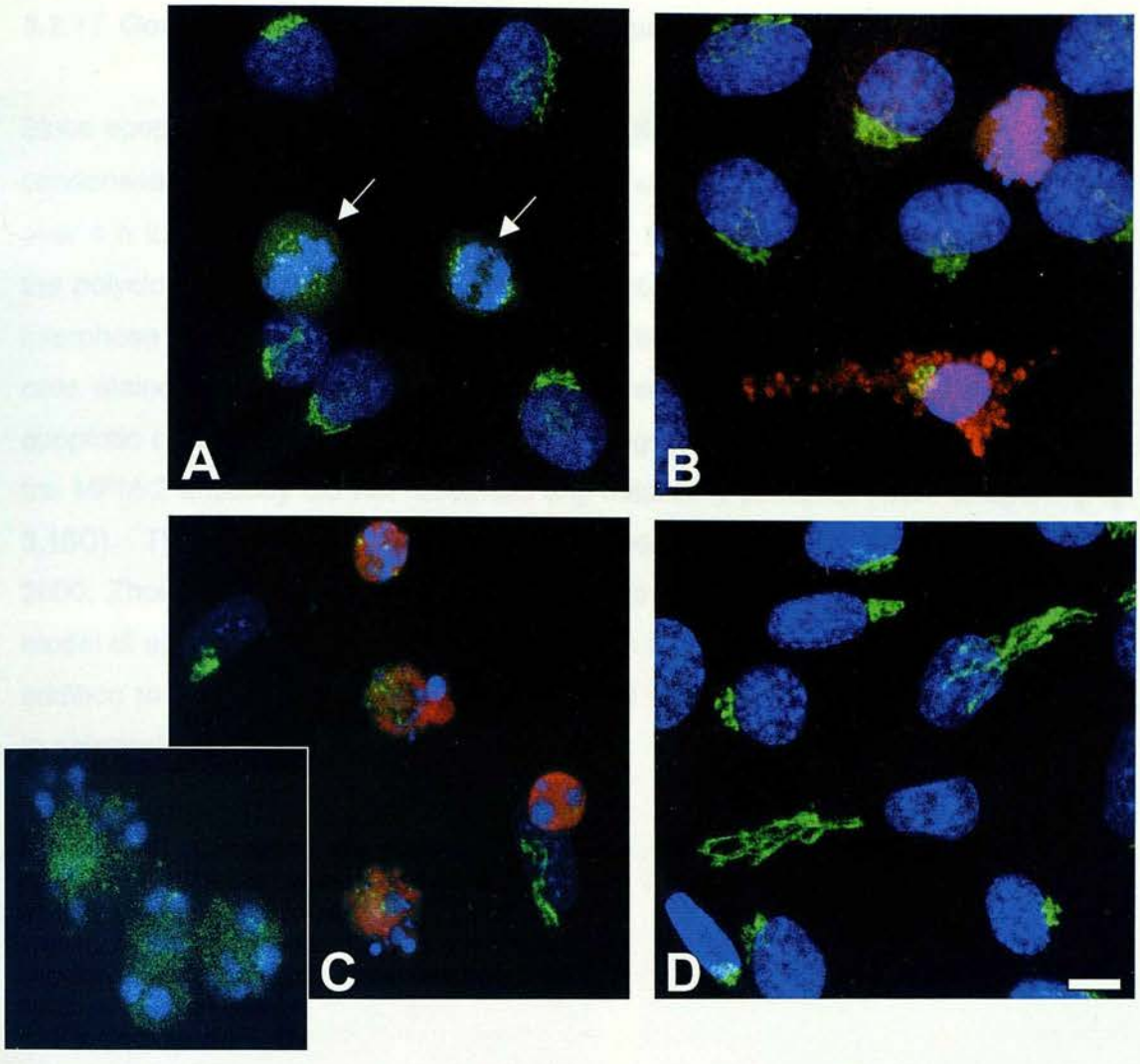

Figure 3.15: Caspases are required for the fragmentation of the Golgi complex during apoptosis. NRK cells were grown on glass coverslips in serum-free medium and treated with or without 10μg/ml CHX for 4 hours. Cells were then fixed with 3% PFA. Immunofluorescence staining of the Golgi apparatus was with the monoclonal antibody against GM130 (green) and the polyclonal antibody against active caspase-3 (red). (A) Untreated NRK cells with typical interphase nuclei and juxtanuclear reticular Golgi. Amongst the cells are two mitotic cells where the Golgi is fragmented (arrows). There is no detectable caspase-3 activity. (B) NRK cells were incubated with CHX for 1 hour and here is an early example of an apoptotic cell that is positively stained for caspase-3 activity, yet the nucleus has not yet pebbled and the Golgi is still intact. (C) NRK cells were treated with CHX for 4 hours after which the nuclei show classical apoptotic nuclear pebbling and are positive for caspase–3 staining; in those cells the Golgi is fragmented. The bottom left picture insert is of NRK cells under the same conditions, without anti-caspase-3 staining to show Golgi fragmentation more clearly. (D) Cells were incubated with 100μM z-VAD-fmk, the broad-spectrum caspase inhibitor, 30 minutes prior to the addition of CHX for 4 hours and the cells have retained their interphase nuclear and Golgi morphology. Data are representative of 2 separate experiments. Scalebar represents 10μm.

3.2.11 Golgi Fragmentation is Specific to Apoptosis

Since apoptosis shares many of the morphological features of mitosis e.g. chromatin condensation, Golgi fragmentation, NRK cells were again treated with 10μg/ ml CHX over 4 h to induce apoptosis and stained with the MPM-2 monoclonal antibody and the polyclonal JPR3 antibody raised against rat liver Golgi membranes. Untreated interphase cells had the characteristic juxtanuclear reticular Golgi staining and mitotic cells stained positively with the MPM-2 monoclonal antibody (Fig. 3.16A&B). In apoptotic cells (identified by nuclear morphology), where the Golgi was fragmented, the MPM-2 antibody did not recognise any mitotically phosphorylated antigens (Fig. 3.16C). Therefore, while CDK activity may occur in apoptotic cells (Harvey *et al.*, 2000; Zhou *et al.*, 1998), not all of the mitotic antigens are phosphorylated in this model of apoptosis. Thus, Golgi fragmentation appears to be specific to apoptosis in addition to mitosis although the mechanism of Golgi fragmentation may be different in apoptosis.

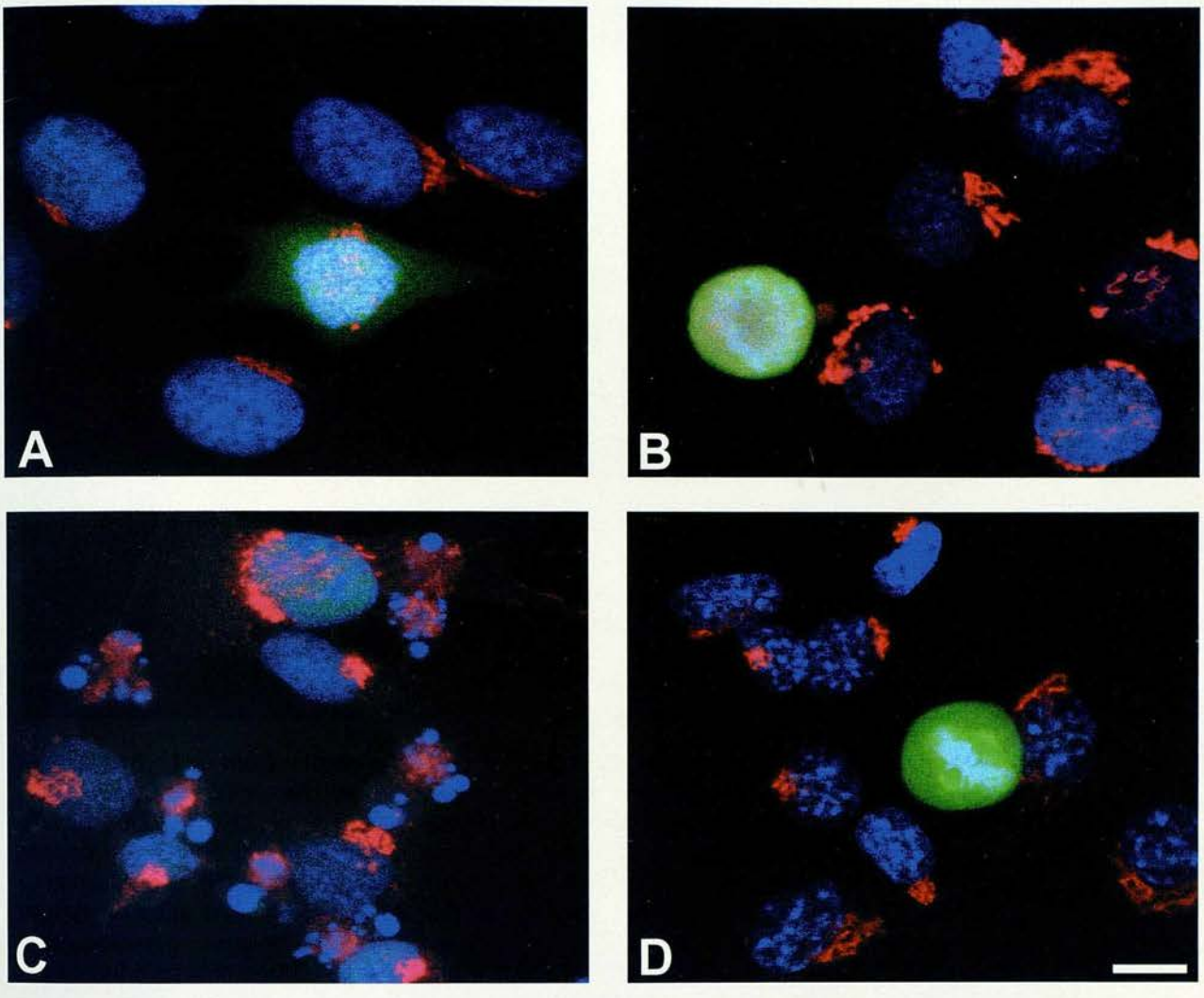

Figure 3.16: The monoclonal antibody MPM-2 does not stain apoptotic NRK cells where the Golgi is fragmented. NRK cells were grown on glass coverslips in serum-free medium and treated with or without 10μg/ml CHX for 4 hours. Cells were stained with the polyclonal JPR3 anti-Golgi-membrane antibody (red) and the monoclonal anti-MPM2 antibody (green). (A) shows an early mitotic NRK cell (prophase) and (B) a prometaphase cell, both staining positively with the anti-mitotic antibody, while interphase cells are not stained by MPM-2. (C) apoptotic NRK cells where the Golgi is fragmented in those cells with pebbled nuclei and the cells are negative for the anti-mitotic antibody. (D) These cells were incubated with z-VAD-fmk alone for 4 hours and the Golgi morphology in interphase cells is the same as the control (A) and again the metaphase cell is brightly stained for the anti-mitotic antibody demonstrating that z-VAD-fmk has no effect on Golgi morphology or mitosis. Data are representative of 2 separate experiments. Scalebar represents 10μm.

3.3 Discussion

The studies herein show that the Golgi fragments during apoptosis in both HeLa and NRK cells treated with SSP or CHX. By electron microscopy, the resulting Golgi fragments are morphologically indistinguishable from those found in the cytosplasm in mitotic cells (J.Lucocq – personal communication). These results were later confirmed in work by Sesso *et al.* (1999) and Lane *et al.* (2002). In addition, Golgi fragmentation during apoptosis was shown to be a caspase-dependent event. Since during mitosis, Golgi fragmentation occurs with a concommittant arrest in the secretory pathway, it is possible that protein transport is also arrested during apoptosis (Lucocq *et al.*, 1988).

Apoptosis occurs constitutively when neutrophils are cultured *in vitro* over 24 h. However, apoptosis may be induced in neutrophils over much shorter time points by incubating cells with various known apoptosis inducing agents, including the anti-FasR monoclonal antibody CH11 and the protein synthesis inhibitor cycloheximide (Ward *et al.*, 1999b). To set up systems of neutrophil apoptosis that could be monitored by different criteria, CH11 was used initially to drive apoptosis, which was monitored by PS externalisation. In the same system, cellular DNA content was measured using PI to estimate apoptosis. Both methods estimated the same rate of apoptosis, indicating that Annexin-V-FITC binding and cellular DNA content are accurate and reliable methods of assessing apoptosis. However, our initial studies on Golgi morphology had to be undertaken using indirect immunofluorescence. Therefore, in addition to using flow cytometry methods to estimate apoptosis, a second marker of apoptosis by indirect immunofluorescence besides nuclear morphology, was required.

The translocation of Bax from the cytosol to the mitochondria is well documented in other cell types and is independent of caspase activity (Granville *et al.*, 1999; Murphy *et al.*, 1999) but only recently has this also been shown to be independent of caspases in neutrophils (Granville *et al.*, 1999; Maianski *et al.*, 2002; Murphy *et al.*, 1999; Nechushtan *et al.*, 2001). Immunofluorescence staining of apoptotic neutrophils showed large clusters of Bax that co-localised with many of the mitochondrial clusters but not all of them. This was consistent with the work of Nechushtan *et al.* (2001), who proposed that Bax initially coats the outer mitochondrial membrane before leaving and clustering with Bak molecules in a

position adjacent to the mitochondria. In addition, they showed that the Bax/ Bak clustering is caspase-independent but Bcl-X_L can inhibit cluster formation. While Bax cluster formation was shown to be caspase-independent, mitochondrial clustering was shown to be caspase-dependent (Fig. 3.4C), consistent with previous work in other cell types (De Vos *et al.*, 1998; Thomas *et al.*, 2000). Interestingly, in z-VAD-fmk treated neutrophils although the mitochondria were not clustered, Bax clusters were still seen in close association with nuclei, suggesting that perhaps Bax can also bind an as yet unidentified organelle or structure involved in the apoptotic program. Thus, Bax translocation is a marker of apoptosis upstream of the execution phase, since cells may still be rescued by the inhibition of caspases. Therefore, using Bax as a marker of upstream events would be a useful marker to determine whether Golgi fragmentation was occurring during the initiation phase or execution phase of apoptosis.

To date, no known studies have shown Golgi staining in neutrophils by indirect immunofluorescence. Using a monoclonal antibody raised against p115, I was able to detect the Golgi complex in freshly isolated neutrophils (Fig. 3.6). Unfortunately, identification of fragments of this relatively small Golgi complex in neutrophils would not have been readily achieved. Since Golgi fragmentation is thought to be an ubiquitous phenomenon to apoptosis, occurring in all cell types studied so far (Lane *et al.*, 2002; Philpott *et al.*, 1996; Sesso *et al.*, 1999), I used cell lines as a model for the study of Golgi morphology during apoptosis.

NRK cells have a large, reticular Golgi complex and all available antibodies specifically stain the Golgi in these cells (Fig. 3.5). Golgi fragmentation during mitosis can be clearly visualised in these cells (Fig. 3.7) and therefore this cell type was used to monitor Golgi morphology during apoptosis. In SSP induced apoptosis in NRK cells, it was shown that the Golgi fragmented. In addition, various stages of apoptosis were identified in terms of nuclear and Golgi morphology (Fig. 3.9). The nuclei condensed before finally fragmenting and the Golgi complex clustered prior to fragmentation in both apoptotic NRK and HeLa cells treated with SSP. At least in the SSP model of Golgi fragmentation in NRK cells, the Golgi fragmented prior to DNA fragmentation (Fig. 3.10), which is dependent on caspase activity (Enari *et al.*, 1998; Sakahira *et al.*, 1998). This finding suggested that Golgi fragmentation is a very early event in this model. To ensure that nuclear condensation was correlated with the onset of apoptosis and not due to SSP alone, we sought a second marker of apoptosis that was known as an early marker. PS exposure on the outer plasma

membrane is known as an early marker of apoptosis (Fadok *et al.*, 1992). However, NRK cells did not bind Annexin-V Alexa-488 reliably despite the presence of clearly apoptotic NRK cells by nuclear morphology. Since this seemed likely to be a peculiarity of NRK cells, I also examined HeLa cells treated with SSP that bound Annexin-V Alexa-488. However, in immunofluorescence analysis, PS exposure correlated with DNA fragmentation or pebbled nuclei, a relatively late event in apoptotic process and did not bind cells where the nucleus was condensed. Therefore, PS exposure was not a useful marker for determining if those cells with condensed nuclei were apoptotic.

Interestingly, the Golgi fragments produced during apoptosis in SSP treated HeLa cells are shown to be morphologically identical to those found in the cytoplasm of mitotic cells (Fig. 3.13). This finding is consistent with studies by (Sesso *et al.*, 1999). The similar size of vesicles present in mitotic cells and apoptotic cells raised the possibility that the mechanism leading to Golgi fragmentation was related.

Using a different stimulus to induce apoptosis, NRK cells were treated with CHX over 4 h to examine whether the Golgi also fragments with a different death stimulus. In addition, a newly available antibody, raised against anti-active caspase-3 antibody was used to detect the early stages of apoptosis. Caspase-3 activation was reported to occur earlier than PS exposure during apoptosis and therefore it was possible that this might precede Golgi fragmentation (Belloc *et al.*, 2000). Apoptotic NRK cells treated with CHX, where caspase-3 activity was detected also had, in most cases, fragmented Golgi (Fig. 3.15C). However, a few cells in the very early stages of apoptosis, preceding loss of adherence and shrinkage were observed (for example see Fig. 3.15B where the nucleus was condensed but the Golgi was still intact). In these cells, the Golgi structure is that of a cell in interphase, juxtanuclear and reticular but there is no evidence of clustering; yet caspase-3 is clearly activated. In the presence of z-VAD-fmk, Golgi fragmentation was inhibited and the morphology indistinct from interphase cells, suggesting that caspase-3 activation preceded Golgi and DNA fragmentation. In addition, in the CHX model of apoptosis in NRK cells, the 'condensed nucleus' morphology was a relatively seldom event, not because it never occurred but because in contrast to the SSP model, it seemed to be a very swift phase and therefore it was seen rarely.

There are several possibilities to explain the apparent differences in the kinetics of morphological apoptosis between the SSP and CHX model. The most obvious being

that in addition to the requirement for caspase activity to fragment DNA, through the cleavage of ICAD (Enari *et al.*, 1998; Sakahira *et al.*, 1998) that caspase-dependent kinase activity may be required. In the case of apoptosis induced by SSP, a broad-range kinase inhibitor, phosphorylation would be inhibited thereby slowing down the morphological changes characteristic of apoptosis. Several studies have reported that CDK activity is upregulated during apoptosis and in some models inhibition of CDKs actually inhibits apoptosis (Gil-Gomez *et al.*, 1998; Harvey *et al.*, 2000; Kim *et al.*, 2001). A number of these studies showed that inhibition of CDK activity reduced DNA cleavage (Hakem *et al.*, 1999; Schroter *et al.*, 1996; Shi *et al.*, 1994). Since SSP is a known inhibitor of CDK activity (Gray *et al.*, 1999) this may be one explanation for the relatively long period between chromatin condensation and visualisation of DNA fragments. Similarly, the 'clustered Golgi' morphology was hardly observed at all in the CHX model of apoptosis, suggesting that the rapid and complete fragmentation of the Golgi complex requires kinase activity and is delayed during SSP induced apoptosis. Since CDK1 is involved in Golgi fragmentation during mitosis, there was a possibility that this pathway of Golgi fragmentation was common to both apoptosis and mitosis. The MPM-2 monoclonal antibody recognises a phosphorylated amino-acid sequence present on more than 40 proteins during mitosis. Therefore, if major mitotic targets were phosphorylated during apoptosis then MPM-2 antibody would react positively (Davis *et al.*, 1983). However, immunofluorescence staining of apoptotic CHX treated NRK cells showed no positive MPM-2 staining. Certainly, this was not entirely unexpected since phosphorylation of all mitotic epitopes would be unlikely to accompany apoptosis. Although, CDK1 is one of many kinases involved in phosphorylating MPM-2 antigens it is by no means alone (Westendorf *et al.*, 1994). Among the kinases involved are MAP kinase, casein kinase II and polo-like kinases (Escargueil *et al.*, 2000; Logarinho & Sunkel, 1998; Westendorf *et al.*, 1994). In addition, while CDKs are active during apoptosis many of their substrates are thought to be different (O'Connor *et al.*, 2000) and importantly their regulation appears to be altered. In non-cycling thymocytes for example, Bcl-2 and Bax were shown to regulate Cdk2 activity. Where overexpression of Bcl-2 was shown to delay the degradation of the Cdk2 inhibitor, $p27^{KIP1}$ and Bax overexpression accelerated it (Gil-Gomez *et al.*, 1998). In summary, whilst these studies are suggestive of distinct kinetics of Golgi fragmentation during apoptosis induced with distinct stimuli, the ultimate outcome in both CHX and SSP induced apoptosis in NRK and HeLa cells is caspase-dependent fragmentation of the Golgi complex.

CHAPTER 4: THE MECHANISM OF GOLGI FRAGMENTATION

4.1 Introduction

The results in Chapter 3 showed that the Golgi complex fragmented during apoptosis in NRK and HeLa cells treated with different apoptosis-inducing agents and that this was inhibited by the broad-range caspase inhibitor z-VAD-fmk. One possibility is that Golgi-associated proteins are targeted in a caspase-dependent manner. This could involve caspase-dependent phosphorylation or direct cleavage of target proteins. GM130, GRASP65, GRASP55, p115 and Rab1 are phosphorylated during mitosis (Bailly *et al.*, 1991; Lin *et al.*, 2000; Lowe *et al.*, 1998; Sohda *et al.*, 1998), concomitant with the fragmentation of the Golgi complex and inhibition of ER to Golgi transport. Since these proteins are targets for phosphorylation during mitosis, it is possible that they are also key targets during apoptosis to initiate Golgi fragmentation.

GRASP65 is predicted to form a cytoplasmically orientated homodimer and is suggested to associate with Golgi membranes *via* an N-myristoylated N-terminus (Barr *et al.*, 1997). This is in contrast to GM130, which has no known domains or modifications that would allow direct interaction with Golgi membranes (Nakamura *et al.*, 1995). GM130 is a peripheral membrane protein, predicted to have six coiled-coil domains separated by spacer sequences and to bind GRASP65 *via* its C-terminus (Barr *et al.*, 1997). GM130 has 25 putative phosphorylation sites, excluding the CDK1 phosphorylation sites, 16 of which are possible casein kinase II sites (Nakamura *et al.*, 1995). GM130 is thought to form a homodimer that binds to the N-terminus of homodimeric p115, where p115's C-terminus forms a rod-like structure with a globular N-terminus (Barr *et al.*, 1997; Lowe *et al.*, 1998). However, only in the case of the interaction between GM130 and p115 has a direct consequence of mitotic phosphorylation been identified. Phosphorylation of GM130 on the *cis*-Golgi prevents binding of p115, present on COPI vesicles and therefore tethering of vesicles is inhibited prior to the action of SNAREs (Linstedt *et al.*, 2000; Lowe *et al.*, 1998). This discovery provided the first explanation for the high number of COPI vesicles present in the mitotic cytosol (Misteli & Warren, 1995).

Since GM130 is the principal binding partner for p115 and is key to vesicle tethering and therefore ER to Golgi transport, we followed the fate of GM130 during apoptosis

(Alvarez *et al.*, 2000; Linstedt *et al.*, 2000; Lowe *et al.*, 1998; Moyer *et al.*, 2001; Nakamura *et al.*, 1997; Seemann *et al.*, 2000).

Activation of caspase-8 through signalling *via* the Fas receptor can trigger two distinct apoptosis-inducing pathways depending on the cell type. In type I cells, a large amount of caspase-8 is able to activate caspase-3 directly (Scaffidi *et al.*, 1998). In contrast, in type II cells such as Jurkat cells, caspase-8 cleaves Bid and tBid then translocates to the mitochondria to induce formation of the apoptosome (Scaffidi *et al.*, 1998). It is thought that the relatively low amounts of caspase-8 present in type II cells are unable to initiate the caspase cascade directly (Scaffidi *et al.*, 1998). For these studies, J.CaM1.6 cells, a derivative of Jurkat cells that constitutively express Fas receptor, were treated with a monoclonal antibody raised against the human Fas-receptor so that we could induce apoptosis by a receptor-mediated pathway as well as by using SSP, which induces apoptosis through the stress pathway.

4.2 Results

4.2.1 Annexin-V-FITC Binding & PI Exclusion by J.CaM1.6 Cells Treated with CH11

To compare the induction of apoptosis by SSP to the induction of apoptosis by the CH11 anti-FasR monoclonal antibody, J.CaM1.6 cells were treated with 500ng/ ml of CH11. Fig. 4.1A is a representative example of untreated cells, where the majority of cells are Annexin-V –ve/ PI –ve. Figure 4.1B shows the SS/ FS properties of untreated J.CaM1.6 cells. J.CaM1.6 cells were treated with 500ng/ ml CH11 over 6 h. At 6 h, approximately 60% of cells were Annexin-V +ve/ PI -ve. The SS/ FS profile (Fig. 4.1D) of these cells is broadly similar to that of the Annexin-V –ve/ PI -ve population of J.CaM1.6 cells, suggesting that apoptotic cells remain intact and have not fragmented into apoptotic bodies. Cells that are Annexin-V +ve/ PI +ve can be seen to have different SS/ FS properties, suggesting that these may have fragmented into apoptotic bodies. Apoptosis, or Annexin-V-FITC binding was inhibited by pre-incubating cells with a neutralising antibody (clone ZB4), raised against human FasR (Fig. 4.1E), for 30 min prior to the addition of CH11. This experiment demonstrated that apoptosis was specific to the induction of the apoptotic Fas signalling pathway. Annexin-V-FITC binding was also inhibited by pre-incubating the cells with z-VAD-fmk (Fig. 4.1G), demonstrating that Annexin-V-FITC binding was caspase-dependent. The SS/ FS of cells treated with z-VAD-fmk and CH11 (Fig. 4.1H) did not differ noticeably from the control SS/ FS.

4.2.2 Annexin-V-FITC Binding & PI Exclusion by J.CaM1.6 Cells Treated with SSP

J.CaM1.6 cells were incubated at 5 x 10^6 cells/ ml in the presence of FCS, with or without 2μM SSP for different times, as indicated. Fig. 4.2(A) is a typical example of an untreated sample of J.CaM1.6 cells, where the vast majority of cells are Annexin-V -ve/ PI -ve. Fig. 4.2(B) shows a typical SS/ FS of untreated J.CaM1.6 cells over 4 h. J.CaM1.6 were treated with SSP over 4 h and samples taken every hour. At 4 h (Fig. 4.2B), ~80% of J.CaM1.6 cells were Annexin-V +ve/ PI –ve. Fig. 4.2(D), the Annexin-V +ve/ PI –ve cells (orange dots) show a different SS/ FS distribution to the

Annexin-V +ve/ PI-ve cells. However, there was no significant difference (p=0.05) in the amount of necrotic cells present per sample SSP treated cells compared to control values. J.CaM1.6 cells that were pre-incubated with z-VAD-fmk for 30 min prior to addition of SSP, did not undergo apoptosis, demonstrating that the effects of SSP were due to caspase activity (Fig. 4.2(E). Again, there was a slight increase in Annexin-V +ve/ PI+ve and Annexin-V –ve/ PI +ve cells but this was not statistically significant (p=0.05). Fig. 4.2(F) shows the FF/SS profile of those cells in Fig. 4.2(E), where again those cells which were Annexin-V +ve/ PI+ve have shifted to the left (orange dots).

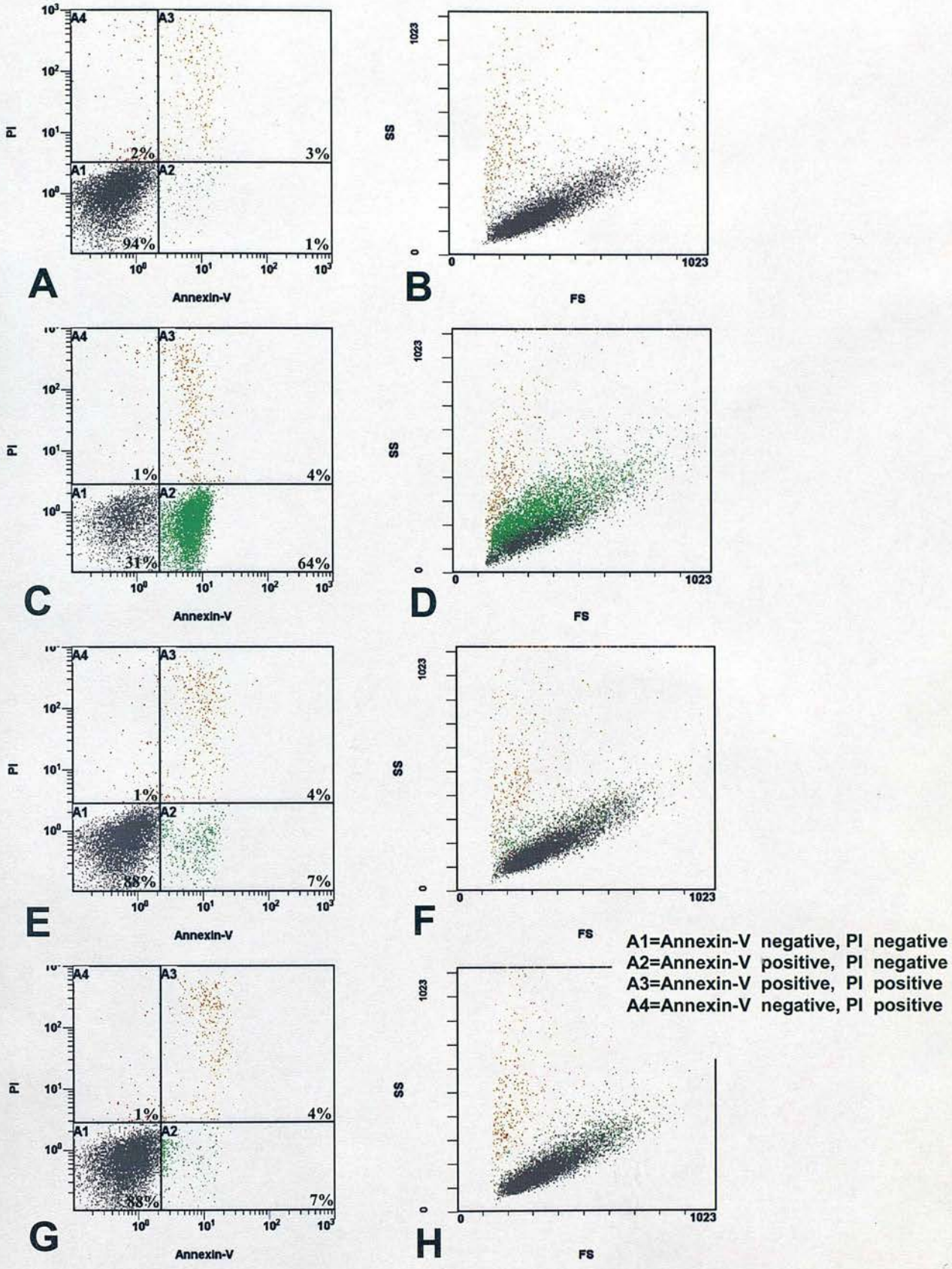

Figure 4.1: Anti-FasR (CH11, 500ng/ml) induced apoptosis in J.CaM1.6 cells. Apoptosis was assessed by Annexin-V binding and PI staining. (A) Untreated cells did not externalise Annexin-V and excluded PI. A scatter plot is shown (B) showing the non-apoptotic cell population distribution. After 6 hours, 64% of cells bound Annexin-V FITC but excluded PI (C). A small percentage of cells had undergone necrosis (PI +ve) and this was also seen as a shift in the SS/FS of those cells (D). ZB4 (E) and z-VAD-fmk (G) inhibited phosphatidylserine expression in CH11 treated cells, where (F) and (H) show the SS/FS. Data are representative of 3 experiments.

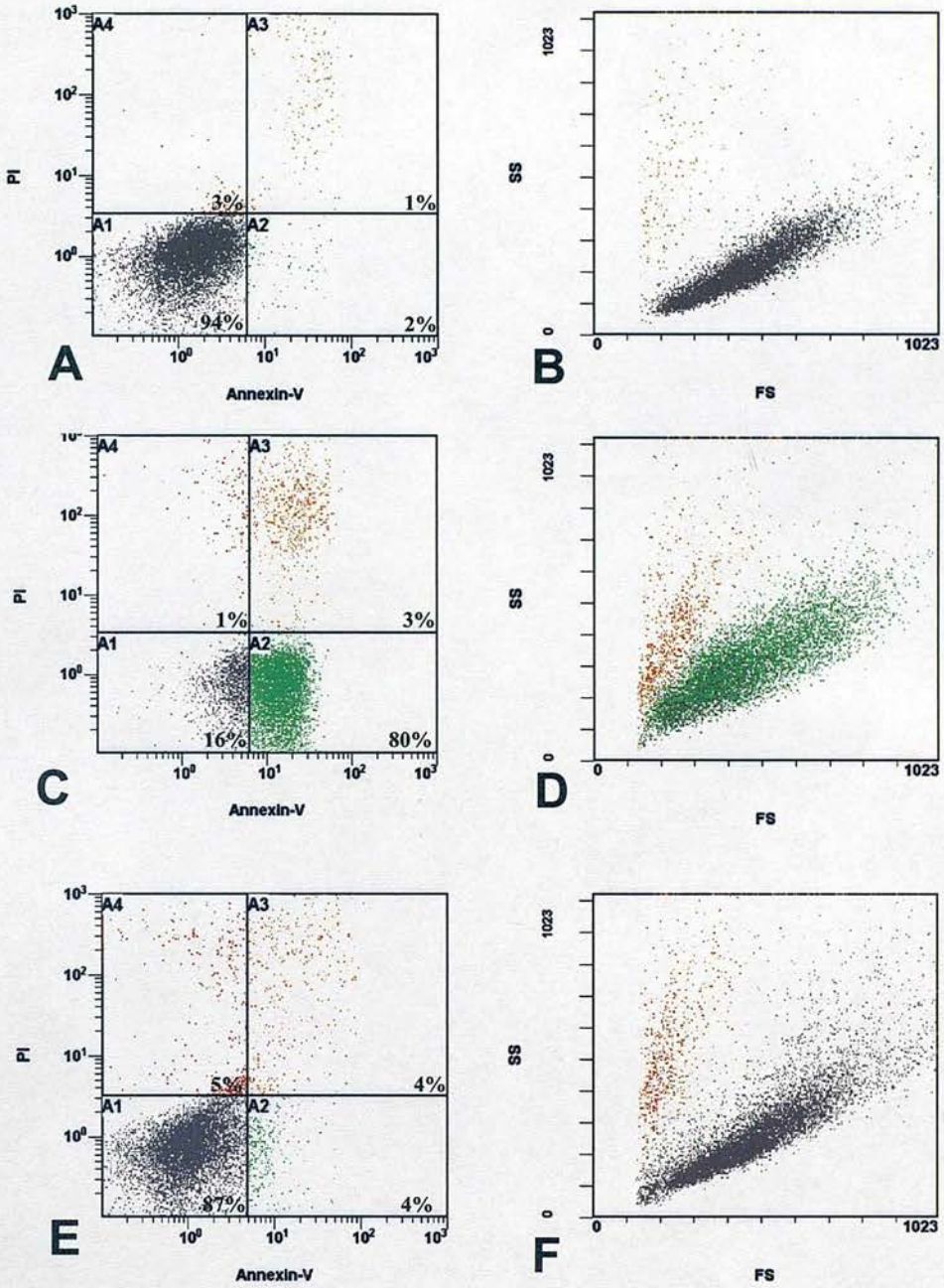

A1=Annexin-V negative, PI negative
A2=Annexin-V positive, PI negative
A3=Annexin-V positive, PI positive
A4=Annexin-V negative, PI positive

Figure 4.2: SSP (2μM) induced apoptosis in J.CaM1.6 cells. Apoptosis was assessed by Annexin-V binding and PI staining. (A) Untreated cells did not externalise Annexin-V and excluded PI. A scatter plot is shown (B) showing the non-apoptotic cell population distribution. After 4 hours, 80% of cells bound Annexin-V FITC but excluded PI (C). A small percentage of cells had undergone necrosis (PI +ve) and this was also seen as a shift in the SS/FS of those cells (D). z-VAD-fmk (E) inhibited phosphatidylserine expression in SSP treated cells, where (F) shows the SS/FS. Data are representative of 3 experiments.

4.2.3 Kinetics of Apoptotis J.CaM1.6 Cells Treated with CH11

J.CaM1.6 cells were treated with 500ng/ ml CH11 in the presence of FCS, over 6 h and the amount of apoptosis, as assessed by Annexin-V-FITC binding and PI exclusion, monitored at 1 hour, 2 h, 4 h and 6 h. At 1 h, the number of apoptotic cells was ~12%, significantly ($p < 0.05$) higher than present in control populations ~2%. The proportion of apoptosis increased up to 4 h, where the amount of apoptosis was ~60%, after which the rate of apoptosis began to decline. At 6 h, the number of apoptotic cells present was ~60%. To ensure the apoptosis inducing stimulus was by induction of the Fas pathway, control samples were pre-incubated with 500ng/ ml ZB4 for 30 min, prior to addition of CH11. ZB4 abolished the apoptotic effect of CH11 of J.CaM1.6 cells and the number of cells, which bound Annexin-V-FITC in these samples ~5% was not significant ($p < 0.05$) from control levels. In addition, z-VAD-fmk completely inhibited Annexin-V-FITC binding 3% which was not significantly ($p < 0.05$) different from control levels.

4.2.4 Kinetics of Apoptosis in J.CaM1.6 cells with SSP

To follow the kinetics of apoptosis induction in J.CaM1.6 cells by 2μM SSP, cells were incubated in the presence of 2μM SSP and FCS, over 4 h (Fig. 4.4). Samples were taken every hour and apoptosis assessed by Annexin-V-FITC binding and exclusion of PI. The results from three separate experiments were then pooled. At 1 hour, the number of apoptotic cells present, ~14%, was already significantly ($p < 0.05$) increased from control cells ~2%. This trend continued up to 4 h, where ~80% of cells bound Annexin-V-FITC and excluded PI. The effect was inhibited by z-VAD-fmk, where the number of cells ~4% binding Annexin-V-FITC was not significantly ($p < 0.05$) different from control levels.

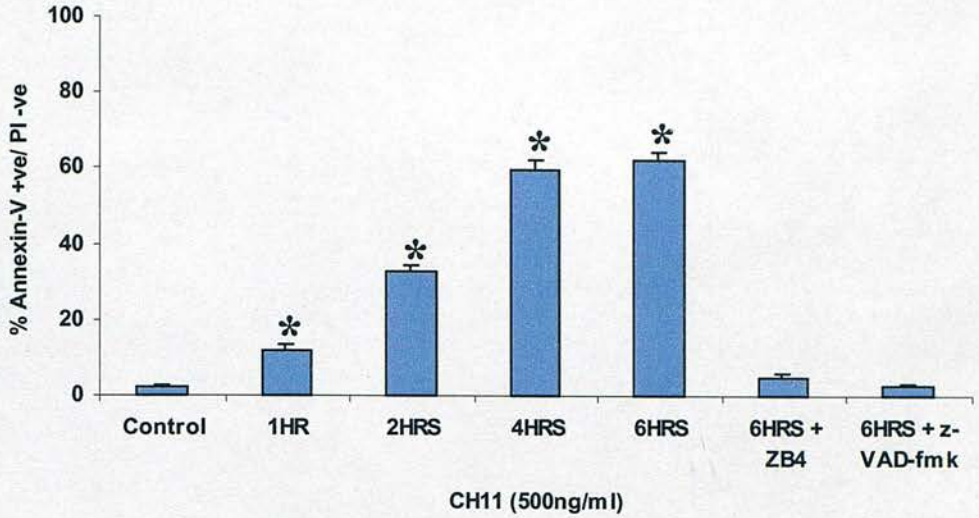

Figure 4.3: Kinetics of anti-FasR (CH11, 500ng/ml) induced apoptosis in J.CaM1.6 cells. Apoptosis was assessed by Annexin-V binding and PI exclusion. Data represent the mean ± SEM of 3 separate experiments. All experiments were performed in triplicate (* = $p < 0.05$ compared with control values).

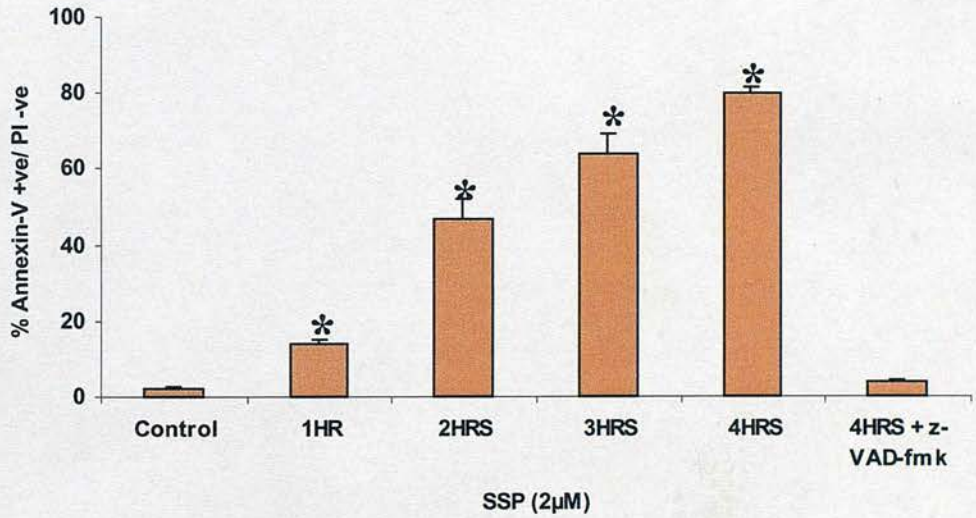

Figure 4.4: Kinetics of SSP (2µM) induced apoptosis in J.CaM1.6 cells. Apoptosis was assessed by Annexin-V binding and PI exclusion. Data represent the mean ± SEM of 3 separate experiments. All experiments were performed in triplicate (* = $p < 0.05$ compared with control values).

4.2.5 Golgi Fragmentation in Apoptotic J.CaM1.6 Cells Stained with a Monoclonal Antibody Raised Against GM130

To confirm that the Golgi also fragmented in apoptotic J.CaM1.6 cells, cells were treated with 500ng/ ml CH11 or 2μM SSP over 4 h to induce apoptosis. Apoptotic cells were identified by 'pebbled' nuclear morphology and by staining with the polyclonal antibody raised against active-caspase-3. No non-specific staining was detected in J.CaM1.6 cells stained with (Fig. 4.5A) rabbit IgG, Alexa 568 (red) and (Fig. 4.5B) mouse IgG, Alexa 488 (green). Untreated cells showing the normal interphase structure of the Golgi complex in J.CaM1.6 cells also had no caspase-3 activity. Caspase-3 activity was also absent in mitotic cells where the Golgi was fragmented (Fig. 4.5C, arrow). In contrast, many of the cells treated with 500ng/ ml CH11 (Fig. 4.5D-F) had caspase-3 activity throughout the cytoplasm and in those cells the nuclei were pebbled and the Golgi fragmented. In cells that had been pre-treated with the FasR neutralising antibody ZB4 or the caspase inhibitor z-VAD-fmk, apoptosis and Golgi fragmentation were prevented. This demonstrated that Golgi fragmentation and nuclear pebbling were specific to FasR signalling in CH11-treated cells and that the morphological changes observed were caspase-dependent. To compare the fragmentation of the Golgi complex during SSP induced apoptosis, J.CaM1.6 cells were treated with 2 μM SSP for 4 h. The proportion of apoptotic cells was higher in SSP treated cells than CH11 treated cells after 4 h with the majority of cells being apoptotic. From the kinetic studies, approximately 80% of SSP treated J.CaM1.6 cells are apoptotic at 4 h (Fig. 4.4). All cells where nuclear fragmentation was detected had caspase-3 activity yet strikingly, a large proportion of these cells still had intact Golgi (Fig. 4.5G-I). Since z-VAD-fmk inhibited DNA fragmentation and caspase-3 activity was not detected, the morphological changes observed were confirmed to be caspase-dependent and not due to broad-range kinase inhibition.

4.2.6 Golgi Fragmentation in Apoptotic J.CaM1.6 Cells Stained with a Monoclonal Antibody Raised Against p115

To confirm that J.CaM1.6 cells treated with SSP appeared to have a delay in the fragmentation of the Golgi complex, the immunofluorescence study was repeated but the Golgi complex stained with another Golgi-marker, a monoclonal antibody raised against p115. Untreated cells did not stain positively for anti-active-caspase-3 (Fig.

4.6A) and Golgi staining with anti-p115 had more punctate cytoplasmic staining compared to anti-GM130 staining (Fig. 4.6A-C), likely due to the fact that p115 is also vesicle-associated as well as to Golgi membranes (Sohda *et al.*, 1998). The same morphological pattern was observed in CH11-treated cells stained with anti-p115 as with anti-GM130. In all cells where caspase-3 is active, the nuclei are pebbled and the Golgi fragmented (Fig. 4.6D-F). Again, caspase-3 activation, nuclear and Golgi fragmentation could be inhibited by pre-incubation with ZB4 or z-VAD-fmk (Fig.4.6J&K). However, in SSP induced apoptosis, caspase-3 activity and pebbled nuclei did not necessarily coincide with fragmented Golgi (Fig. 4.6G-I) confirming the previous result when cells were stained with anti-GM130.

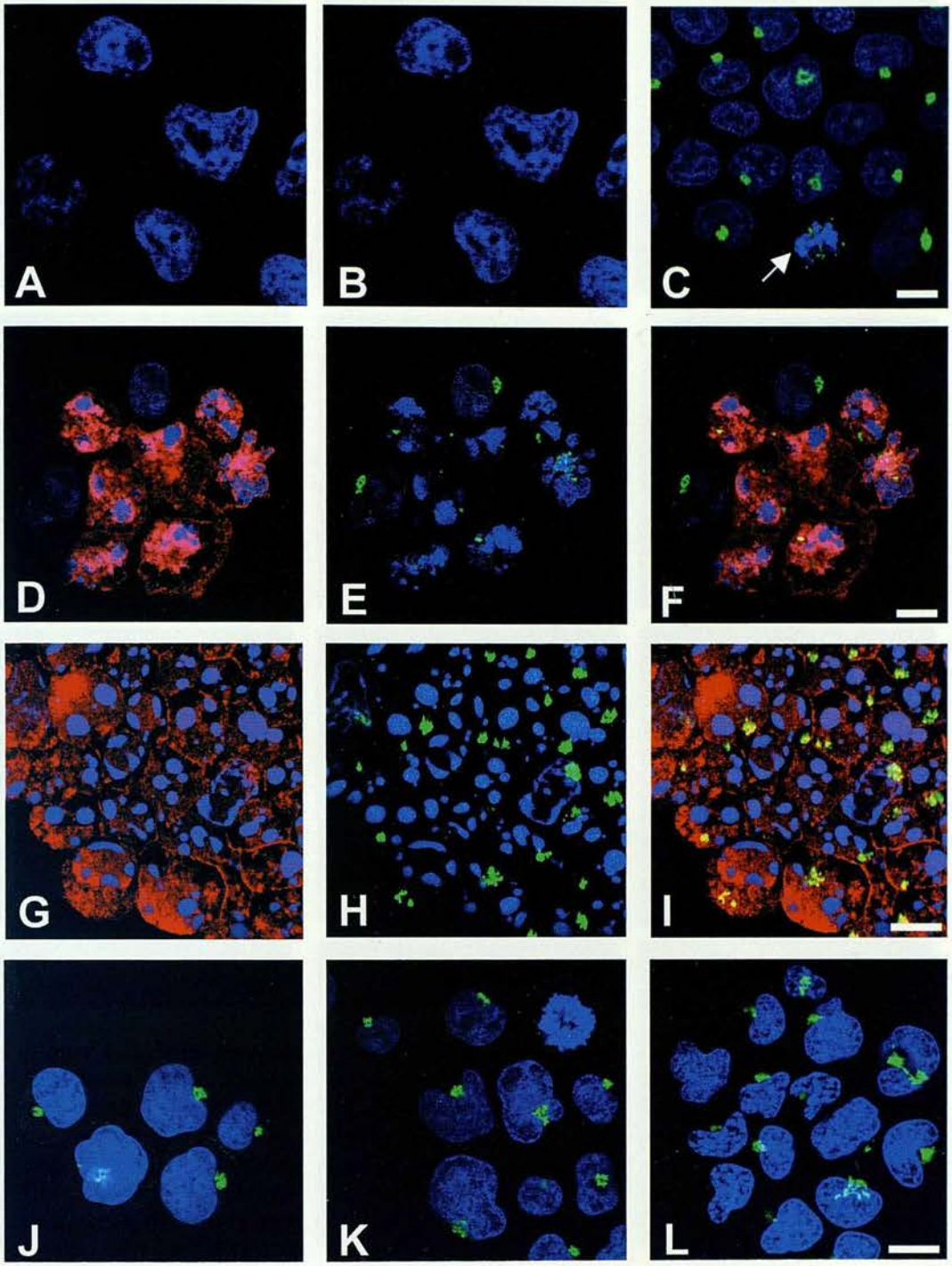

Figure 4.5: Golgi morphology in J.CaM1.6 cells treated with 500ng/ml CH11 or 2μM SSP for 4 hours. Cells were stained with anti-active-caspase-3, Alexa 568 (red) and anti-GM130, Alexa 488 (green) and the nuclei with TO-PRO-3 (blue). J.CaM1.6 cells stained with (A) rabbit IgG, Alexa 568 and (B) mouse IgG, Alexa 488. (C) Untreated cells stained with anti-GM130 and anti-active-caspase-3 (arrow indicates mitotic cell). Cells treated with 500ng/ml CH11 over 4 hours (D-F), where (D) shows anti-active-caspase-3, (E) shows anti-GM130 and (F) is the composite micrograph of (D&E). Cells treated with 2μM SSP over 4 hours (G-I), where (G) shows anti-active-caspase-3, (H) shows anti-GM130 and (I) is the composite micrograph of (G&H). Composite micrograph of cells treated with CH11 in presence of (J) ZB4, (K) z-VAD-fmk. Cells treated with SSP in presence of z-VAD-fmk (L). Data are representative of 3 separate experiments. Scalebars represent 10μm.

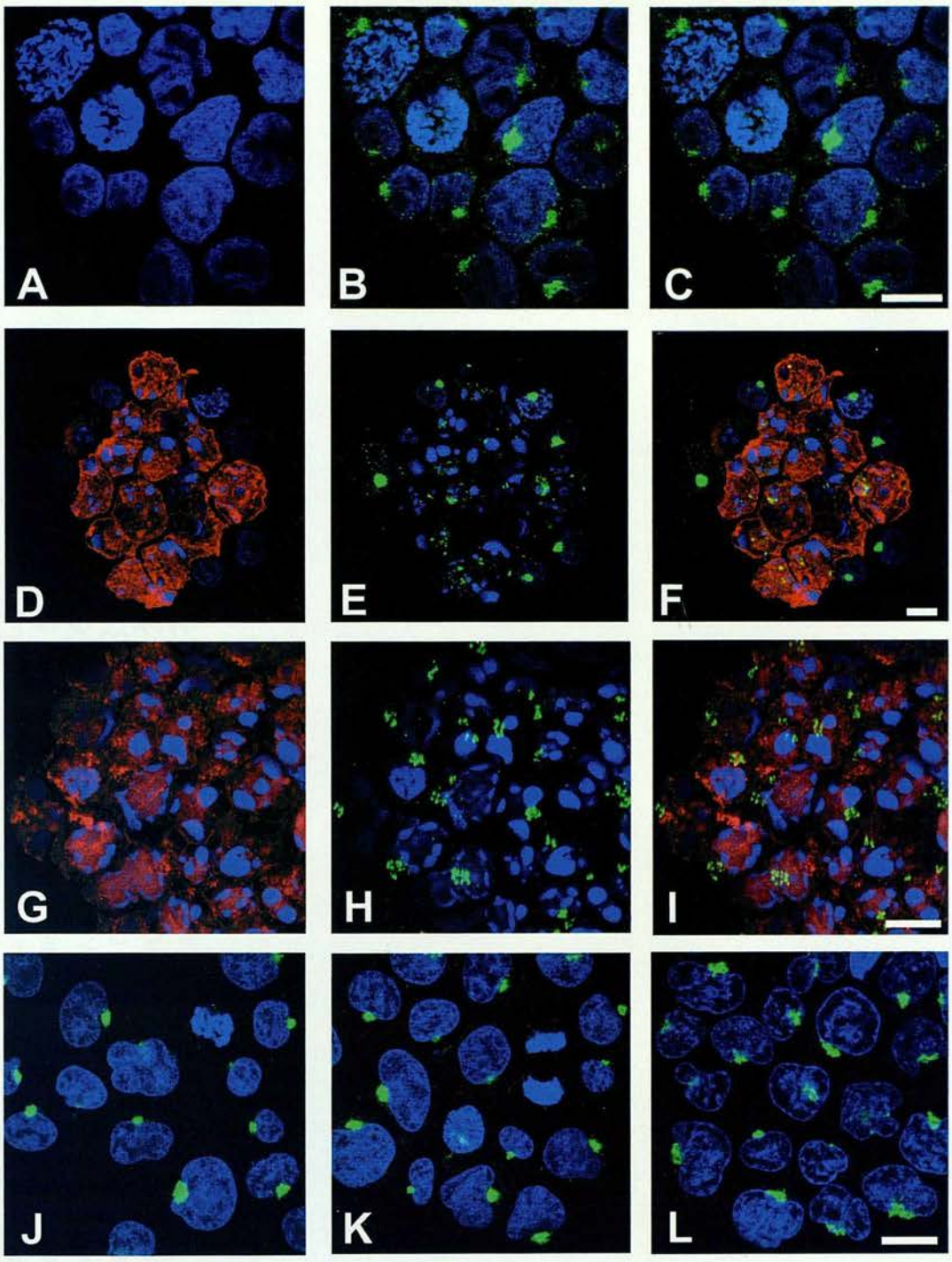

Figure 4.6: Golgi morphology in J.CaM1.6 cells treated with 500ng/ml CH11 or 2μM SSP for 4 hours. Cells were stained with anti-active-caspase-3 followed by Alexa 568 (red) and anti-p115 followed by Alexa 488 (green) and the nuclei with TO-PRO-3 (blue). (A-C) Untreated cells stained with anti-p115, where (A) shows anti-active-caspase-3 staining, (B) anti-p115 staining and (C) is the composite micrograph of (A&B). Cells treated with 500ng/ml CH11 over 4 hours (D-F), where (D) shows anti-active-caspase-3, (E) shows anti-p115 and (F) is the composite micrograph of (D&E). Cells treated with 2μM SSP over 4 hours (G-I), where (G) shows anti-active-caspase-3, (H) shows anti-p115 and (I) is the composite micrograph of (G&H). Composite micrographs of cells treated with CH11 in presence of (J) ZB4, (K) z-VAD-fmk. Composite micrograph of cells treated with SSP in presence of z-VAD-fmk (L). Data are representative of 3 experiments. Data are representative of 3 separate experiments. Scalebars represent 10μm.

4.2.7 GM130 is Cleaved During CH11 Induced Apoptosis

Immunofluorescence studies suggested that the kinetics of Golgi fragmentation in apoptotic cells treated with SSP were different to the kinetics of Golgi fragmentation in cells treated with CH11. Of particular interest was the fate of the Golgi matrix protein GM130 during apoptosis and the tethering factor p115, both shown to be essential for ER to Golgi transport (Allan *et al.*, 2000; Alvarez *et al.*, 1999; Lowe *et al.*, 1998; Lowe *et al.*, 2000; Nakamura *et al.*, 1997; Seemann *et al.*, 2000; Sohda *et al.*, 1998). J.CaM1.6 cells were incubated with 500ng/ ml of CH11 over 6 h and apoptosis and necrosis was assessed by Annexin-V and PI staining. After 1 h, when low levels of apoptotic cells were present (~7%), as assessed by Annexin-V binding, no evidence of GM130, p115 and pro-caspase-3 was seen (Fig. 4.7, lane 2) and comparable to untreated cells (Fig. 4.7, lane 1). Similarly, at 2 h, although apoptosis had increased to ~30%, GM130, p115, pro-caspase-3 and actin were still present (Fig. 4.7, lane 3). By contrast after 4 h, ~55% of cells were apoptotic and pro-caspase-3 was completely cleaved and there was a concomitant decrease in GM130 compared to control levels, although p115 and actin levels were similar to control (Fig. 4.7, lane 4). At 6 h, no further apoptosis was seen (~55%), when compared with 4 h. Interestingly, GM130 was almost completely cleaved, although p115 and actin levels (Fig. 4.7, lane 5) remained comparable to control levels. Pro-caspase-3 cleavage and apoptosis was inhibited by ZB4, a neutralising antibody to CH11, demonstrating that apoptosis was specific to anti-FasR (Fig. 4.7, lane 6). Pro-caspase-3 cleavage was also completely inhibited by z-VAD-fmk (Fig. 4.7, lane 7) and the rate of apoptosis, by Annexin-V binding, similar to control levels. GM130 cleavage was inhibited by both ZB4 and z-VAD-fmk, demonstrating that this was specific to anti-FasR induced apoptosis and caspase-dependent.

4.2.8 GM130 Cleavage is Inhibited During SSP Induced Apoptosis

To investigate the apparent morphological differences between the kinetics of Golgi fragmentation in CH11 and SSP induced apoptosis, we followed the fate of GM130 and p115 in SSP induced apoptosis in J.CaM1.6 cells. J.CaM1.6 cells were incubated with 2μM staurosporine over 4 h and apoptosis assessed by Annexin-V-FITC binding and exclusion of PI. After 1 hour, ~13% of cells were apoptotic, compared to ~2% in untreated cells but GM130, p115 and pro-caspase-3 were not

affected (Fig. 4.8, lane 2) and comparable to untreated cells (Fig. 4.8, lane 1). By 2 h however, the rate of apoptosis had increased to ~54% and procaspase-3 was no longer detected but GM130, p115 and actin were not diminished (Fig. 4.8, lane 3). After 3 and 4 h, despite procaspase-3 processing and ~ 80% apoptosis, GM130 was still not cleaved and comparable to untreated cells (Fig. 4.8, lanes 4 & 5). Pro-caspase-3 cleavage was completely inhibited by z-VAD-fmk and the rate of apoptosis, by Annexin-V-FITC binding, similar to control levels. GM130 is therefore resistant to caspase-dependent cleavage in the presence of SSP, perhaps reflecting the apparent inhibition of Golgi fragmentation by morphology in SSP treated J.CaM1.6 cells.

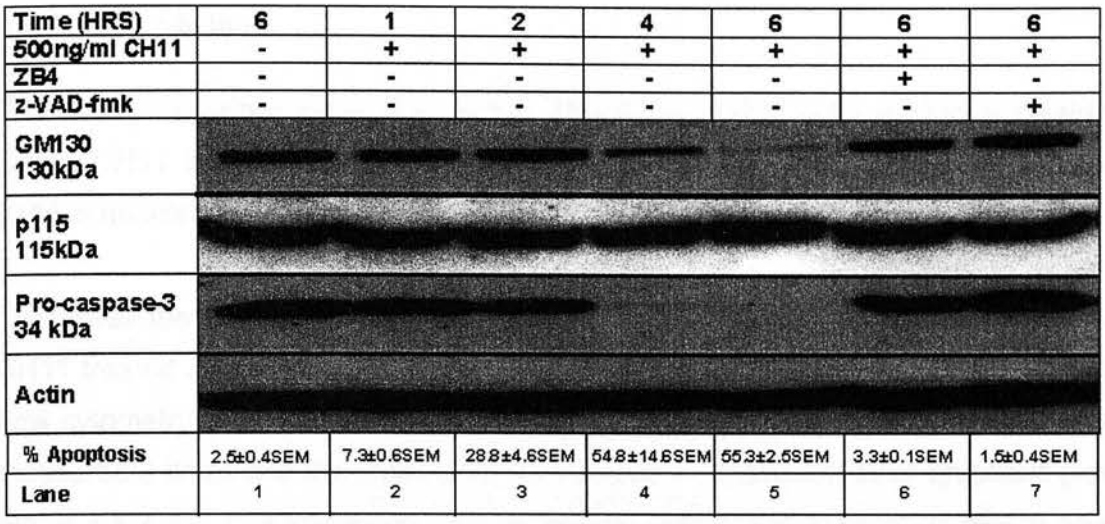

Figure 4.7: GM130 is cleaved during CH11 induced apoptosis in J.CaM1.6 cells. J.CaM1.6 cells were incubated at 2.5 x 10^6 cells/ ml in whole RPMI 1640 with or without 500ng/ml CH11 over 6 hours and samples solubilised in SDS lysis buffer. Nitrocellulose was probed with the monoclonal antibodies GM130, p115, pro-caspase-3 and actin. Lane 1: Untreated cells. Lane 4: procaspase-3 is cleaved and there is some cleavage of GM130. Lane 5: GM130 is almost completely cleaved and this effect is inhibited by ZB4 (Lane 6) and by z-VAD-fmk (Lane 7). % Apoptosis: Annexin-V-FITC binding/ PI exclusion was monitored and data represent the mean ± SEM of triplicate samples. Data are representative of 3 separate experiments.

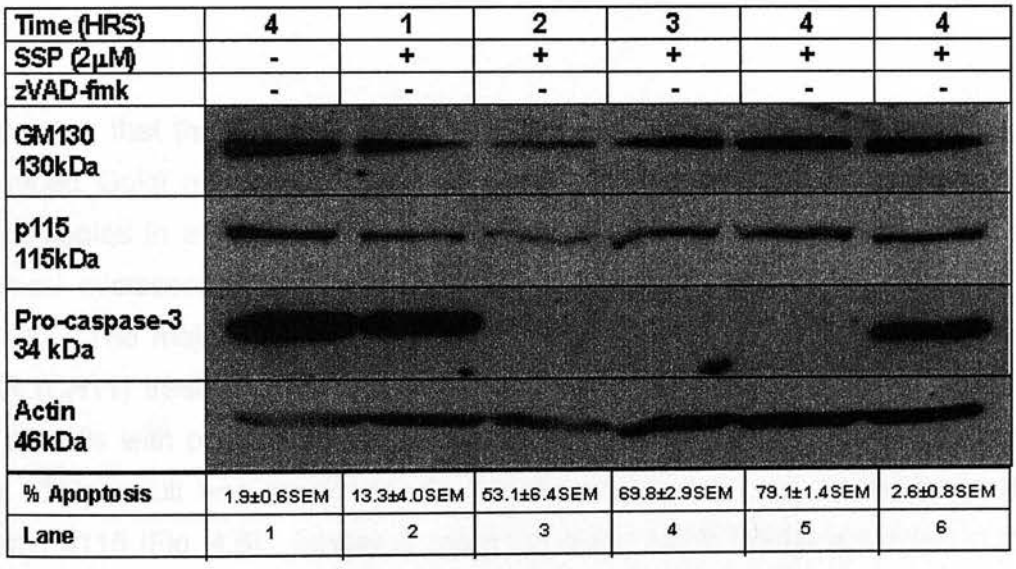

Figure 4.8: GM130 Cleavage is inhibited during SSP induced apoptosis in J.CaM1.6 cells. J.CaM1.6 cells were incubated at 2.5 x 10^6 cells/ ml in whole RPMI 1640 with or without 2µM SSP over 4 hours and samples solubilised in SDS lysis buffer. Nitrocellulose was probed with the monoclonal antibodies GM130, p115, pro-caspase-3 and actin. Lane 1: Untreated cells. Lane 3: procaspase-3 is cleaved but both GM130 and p115 are similar to untreated cells. Lane 5: GM130 is is not cleaved despite almost 80% apoptosis. Lane 6: pro-caspase-3 cleavage was inhibited by z-VAD-fmk. % Apoptosis: Annexin-V-FITC binding/ PI exclusion was monitored and data represent the mean ± SEM of triplicate samples. Data are representative of 3 separate experiments.

4.3 Discussion

The results described within this chapter show that GM130 but not p115 is cleaved during CH11 induced apoptosis in J.CaM1.6 cells. However, neither GM130 nor p115 is affected in SSP induced apoptosis over 4 h.

To assess the rate of apoptosis and to ensure the absence of necrosis in SSP or CH11 treated J.CaM1.6 cells we measured Annexin-V-FITC binding/ PI exclusion by flow cytometry (Fig. 4.1 & 4.2). The kinetics of apoptosis using both stimuli, were measured 3 times and the data pooled to establish a kinetic profile of apoptosis (see Fig. 4.3 & 4.4). It is interesting to note that the rate of apoptosis in J.CaM1.6 cells following Fas ligation appeared to decrease between 4 and 6 h, whereas in SSP-treated cells the rate of apoptosis was time dependent. One possible explanation for this is that in CH11 treated populations dividing cells could still be observed, whereas in SSP treated cultures mitotic cells were absent. In both SSP and Fas induced apoptosis, Annexin-V-FITC binding was inhibited by z-VAD-fmk, demonstrating that PS externalisation was caspase-dependent in this system. Additionally, in CH11 treated J.CaM1.6 cells, ZB4 a neutralising antibody raised against the FasR, was able to prevent PS exposure demonstrating that apoptosis was specific to the Fas pathway.

To confirm that the Golgi also fragmented during apoptosis in J.CaM1.6 cells, we examined Golgi morphology by indirect immunofluorescence. Surprisingly, Golgi morphologies in apoptotic J.CaM1.6 cells treated with CH11 and SSP differed by confocal microscopy when stained with a monoclonal antibody raised against rat GM130. The majority of cells that stained positively for active-caspase-3 in anti-FasR (CH11) treated cells had fragmented Golgi. In contrast, in SSP treated cells not all cells with positive anti-active-caspase-3 staining had fragmented Golgi (Fig. 4.5). This result was confirmed when cells were stained with an antibody raised against p115 (Fig. 4.6). However, since full Golgi fragmentation did occur in many cells treated with SSP, it is likely that while the kinetics and sequence of cleavage of key Golgi proteins differ, ultimately cleavage of Golgi substrates must take place. To delineate the underlying mechanism behind this apparent difference in the kinetics of Golgi fragmentation, we followed the fate of two of the proteins that are known targets during mitotic Golgi fragmentation, p115 and GM130, for which antibodies were commercially available.

GM130 but not p115 was identified as a target for caspase cleavage during CH11 induced apoptosis in J.CaM1.6 cells (Fig. 4.7). Pro-caspase-3 was no longer detected at 4 h (Fig. 4.7, lane 5), suggesting that most of pro-caspase-3 had been proteolytically processed and activated. There was a concomitant reduction in GM130 detection with pro-caspase-3 detection at 4 h (Fig. 4.7, lane 5). At 6 h, there was a further decrease in GM130 detected despite a slowed rate of apoptosis (Fig. 4.7, lane 5). This was not due to non-specific proteolysis since p115, nor actin was affected. ZB4 inhibited GM130 and pro-caspase-3 cleavage showing that the apoptosis observed was specific to CH11 (Fig. 4.7, lane 6). Furthermore, cleavage of procaspase-3 and GM130 was completely inhibited by z-VAD-fmk, demonstrating that GM130 cleavage was caspase-dependent (Fig. 4.7, lane 7). However, in SSP induced apoptosis neither GM130 nor p115 was cleaved in spite of a significantly higher percentage of apoptosis (~25%) at 4 h than in CH11 treated cells at 6 h. More specifically, despite cleavage of pro-caspase-3 at 2 h (Fig. 4.8, lane 3) and ~80% apoptosis after 4 h, GM130 was not cleaved and the band intensity comparable to non-apoptotic cells. This was in direct contrast to CH11 treated cells, where after 6 h ~55% of cells were apoptotic and yet the band intensity was significantly reduced compared to control.

The monoclonal antibody used to detect GM130 (986 a.a.), was raised against the c-terminal region of rat-GM130 (a.a. 869-982) (Nakamura *et al.*, 1997). Since no cleavage products were detected (Fig. 4.7), it is predicted that GM130 is cleaved at the c-terminal portion, very close to the antibody binding region. This would explain the lack of a cleavage product since the resulting C-terminal fragment would be too small to detect on a 8% polyacrylamide gel. If GM130 is cleaved prior to the antibody binding region as predicted, GM130 would no longer be able to associate with GRASP65, since the GRASP65 binding region is at the very C-terminal portion (Fig. 4.9) (Barr *et al.*, 1998) and thus no longer be able to bind Golgi membranes during apoptosis. Interestingly, in a recent study using a truncated form of GM130, which lacks the GRASP65 binding site but contains the p115 binding site, truncated GM130 did not associate with Golgi membranes. In fact, truncated GM130 became associated with the early intermediate compartment (IC) through its interaction with p115 (Marra *et al.*, 2001). In addition, cells transfected with GM130 containing the GRASP65 binding region but not the p115 binding region, had a significantly reduced capacity to deliver protein cargo from the ER to the Golgi complex (Marra *et al.*,

2001). This suggests that any disruption of the p115-GM130-GRASP65 interaction leads to an inhibition of protein transport.

There are at least two possibilities to explain the inhibition of GM130 cleavage during SSP induced apoptosis. Firstly, SSP could be inhibiting an upstream kinase-dependent apoptotic pathway. Secondly, SSP could prevent caspase-dependent phosphorylation of GM130, necessary for cleavage during apoptosis. From mitotic studies of GM130 and p115 interactions, it was shown that CK1 phosphorylates GM130 rendering p115 unable to bind, thus contributing to the inhibition of ER to Golgi transport (Linstedt *et al.*, 2000; Nakamura *et al.*, 1997; Seemann *et al.*, 2000). CDK activity has also been reported to be activated during apoptosis and in some systems appears to be necessary for apoptosis (Choi *et al.*, 1999; Gil-Gomez *et al.*, 1998; Hakem *et al.*, 1999; Harvey *et al.*, 2000; Kim *et al.*, 2001; Ojala *et al.*, 2000; Takizawa & Morgan, 2000). p115 can be inhibited from binding Golgi membranes in a cell-free system, when mitotic cytosols are treated with staurosporine, or the specific CDK inhibitors, olomoucine and roscovitine prior to incubation with Golgi membranes (Levine *et al.*, 1996). Therefore it is possible, although the MPM-2 antibody does not react to apoptotic cells, that CDK activity is nevertheless responsible for GM130 phosphorylation in apoptotic cells and that this phosphorylation event is required for efficient caspase cleavage. Cells treated with SSP however, would be unable to phosphorylate GM130 due to inhibition of CDK1 and hence the kinetics of Golgi fragmentation would be slowed.

As mentioned in the introduction, GM130 has 25 putative phosphorylation sites, excluding the CDK1 phosphorylation sites. 16 of those sites are possible casein kinase II sites (Nakamura *et al.*, 1995). However, it is unlikely that casein kinase II is involved in the SSP-mediated inhibition of GM130 cleavage since its activity is not inhibited by SSP (Meggio *et al.*, 1995). In any case, it will be necessary to determine whether direct phosphorylation of GM130 is required for its cleavage by caspases in the first instance.

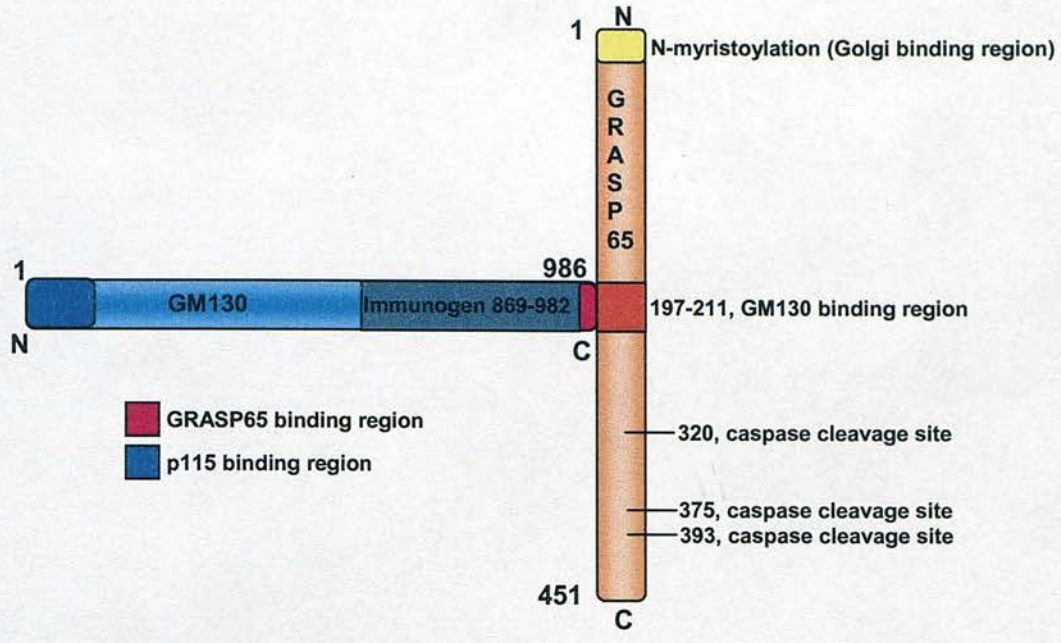


```
1   mseetrqskl aaakkklrey qqknspgvpa gakkkkkikn ghspertsas dcqsaenvpt
61   dhtapappst aaatmflgvv pspdadliqs hdagncsnll eetktfsste slrqlsqqln
121 glvsestsyi ngegltssnm kelesryqel avaldssyvt nkqlsstiee lkqqnqdtld
181 qlekekkdyq qklakeqgal reqlqvhiqt igilvsekae lqtalahtqq aarqkagese
241 dlasrlqssr qrvgelertl stvstqqkqa drynkdltke rdalklelyk ngksnedlrq
301 qnseleeklr vlvaekaaaq lgaeelqkkl emselllqqf ssqseasgsn eqlqqameer
361 aqleshvgql meslkqlqve rdqyaenlkg esamwqqrvq qmaeqvhalk eekeqresqv
421 qeleaslael rsqmeepppp epptgpseae erlqqeveql qkelegltgq lraqvqdnes
481 lshlnreqeg rmlelereaq hwseqaeerk qilesmqsdr ttisralsqn relkeqlael
541 qngfvrltne nmeitsalqs eqhvkkelar klgelqerlg elketvelks qeaqglqeqr
601 dqclshlqqy aaayqqhlta yeqltsekea lhkqlllqtq lmdqlqheev qgkmaaemar
661 qelqeaqerl kassqenqql qaqlsllvlp gedmdqeeqd eevpqpslti pedlvsream
721 vafcnaaiar aeeeqarlrv qlreqkarcr slahlaapvq sklekeavvp rdmgdsvsee
781 snqalhvame klqsrflevm qekvelkerv eelehcciql sgetdtigey ialyqnqrav
841 lkarhlekee yisrlaqdke emkvkllelq elvlrlvner newqgkflav sqnpadvpap
901 vptgsqefga adqqgdlrev sladdtepaq geagvpapqe nptaqqimql lreiqnpqer
961 pglgsnpcip ffyradende vkimvi
```

Figure 4.9: GM130-GRASP65 interaction and amino acid sequence of GM130 (Rattus norvegicus). (NP_072118, National Centre for Biotechnology Information (NCBI)). The GM130 monoclonal antibody was raised against amino acids 869-982 (gray text), blue text = p115 binding region, underlined blue text=putative CDK1 phosphorylation sites, pink text = GRASP65 binding region. Caspase- cleavage sites on GRASP65 are indicated in schematic of GM130-GRASP65 interaction.

Recently, it was shown that GRASP65, a Golgi stacking protein, was cleaved by caspase-3, contributing to Golgi fragmentation during apoptosis (Lane *et al.*, 2002). Furthermore, it was shown that GRASP65 is cleaved after the GM130 binding region, to a 30-35kDa fragment during apoptosis in SSP treated NRK cells. Whether the cleaved form of GRASP65 could still bind GM130 was not assessed. Cleavage of GRASP65 was shown to be mediated by caspase-3 *in vitro*, where incubation of Golgi membranes with apoptotic cytosol obtained from caspase-3 deficient MCF-7 cytosols had no GRASP65 cleavage. NRK cells were treated with 1μM SSP for 4 h and using a polyclonal antibody against GM130 and monoclonal against GRASP65, the authors showed that immunofluorescence staining of GRASP65 was diminished as compared to the fluorescence staining of GM130 in the same cell. However, this is not surprising since in the studies shown herein, where J.CaM1.6 cells were treated with CH11, GM130 was shown to be cleaved but this was inhibited by SSP. Although, the evidence the authors presented for GRASP65 cleavage was compelling, it is likely that SSP also inhibits GM130 cleavage in their system. Furthermore, using HeLa cells transfected with a mutant form of GRASP-65-GFP, resistant to caspase-3 cleavage, it was shown that Golgi fragmentation in these cells was slowed down.

It was also shown that GRASP65 cleavage occurs prior to Golgi fragmentation in SSP treated cells (Lane *et al.*, 2002). These studies on the kinetics of Golgi fragmentation were performed using NRK cells treated with SSP. Inherently problematic in the chosen system is the 'unknown factor', where multiple signalling pathways must be inhibited. The question to answer would be: 'does GM130 cleavage precede GRASP-65 cleavage in a physiologically relevant model of apoptosis?' Golgi fragmentation may in actual fact be initiated prior to GRASP-65 cleavage in a more physiologically relevant model of apoptosis. For example, it is possible that in CH11-mediated apoptosis, GM130 is cleaved prior to GRASP-65, leading to the inability of COPI vesicles to bind and the accumulation of COPI vesicles in the cytosol. More importantly, in this model of Golgi fragmentation during apoptosis, GM130 cleavage would likely result in an inhibition of ER to Golgi transport. Interestingly, a mutant form of GM130, lacking the GRASP65 binding region was found to be unable to associate with the *cis*-Golgi (Marra *et al.*, 2001). Since GRASP65 is cleaved after the GM130 binding region, it is possible that this does not affect the GM130-GRASP65 binding interaction and hence incoming COPI vesicles would still be able to associate with the *cis*-Golgi (Fig. 4.9). In *in vitro* studies the interaction between GM130 and GRASP65 was not affected by the

deletions of the C-terminus of GRASP65 to positions 237 or 314 (Barr *et al.*, 1998). Considering that caspase-mediated cleavage of GRASP65 was shown to be at positions 320, 375 and 393 (Fig. 4.9) it is unlikely that this would have a significant impact on ER to Golgi transport (Lane *et al.*, 2002). In support of this, the authors claimed that GM130 and p115 remained associated with Golgi membranes during apoptosis. Furthermore, they concluded that GM130 and p115 were therefore not involved in the morphological changes observed in Golgi structure during apoptosis. Intuitively, it seems that GRASP65 cleavage would not result in an increase in COPI vesicles in the cytosol of apoptotic cells, whereas GM130 cleavage would. Therefore, the exact significance of GRASP65 cleavage during apoptosis remains to be determined.

In summary, GM130 was identified as a key target for caspase-mediated cleavage during apoptosis induced by CH11 but not SSP in J.CaM1.6 cells. GM130 is also a major target during mitosis, where its phosphorylation renders p115 unable to bind. Disruption of the GM130-p115 interaction, has been shown to inhibit ER to Golgi transport (Marra *et al.*, 2001). Therefore, we sought to directly study delivery of protein cargo from the ER to Golgi to plasma membrane in apoptotic cells (Chapter 5).

CHAPTER 5: ER TO GOLGI TRANSPORT DURING APOPTOSIS

5.1 Introduction

During mitosis, the Golgi fragments into thousands of vesicles, coinciding with an arrest of ER to Golgi transport. Golgi fragmentation was also shown to occur during apoptosis (Chapter 3). One of the key proteins, GM130, involved in vesicle tethering during ER to Golgi transport was shown to be cleaved, during Fas-induced apoptosis in J.CaM.1.6 cells (Chapter 4). Cleavage of GM130 may result in an inability to bind GRASP65, associated with the *cis*-Golgi. This suggests that vesicle tethering and therefore ER to Golgi transport is inhibited during apoptosis.

The Vesicular Stomatitis Virus (VSV) is a small negative-stranded RNA virus and has been used extensively in the past to study the constitutive secretory pathway (Robbins *et al.*, 1977; Tabas & Kornfeld, 1978). The VSV genome encodes five proteins of which there is only one glycoprotein that forms part of the membrane of the mature virion. During infection, the VSV glycoprotein (VSVG) is synthesised using host cell machinery and is transported through the constitutive secretory pathway (Lenard, 1978). Like the many secretory proteins, VSVG is subject to oligosaccharide processing in the ER and Golgi complex (Tabas & Kornfeld, 1978).

The role of oligosaccharide addition in the ER appears to be mainly related to quality control, especially in promoting correct protein folding (Helenius, 1994). Most proteins destined for secretion or the plasma membrane, are subject to carbohydrate modification. Mature glycoproteins are structurally diverse and vary between cell type and species. Addition of glycans begins in the ER, often as the protein is still being synthesised by the ribosome (Helenius & Aebi, 2001). Fourteen sugar oligosaccharides are added cotranslationally to the growing polypeptide chain, which is translocated into the ER lumen through a translocation pore. The core 14 sugar oligosaccharide is composed of N-acetylglucosamine, mannose and glucose. Transfer of core oligosaccharides is mediated by the ER enzyme oligosaccharyltransferase, which recognises the Asn-X-Ser/ Thr sequence, where X is any amino acid except proline (Silberstein & Gilmore, 1996). Also, immunoglobulin heavy chain binding protein (BiP), a member of the Hsp70 chaperone family and the oxidoreductase protein-disulfide isomerase (PDI) associate either co-translationally, or posttranslationally to accommodate protein folding (Mori, 2000). After the addition of the core oligosaccharide, glucose and mannose residues are removed by ER

resident glucosidases and mannosidases (Kornfeld & Kornfeld, 1985). Oligosaccharide addition and processing in the ER is relatively homogeneous from protein to protein, it is in the Golgi where further carbohydrate processing results in the diversity of N-linked glycoproteins (Helenius & Aebi, 2001). Glycosylation of proteins renders them subject to the calnexin-calreticulin cycle, which is essential to ensure proper protein folding and oligomerisation (Parodi, 2000). After removal of two of the attached glucoses by glucosidases I and II, monoglycosylated glycans are recognised by the molecular chaperones calnexin and/ or calreticulin. Calnexin is a type I transmembrane protein located in the ER, while its homologue, calreticulin is a soluble protein of the ER lumen (Parodi, 2000). Erp57, a member of the PDI family, then binds to the calnexin/ calreticulin/ protein complex promoting the formation of correctly paired disulfide bonds (Frickel *et al.*, 2002). Removal of the third glucose residue results in the dissociation of this complex and if correctly folded, the protein is no longer recognised by glucosyltransferase and lacking any glucose residues, it will no longer bind to calnexin or calreticulin (Cannon & Helenius, 1999; Parodi, 1999; Parodi, 2000). Correctly folded proteins are then transported from the ER to the Golgi complex, where further oligosaccharide trimming takes place and also is the site of O-glycosylation (Roth, 1987).

Carbohydrate processing in the Golgi complex results in the generation of three major N-linked glycoprotein families: 1. high mannose type: contains all mannose outside the core oligosaccharide. 2. hybrid type: contains N-acetylglucosaminyl (GlcNAc) and galactose (Gal) in addition to mannose residues 3. complex type: contains no mannose residues outside the core structure but may contain N-acetyl galactosaminyl (GalNAc), fucose and sialic acid outwith the core structure (Helenius & Aebi, 2001). The VSVG obtains two complex N-linked oligosaccharides as it reaches the Golgi complex (Reading *et al.*, 1978). It is this feature that has made it so useful for ER to Golgi transport studies. Using the enzyme endoglycosidase H (Endo H), it is possible to distinguish between the ER and the Golgi forms of the VSVG. Endo H will cleave the mannose-rich oligosaccharides of the VSVG, but not the complex type oligosaccharides that it acquires after processing in the Golgi complex. Cleavage of the mannose-rich oligosaccharides, attached to the VSVG, results in a clear reduction in molecular weight (Robbins *et al.*, 1977).

To demonstrate that ER to Golgi transport was inhibited during mitosis, synchronised Chinese hamster ovary (CHO) cells, blocked in mitosis were infected with VSV (Warren et al., 1983). In transport studies where VSV was used as a tool to study

the constitutive secretory pathway, VSV infected ~90% of cells as standard. Cells were then labelled with [^{35}S-methionine] and the radiolabelled VSVG protein was digested with Endo H and immunoprecipitated. Subsequent autoradiographs showed that in mitotic cells there was a reduction in the molecular weight of VSVG, compared to interphase cells where the VSVG was resistant to Endo H digestion. This demonstrated that during mitosis, VSVG is not transported out of the ER where the ER form is sensitive to Endo H digestion after extraction from whole cells, whereas in interphase cells the VSVG is transported to the cell surface through the Golgi apparatus, where it becomes resistant to Endo H processing due to carbohydrate modifications.

To investigate whether ER to Golgi transport is also inhibited during apoptosis as in mitosis, by biochemical means, the same method should be employed. However, it was shown that VSV infection results in the induction of apoptosis in HeLa cells by 4 h and by 10 h over 80% of cells were apoptotic (Koyama, 1995). Since most methods of inducing apoptosis require incubations of several h with the apoptotic stimuli, the use of whole virus infection for apoptotic studies should be avoided. The VSVG gene is also available in an expression vector and the use of transfection with this expression vector would circumvent any possible problems associated with infection of cells with whole virus. However, obtaining equivalent transfection efficiencies of 95%, as is achieved during whole virus infection would be difficult. In addition, VSV mutational studies resulted in the generation of a temperature-sensitive form of VSVG, designated VSVGts045 that is not transported from the ER at 39°C, but at 32°C is folded properly, able to exit the ER and be transported to the plasma membrane through the Golgi normally (Gallione & Rose, 1985). While, as a tool, the temperature sensitive VSVG is superior to non-temperature sensitive VSVG, careful monitoring of apoptosis would be necessary since the accumulation of unfolded VSVG in the ER could likely induce apoptosis *via* the UPR.

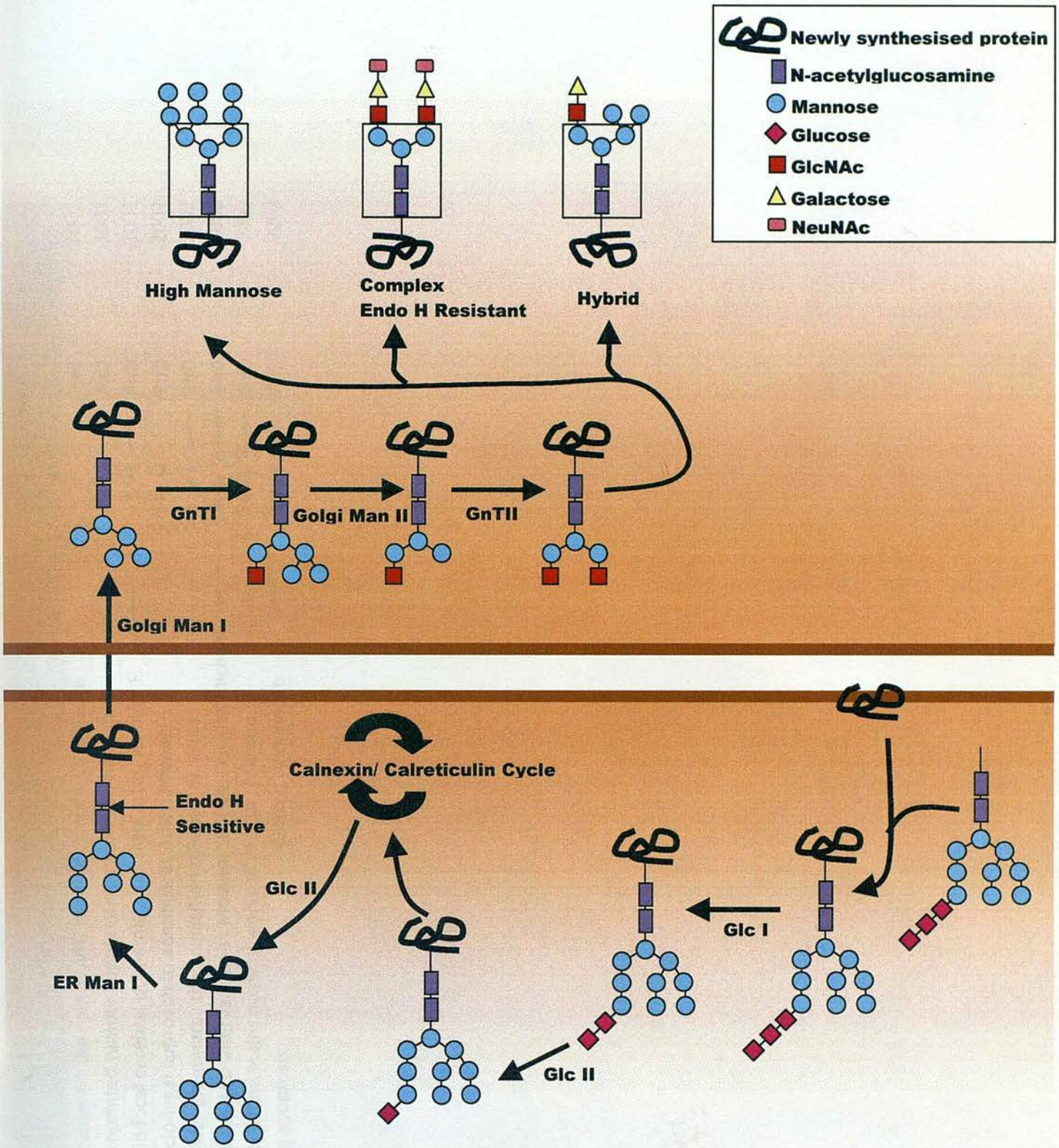

Figure 5.1: Overview of N-linked oligosaccharide processing in the ER through to the Golgi. Pre-formed core oligosaccharide is transferred to growing polypeptide chains. The oligosaccharyltransferase enzyme transfers the pre-formed oligosaccharide only to the sequence Asn-X-Ser/ Thr, where X is any amino acid except proline. When the glycoprotein has folded and reached the Golgi complex, additional trimming takes place but also with the addition of new terminal sugars. N-linked glycoproteins all contain a common core of oligosaccharide (boxed areas) attached to the polypeptide. This core consists of three mannose residues and two GlcNAc. A variety of other sugars are attached to this core and comprise three major N-linked families: 1. High mannose type 2. Hybrid type 3. Complex type. The VSVG has the complex N-linked glycoprotein addition, rendering it resistant to Endo H digestion once it has reached the Golgi. Glc I & II = glucosidase I & II, ER Man I = ER mannosidase I, Golgi Man I = Golgi mannosidase I, GnTI = GlcNAc tranferase I, Golgi Man II = Golgi mannosidase II, GnTII = GlcNAc tranferase II.

5.2 Results

5.2.1 Transfection of Mammalian Cell Lines with JC119/ ts045

Previous attempts to transfect neutrophils in the laboratory were unsuccessful (J. Pryde – personal communication). Therefore, cell lines were used instead to model VSVGts045 progression through the constitutive secretory pathway during apoptosis. Various cell lines were transfected with both JC119/ ts045 to find the cell type that would yield the highest transfection efficiency. Spinner HeLa (sHeLa) cells were transfected initially as they were the ideal cell type for future immunofluorescence, metabolic labelling and flow cytometry studies due to their ability to grow either in suspension or as a monolayer. Using the protocol given by the EquiBio Electroporator manufacturers, sHeLa cells were electroporated and the amount of GFP protein expression measured by flow cytometry over 48 h (Fig. 5.2). After 24 h, 28% of sHeLa cells transfected with 10 μg and 20 μg PEGFP-N1, expressed GFP. 31% of sHeLa cells transfected with 40 μg PEGFP-N1 expressed GFP after 24 h. After 48 h, 47% of sHeLa cells transfected with 10 μg PEGFP-N1 expressed GFP. 53% of cells expressed GFP when transfected with 20 μg PEGFP-N1 and 52% of cells expressed GFP when transfected with 40 μg PEGFP-N1. After 72 h, 42% of cells transfected with 10 μg of PEGFP-N1 expressed GFP, 46% of cells transfected with 20 μg of PEGFP-N1 expressed GFP and 44% of cells transfected with 40 μg of PEGFP-N1 expressed GFP.

Since the highest GFP expression was found to occur at 48 h using 20 μg of PEGFP-N1 this DNA concentration was maintained, as was the time post-transfection, to allow maximal protein expression.

Maintaining the same conditions, sHeLa cells were transfected with JC119/ ts045. However, no protein expression was detected either by flow cytometry or by indirect immunofluorescence. As an alternative to sHeLa cells, HeLa cells were transfected using slightly different electroporation conditions. The electroporation medium was optimised by using Hank's medium, which contains 500 mM glucose to provide the cells with an immediate glycolysis substrate, ATP so that any intracellular loss during the electroporation could be temporarily provided for and 50 mM glutathione so that the cells were under reducing conditions. HeLa cells were transfected with JC119/ ts045 by electroporation using 250 V, 1500 μF as per the manufacturers

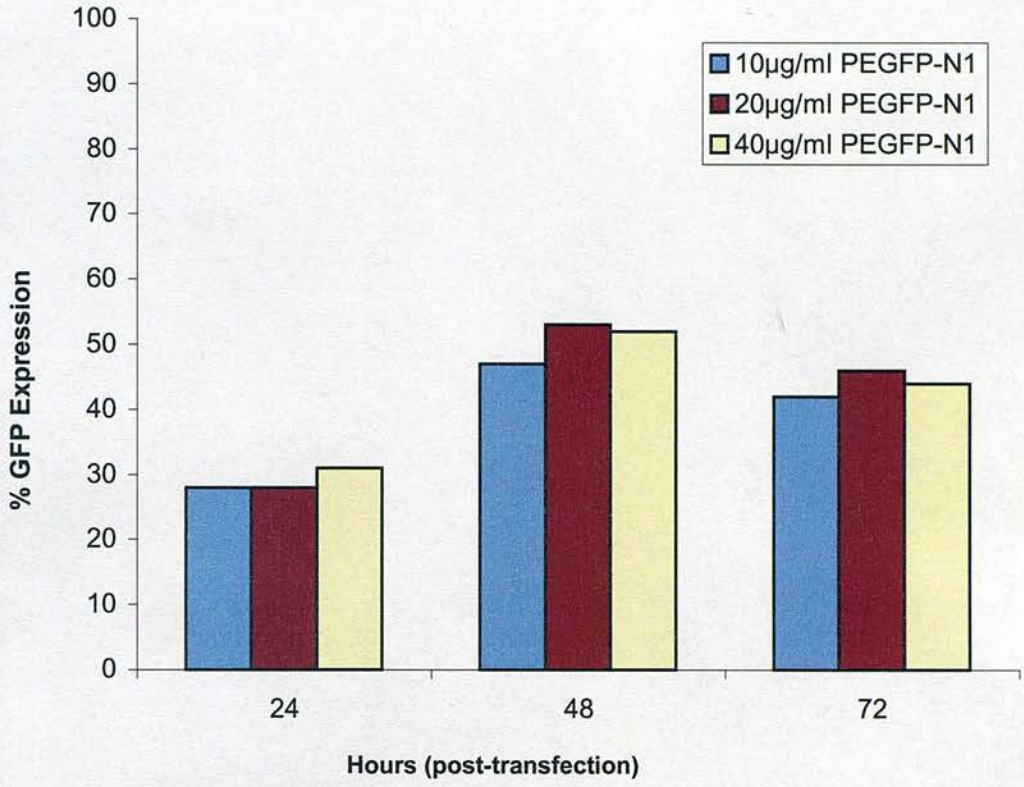

Figure 5.2: Optimisation of DNA concentration and time required for protein expression in sHeLa cells. 24 hours after transfection with PEGFP-N1, sHeLa cells transfected with 10, 20 and 40µg/ml PEGFP-N1. 24 hours after transfection, GFP expression was marginally higher in those cells transfected with 40µg/ml PEGFP-N1 (30% expression) compared to the lower DNA concentrations, where in both cases 28% of cells expressed GFP. 48 hours after transfection, GFP expression was highest in those cells transfected with 20µg/ml PEGFP-N1 (57% expression) compared to the lower DNA concentrations. Tranfection efficiency again was highest in those cells transfected with 20µg/ml PEGFP-N1 after 72 hours (48%), but was lower than at 24 hours. n =1

recommendations. After 48 h, protein expression was assessed by indirect immunofluorescence microscopy. Only 5 % of JC119/ ts045 transfected HeLa cells expressed VSVGts045. This was not sufficient expression to yield enough VSVGts045 to detect the protein by future metabolic labelling experiments. Therefore, another cell line was tested for its ability to express VSVGts045. Hek-293 cells were electroporated under the same conditions as HeLa cells, however only ~5% of cells expressed VSVGts045. Although, not the first transfection method of choice for these studies, FuG6 (Qiagen) was also tested to determine if transfection efficiency could be increased in HeLa cells by this method. Efficiency was increased to ~8%, this however, was still not sufficient. Furthermore, the morphology of the cells following incubation with FuG6 was abnormal. Nuclei were condensed and many cells appeared to be fused by the plasma membrane.

COS-7 cells were also electroporated under the same conditions and protein expression was ~10% in this cell line. To capitalise on this increase in protein expression, COS-7 cells were electroporated with a double pulse as per the manufacturers instructions. This resulted in a large increase in the number of cells expressing VSVGts045, with protein expression ~35%. NRK cells were then also electroporated under the double pulse conditions, but again, only ~5% of cells expressed VSVG/ ts045. NRK cells were also transfected by the FuG6 method and by the Superfect method and again there was no protein expression using either method. J.CaM1.6 cells were transfected under double pulse conditions but this time there was no protein expression.

COS-7 cells were the only cell line that expressed sufficient protein for metabolic labelling experiments under any of the electroporation conditions tested. However, this cell line was not the ideal choice of cell due to their resistance to most apoptotic stimuli. Therefore, to try and obtain sufficient protein expression in the other cell lines already tested, the VSVGts045 gene in the JC119 expression vector was sub-cloned into a more modern CMV based vector. The JC119 expression vector, in which the ts045 gene had been cloned in the early 1980s, is based on the SV40 promoter. SV40 promoters are generally relatively inefficient compared to CMV promoters (Colosimo *et al.*, 2000) and therefore, sub-cloning of the VSVGts045 gene into a modern CMV expression vector could enhance protein expression, as well as transfection efficiencies not only in COS-7 cells but also in other cell lines.

Cell Type	Vector	Method	Buffer	Conditions	Approximate Efficiency
sHeLa	PEGFP-N1	Electroporation	Phosphate Buffered Sucrose	400V, 25 µF	40%
	JC119/ ts045	Electroporation	Phosphate Buffered Sucrose	400V, 25 µF	NO EXPRESSION
COS-7	JC119/ ts045	Electroporation	Hank's/ 1mM Glutathione/ 1mM ATP	250V, 1500 µF	10%
	JC119/ ts045	Electroporation	Hank's/ 1mM Glutathione/ 1mM ATP	750V, 25 µF 100V, 1500 µF	35%
HeLa	JC119/ ts045	Electroporation	Hank's/ 1mM Glutathione/ 1mM ATP	250V, 1500 µF	5%
	JC119/ ts045	FuG6			8%
Hek-293	JC119/ ts045	Electroporation	Hank's/ 1mM Glutathione/ 1mM ATP	250V, 1500 µF	5%
NRK	JC119/ ts045	Electroporation	Hank's/ 1mM Glutathione/ 1mM ATP	750V, 25 µF 100V, 1500 µF	5%
	JC119/ ts045	FuG6			NO EXPRESSION
	JC119/ ts045	SuperFect			NO EXPRESSION
J.CaM1.6	JC119/ ts045	Electroporation	Hank's/ 1mM Glutathione/ 1mM ATP	750V, 25 µF 100V, 1500 µF	NO EXPRESSION

Table 5.1: Transfection of mammalian cell lines by electroporation. 5 x 10^6 cells were pelleted and resuspended in 800µl of transfection buffer and transferred to an electroporation cuvette. Cells were pulsed and immediately transferred to warmed (37°C) growth medium and left overnight. Cells were then sub-cultured and incubated for a further 24 hours before the total VSVG expression was determined. Cells were fixed and permeabilised and stained with anti-VSVG, followed by Alexa-488 (green). 100 cells/ electroporation were counted to estimate transfection efficiency. In COS-7 cells, % cell loss 24 hours post-transfection was 50-60%.

5.2.2 Sub-cloning of VSVGts045

The full restriction map of JC119 was unavailable, although from the published work the 1.7Kb gene had been cloned originally into JC119 using XhoI cuts (Sprague *et al.*, 1983). Therefore, the JC119 expression vector was digested with XhoI to excise the VSVG gene. Fig. 5.2A shows the 1.7Kb band produced upon XhoI digestion. The new pcDNA3 vector was prepared in the same way to produce XhoI sticky ends but in addition, was treated with shrimp alkaline phosphatase to remove the 5' phosphates, preventing self-ligation of the vector Fig. 5.2B.

After purification of the 1.7Kb band and the linearised pcDNA3, ligation reactions were performed using T4 DNA ligase using different vector:gene ratios. Competent *Escherichia coli* (*E. coli*) DH5α cells were then transformed and plated onto ampicillin-containing agar petri dishes. The plates containing the most colonies were considered to be the most successful ligation reactions and the colonies were initially screened for pcDNA3/ VSVG gene constructs using XhoI digests.

After XhoI digestion of the potential new clones it was found that the majority of clones appeared to contain the 1.7Kb band but the vector size was above 5.4Kb (Fig. 5.3) indicating that this was not a pcDNA3/ ts045 construct. In Fig. 5.3, one clone appeared to have the correct vector size and gene size. The potential construct was digested with EcoRV to check that the orientation of the gene was correct. There is an EcoRV restriction site in the multi-cloning region of pcDNA3 before the XhoI site and also at position 1.6KB of the VSVG gene. If the gene was present in the correct orientation the resulting DNA fragments would be approximately 5.5Kb and 1.6Kb and ~7Kb if in the wrong orientation. Fig. 5.4 shows that the gene was present in the correct orientation. To check that the gene was present as a single-copy only, a double restriction digest was performed with XbaI and NotI. The NotI restriction site is present directly before the XhoI site in the multi-cloning region of the pcDNA3 expression vector and the XbaI site directly after the XhoI site. Therefore, if the gene was present as a single copy only, then the resulting DNA fragment would be approximately 1.7Kb. Fig. 5.4 shows that while the gene was present in the correct orientation, the NotI/XbaI digests resulted in a 3.4Kb band, demonstrating that 2 copies of the gene had ligated into pcDNA3.

Since most of the clones contained the 1.7Kb band but the vector size was too large to be pcDNA3, it was concluded that the initial purification step may have contained

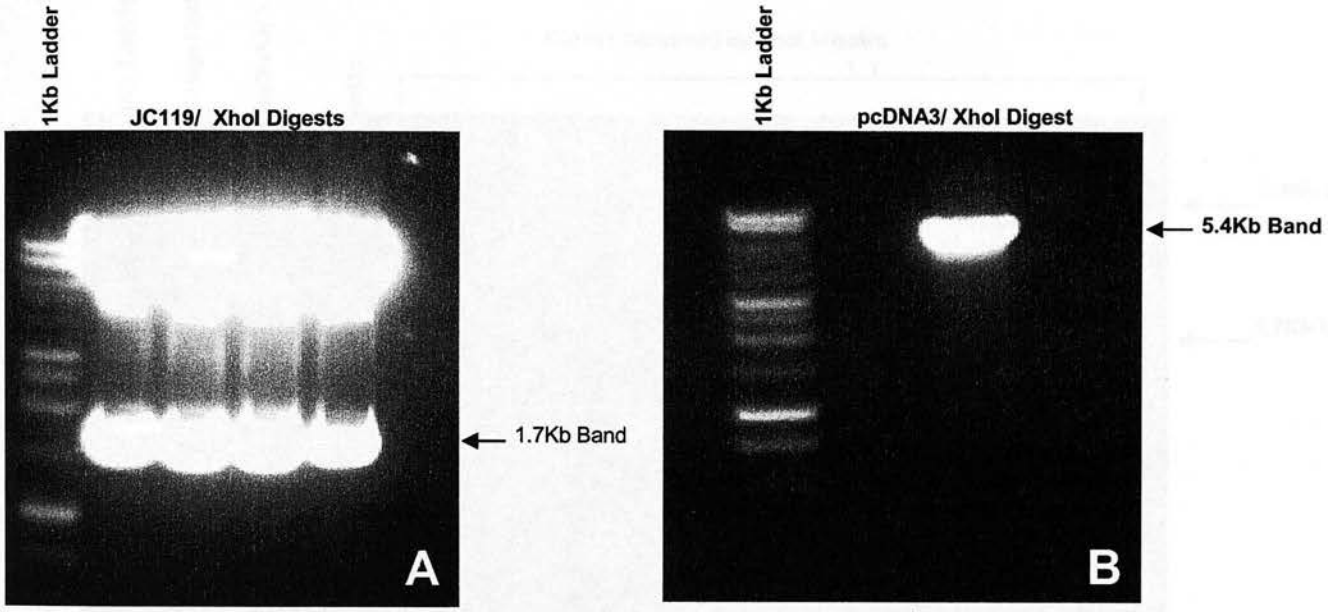

Figure 5.3: pcDNA3 preparation and ex*ci*sion of the ts045 gene from the SV40 based expression vector JC119. JC119 was digested with XhoI (A) to ex*cis*e the VSVG 1.7Kb ts045 gene. The 1.7Kb band was then separated on a 1% agarose gel and purified. (B) pcDNA3 was digested with XhoI to linearise the vector with XhoI sticky ends. The 5.4Kb band was then gel purified and treated with shrimp alkaline phosphatase to remove the 5' phosphates to prevent self-ligation.

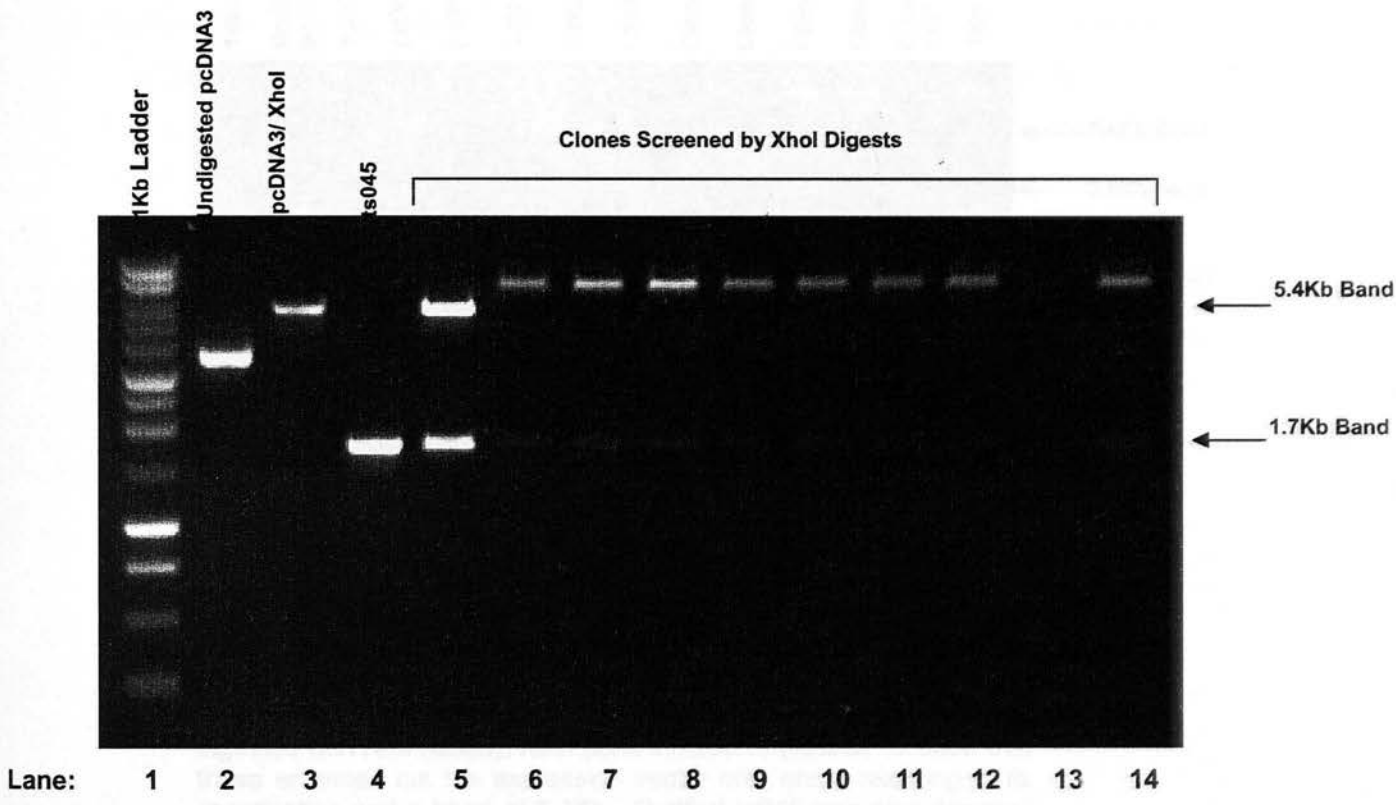

Figure 5.4: Screening for pcDNA3/ ts045. Undigested pcDNA3 (lane 2), XhoI digested pcDNA3 (lane 3) and ts045 (lane 4). 10 (lanes 5-14) potential pcDNA/ ts045 expression vectors were screened. One clone (lane 5) had the correct fragment sizes expected from pcDNA3/ ts045 digested with XhoI 5.4Kb and 1.7Kb.

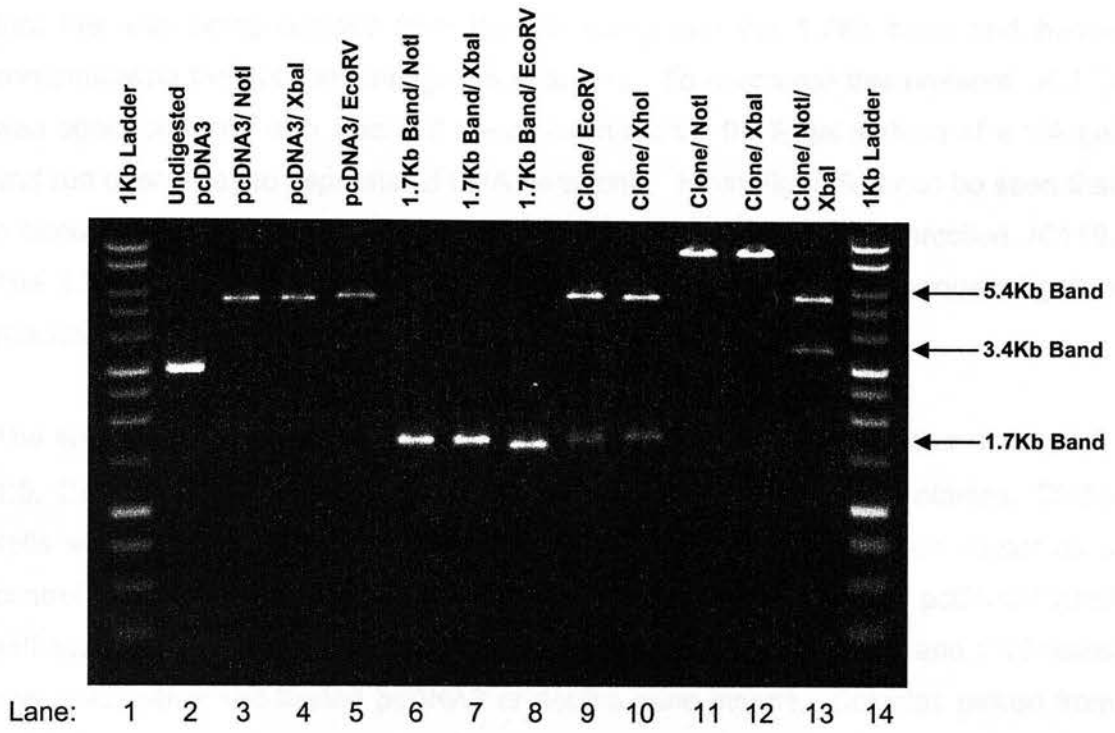

Figure 5.5: Diagnostic restriction digests of putative pcDNA3/ ts045. Undigested pcDNA3 (lane 2) was run alongside samples to control for any undigested samples. pcDNA3 alone was then digested with NotI (lane3), XbaI (lane 4), EcoRV (lane 5) to show that these enzymes cut the expression vector only once, resulting in its linearisation and a band at 5.4Kb. Purified ts045 was also digested with NotI (lane 6) and XbaI (lane7) to show that the 1.7Kb band is not cleaved by these enzymes but is cleaved by EcoRV (lane 8) as can be seen by the slight decrease in fragment size. As expected, the putative pcDNA3/ ts045 clone, upon digestion with EcoRV (lane 9) and XhoI (lane 10), yielded 2 fragments (5.4Kb and 1.7Kb). Digestion with NotI (lane 11) and XbaI (lane 12) resulted in one fragment as expected, however the fragment produced was too large to be pcDNA3/ ts045. When digested with both NotI and XbaI (lane 13), it was found that the clone contained a double copy of the gene, since in addition to the 5.4Kb band expected, there was a fragment of 3.4Kb, double the size of the expected 1.7Kb band.

small amounts of supercoiled undigested vector which would preferentially transform competent *E. Coli* DH5α cells. When clones were initially screened with EcoRV to check gene orientation, the clones with the wrong vector size showed a band pattern of ~3.5Kb, 3Kb and 2.3Kb. When the original vector was digested with EcoRV, the exact same band pattern was observed (Fig. 5.5), confirming that undigested supercoiled JC119/ ts045 was running in the vicinity of the digested 1.7Kb band and that this was being excised from the gel along with the 1.7Kb band and hence contaminating the subsequent ligation reactions. To overcome this problem, JC119 was again digested with XhoI but the digest run on a 0.7% gel instead of a 1% gel and run over a day to separate all DNA fragments. From Fig. 5.6, it can be seen that a band is present around 4Kb which is likely to be undigested supercoiled JC119. The 1.7Kb band was excised and gel purified and used in the subsequent ligation reactions.

The subsequent ligation reactions were performed at vector:insert ratios of 1:1, 1:3, 1:5, 1:7, 1:10, 1:12. Resulting DH5α colonies ranged from 10 to 15 colonies. DH5α cells were also transformed with SAP treated pcDNA3/ XhoI digested vector as a control to estimate the number of colonies produced as a result of pcDNA3/ XhoI self-ligation of which 5 were counted. Colonies picked from the 1:10 and 1:12 ratios contained either self-ligated pcDNA3 or double gene inserts. Colonies picked from 1:3 to 1:7 ratios contained successful ligations. Colonies were screened for pcDNA3/ 1.7Kb insert by EcoRV digestion and from Fig. 5.7, lanes 3, 4, 6, 9, 10, 11 and 12 these colonies contained self-ligated pcDNA3/ XhoI. Two colonies contained the 1.7Kb insert but in the wrong orientation, demonstrated by the 7.1Kb bands. Lane 1 however, contained the band pattern expected, a 5.5Kb band and 1.6Kb band, of pcDNA3 containing the 1.7Kb gene present as a single copy and in the right orientation.

The candidate pcDNA3/ ts045 was further digested to confirm that the gene was present as a single copy only. The vector was digested with EcoRV (Fig. 5.8, lane 5) to confirm the previous result that the gene was present in the right orientation. Separate digests were performed with NotI and XbaI to show that these restriction enzymes cut only in one place in the candidate pcDNA3/ ts045 as expected, resulting in 7.1Kb bands (Fig. 5.8, lanes 6, 7). A double digest with NotI and XbaI resulted in two bands: 5.4Kb and 1.7Kb, confirming that the gene was present as a single-copy only.

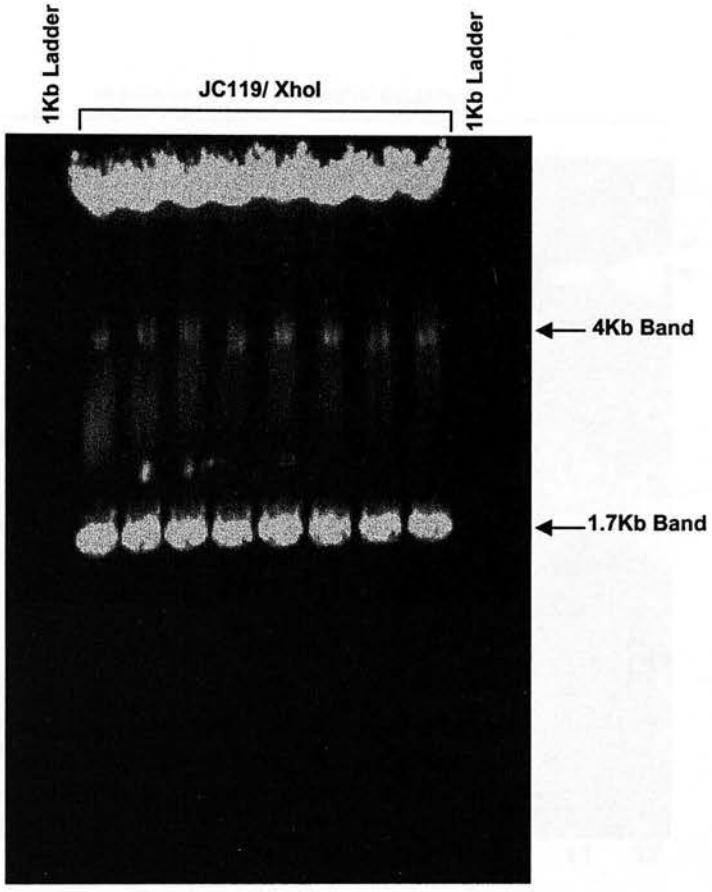

Figure 5.7: Gel purification of ts045. JC119/ ts045 was incubated overnight with XhoI and the DNA separated on a 0.7% gel. The 1.7Kb bands were cut from the gel, avoiding the top portion of the bands so as not to co-purify supercoiled JC119/ ts045.

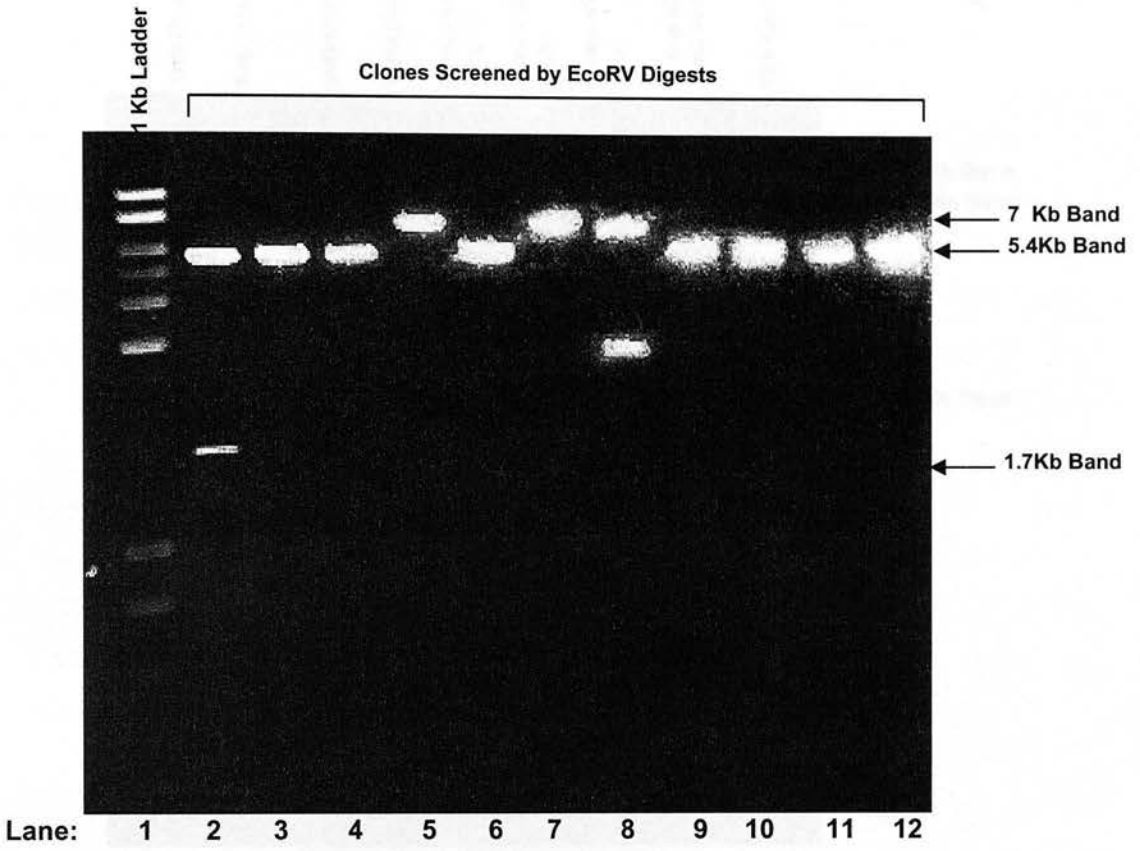

Figure 5.8: Screening for pcDNA3/ ts045 by EcoRV restriction digests. 11 potential pcDNA/ ts045 expression vectors (lanes 2-12) were screened by restriction digest using EcoRV. All DNA fragment sizes were consistent with either pcDNA3 only (5.4Kb, lanes 3,4, 9-12), pcDNA3 containing a double copy of ts045 (5.4Kb, 3.4Kb, lane 8), pcDNA3 with one copy of ts045 (7.1Kb, lanes 5 & 7) or pcDNA3 containing ts045 in the correct orientation (5.4Kb, 1.7Kb, lane 1). None of the clones contained the old vector JC119/ ts045, suggesting that the new method of gel purifying and ex*ci*sing ts045 was successful.

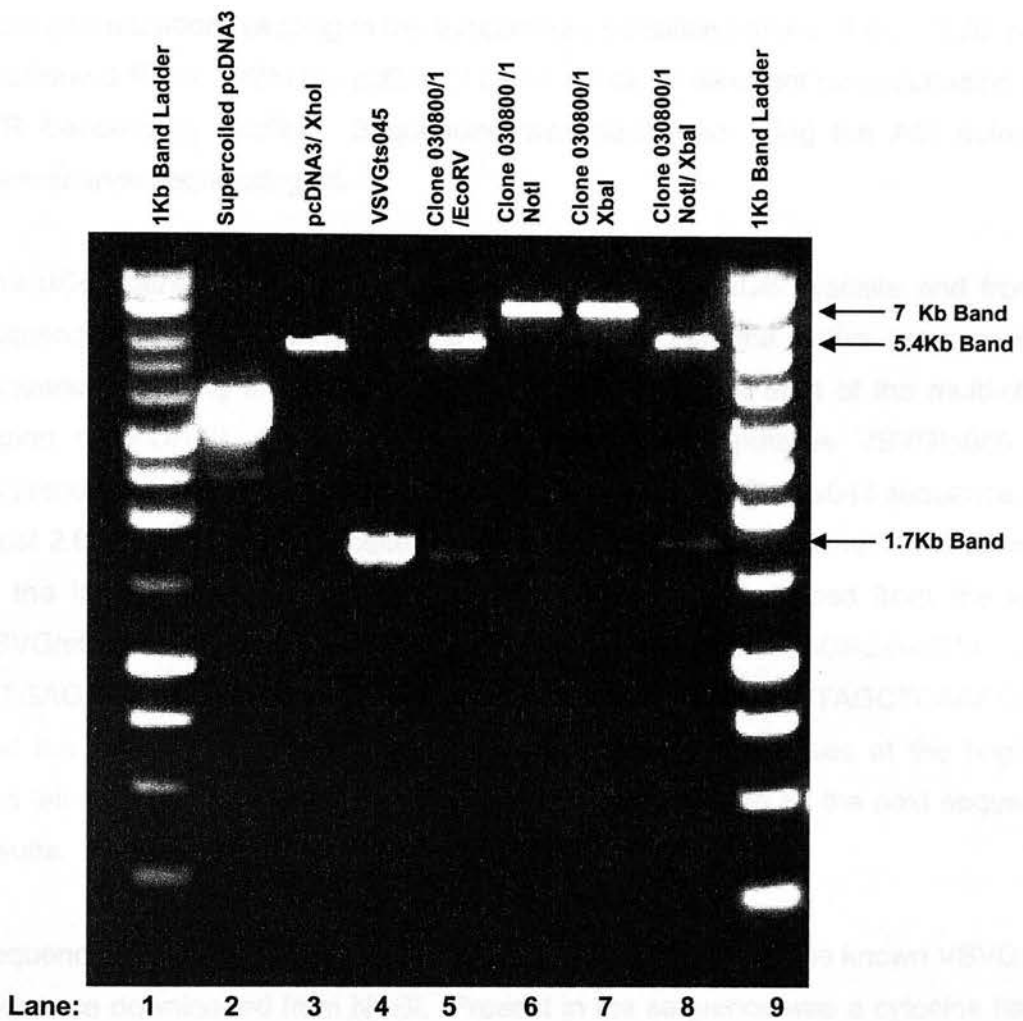

Figure 5.9: Diagnostic restriction digests of putative pcDNA3/ ts045 clones. Undigested pcDNA3 (lane 2) was run alongside samples to control for partially digested samples. pcDNA3 alone was then digested with XhoI (lane3). Clone 030800/1 was digested with EcoRV (lane 5) and as would be expected if the ts045 gene had ligated with the right copy number and in the right orientation, there was a 5.4Kb band and a 1.7Kb band. To ensure that the ts045 gene was present as a single copy only, 030800/1 was linearised with NotI (lane 6) and XbaI (lane7) which in both digests yielded a single band of the correct size 7.1Kb. To further verify that pcDNA3 contained the ts045 gene in a single copy only, a double restriction digest was performed with NotI and XbaI and as expected, there were 2 bands of 5.4Kb and 1.7Kb (lane 8), confirming that 030800/1 was the mammalian expression vector pcDNA3 containing the ts045 gene.

5.2.3 Sequencing of pcDNA3/ ts045

To confirm that the 1.7Kb band was the ts045 gene and that it contained the single base pair mutation resulting in the temperature sensitive mutant of the VSVG protein (Gallione & Rose, 1985) the pcDNA3/ ts045 construct was sent for sequencing at the CIR Sequencing Facility. Sequencing was performed using the ABI automated fluorescence sequencing kit.

The ts045 gene sequence was downloaded from the NCBI website and from the sequence, 3 forward primers were designed so that the entire gene could be sequenced. Using the T7 primer which is located at the start of the multi-cloning region of pcDNA3, the first ~650 base pairs of the putative VSVGts045 were sequenced and the sequence compared with the known VSVGts045 sequence using Blast 2.0.14 at the NCBI website. The first ~650 base pairs showed 96% homology to the known VSVG sequence. Three primers were designed from the known VSVGts045 sequence; from 0.5Kb (TTGTTGATGAATACACAGGAGA), 9.0Kb (TTGAGAGGATCTTGGATTATTC) and 12.6Kb (ATCTTCATCTTAGCTCAAAGG) so that the sequencing ranges overlapped allowing for inaccuracies at the beginning and tail-ends of the sequencing reactions could be checked by the next sequencing results.

Sequencing from 0.5Kb to ~ 1.1Kb showed 99% homology to the known VSVGts045 sequence downloaded from NCBI. Present in the sequence was a cytosine base at position 0.64Kb, which in the non-temperature sensitive VSVG gene is a thymine base, confirming that VSVG gene was the temperature sensitive mutant ts045. This single base pair mutation results in the replacement of phenylalanine by serine in the VSVG, producing the temperature sensitive VSVG (Gallione & Rose, 1985). The sequence obtained using the 0.9Kb primer was 98% homologous to the published ts045 sequence and the sequence obtained from the 12.6Kb primer was 97% homologous, confirming that the 1.7Kb band that was sub-cloned into pcDNA3 was the VSVGts045 gene. (For sequencing results see Appendix, Fig. A1).

5.2.4 *Transfection of Mammalian Cell Lines with pcDNA3/ ts045*

sHeLa, COS-7, HeLa, Hek-293, NRK and J.CaM1.6 cells were transfected by electroporation again with the new pcDNA3/ ts045 CMV based expression vector. However, in all of the cell lines tested, except for COS-7 cells, there was no protein expression using the new construct or protein expression was reduced compared to the old SV40 based construct JC119 containing ts045. Under single pulse conditions, <1% of COS-7 cells transfected with pcDNA3/ ts045, expressed VSVGts045. This was increased to 10% of COS-7 cells (Table 5.2) when cells were electroporated under double pulse conditions, although protein expression compared poorly to the ~35% achieved in JC119/ ts045 transfected COS-7 cells (Table 5.1).

5.2.5 *Temperature Sensitivity of VSVGts045 Expressed in COS-7 Cells*

To further confirm that the expression vectors JC119/ ts045 and pcDNA3/ ts045 contained the temperature sensitive VSVG, COS-7 cells were transfected with either vector and held at the restrictive temperature (40°C) for 12 h to accumulate VSVG protein within the ER (Gallione & Rose, 1985). The ER was stained with the antibody to the ER marker calnexin and at the restrictive temperature the VSVG protein co-localised with the reticular membrane structure that encircled the nucleus and extended out to the plasma membrane, characteristic of the ER (Fig. 5.10A&E) (Louvard *et al.*, 1982). After a 15 min chase in the presence of CHX to prevent synthesis of new VSVG protein, a bolus of viral protein moved out of the ER to a reticular membrane compartment that was restricted to a juxtanuclear position (Fig. 5.10B&F). VSVG protein started to reach the cell surface following a 30 min chase but the majority of VSVG is positioned juxtanuclearly (Fig. 5.10C&G). However after a 120 min chase, VSVG can no longer be seen in intracellular compartments and no longer co-localises with the ER (Fig. 5.10D&H).

The VSVGts045 in both the mammalian expression vectors JC119 and pcDNA3 performed as expected at the restrictive and permissive temperatures as described in previous work (Gallione & Rose, 1985). Therefore, this was further confirmation that the gene in pcDNA3 was the same as in JC119 and that the differences in transfection efficiency were expression vector specific.

Cell Type	Vector	Method	Buffer	Conditions	Approximate Efficiency
sHeLa	pcDNA3/ ts045	Electroporation	Phosphate Buffered Sucrose	400V, 25 μF	NO EXPRESSION
COS-7	pcDNA3/ ts045	Electroporation	Hank's/ 1mM Glutathione/ 1mM ATP	250V, 1500 μF	<1%
	pcDNA3/ ts045	Electroporation	Hank's/ 1mM Glutathione/ 1mM ATP	750V, 25 μF 100V, 1500 μF	~10%
HeLa	pcDNA3/ ts045	Electroporation	Hank's/ 1mM Glutathione/ 1mM ATP	250V, 1500 μF	NO EXPRESSION
HeK-293	pcDNA3/ ts045	Electroporation	Hank's/ 1mM Glutathione/ 1mM ATP	250V, 1500 μF	NO EXPRESSION
	pcDNA3/ ts045	Electroporation	Hank's/ 1mM Glutathione/ 1mM ATP	750V, 25 μF 100V, 1500 μF	NO EXPRESSION
	pcDNA3/ ts045	FuG6			NO EXPRESSION
J.CaM1.6	pcDNA3/ ts045	Electroporation	Hank's/ 1mM Glutathione/ 1mM ATP	750V, 25 μF 100V, 1500 μF	NO EXPRESSION

Table 5.2: Transfection of mammalian cell lines by electroporation. 5 x 10^6 cells were pelleted and resuspended in 800μl of transfection buffer and transferred to an electroporation cuvette. Cells were pulsed and immediately transferred to warmed (37°C) growth medium and left overnight. Cells were then sub-cultured and incubated for a further 24 hours before the total VSVG expression was determined. Cells were fixed and permeabilised and stained with anti-VSVG, followed by Alexa-488 (green). 100 cells/ electroporation were counted to estimate transfection efficiency. In COS-7 cells, the typical % cell loss 24 hours post-transfection was between 80-90%.

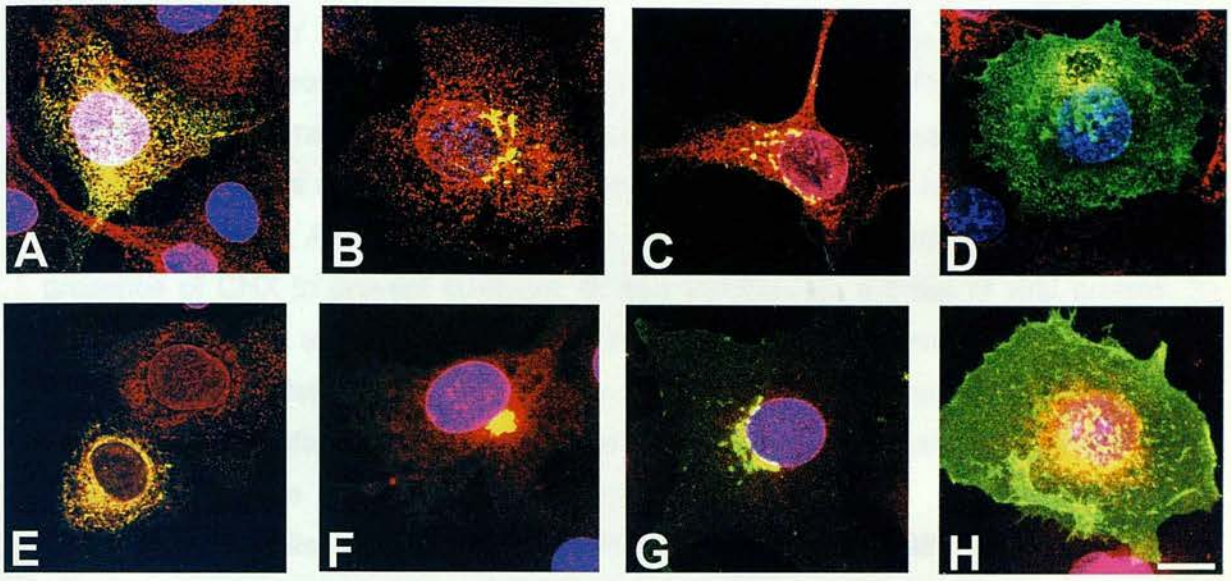

Figure 5.10: Time course of delivery of the VSVGts045 from the ER to the cell surface in COS-7 cells transfected with pcDNA3/ts045 (A-D) and JC119/ts045 (E-H). Transfected cells were incubated at 40°C for 12 hours to allow VSVGts045 to accumulate in the ER and then treated with 50µg/ml CHX for 30 minutes prior to shifting cells to the permissive temperature. Samples were stained with an anti-VSVG monoclonal antibody (green) and a polyclonal anti-calnexin (ER marker) antibody. (A & E) At time 0, cells incubated at the restrictive temperature of 40°C, where the VSVGts045 co-localised (yellow) with the ER. At 15 minutes (B & F), the VSVG has started to proceed through the secretory pathway in a bolus. After 30 minutes at 32°C, the VSVG protein no longer co-localises with the ER but still appears in an internal structure (C & G), probably the Golgi, en-route to the cell surface. At 120 minutes (D&H), delivery to the cell surface is complete and there is no more co-localisation with the ER (D) after this time point. Data are representative of at least 3 separate experiments. Scalebar represents 10µm.

5.2.6 ER to Golgi Transport is Arrested in SSP Treated COS-7 cells

Progression of VSVGts045 through the constitutive secretory pathway (Gallione & Rose, 1983) was used to assess the secretory function in apoptotic COS-7 cells. Transfected cells were held at 40°C for 12 h to accumulate VSVG protein in the ER and in the presence of the PI3-kinase inhibitor, LY294002 to sensitise the cells to apoptosis (Gallaher *et al.*, 2001; Gluzman, 1981; Valentinis *et al.*, 1994). At 40°C, VSVGts045 was seen to co-localise with the ER-marker calnexin (Fig. 5.11A-C). The ER is a reticular membrane compartment that extends all the way to the plasma membrane and has a characteristic ring-like structure around the nucleus (Powell & Latterich, 2000). After a 15 min chase at the permissive temperature, in the presence of CHX to prevent synthesis of new VSVGts045, a bolus of viral protein moved out the ER and co-localised with markers for the Golgi complex (Fig. 5.11D-F). LY294002 in itself had no effect on the ability of cells to transport VSVGts045 to cell surface and after a 120 min chase at the permissive temperature, delivery of VSVGts045 to the cell surface was complete (Fig. 5.11G-I). While LY294002 sensitised the cells to apoptosis, the PI3-kinase inhibitor itself did not induce apoptosis, as caspase-3 activity was not detected in transfected cells held at the restrictive temperature in the presence of LY294002 (Fig. 5.11J-L). After an 8 h incubation with SSP, CHX was added to the samples to prevent any new synthesis of VSVGts045 and z-VAD-fmk to halt the progression of apoptosis. Cells were then shifted to the permissive temperature for 2 h to allow progression of the VSVGts045 to the cell surface. Transfected cells with pebbled nuclei, characteristic of apoptosis and caspase-3 activity were examined. The majority of those cells did not appear to have cell surface staining; instead the VSVGts045 appeared to be held in an internal structure (Fig. 5.11M-O). When these cells were double-labelled with the ER marker calnexin and antibodies to VSVGts045, the viral protein was shown to co-localise with the ER demonstrating that in this system ER to Golgi transport is inhibited during apoptosis (Fig. 5.11P-Q). SSP alone did not cause this arrest in transport since cells where SSP was added in combination with z-VAD-fmk to inhibit apoptosis 30 min prior to shifting to the permissive temperature, were still able to transport VSVGts045 to the cell surface (Fig. 5.11S). The arrest of protein transport was shown, like Golgi fragmentation, to be caspase-dependent since cells pre-incubated with z-VAD-fmk prior to the addition of SSP were able to transport VSVGts045 to the cell surface (Fig. 5.11T).

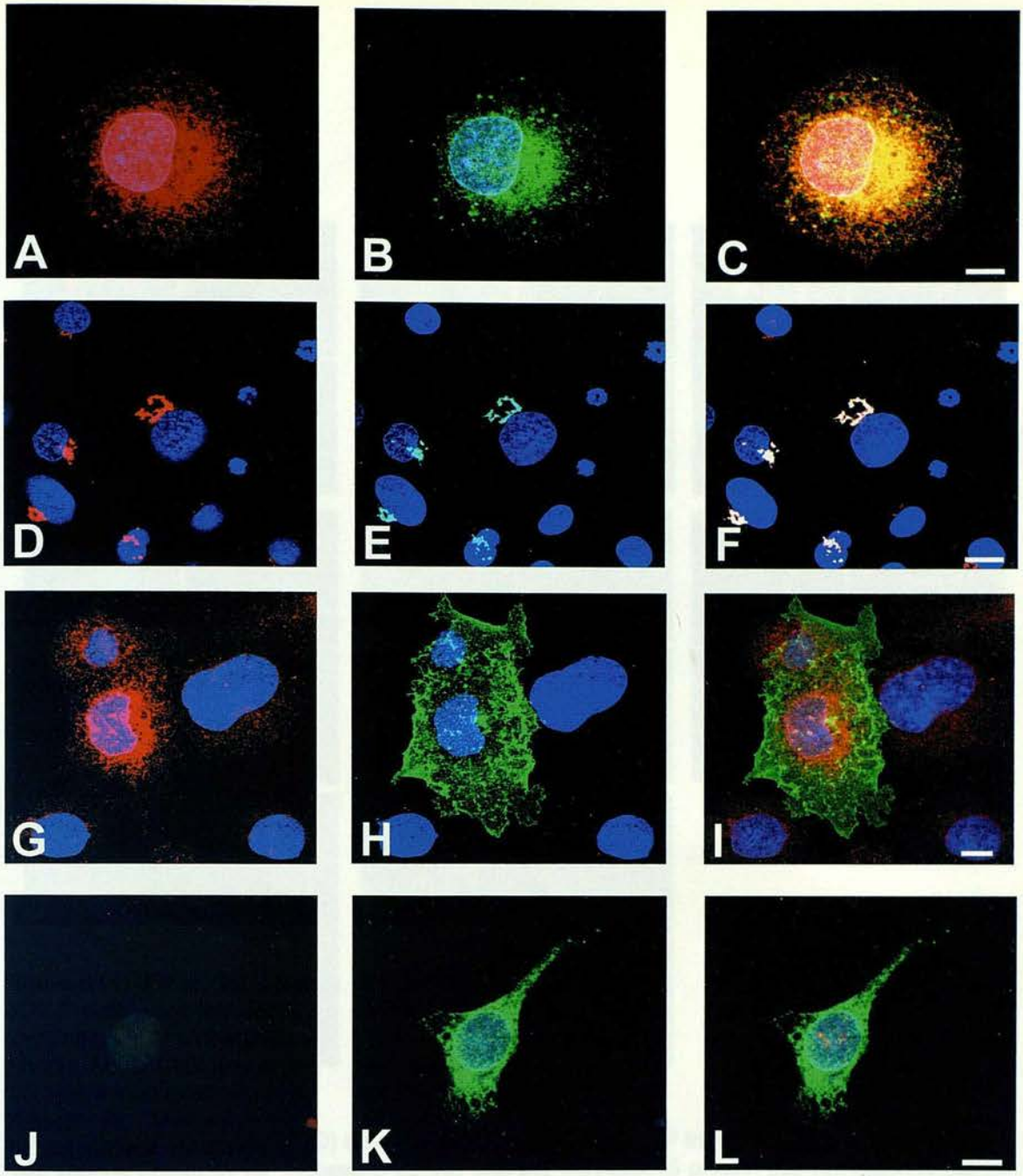

Figure 5.11: ER to Golgi transport is arrested during SSP induced apoptosis in COS-7 cells. COS-7 cells were transiently transfected with VSVGts045 and incubated in serum-free medium containing 20μM LY294002 overnight at 40°C and 30 minutes prior to the addition of 2μM SSP for 8 hours, 50μM CHX was added to each sample. 30 minutes prior to the temperature shift, z-VAD-fmk was added to all samples, except those already containing z-VAD-fmk, to inhibit the progress of apoptosis. The cells were then shifted to 32°C for 2 hours to allow transport of VSVGts045 to the cell surface. (A-C) Cells were incubated with CHX alone, without incubation at the permissive temperature. COS-7 cells were stained with anti-calnexin to mark the ER (A) and anti-VSVG to stain the VSVGts045 protein (B), which co-localised with the ER (C). (D-F) After 15 minutes at the permissive temperature, the VSVGts045 (E) had left the ER and was transported through the Golgi complex (D, Golgi marker is anti-p115) towards the plasma membrane. (G-H) After 2 hours at the permissive temperature, the VSVGts045 (H) protein was no longer present in the ER (G) and was delivered to the cell surface (I). (J-L) Control cells only and held at 40°C without incubation at the permissive temperature. (J) shows that there was no detectable caspase-3 activity and the VSVG ts045 protein shows ER-like staining (H). (L) is the overlay of (J&K). Scalebars represent 10μm.

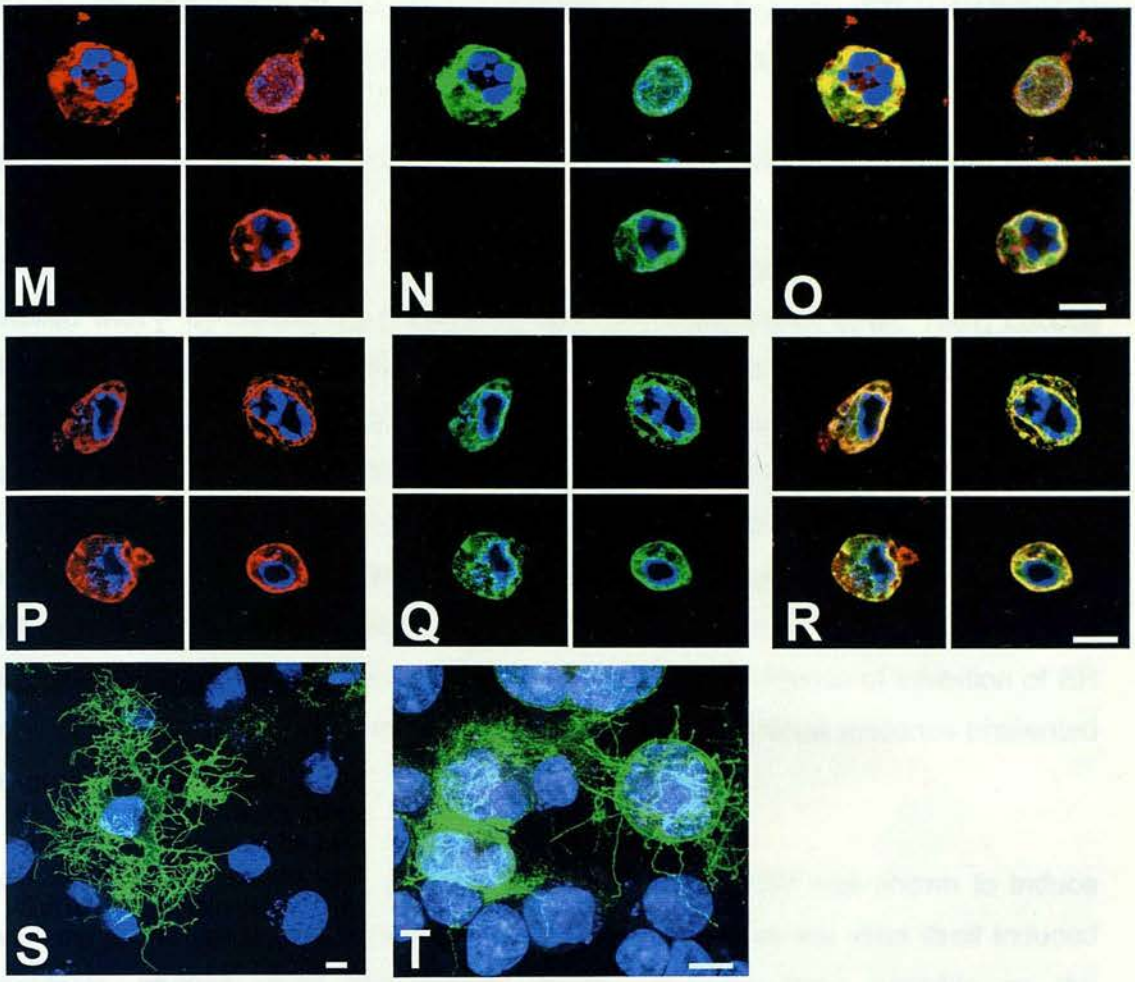

Figure 5.11 continued: (M-O) shows a cell incubated with SSP for 8 hours where (M) shows the cell stained positively for caspase-3 activity and the VSVGts045 protein has not reached the cell surface, but appears to be held in an internal structure (N). (O) is the composite of (M&N). (P-R) An apoptotic transfected cell, where the ER was stained with anti-calnexin (P) and the VSVGts045 protein (Q) again was not present on the cell surface but the staining co-localised with the ER (R, yellow), indicating a block in the constitutive secretory pathway at the ER during apoptosis. SSP nor LY294002 themselves inhibited transport of the VSVGts045 to the plasma membrane. SSP was added 30 minutes prior to the temperature drop to cells incubated with serum-free medium containing 20μM LY294002 alone. These cells were still able to transport VSVGts045 to the cell surface (S). The arrest of ER to Golgi transport in apoptotic cells was inhibited by 100μM z-VAD-fmk (T). Data are representative of 3 separate experiments. Scalebars represent 10μm.

5.3 Discussion

The results shown herein have demonstrated that exit from the ER is inhibited in apoptotic COS-7 cells treated with SSP by indirect immunofluorescence.

Many of the original studies that demonstrated a block in ER to Golgi transport were performed using whole VSV. In these studies, 95% of cells were routinely infected, providing enough VSVG for metabolic labelling experiments, where VSVG was labelled with [^{35}S]-methionine (Featherstone *et al.*, 1985; Green *et al.*, 1981; Lucocq *et al.*, 1991; Lucocq & Warren, 1987; Warren *et al.*, 1983). The mannose-rich oligosaccharide side chains of the ER form of VSVG are sensitive to digestion with Endo H, while VSVG that has reached the Golgi complex acquires complex type oligosaccharide side chains which are resistant to Endo H cleavage and therefore the two forms of VSVG can be distinguished by molecular weight. The long-term aim is that the system that has been developed and adapted to look at constitutive secretion during apoptosis, will also provide biochemical evidence of inhibition of ER to Golgi transport, in addition to the indirect immunofluorescence evidence presented herein.

In a study by Koyama *et al.*, (1995), infection of whole VSV was shown to induce over 80% apoptosis 8 h post-infection in HeLa cells. Since the virus itself induced apoptosis, studies using this system would not have been possible as the mechanism of apoptosis would be undefined and furthermore induction of apoptosis would be uncontrolled. Therefore, instead of using whole virus to infect cells and follow the VSVGts045 through the secretory pathway, an expression vector containing the VSVGts045 gene alone was used instead, to circumvent induction of apoptosis by VSV. To increase the efficiency of transfection obtained with the JC119/ ts045 SV40 based vector in a number of cell lines, the ts045 gene was sub-cloned into the CMV-based expression vector, pcDNA3. Efficiency of transfection was reduced in all cell lines transfected with pcDNA3/ ts045 compared to JC119/ ts045 transfected cells. The results were surprising since pcDNA3 is a CMV-based expression vector, which is a stronger promoter than SV40 in the JC119 expression vector (Colosimo *et al.*, 2000). However, when COS-7 cells were transfected under double pulse conditions, there was an increase in cell loss, 24 h post-transfection in pcDNA3/ ts045 transfected cells compared to JC119/ ts045 transfected cells. In addition, in pcDNA3/ ts045 transfected COS-7 cells, there was an increase in cell

loss compared to COS-7 cells transfected with empty pcDNA3 alone, suggesting that the ts045 gene conferred a certain degree of lethality on its own. It is possible that in this case, the increased efficiency of protein expression in the CMV based vector pcDNA3 would in fact result in a decrease in transfection efficiency. Incubation at 37°C, while allowing a little VSVG to move to the cell surface, still inhibits correct folding of the VSVG/ ts045 and therefore the VSVG/ ts045 accumulates in the ER. Accumulation of protein in the ER is known to induce apoptosis, also known as the unfolded protein response (Yoneda *et al.*, 2001). COS-7 cells are remarkably recalcitrant to apoptotic stimuli, probably why they had the highest transfection efficiency of all the cell lines tested. However, it seems that the CMV based vector may have increased the expression of VSVGts045 too much, causing the induction of apoptosis. In contrast, it is clear that the SV40 based vector JC119, while maintaining satisfactory transfection efficiencies, is expressed at a tolerable level for these cells. The ability of COS-7 cells to withstand an accumulation of misfolded proteins in the ER more than other cell types may involve defective stress signalling molecules. While the precise defects in the apoptotic signalling pathways are unknown in COS-7 cells, stimulation of the FasR (Memon *et al.*, 1998) or overexpression of caspase-2 (Wang *et al.*, 1994) does not induce apoptosis in these cells.

While the relative resistance of COS-7 cells is probably an advantage if high transfection efficiencies are required as was the case here, the induction of apoptosis is problematic. In addition, apoptosis induction had to be rapid as leaving the transfected cells longer than overnight, at the restrictive temperature, may have initiated ER stress responses if unfolded VSVG was allowed to accumulate beyond this time frame. Insulin-like growth factor-1 (IGF-1), mediates multiple cellular responses, including stimulation of both proliferative and anti-apoptotic pathways *via* PI3-kinase activation and is constitutively activated in COS-7 cells (Gallaher *et al.*, 2001; Gluzman, 1981; Valentinis *et al.*, 1994). To reduce the anti-apoptotic effect of IGF-1, transfected COS-7 cells were incubated with the specific PI3-kinase inhibitor LY294002 overnight. This in itself did not induce apoptosis, but sensitised the cells to SSP induced apoptosis, allowing a more rapid induction of apoptosis. While SSP was not the ideal stimulus of choice to induce apoptosis, out of the reagents tried (CHX, mitomycin c and etoposide), it was the only method that was sufficiently effective. Moreover, it was shown that neither LY294002 nor SSP inhibit the secretory pathway in themselves. This was demonstrated by incubating COS-7 cells in LY294002 overnight as usual and 30 min prior to shifting to the permissive

temperature, adding SSP together with z-VAD-fmk. While the morphology of those cells was clearly different from untreated cells, VSVGts045 was still transported to the cell surface (Fig. 5.11S).

Since SSP was shown to slow the kinetics of Golgi fragmentation compared to other apoptotic stimuli (Chapters 3,4), only cells with pebbled nuclei were examined for their ability to transport VSVG/ ts045 to the cell surface. Before the shift to the permissive temperature, cells were incubated with z-VAD-fmk, halting all caspase-activity and preventing apoptosis occurring or proceeding during incubation at the permissive temperature. This was important since without pre-incubation with z-VAD-fmk prior to the temperature shift, some cells may have initiated the apoptotic program during incubation at the permissive temperature. This would result in many cells having delivered VSVGts045 to the cell surface before acquiring the apoptotic morphology. During apoptosis the ER appears to retain its structure (Fig. 5.11P), in agreement with other reports where the ER was shown to be dilated but intact in apoptotic cells (Chu-Wang I.W., 1978; Sesso *et al.*, 1999). In the vast majority of apoptotic COS-7 cells, VSVGts045 was retained in the ER during apoptosis (Fig. 5.11R). Confirming that ER to Golgi transport is inhibited during apoptosis. In addition, inhibition of ER to Golgi transport was shown to be dependent on caspase activity, since pre-incubation of transfected COS-7 cells with z-VAD-fmk allows transport of the VSVGts045 to the cell surface in SSP treated cells (Fig. 5.11T).

BAP31 is a ubiquitously expressed 28kDa integral membrane protein of the ER that is constantly recycled between the ER and Golgi complex (Annaert *et al.*, 1997; Mosser *et al.*, 1994). It is involved in the export from the ER of cellubrevin, a protein largely localised to the endocytic pathway and functions in the exocytic pathway but its expression is cell type specfiic (Annaert *et al.*, 1997; Chilcote *et al.*, 1995), . However, BAP31 has received the most attention for its role in apoptosis. The cytosolic tail contains a death effector domain flanked by caspase cleavage sites, preferentially cleaved by caspase-8 and weakly cleaved by caspase-3 (Ng *et al.*, 1997; Ng & Shore, 1998). Caspase-8 mediated cleavage results in a 20kDa membrane-integrated BAP31 product which when transfected is a potent inducer of apoptosis. It was shown that in cells transfected with the 20kDa cleavage product of BAP31 to induce apoptosis and infected with Semliki Forest Virus (SFV) (where the coat glycoprotein may also be followed through the secretory pathway in a similar manner to VSVG), that transport from the ER to the Golgi was inhibited (Maatta *et al.*, 2000) in agreement with the data presented herein. Since cellubrevin is also

involved in the exocytic pathway in some cells, the authors suggested that inhibition of ER to Golgi transport could be attributed to BAP31 cleavage alone. However, their system was fundamentally flawed since truncated BAP31, while no longer able to export cellubrevin, is still able to export the transferrin receptor (Annaert *et al.*, 1997). This suggests that BAP31 is involved in the export of specific proteins but its cleavage alone does not result in a global inhibition of ER to Golgi transport. BAP31 has also been shown to interact with procaspase-8, Bcl-2 and Bcl-XL (Ng *et al.*, 1997; Ng & Shore, 1998), which is more suggestive of a role as a global sensor to death signals rather than being directly linked to the inhibition of the secretory pathway. Their results are in agreement with the data shown herein, however it is likely that the inhibition of ER to Golgi transport reported by the authors was due to cleavage of specific tethering/ docking factors and not a direct result of BAP31 cleavage.

The results shown herein are the first formal demonstration that protein exit from the ER is inhibited during apoptosis. Inhibition of the secretory pathway is likely to play a significant role in 'isolating' the apoptotic cell from its extracellular milieu. Since Golgi fragmentation occurred in a variety of cell lines and with different apoptotic stimuli, it is predicted that ER to Golgi transport is also a ubiquitous occurrence during apoptosis. Therefore, the apoptotic neutrophils' inability to respond to inflammatory mediators (Whyte *et al.*, 1993) is likely to occur due in part to a shut down of the constitutive secretory pathway. Receptor molecules, already present on the cell surface before the induction of apoptosis, will have a finite half-life resulting in the net loss of receptors and therefore the cells ability to respond to extracellular signals as apoptosis progresses.

CHAPTER 6: SUMMARY & FUTURE DIRECTION

Modulation of neutrophil secretion may provide a key therapeutic target in preventing tissue damage often associated with inflammatory disease. Phagocytosis of apoptotic neutrophils before they undergo secondary necrosis is thought to be a major mechanism preventing the inappropriate release of neutrophil granules. However, there is a time window where apoptotic neutrophils could still degranulate at the inflammatory site before phagocytosis takes place. However, Whyte *et al.* (1993) demonstrated that apoptotic neutrophils do not degranulate in response to inflammatory stimuli. Therefore, not only does apoptosis mark the neutrophil for removal, it also prevents the cell from exacerbating the inflammatory response by releasing its granule contents. This inability of the neutrophil to respond to inflammatory stimuli may in part be due to an inhibition of the secretory pathway, which would result in the failure of cell surface receptors to reach the plasma membrane, effectively cutting off the cells' ability to respond to stimuli.

6.1 Golgi Morphology During Apoptosis

The work presented in this thesis has for the first time sought to investigate the mechanism by which neutrophils become functionally static when apoptotic. The Golgi apparatus was identified by indirect immunofluorescence for the first time in neutrophils, however the resolution of this structure was not sufficient for morphological studies. Using cell lines that have a large, well-defined Golgi apparatus the fate of this organelle was investigated during apoptosis. Golgi fragmentation was used as a preliminary indicator of an arrest in the constitutive secretory pathway and initially Golgi fragmentation was shown to occur in apoptotic SSP-treated NRK cells. Golgi fragmentation during apoptosis was then also shown to occur in other cell lines using a variety of apoptotic stimuli, suggesting that this is a ubiquitous morphological event, in agreement with other studies (Lane *et al.*, 2002; Philpott *et al.*, 1996; Sesso *et al.*, 1999). Additionally, Golgi fragmentation was shown to be a caspase-dependent event and therefore part of the execution phase of apoptosis. Furthermore, the Golgi-derived vesicles in apoptotic cells were found to be morphologically identical to those found in the cytoplasm of mitotic cells (John Lucocq – personal communication), indicating that the target Golgi-associated proteins during mitosis that lead to Golgi fragmentation may be the same during

apoptosis. It is quite likely that at the EM level Golgi structure in neutrophils could be defined during apoptosis. Therefore, to confirm that Golgi fragmentation also occurs in neutrophils during apoptosis, the antibody against p115 that specifically stained the Golgi apparatus in neutrophils by indirect immunofluorescence, could be used to perform immunogold labelling for EM.

6.2 Cleavage of GM130 During Apoptosis

One of the key target Golgi-associated proteins, GM130 that is phosphorylated during mitosis and believed to play a significant role in Golgi fragmentation and inhibition of ER to Golgi transport during mitosis (Alvarez *et al.*, 2000; Barr *et al.*, 1998; Linstedt *et al.*, 2000; Moyer *et al.*, 2001) was also shown to be targeted during apoptosis. GM130 was demonstrated to be cleaved in a caspase-dependent manner when apoptosis was induced *via* the Fas pathway by ligation of the FasR with the monoclonal antibody CH11. However, GM130 cleavage was inhibited when apoptosis was induced by SSP, despite caspase activation. These differences between Golgi fragmentation in CH11-treated cells and SSP-treated cells were strikingly reflected in the rate of Golgi fragmentation between the 2 treatments when these cells were viewed by indirect immunofluorescence. SSP is a broad-range kinase inhibitor and therefore it is possible that phosphorylation of GM130 is required to sensitise it to caspase cleavage. To verify if this is the case, labelling with 32P-phosphate should identify phosphorylation of GM130 prior to caspase cleavage in the first instance. The fact that Golgi fragmentation was delayed in cells where GM130 was not cleaved, implicates GM130 as a central molecule involved in the maintenance of Golgi structure, which is related to its role in tethering incoming secretory vesicles. This is the first demonstration that GM130 is cleaved during apoptosis and is in direct opposition to the work of Lane *et al.*, (2002) who stated that GM130 was not cleaved during apoptosis. However, since one of their main methods of inducing apoptosis was by SSP, it is likely that GM130 cleavage was also inhibited in their system.

The monoclonal antibody used to detect GM130 by Western blotting is the only antibody commercially available. However, the immunogen against which it was raised presides on the C-terminal end of GM130, presumably just before the putative GM130 caspase cleavage site. No cleavage products and therefore the size of fragment or fragments produced were obtained to allow a more accurate estimation

of where the caspase cleavage site may lie. However, Walker *et al.*, (2002) were able to detect a proteolytic fragment of GM130 of about ~111kDa using a polyclonal antibody in apoptotic NRK cells and in a cell-free system using apoptotic neutrophil cytosol (Pryde et al., 2000) and rat liver Golgi membranes. This confirmed the prediction that the GM130 cleavage site lies close to the C-terminal end. Walker *et al.*, (2002) further examined the GM130 amino acid sequence and identified a potential caspase cleavage site at the $DMGD^{775}$ position. Cleavage at this site would be consistent with not only the loss of the C-terminal domain amino acids 869-982 but also with the molecular mass of the remaining N-terminal fragment.

Future studies using an expression vector containing the GM130 sequence, would allow GM130 to be translated *in vitro* and incubated with recombinant effector caspases, to identify the caspase or caspases that cleave GM130. To formally identify the precise caspase recognition site, cells could be transfected with an expression vector containing the GM130 sequence mutated in the predicted cleavage site. Resistance of mutant GM130 to caspase-mediated cleavage would then formally identify the caspase cleavage site. In addition, it would be interesting to transfect cells with an expression vector encoding a truncated form of GM130 identical to GM130 after caspase cleavage. From this, cells could be co-transfected with expression vectors containing VSVGts045 and truncated GM130 to assess the impact that cleaved GM130 alone has on ER to Golgi transport.

6.3 ER to Golgi Transport During Apoptosis

ER to Golgi transport was demonstrated to be inhibited in apoptotic COS-7 cells transfected with VSVGts045 by indirect immunofluorescence. This is the first formal demonstration of an inhibition of the constitutive secretory pathway during apoptosis. Walker et al., 2002 were able to continue this work using the system described herein, to demonstrate a block in the ER to Golgi transport during apoptosis by biochemical means. Endo-H only cleaves the mannose-rich oligosaccharides of the VSVGts045 acquired in ER. Transport of VSVGts045 to the Golgi complex results in the further processing of its oligosaccharide side chains to the complex form that is resistant to Endo-H digestion, providing a convenient biochemical method for monitoring VSVGts045 progress through the constitutive secretory pathway. Walker et al., 2002 showed that in apoptotic COS-7 cells treated with SSP VSVGts045 remained sensitive to oligosaccaride removal by Endo-H indicating that in apoptotic

cells the VSVGts045 was unable to reach the Golgi apparatus. Furthermore, pre-incubation with z-VAD-fmk allowed transport of VSVGts045 to the Golgi apparatus since VSVGts045 was resistant to Endo-H digestion in these cells.

COS-7 cells are unusually resistant to apoptosis, which may explain why this cell type yielded the highest transfection efficiencies. It was shown that inducing apoptosis with SSP results in differential kinetics of Golgi fragmentation and in addition that GM130 cleavage is inhibited in SSP treated J.CaM1.6 cells, a derivative of Jurkat cells. However, SSP in combination with LY294002 was the only stimuli tested that induced a sufficient amount of apoptosis within a relatively short time frame. It may be possible however to initiate apoptosis in COS-7 cells by a more physiological method by co-transfecting cells with a vector containing a chimeric FasR that is fused with the cytoplasmic procaspase-8 molecule as described by Memon *et al.*, (1998). COS-7 cells undergo apoptosis when treated with the DNA damaging agent mitomycin c, although the kinetics of apoptosis are too slow for the requirements of the system used (Mahajan *et al.*, 1999). However, transfecting COS-7 cells with for example the pro-apoptotic Bcl-2 family member Bax may sensitise the cells to mitomycin c induced apoptosis. The advantage of these alternative methods of killing would be the avoidance of SSP-mediated inhibition of GM130 cleavage. While inhibition of ER to Golgi transport was demonstrated to occur in the SSP system, a more physiological method of killing would allow a greater understanding of the kinetics of this inhibition. To transfer this system to neutrophils to demonstrate a block in ER to Golgi transport would appear to be problematic since previous attempts to transfect neutrophils were unsuccessful (J. Pryde – personal communication). In addition, it is likely that the presence of viral DNA/ protein would result in a rapid induction of apoptosis. Also, the size of the Golgi apparatus in neutrophils is indicative of a low level of protein trafficking through the constitutive secretory pathway, which would make detection of any protein trafficking through this route difficult. It may therefore be better to model inhibition of ER to Golgi transport during apoptosis in cell lines but identify the caspase-dependent cleavage of key trafficking molecules leading to this inhibition, verify their existence in neutrophils and show that they are also cleaved in apoptotic neutrophils. This together with morphological studies showing Golgi fragmentation by EM in neutrophils would be highly indicative that constitutive exocytosis is also inhibited in these cells during apoptosis.

PUBLICATIONS

Abstracts:

Walker, A., Lucocq, J.M., Haslett C., Pryde, J.G. Fragmentation of the Golgi Complex During Apoptosis. *Keystone Symposia, Colorado (Molecular Mechanisms of Apoptosis)*. January 16-22, 2001, Poster 448.

Walker, A., Pryde, J.G. The Golgi Fragments During Apoptosis. *Biochem. Soc. Trans.* 1999. 27 (Part 5, No 12). A146.

Publications:

Walker, A., Sheldrake, T., Haslett, C., Pryde, J.G. Exocytic transport between the endoplasmic reticulum and the Golgi complex is arrested during apoptosis. *In preparation.*

Pryde, J.G., Walker, A., Rossi, A., Hannah, S., Haslett, C. 2000. Temperature-dependent arrest of neutrophil apoptosis: failure of bax insertion into mitochondria at 15°C prevents the release of cytochrome c. *J. Biol. Chemistry*. 275 (No.43), 33574-33584.

APPENDIX

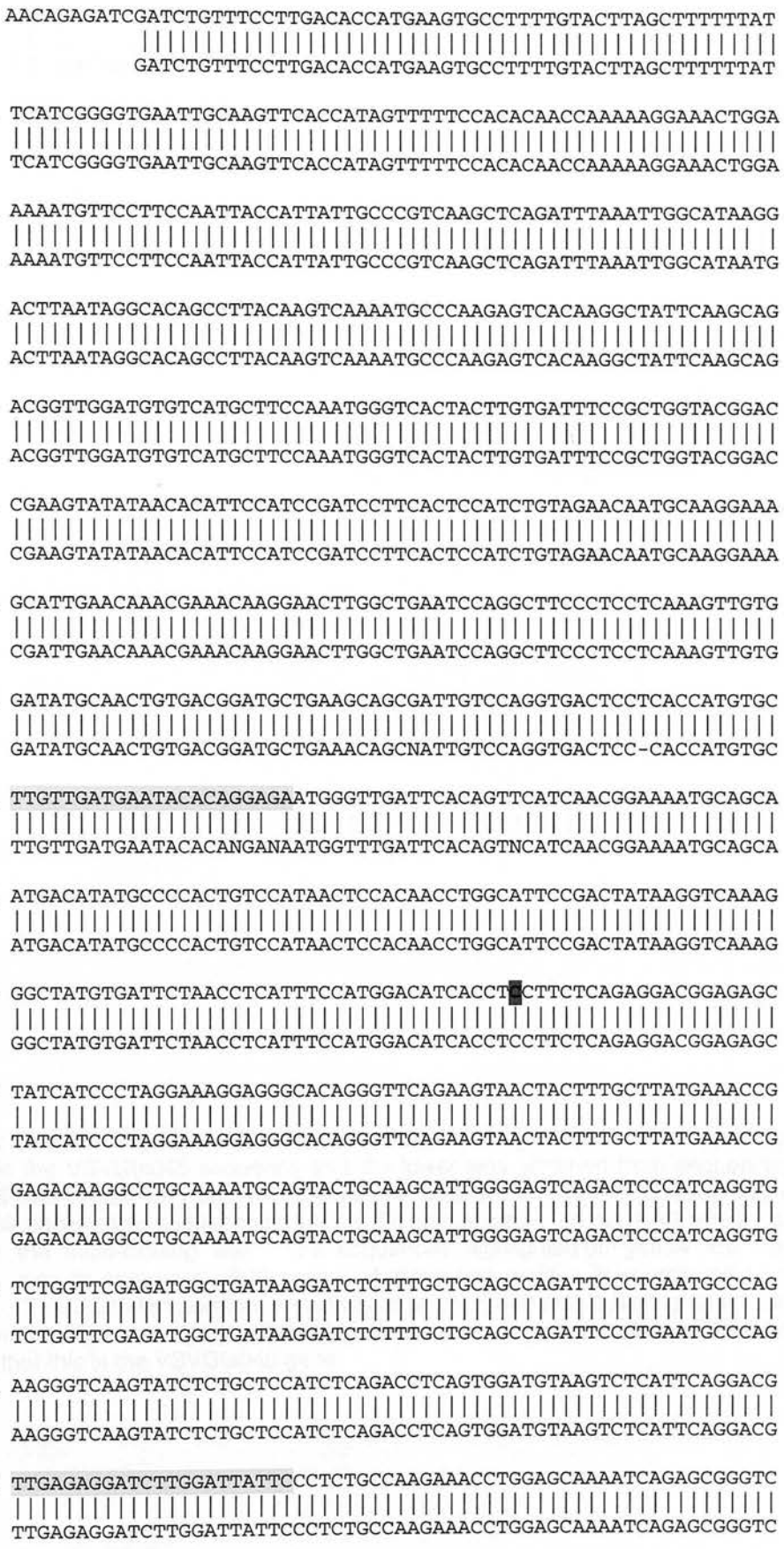
1 AACAGAGATCGATCTGTTTCCTTGACACCATGAAGTGCCTTTTGTACTTAGCTTTTTTAT
GATCTGTTTCCTTGACACCATGAAGTGCCTTTTGTACTTAGCTTTTTTAT
61 TCATCGGGGTGAATTGCAAGTTCACCATAGTTTTTCCACACAACCAAAAAGGAAACTGGA
TCATCGGGGTGAATTGCAAGTTCACCATAGTTTTTCCACACAACCAAAAAGGAAACTGGA
121 AAAATGTTCCTTCCAATTACCATTATTGCCCGTCAAGCTCAGATTTAAATTGGCATAAGG
AAAATGTTCCTTCCAATTACCATTATTGCCCGTCAAGCTCAGATTTAAATTGGCATAATG
181 ACTTAATAGGCACAGCCTTACAAGTCAAAATGCCCAAGAGTCACAAGGCTATTCAAGCAG
ACTTAATAGGCACAGCCTTACAAGTCAAAATGCCCAAGAGTCACAAGGCTATTCAAGCAG
241 ACGGTTGGATGTGTCATGCTTCCAAATGGGTCACTACTTGTGATTTCCGCTGGTACGGAC
ACGGTTGGATGTGTCATGCTTCCAAATGGGTCACTACTTGTGATTTCCGCTGGTACGGAC
301 CGAAGTATATAACACATTCCATCCGATCCTTCACTCCATCTGTAGAACAATGCAAGGAAA
CGAAGTATATAACACATTCCATCCGATCCTTCACTCCATCTGTAGAACAATGCAAGGAAA
361 GCATTGAACAAACGAAACAAGGAACTTGGCTGAATCCAGGCTTCCCTCCTCAAAGTTGTG
CGATTGAACAAACGAAACAAGGAACTTGGCTGAATCCAGGCTTCCCTCCTCAAAGTTGTG
421 GATATGCAACTGTGACGGATGCTGAAGCAGCGATTGTCCAGGTGACTCCTCACCATGTGC
GATATGCAACTGTGACGGATGCTGAAACAGCNATTGTCCAGGTGACTCC-CACCATGTGC
481 TTGTTGATGAATACACAGGAGAATGGGTTGATTCACAGTTCATCAACGGAAAATGCAGCA
TTGTTGATGAATACACANGANAATGGTTTGATTCACAGTNCATCAACGGAAAATGCAGCA
541 ATGACATATGCCCCACTGTCCATAACTCCACAACCTGGCATTCCGACTATAAGGTCAAAG
ATGACATATGCCCCACTGTCCATAACTCCACAACCTGGCATTCCGACTATAAGGTCAAAG
601 GGCTATGTGATTCTAACCTCATTTCCATGGACATCACCTCCTTCTCAGAGGACGGAGAGC
GGCTATGTGATTCTAACCTCATTTCCATGGACATCACCTCCTTCTCAGAGGACGGAGAGC
661 TATCATCCCTAGGAAAGGAGGGCACAGGGTTCAGAAGTAACTACTTTGCTTATGAAACCG
TATCATCCCTAGGAAAGGAGGGCACAGGGTTCAGAAGTAACTACTTTGCTTATGAAACCG
721 GAGACAAGGCCTGCAAAATGCAGTACTGCAAGCATTGGGGAGTCAGACTCCCATCAGGTG
GAGACAAGGCCTGCAAAATGCAGTACTGCAAGCATTGGGGAGTCAGACTCCCATCAGGTG
781 TCTGGTTCGAGATGGCTGATAAGGATCTCTTTGCTGCAGCCAGATTCCCTGAATGCCCAG
TCTGGTTCGAGATGGCTGATAAGGATCTCTTTGCTGCAGCCAGATTCCCTGAATGCCCAG
841 AAGGGTCAAGTATCTCTGCTCCATCTCAGACCTCAGTGGATGTAAGTCTCATTCAGGACG
AAGGGTCAAGTATCTCTGCTCCATCTCAGACCTCAGTGGATGTAAGTCTCATTCAGGACG
901 TTGAGAGGATCTTGGATTATTCCCTCTGCCAAGAAACCTGGAGCAAAATCAGAGCGGGTC
TTGAGAGGATCTTGGATTATTCCCTCTGCCAAGAAACCTGGAGCAAAATCAGAGCGGGTC

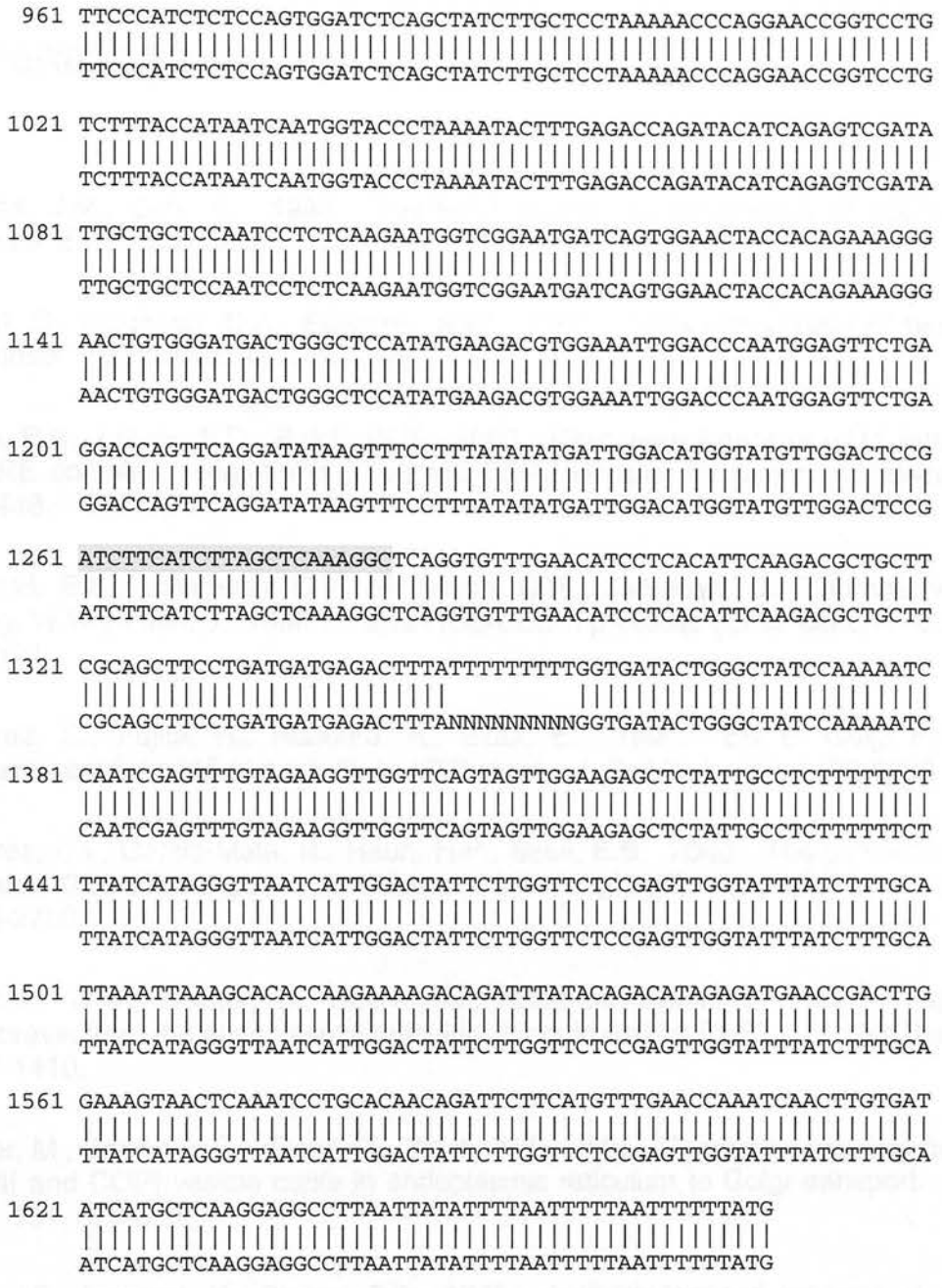

Figure A1: Sequencing of VSVGts045 sub-cloned into pcDNA3. The upper nucleotide sequence is the VSVGts045 sequence and the lower was obtained from sequencing of the VSVGts045 sub-cloned into pcDNA3 (Sequence data was from CIR Sequencing Facility). The first 480 bases were sequenced from the T7 primer within the pcDNA3 construct located just before the multi-cloning site. The sequences highlighted in yellow are the primer sequences used to sequence ~500 bases. A thymidine residue is substituted by cytosine resulting in VSVGts045 temperature sensitivity at position 640 and is highlighted in pink. This can be seen to be present in the VSVGts045 sequence obtained from the pcDNA3 construct, confirming that this is the VSVGts045 gene.

REFERENCES

Adams, J.M., Cory, S. 1998. The Bcl-2 protein family: arbiters of cell survival. *Science* 281, 1322-1326.

Akgul, C., Moulding, D.A., Edwards, S.W. 2001. Molecular control of neutrophil apoptosis. *FEBS Lett.* 487, 318-322.

Allan, B.B., Moyer, B.D., Balch, W.E. 2000. Rab1 recruitment of p115 into a *cis*-SNARE complex: programming budding COPII vesicles for fusion. *Science* 289, 444-448.

Alnemri, E.S., Livingston, D.J., Nicholson, D.W., Salvesen, G., Thornberry, N.A., Wong, W.W., Yuan, J. 1996. Human ICE/CED-3 protease nomenclature. *Cell* 87 , 171-171.

Alvarez, C., Fujita, H., Hubbard, A., Sztul, E. 1999. ER to Golgi transport: Requirement for p115 at a pre-Golgi VTC stage. *J. Cell Biol.* 147, 1205-1222.

Alvarez, C.I., Garcia-Mata, R., Hauri, H.P., Sztul, E.S. 2000. The p115-interactive proteins, GM130 and giantin participate in ER- Golgi traffic. *J. Biol. Chem.* 276 (4), 2693-2700.

Annaert, W.G., Becker, B., Kistner, U., Reth, M., Jahn, R. 1997. Export of cellubrevin from the endoplasmic reticulum is controlled by BAP31. *J. Cell Biol.* 139, 1397-1410.

Aridor, M., Bannykh, S.I., Rowe, T., Balch, W.E. 1995. Sequential coupling between COPII and COPI vesicle coats in endoplasmic reticulum to Golgi transport. *J. Cell Biol.* 131, 875-893.

Ash, J.F., Louvard, D., Singer, S.J. 1977. Antibody-induced linkages of plasma membrane proteins to intracellular actomyosin-containing filaments in cultured fibroblasts. *Proc. Natl. Acad. Sci. U.S.A* 74, 5584- 5588.

Ashkenazi, A., Dixit, V.M. 1998. Death receptors: signaling and modulation. *Science* 281, 1305-1308.

Ashkenazi, A., Dixit, V.M. 1999. Apoptosis control by death and decoy receptors. *Curr. Opin. Cell Biol.* 11, 255-260.

Bailly, E., McCaffrey, M., Touchot, N., Zahraoui, A., Goud, B., Bornens, M. 1991. Phosphorylation of two small GTP-binding proteins of the Rab family by $p34^{cdc2}$. *Nature* 350, 715-718.

Bainton, D.F. 1973. Sequential degranulation of the two types of polymorphonuclear leukocyte granules during phagocytosis of microorganisms. *J. Cell Biol.* 58, 249-264.

Bainton, D.F., Ullyot, J.L., Farquhar, M.G. 1971. The development of neutrophilic polymorphonuclear leukocytes in human bone marrow. *J. Exp. Med.* 134, 907-934.

Balch, W.E., Glick, B.S., Rothman, J.E. 1984. Sequential intermediates in the pathway of intercompartmental transport in a cell-free system. *Cell* 39, 525-536.

Barlowe, C., Orci, L., Yeung, T., Hosobuchi, M., Hamamoto, S., Salama, N., Rexach, M.F., Ravazzola, M., Amherdt, M., Schekman, R. 1994. COPII: a membrane coat formed by Sec proteins that drive vesicle budding from the endoplasmic reticulum. *Cell* 77, 895-907.

Barlowe, C., Schekman, R. 1993. SEC12 encodes a guanine-nucleotide-exchange factor essential for transport vesicle budding from the ER. *Nature* 365, 347-349.

Barr, F.A., Nakamura, N., Warren, G. 1998. Mapping the interaction between GRASP65 and GM130, components of a protein complex involved in the stacking of Golgi cisternae. *EMBO J.* 17, 3258-3268.

Barr, F.A., Puype, M., Vandekerckhove, J., Warren, G. 1997. GRASP65, a protein involved in the stacking of Golgi cisternae. *Cell* 91, 253-262.

Baumert, M., Maycox, P.R., Navone, F., De Camilli, P., Jahn, R. 1989. Synaptobrevin: an integral membrane protein of 18,000 daltons present in small synaptic vesicles of rat brain. *EMBO J.* 8, 379-384.

Beckers, C.J., Plutner, H., Davidson, H.W., Balch, W.E. 1990. Sequential intermediates in the transport of protein between the endoplasmic reticulum and the Golgi. *J. Biol. Chem.* 265, 18298-18310.

Bedner, E., Li, X., Gorczyca, W., Melamed, M.R., Darzynkiewicz, Z. 1999. Analysis of apoptosis by laser scanning cytometry. *Cytometry* 35, 181-195.

Belloc, F., Belaud-Rotureau, M.A., Lavignolle, V., Bascans, E., Braz-Pereira, E., Durrieu, F., Lacombe, F. 2000. Flow cytometry detection of caspase 3 activation in preapoptotic leukemic cells. *Cytometry* 40, 151 -160.

Berger, M., O'Shea, J., Cross, A.S., Folks, T.M., Chused, T.M., Brown, E.J., Frank, M.M. 1984. Human neutrophils increase expression of C3bi as well as C3b receptors upon activation. *J. Clin. Invest* 74, 1566-1571.

Berger, M., Wetzler, E.M., Welter, E., Turner, J.R., Tartakoff, A.M. 1991. Intracellular sites for storage and recycling of C3b receptors in human neutrophils. *Proc. Natl. Acad. Sci. U.S.A* 88, 3019-3023.

Block, M.R., Glick, B.S., Wilcox, C.A., Wieland, F.T., Rothman, J.E. 1988. Purification of an N-ethylmaleimide-sensitive protein catalyzing vesicular transport. *Proc. Natl. Acad. Sci. U.S.A* 85, 7852-7856.

Borregaard, N., Cowland, J.B. 1997. Granules of the human neutrophilic polymorphonuclear leukocyte. *Blood* 89, 3503-3521.

Borregaard, N., Sehested, M., Nielsen, B.S., Sengelov, H., Kjeldsen, L. 1995. Biosynthesis of granule proteins in normal human bone marrow cells. Gelatinase is a marker of terminal neutrophil differentiation. *Blood* 85, 812-817.

Brumell, J.H., Volchuk, A., Sengelov, H., Borregaard, N., Cieutat, A.M., Bainton, D.F., Grinstein, S., Klip, A. 1995. Subcellular distribution of docking/fusion proteins in neutrophils, secretory cells with multiple exocytic compartments. *J. Immunol.* 155, 5750-5759.

Burke B, Griffiths G, Reggio H, Louvard D, Warren G. 1982. A monoclonal antibody against a 135-K Golgi membrane protein. *EMBO J.* 1, 1621-1628.

Cannistra, S.A., Griffin, J.D. 1988. Regulation of the production and function of granulocytes and monocytes. *Semin. Hematol.* 25, 173-188.

Cannon, K.S., Helenius, A. 1999. Trimming and readdition of glucose to N-linked oligosaccharides determines calnexin association of a substrate glycoprotein in living cells. *J. Biol. Chem.* 274, 7537-7544.

Cao, X., Ballew, N., Barlowe, C. 1998. Initial docking of ER-derived vesicles requires Uso1p and Ypt1p but is independent of SNARE proteins. *EMBO J.* 17, 2156-2165.

Chai, J., Du, C., Wu, J.W., Kyin, S., Wang, X., Shi, Y. 2000. Structural and biochemical basis of apoptotic activation by Smac/DIABLO. *Nature* 406, 855-862.

Chao, J.R., Wang, J.M., Lee, S.F., Peng, H.W., Lin, Y.H., Chou, C.H., Li, J.C., Huang, H.M., Chou, C.K., Kuo, M.L., Yen, J.J., Yang-Yen, H.F. 1998. mcl-1 is an immediate-early gene activated by the granulocyte- macrophage colony-stimulating factor (GM-CSF) signaling pathway and is one component of the GM-CSF viability response. *Mol. Cell Biol.* 18, 4883-4898.

Chen, Y.A., Scales, S.J., Patel, S.M., Doung, Y.C., Scheller, R.H. 1999. SNARE complex formation is triggered by Ca^{2+} and drives membrane fusion. *Cell* 97, 165-174.

Chen, Y.A., Scheller, R.H. 2001. SNARE-mediated membrane fusion. *Nat. Rev. Mol. Cell Biol.* 2, 98-106.

Chilcote, T.J., Galli, T., Mundigl, O., Edelmann, L., McPherson, P.S., Takei, K., De Camilli, P. 1995. Cellubrevin and synaptobrevins: similar subcellular localization and biochemical properties in PC12 cells . *J. Cell Biol.* 129, 219-231.

Choi, K.S., Eom, Y.W., Kang, Y., Ha, M.J., Rhee, H., Yoon, J.W., Kim, S.J. 1999. Cdc2 and Cdk2 kinase activated by transforming growth factor-beta1 trigger apoptosis through the phosphorylation of retinoblastoma protein in FaO hepatoma cells. *J. Biol. Chem.* 274, 31775-31783.

Chou, J.J., Matsuo, H., Duan, H., Wagner, G. 1998. Solution structure of the RAIDD CARD and model for CARD/CARD interaction in caspase-2 and caspase-9 recruitment. *Cell* 94, 171-180.

Chu-Wang I.W. 1978. Cell Death of Motoneurons in the Chick Embryo Spinal Cord. *J. of Comp. Neur.* 177, 33 -57.

Chuang, P.I., Yee, E., Karsan, A., Winn, R.K., Harlan, J.M. 1998. A1 is a constitutive and inducible Bcl-2 homologue in mature human neutrophils. *Biochem. Biophys. Res. Commun.* 249, 361-365.

Clarke, P.R., Karsenti, E. 1991. Regulation of p34cdc2 protein kinase: new insights into protein phosphorylation and the cell cycle. *J. Cell Sci.* 100, 409-414.

Clary, D.O., Griff, I.C., Rothman, J.E. 1990. SNAPs, a family of NSF attachment proteins involved in intracellular membrane fusion in animals and yeast. *Cell* 61, 709-721.

Cluett, E.B., Brown, W.J. 1992. Adhesion of Golgi cisternae by proteinaceous interactions: intercisternal bridges as putative adhesive structures. *J. Cell Sci.* 103, 773-784.

Colosimo, A., Goncz, K.K., Holmes, A.R., Kunzelmann, K., Novelli, G., Malone, R.W., Bennett, M.J., Gruenert, D.C. 2000. Transfer and expression of foreign genes in mammalian cells . *Biotechniques* 29, 314-2, 324.

Cox, J.S., Walter, P. 1996. A novel mechanism for regulating activity of a transcription factor that controls the unfolded protein response. *Cell* 87, 391-404.

Crepaldi, L., Gasperini, S., Lapinet, J.A., Calzetti, F., Pinardi, C., Liu, Y., Zurawski, S., de Waal, M.R., Moore, K.W., Cassatella, M.A. 2001. Up-regulation of IL-10R1 expression is required to render human neutrophils fully responsive to IL-10. *J. Immunol.* 167, 2312-2322.

Crockett-Torabi, E., Fantone, J.C. 1995. The selectins: insights into selectin-induced intracellular signaling in leukocytes. *Immunol. Res.* 14, 237-251.

Crockett-Torabi, E., Sulenbarger, B., Smith, C.W., Fantone, J.C. 1995. Activation of human neutrophils through L-selectin and Mac-1 molecules. *J. Immunol.* 154, 2291-2302.

Daigle, I., Simon, H.U. 2001. Critical role for caspases 3 and 8 in neutrophil but not eosinophil apoptosis. *Int. Arch. Allergy Immunol.* 126, 147-156.

Davis, F.M., Tsao, T.Y., Fowler, S.K., Rao, P.N. 1983. Monoclonal antibodies to mitotic cells. *Proc. Natl. Acad. Sci. U.S.A* 80, 2926-2930.

De Vos, K., Goossens, V., Boone, E., Vercammen, D., Vancompernolle, K., Vandenabeele, P., Haegeman, G., Fiers, W., Grooten, J. 1998. The 55-kDa tumor necrosis factor receptor induces clustering of mitochondria through its membrane-proximal region. *J. Biol. Chem.* 273, 9673-9680.

Desagher, S., Martinou, J.-C. 2000. Mitochondria as the central control point of apoptosis. *Trends Cell Biol.* 10, 369-377.

Desagher, S., Osen-Sand, A., Montessuit, S., Magnenat, E., Vilbois, F., Hochmann, A., Journot, L., Antonsson, B., Martinou, J.C. 2001. Phosphorylation of bid by casein kinases I and II regulates its cleavage by caspase 8. *Mol. Cell* 8, 601-611.

Deveraux, Q.L., Roy, N., Stennicke, H.R., Van Arsdale, T., Zhou, Q., Srinivasula, S.M., Alnemri, E.S., Salvesen, G.S., Reed, J.C. 1998. IAPs block apoptotic events induced by caspase-8 and cytochrome c by direct inhibition of distinct caspases. *EMBO J.* 17, 2215-2223.

Deveraux, Q.L., Takahashi, R., Salvesen, G.S., Reed, J.C. 1997. X-linked IAP is a direct inhibitor of cell-death proteases. *Nature* 388, 300-304.

Dirac-Svejstrup, A.B., Shorter, J. , Waters, M.G., Warren, G. 2000. Phosphorylation of the vesicle-tethering protein p115 by a casein kinase II-like enzyme is required for Golgi reassembly from isolated mitotic fragments. *J. Cell Biol.* 150, 475-488.

Downward, J. 1999. How BAD phosphorylation is good for survival [news]. *Nat. Cell Biol.* 1, E33-E35.

Draviam, V.M., Orrechia, S., Lowe, M., Pardi, R., Pines, J. 2001. The localization of human cyclins B1 and B2 determines CDK1 substrate specificity and neither enzyme requires MEK to disassemble the Golgi apparatus. *J. Cell Biol.* 152, 945-958.

Droin, N., Bichat, F., Rebe, C., Wotawa, A., Sordet, O., Hammann, A., Bertrand, R., Solary, E. 2001. Involvement of caspase-2 long isoform in Fas-mediated cell death of human leukemic cells. *Blood* 97, 1835-1844.

Du, C., Fang, M., Li, Y., Li, L., Wang, X. 2000. Smac, a mitochondrial protein that promotes cytochrome c-dependent caspase activation by eliminating IAP inhibition. *Cell* 102, 33-42.

Duan, H., Dixit, V.M. 1997. RAIDD is a new 'death' adaptor molecule. *Nature* 385, 86-89.

Earnshaw, W.C., Martins, L.M., Kaufmann, S.H. 1999. Mammalian caspases: Structure, activation, substrates, and functions during apoptosis. *Ann. Rev. Biochem.* 68, 383-424.

Ekert, P.G., Silke, J., Vaux, D.L. 1999. Caspase inhibitors. *Cell Death Differ.* 6, 1081-1086.

Enari, M., Sakahira, H., Yokoyama, H., Okawa, K., Iwamatsu, A., Nagata, S. 1998. A caspase-activated DNase that degrades DNA during apoptosis, and its inhibitor ICAD. *Nature* 391, 43-50.

Escargueil, A.E., Plisov, S.Y., Filhol, O., Cochet, C., Larsen, A.K. 2000. Mitotic phosphorylation of DNA topoisomerase II alpha by protein kinase CK2 creates the MPM-2 phosphoepitope on Ser-1469. *J. Biol. Chem.* 275, 34710-34718.

Eystathioy, T., Jakymiw, A., Fujita, D.J., Fritzler, M.J., Chan, E.K. 2000. Human autoantibodies to a novel Golgi protein golgin-67: high similarity with golgin-95/gm 130 autoantigen. *J. Autoimmun.* 14 , 179-187.

Fadok, V.A., Voelker, D.R., Campbell, P.A., Cohen, J.J., Bratton, D.L., Henson, P.M. 1992. Exposure of phosphatidylserine on the surface of apoptotic lymphocytes triggers specific recognition and removal by macrophages. *J. Immunol.* 148, 2207-2216.

Featherstone, C., Griffiths, G., Warren, G. 1985. Newly synthesized G protein of vesicular stomatitis virus is not transported to the Golgi complex in mitotic cells. *J. Cell Biol.* 101, 2036-2046.

Ferri, K.F., Kroemer, G. 2001. Organelle-specific initiation of cell death pathways. *Nat. Cell Biol.* 3, E255-E263.

Frickel, E.M., Riek, R., Jelesarov, I., Helenius, A., Wuthrich, K., Ellgaard, L. 2002. TROSY-NMR reveals interaction between ERp57 and the tip of the calreticulin P-domain. *Proc. Natl. Acad. Sci. U.S.A* 99, 1954-1959.

Gallaher, B.W., Hille, R., Raile, K., Kiess, W. 2001. Apoptosis: live or die--hard work either way! *Horm. Metab. Res.* 33, 511-519.

Gallione, C.J., Rose, J.K. 1985. A single amino acid substitution in a hydrophobic domain causes temperature-sensitive cell-surface transport of a mutant viral glycoprotein. *J. Virol.* 54, 374-382.

Gil-Gomez, G., Berns, A., Brady, H.J. 1998. A link between cell cycle and cell death: Bax and Bcl-2 modulate Cdk2 activation during thymocyte apoptosis. *EMBO J.* 17, 7209-7218.

Girard, D., Paquet, M.E., Paquin, R., Beaulieu, A.D. 1996. Differential effects of interleukin-15 (IL-15) and IL-2 on human neutrophils: modulation of phagocytosis, cytoskeleton rearrangement, gene expression, and apoptosis by IL-15. *Blood* 88, 3176-3184.

Girard, D., Paquin, R., Beaulieu, A.D. 1997. Responsiveness of human neutrophils to interleukin-4: induction of cytoskeletal rearrangements, de novo protein synthesis and delay of apoptosis. *Biochem. J.* 325, 147-153.

Gluzman, Y. 1981. SV40-transformed simian cells support the replication of early SV40 mutants. *Cell* 23, 175-182.

Goping, I.S., Gross, A., Lavoie, J.N., Nguyen, M., Jemmerson, R., Roth, K., Korsmeyer, S.J., Shore, G.C. 1998. Regulated targeting of BAX to mitochondria. *J. Cell Biol.* 143, 207-215.

Gotte, M., von Mollard, G.F. 1998. A new beat for the SNARE drum. *Trends Cell Biol.* 8, 215-218.

Granville, D.J., Shaw, J.R., Leong, S., Carthy, C.M., Margaron, P., Hunt, D.W., McManus, B.M. 1999. Release of cytochrome c, Bax migration, Bid cleavage, and activation of caspases 2, 3, 6, 7, 8, and 9 during endothelial cell apoptosis. *Am. J. Pathol.* 155, 1021-1025.

Gray, N., Detivaud, L., Doerig, C., Meijer, L. 1999. ATP-site directed inhibitors of cyclin-dependent kinases. *Curr. Med. Chem.* 6, 859-875.

Green, J., Griffiths, G., Louvard, D., Quinn, P., Warren, G. 1981. Passage of viral membrane proteins through the Golgi complex. *J. Mol. Biol.* 152, 663-698.

Grenier, A., Dehoux, M., Boutten, A., Arce-Vicioso, M., Durand, G., Gougerot-Pocidalo, M.A., Chollet-Martin, S. 1999. Oncostatin M production and regulation by human polymorphonuclear neutrophils. *Blood* 93, 1413-1421.

Hakem, A., Sasaki, T., Kozieradzki, I., Penninger, J.M. 1999. The cyclin-dependent kinase Cdk2 regulates thymocyte apoptosis. *J. Exp. Med.* 189, 957-968.

Harding, H.P., Zhang, Y., Ron, D. 1999. Protein translation and folding are coupled by an endoplasmic-reticulum- resident kinase. *Nature* 397, 271-274.

Hart, S.P., Ross, J.A., Ross, K., Haslett, C., Dransfield, I. 2000. Molecular characterization of the surface of apoptotic neutrophils: implications for functional downregulation and recognition by phagocytes. *Cell Death Differ.* 7, 493-503.

Harvey, K.J., Lukovic, D., Ucker, D.S. 2000. Caspase-dependent Cdk activity is a requisite effector of apoptotic death events. *J. Cell Biol.* 148, 59-72.

Haslett, C. 1992. Resolution of acute inflammation and the role of apoptosis in the tissue fate of granulocytes. *Clin. Sci. (Lond)* 83, 639-648.

Haslett, C., Guthrie, L.A., Kopaniak, M.M., Johnston, R.B., Jr., Henson, P.M. 1985. Modulation of multiple neutrophil functions by preparative methods or trace concentrations of bacterial lipopolysaccharide. *Am. J. Pathol.* 119, 101-110.

Haslett, C., Savill, J.S., Meagher, L. 1989. The neutrophil. *Curr. Opin. Immunol.* 2, 10-18.

Haslett, C., Savill, J.S., Whyte, M.K., Stern, M., Dransfield, I., Meagher, L.C. 1994. Granulocyte apoptosis and the control of inflammation. *Philos. Trans. R. Soc. Lond B Biol. Sci.* 345, 327-333.

Hauri, H.P., Schweizer, A. 1992. The endoplasmic reticulum-Golgi intermediate compartment. *Curr. Opin. Cell Biol.* 4, 600-608.

Hay, J.C., Chao, D.S., Kuo, C.S., Scheller, R.H. 1997. Protein interactions regulating vesicle transport between the endoplasmic reticulum and Golgi apparatus in mammalian cells. *Cell* 89, 149-158.

Hay, J.C., Hirling, H., Scheller, R.H. 1996. Mammalian vesicle trafficking proteins of the endoplasmic reticulum and Golgi apparatus. *J. Biol. Chem.* 271, 5671-5679.

Hay, J.C., Klumperman, J., Oorschot, V., Steegmaier, M., Kuo, C.S., Scheller, R.H. 1998. Localization, dynamics, and protein interactions reveal distinct roles for ER and Golgi SNAREs. *J. Cell Biol.* 141, 1489-1502.

Hay, J.C., Scheller, R.H. 1997. SNAREs and NSF in targeted membrane fusion. *Curr. Opin. Cell Biol.* 9, 505-512.

Haze, K., Yoshida, H., Yanagi, H., Yura, T., Mori, K. 1999. Mammalian transcription factor ATF6 is synthesized as a transmembrane protein and activated by proteolysis in response to endoplasmic reticulum stress. *Mol. Biol. Cell* 10, 3787-3799.

Helenius, A. 1994. How N-linked oligosaccharides affect glycoprotein folding in the endoplasmic reticulum. *Mol. Biol. Cell* 5, 253-265.

Helenius, A., Aebi, M. 2001. Intracellular functions of N-linked glycans. *Science* 291, 2364 -2369.

Hiller, G., Weber, K. 1982. Golgi detection in mitotic and interphase cells by antibodies to secreted galactosyltransferase. *Exp. Cell Res.* 142, 85-94.

Hu, Y., Benedict, M.A., Ding, L., Nunez, G. 1999. Role of cytochrome c and dATP/ATP hydrolysis in Apaf-1-mediated caspase- 9 activation and apoptosis. *EMBO J.* 18, 3586-3595.

Hunt, J.M., Bommert, K., Charlton, M.P., Kistner, A., Habermann, E., Augustine, G.J., Betz, H. 1994. A post-docking role for synaptobrevin in synaptic vesicle fusion. *Neuron* 12, 1269-1279.

Iwai, K., Miyawaki, T., Takizawa, T., Konno, A., Ohta, K., Yachie, A., Seki, H., Taniguchi, N. 1994. Differential expression of bcl-2 and susceptibility to anti-Fas-mediated cell death in peripheral blood lymphocytes, monocytes, and neutrophils. *Blood* 84, 1201-1208.

Jin, Y.H., Yoo, K.J., Lee, Y.H., Lee, S.K. 2000. Caspase 3-mediated Cleavage of p21WAF1/CIP1 Associated with the Cyclin A-Cyclin-dependent Kinase 2 Complex Is a Prerequisite for Apoptosis in SK-HEP-1 Cells. *J. Biol. Chem.* 275, 30256-30263.

Jost, C.R., Gaillard, M.L., Fransen, J.A., Daha, M.R., Ginsel, L.A. 1991. Intracellular localization of glycosyl-phosphatidylinositol-anchored CD67 and FcRIII (CD16) in affected neutrophil granulocytes of patients with paroxysmal nocturnal hemoglobinuria. *Blood* 78, 3030-3036.

Jost, C.R., Huizinga, T.W., de Goede, R., Fransen, J.A., Tetteroo, P.A., Daha, M.R., Ginsel, L.A. 1990. Intracellular localization and de novo synthesis of FcRIII in human neutrophil granulocytes. *Blood* 75, 144-151.

Kaiser, C., Ferro-Novick, S. 1998. Transport from the endoplasmic reticulum to the Golgi . *Curr. Opin. Cell Biol.* 10, 477-482.

Karsan, A., Yee, E., Kaushansky, K., Harlan, J.M. 1996. Cloning of human Bcl-2 homologue: inflammatory cytokines induce human A1 in cultured endothelial cells. *Blood* 87, 3089-3096.

Kelekar, A., Thompson, C.B. 1998. Bcl-2-family proteins: the role of the BH3 domain in apoptosis. *Trends Cell Biol.* 8, 324-330.

Kerr, J.F., Wyllie, A.H., Currie, A.R. 1972. Apoptosis: a basic biological phenomenon with wide-ranging implications in tissue kinetics. *Br. J. Cancer* 26, 239-257.

Kiener, P.A., Davis, P.M., Starling, G.C., Mehlin, C., Klebanoff, S.J., Ledbetter, J.A., Liles, W.C. 1997. Differential induction of apoptosis by Fas-Fas ligand interactions in human monocytes and macrophages. *J. Exp. Med.* 185, 1511-1516.

Kim, S.G., Kim, S.N., Jong, H.S., Kim, N.K., Hong, S.H., Kim, S.J., Bang, Y.J. 2001. Caspase-mediated Cdk2 activation is a critical step to execute transforming growth factor-beta1-induced apoptosis in human gastric cancer cells. *Oncogene* 20, 1254-1265.

Kischkel, F.C., Lawrence, D.A., Tinel, A., LeBlanc, H., Virmani, A., Schow, P., Gazdar, A., Blenis, J., Arnott, D., Ashkenazi, A. 2001. Death receptor recruitment of endogenous caspase-10 and apoptosis initiation in the absence of caspase-8. *J. Biol. Chem.* 276, 46639-46646.

Kjeldsen, L., Bjerrum, O.W., Askaa, J., Borregaard, N. 1992. Subcellular localization and release of human neutrophil gelatinase, confirming the existence of separate gelatinase-containing granules. *Biochem. J.* 287, 603-610.

Kluck, R.M., Bossy-Wetzel, E., Green, D.R., Newmeyer, D.D. 1997. The release of cytochrome c from mitochondria: a primary site for Bcl-2 regulation of apoptosis. *Science* 275, 1132-1136.

Kluck, R.M., Esposti, M.D., Perkins, G., Renken, C., Kuwana, T., Bossy-Wetzel, E., Goldberg, M., Allen, T., Barber, M.J., Green, D.R., Newmeyer, D.D. 1999. The pro-apoptotic proteins, Bid and Bax, cause a limited permeabilization of the mitochondrial outer membrane that is enhanced by cytosol. *J. Cell Biol.* 147, 809-822.

Kornfeld, R., Kornfeld, S. 1985. Assembly of asparagine-linked oligosaccharides. *Annu. Rev. Biochem.* 54, 631-664.

Koyama, A.H. 1995. Induction of apoptotic DNA fragmentation by the infection of vesicular stomatitis virus. *Virus Res.* 37, 285-290.

Kuehn, M.J., Herrmann, J.M., Schekman, R. 1998. COPII-cargo interactions direct protein sorting into ER-derived transport vesicles. *Nature* 391, 187-190.

Kuijpers, T.W., Tool, A.T., van der Schoot, C.E., Ginsel, L.A., Onderwater, J.J., Roos, D., Verhoeven, A.J. 1991. Membrane surface antigen expression on neutrophils: a reappraisal of the use of surface markers for neutrophil activation. *Blood* 78, 1105-1111.

Kumar, S. 1999. Mechanisms mediating caspase activation in cell death. *Cell Death. Differ.* 6, 1060-1066.

Laemmli, U.K. 1970. Cleavage of structural proteins during the assembly of the head of bacteriophage T4. *Nature* 227, 680-685.

Lane, J.D., Lucocq, J., Pryde, J., Barr, F.A., Woodman, P.G., Allan, V.J., Lowe, M. 2002. Caspase-mediated cleavage of the stacking protein GRASP65 is required for Golgi fragmentation during apoptosis. *J. Cell Biol.* 156(3), 495-509.

Leist, M., Jaattela, M. 2001. Four deaths and a funeral: from caspases to alternative mechanisms. *Nat. Rev. Mol. Cell Biol.* 2, 589-598.

Lenard, J. 1978. Virus envelopes and plasma membranes. *Annu. Rev. Biophys. Bioeng.* 7, 139-165.

Lesa, G.M., Seemann, J., Shorter, J., Vandekerckhove, J., Warren, G. 2000. The amino-terminal domain of the Golgi protein giantin interacts directly with the vesicle-tethering protein p115. *J. Biol. Chem.* 275, 2831-2836.

Levine, T.P., Rabouille, C., Kieckbusch, R.H., Warren, G. 1996. Binding of the vesicle docking protein p115 to Golgi membranes is inhibited under mitotic conditions. *J. Biol. Chem.* 271, 17304-17311.

Lew, P.D., Monod, A., Waldvogel, F.A., Dewald, B., Baggiolini, M., Pozzan, T. 1986. Quantitative analysis of the cytosolic free calcium dependency of exocytosis from three subcellular compartments in intact human neutrophils. *J. Cell Biol.* 102, 2197-2204.

Li, F., Ambrosini, G., Chu, E.Y., Plescia, J., Tognin, S., Marchisio, P.C., Altieri, D.C. 1998. Control of apoptosis and mitotic spindle checkpoint by survivin. *Nature* 396, 580-584.

Li, P., Nijhawan, D., Budihardjo, I., Srinivasula, S.M., Ahmad, M., Alnemri, E.S., Wang, X. 1997. Cytochrome c and dATP-dependent formation of Apaf-1/caspase-9 complex initiates an apoptotic protease cascade. *Cell* 91, 479-489.

Li, X., Weinman, S.A. 2002. CHLORIDE CHANNELS AND HEPATOCELLULAR FUNCTION: Prospects for Molecular Identification. *Annu. Rev. Physiol.* 64, 609-633.

Liles, W.C., Kiener, P.A., Ledbetter, J.A., Aruffo, A., Klebanoff, S.J. 1996. Differential expression of Fas (CD95) and Fas ligand on normal human phagocytes: implications for the regulation of apoptosis in neutrophils. *J. Exp. Med.* 184, 429-440.

Lin, C.Y., Madsen, M.L., Yarm, F.R., Jang, Y.J., Liu, X., Erikson, R.L. 2000. Peripheral Golgi protein GRASP65 is a target of mitotic polo-like kinase (Plk) and Cdc2. *Proc. Natl. Acad. Sci. U.S.A* 97, 12589-12594.

Lin, R.C., Scheller, R.H. 1997. Structural organization of the synaptic exocytosis core complex. *Neuron* 19, 1087-1094.

Linstedt, A.D., Jesch, S.A., Mehta, A., Lee, T.H., Garcia-Mata, R., Nelson, D.S., Sztul, E. 2000. Binding relationships of membrane tethering components. The giantin N terminus and the GM130 N terminus compete for binding to the p115 C terminus. *J. Biol. Chem.* 275, 10196-10201.

Logarinho, E., Sunkel, C.E. 1998. The Drosophila POLO kinase localises to multiple compartments of the mitotic apparatus and is required for the phosphorylation of MPM2 reactive epitopes. *J. Cell Sci.* 111, 2897-2909.

Louvard, D., Reggio, H., Warren, G. 1982. Antibodies to the Golgi complex and the rough endoplasmic reticulum. *J. Cell Biol.* 92, 92-107.

Lowe, M., Gonatas, N.K., Warren, G. 2000. The mitotic phosphorylation cycle of the *cis*-Golgi matrix protein GM130. *J. Cell Biol.* 149, 341-356.

Lowe, M., Rabouille, C., Nakamura, N., Watson, R., Jackman, M., Jamsa, E., Rahman, D., Pappin, D.J., Warren, G. 1998. Cdc2 kinase directly phosphorylates the *cis*-Golgi matrix protein GM130 and is required for Golgi fragmentation in mitosis. *Cell* 94, 783-793.

Lucocq, J., Warren, G., Pryde, J. 1991. Okadaic acid induces Golgi apparatus fragmentation and arrest of intracellular transport. *J. Cell Sci.* 100, 753-759.

Lucocq, J.M., Pryde, J.G., Berger, E.G., Warren, G. 1988. A mitotic form of the Golgi apparatus identified using immuno- electronmicroscopy. *Prog. Clin. Biol. Res.* 270, 431-440.

Lucocq, J.M., Warren, G. 1987. Fragmentation and partitioning of the Golgi apparatus during mitosis in HeLa cells. *EMBO J.* 6, 3239-3246.

Määttä, J., Hallikas, O., Welti, S., Hilden, P., Schroder, J., Kuismanen, E. 2000. Limited caspase cleavage of human BAP31. *FEBS Lett.* 484, 202-206.

Mackay, D., Kieckbusch, R., Adamczewski, J., Warren, G. 1993. Cyclin A-mediated inhibition of intra-Golgi transport requires $p34^{cdc2}$. *FEBS Lett.* 336, 549-554.

Mahajan, N.P., Harrison-Shostak, D.C., Michaux, J., Herman, B. 1999. Novel mutant green fluorescent protein protease substrates reveal the activation of specific caspases during apoptosis. *Chem. Biol.* 6, 401-409.

Maianski, N.A., Mul, F.P., van Buul, J.D., Roos, D., Kuijpers, T.W. 2002. Granulocyte colony-stimulating factor inhibits the mitochondria-dependent activation of caspase-3 in neutrophils. *Blood* 99, 672-679.

Mancini, M., Machamer, C.E., Roy, S., Nicholson, D.W., Thornberry, N.A., Casciola-Rosen, L.A., Rosen, A. 2000. Caspase-2 is localized at the Golgi complex and cleaves golgin-160 during apoptosis. *J. Cell Biol.* 149, 603-612.

Marra, P., Maffucci, T., Daniele, T., Tullio, G.D., Ikehara, Y., Chan, E.K., Luini, A., Beznoussenko, G., Mironov, A., De Matteis, M.A. 2001. The GM130 and GRASP65 Golgi proteins cycle through and define a subdomain of the intermediate compartment. *Nat. Cell Biol.* 3, 1101-1113.

Martin-Martin, B., Nabokina, S.M., Blasi, J., Lazo, P.A., Mollinedo, F. 2000. Involvement of SNAP-23 and syntaxin 6 in human neutrophil exocytosis. *Blood* 96, 2574-2583.

McCullough, K.D., Martindale, J.L., Klotz, L.O., Aw, T.Y., Holbrook, N.J. 2001. Gadd153 sensitizes cells to endoplasmic reticulum stress by down- regulating Bcl2 and perturbing the cellular redox state. *Mol. Cell Biol.* 21, 1249-1259.

Meagher, L.C., Savill, J.S., Baker, A., Fuller, R.W., Haslett, C. 1992. Phagocytosis of apoptotic neutrophils does not induce macrophage release of thromboxane B2. *J. Leukoc. Biol.* 52, 269-273.

Meggio, F., Donella, D.A., Ruzzene, M., Brunati, A.M., Cesaro, L., Guerra, B., Meyer, T., Mett, H., Fabbro, D., Furet, P., . 1995. Different susceptibility of protein kinases to staurosporine inhibition. Kinetic studies and molecular bases for the resistance of protein kinase CK2. *Eur. J. Biochem.* 234, 317-322.

Memon, S.A., Hou, J., Moreno, M.B., Zacharchuk, C.M. 1998. Apoptosis induced by a chimeric Fas/FLICE receptor: lack of requirement for Fas- or FADD-binding proteins. *J. Immunol.* 160, 2046-2049.

Miller, T.M., Moulder, K.L., Knudson, C.M., Creedon, D.J., Deshmukh, M., Korsmeyer, S.J., Johnson, E.M., Jr. 1997. Bax deletion further orders the cell death

pathway in cerebellar granule cells and suggests a caspase-independent pathway to cell death. *J. Cell Biol.* 139, 205- 217.

Misteli, T., Warren, G. 1995. Mitotic disassembly of the Golgi apparatus *in vivo*. *J. Cell Sci.* 108, 2715-2727.

Mori, K. 2000. Tripartite management of unfolded proteins in the endoplasmic reticulum. *Cell* 101, 451- 454.

Mosser, J., Sarde, C.O., Vicaire, S., Yates, J.R., Mandel, J.L. 1994. A new human gene (DXS1357E) with ubiquitous expression, located in Xq28 adjacent to the adrenoleukodystrophy gene. *Genomics* 22, 469-471.

Moulding, D.A., Akgul, C., Derouet, M., White, M.R., Edwards, S.W. 2001. BCL-2 family expression in human neutrophils during delayed and accelerated apoptosis. *J. Leukoc. Biol.* 70, 783-792.

Moulding, D.A., Quayle, J.A., Hart, C.A., Edwards, S.W. 1998. Mcl-1 expression in human neutrophils: regulation by cytokines and correlation with cell survival. *Blood* 92, 2495-2502.

Moyer, B.D., Allan, B.B., Balch, W.E. 2001. Rab1 interaction with a GM130 effector complex regulates COPII vesicle *cis*-Golgi tethering. *Traffic* 2, 268-276.

Murphy, K.M., Streips, U.N., Lock, R.B. 1999. Bax membrane insertion during Fas(CD95)-induced apoptosis precedes cytochrome c release and is inhibited by Bcl-2. *Oncogene* 18, 5991-5999.

Muzio, M., Stockwell, B.R., Stennicke, H.R., Salvesen, G.S., Dixit, V.M. 1998. An induced proximity model for caspase-8 activation. *J. Biol. Chem.* 273, 2926-2930.

Nakagawa, T., Zhu, H., Morishima, N., Li, E., Xu, J., Yankner, B.A., Yuan, J. 2000. Caspase-12 mediates endoplasmic-reticulum-specific apoptosis and cytotoxicity by amyloid-beta. *Nature* 403, 98- 103.

Nakamura, K., Zuppini, A., Arnaudeau, S., Lynch, J., Ahsan, I., Krause, R., Papp, S., De Smedt, H., Parys, J.B., Muller-Esterl, W., Lew, D.P., Krause, K.H., Demaurex, N., Opas, M., Michalak, M. 2001. Functional specialization of calreticulin domains. *J. Cell Biol.* 154, 961-972.

Nakamura, N., Lowe, M., Levine, T.P., Rabouille, C., Warren, G. 1997. The vesicle docking protein p115 binds GM130, a *cis*-Golgi matrix protein, in a mitotically regulated manner. *Cell* 89, 445-455.

Nakamura, N., Rabouille, C., Watson, R., Nilsson, T., Hui, N., Slusarewicz, P., Kreis, T.E., Warren, G. 1995. Characterization of a *cis*-Golgi matrix protein, GM130. *J. Cell Biol.* 131, 1715-1726.

Narita, M., Shimizu, S., Ito, T., Chittenden, T., Lutz, R.J., Matsuda, H., Tsujimoto, Y. 1998. Bax interacts with the permeability transition pore to induce permeability transition and cytochrome c release in isolated mitochondria. *Proc. Natl. Acad. Sci. U.S.A* 95, 14681-14686.

Nechushtan, A., Smith, C.L., Lamensdorf, I., Yoon, S.H., Youle, R.J. 2001. Bax and Bak coalesce into novel mitochondria-associated clusters during apoptosis. *J. Cell Biol.* 153, 1265-1276.

Newmeyer, D.D., Farschon, D.M., Reed, J.C. 1994. Cell-free apoptosis in *Xenopus* egg extracts: inhibition by Bcl-2 and requirement for an organelle fraction enriched in mitochondria. *Cell* 79, 353-364.

Ng, F.W., Nguyen, M., Kwan, T., Branton, P.E., Nicholson, D.W., Cromlish, J.A., Shore, G.C. 1997. p28 Bap31, a Bcl-2/Bcl-XL- and procaspase-8-associated protein in the endoplasmic reticulum. *J. Cell Biol.* 139, 327-338.

Ng, F.W., Shore, G.C. 1998. Bcl-XL cooperatively associates with the Bap31 complex in the endoplasmic reticulum, dependent on procaspase-8 and Ced-4 adaptor. *J. Biol Chem.* 273, 3140-3143.

Nicholson, D.W. 1999. Caspase structure, proteolytic substrates, and function during apoptotic cell death. *Cell Death Differ.* 6, 1028-1042.

Novick, P., Zerial, M. 1997. The diversity of Rab proteins in vesicle transport. *Curr. Opin. Cell Biol.* 9, 496-504.

O'Connor, L., Huang, D.C., O'Reilly, L.A., Strasser, A. 2000. Apoptosis and cell division. *Curr. Opin. Cell Biol.* 12, 257-263.

Obaya, A.J., Sedivy, J.M. 2002. Regulation of cyclin-Cdk activity in mammalian cells. *Cell Mol. Life Sci.* 59, 126-142.

Ojala, P.M., Yamamoto, K., Castanos-Velez, E., Biberfeld, P., Korsmeyer, S.J., Makela, T.P. 2000. The apoptotic v-cyclin-CDK6 complex phosphorylates and inactivates Bcl- 2. *Nat. Cell Biol* 2, 819-825.

Ottonello, L., Tortolina, G., Amelotti, M., Dallegri, F. 1999. Soluble Fas ligand is chemotactic for human neutrophilic polymorphonuclear leukocytes. *J. Immunol.* 162, 3601-3606.

Pan, G., Humke, E.W., Dixit, V.M. 1998a. Activation of caspases triggered by cytochrome c in vitro. *FEBS Lett.* 426, 151-154.

Pan, G., O'Rourke, K., Dixit, V.M. 1998b. Caspase-9, Bcl-XL, and Apaf-1 form a ternary complex. *J. Biol. Chem.* 273, 5841-5845.

Parodi, A.J. 1999. Reglucosylation of glycoproteins and quality control of glycoprotein folding in the endoplasmic reticulum of yeast cells. *Biochim. Biophys. Acta* 1426, 287-295.

Parodi, A.J. 2000. Role of N-oligosaccharide endoplasmic reticulum processing reactions in glycoprotein folding and degradation. *Biochem. J.* 348, 1-13.

Patel, K.D., Modur, V., Zimmerman, G.A., Prescott, S.M., McIntyre, T.M. 1994. The necrotic venom of the brown recluse spider induces dysregulated endothelial cell-dependent neutrophil activation. Differential induction of GM-CSF, IL-8, and E-selectin expression. *J. Clin. Invest.* 94, 631-642.

Pevsner, J., Hsu, S.C., Braun, J.E., Calakos, N., Ting, A.E., Bennett, M.K., Scheller, R.H. 1994. Specificity and regulation of a synaptic vesicle docking complex. *Neuron* 13, 353-361 .

Pfeffer, S.R. 1999. Transport-vesicle targeting: tethers before SNAREs. *Nat. Cell Biol.* 1, E17-E22.

Philpott, K.L., McCarthy, M.J., Becker, D., Gatchalian, C., Rubin, L.L. 1996. Morphological and biochemical changes in neurons: apoptosis versus mitosis. *Eur. J. Neurosci.* 8, 1906-1915.

Powell, K.S., Latterlich, M. 2000. The making and breaking of the endoplasmic reticulum. *Traffic* 1, 689-694.

Pryde, J.G. 1994. A group of integral membrane proteins of the rat liver Golgi contains a conserved protein of 100kDa. *J. Cell Sci.* 107, 3425-3436.

Pryde, J.G., Farmaki, T., Lucocq, J.M. 1998. Okadaic acid induces selective arrest of protein transport in the rough endoplasmic reticulum and prevents export into COPII-coated structures. Mol. Cell. Biol. 18, 1125-1135.

Pryde, J.G., Walker, A., Rossi, A.G., Hannah, S., Haslett, C. 2000. Temperature-dependent arrest of neutrophil apoptosis: failure of bax insertion into mitochondria at 15°C prevents the release of cytochrome c. *J. Biol. Chem.* 276 (43), 33574-33584.

Rabouille, C., Levine, T.P., Peters, J.M., Warren, G. 1995. An NSF-like ATPase, p97, and NSF mediate cisternal regrowth from mitotic Golgi fragments. *Cell* 82, 905-914.

Raff, M.C. 1992. Social controls on cell survival and cell death. *Nature* 356, 397-400.

Reading, C.L., Penhoet, E.E., Ballou, C.E. 1978. Carbohydrate structure of vesicular stomatitis virus glycoprotein. *J. Biol. Chem.* 253, 5600-5612.

Rice, W.G., Ganz, T., Kinkade, J.M., Jr., Selsted, M.E., Lehrer, R.I., Parmley, R.T. 1987. Defensin-rich dense granules of human neutrophils. *Blood* 70, 757-765.

Robbins, P.W., Hubbard, S.C., Turco, S.J., Wirth, D.F. 1977. Proposal for a common oligosaccharide intermediate in the synthesis of membrane glycoproteins. *Cell* 12, 893-900.

Rossi, A.G., Haslett, C. 1998. Inflammation, Cell Injury, and Apoptosis. Chapter 2. In: *Pro-inflammatory and Anti-inflammatory Peptides*, ed. Said, S.I. Volume 112. In the series: Lung Biology in Health and Disease, (Series ed. Lenfant, C.) Marcel Dekker, Inc., New York, pp. 9-24.

Roth, J. 1987. Subcellular organization of glycosylation in mammalian cells. *Biochim. Biophys. Acta* 906, 405-436.

Rothman, J.E. 1994. Mechanisms of intracellular protein transport. *Nature* 372, 55-63.

Roy, N., Deveraux, Q.L., Takahashi, R., Salvesen, G.S., Reed, J.C. 1997. The c-IAP-1 and c-IAP-2 proteins are direct inhibitors of specific caspases. *EMBO J.* 16, 6914-6925.

Sakahira, H., Enari, M., Nagata, S. 1998. Cleavage of CAD inhibitor in CAD activation and DNA degradation during apoptosis. *Nature* 391, 96-99.

Saleh, A., Srinivasula, S.M., Acharya, S., Fishel, R., Alnemri, E.S. 1999. Cytochrome c and dATP-mediated oligomerization of Apaf-1 is a prerequisite for procaspase-9 activation. *J. Biol. Chem.* 274, 17941-17945.

Santos-Beneit, A.M., Mollinedo, F. 2000. Expression of genes involved in initiation, regulation, and execution of apoptosis in human neutrophils and during neutrophil differentiation of HL-60 cells. *J. Leukoc. Biol.* 67, 712-724 .

Saraste, J., Kuismanen, E. 1984. Pre- and post-Golgi vacuoles operate in the transport of Semliki Forest virus membrane glycoproteins to the cell surface. *Cell* 38, 535-549.

Savill, J. 1997. Apoptosis in resolution of inflammation. *J. Leukoc. Biol.* 61, 375-380.

Savill, J., Fadok, V., Henson, P., Haslett, C. 1993. Phagocyte recognition of cells undergoing apoptosis. *Immunol. Today* 14, 131-136.

Savill, J., Haslett, C. 1995. Granulocyte clearance by apoptosis in the resolution of inflammation. *Semin. Cell Biol.* 6, 385-393.

Savill, J.S., Wyllie, A.H., Henson, J.E., Walport, M.J., Henson, P.M., Haslett, C. 1989. Macrophage phagocytosis of aging neutrophils in inflammation. Programmed cell death in the neutrophil leads to its recognition by macrophages. *J. Clin. Invest* 83, 865-875.

Scaffidi, C., Fulda, S., Srinivasan, A., Friesen, C., Li, F., Tomaselli, K.J., Debatin, K.M., Krammer, P.H., Peter, M.E. 1998. Two CD95 (APO-1/Fas) signaling pathways. *EMBO J.* 17, 1675-1687.

Scales, S.J., Chen, Y.A., Yoo, B.Y., Patel, S.M., Doung, Y.C., Scheller, R.H. 2000. SNAREs contribute to the specificity of membrane fusion. *Neuron* 26, 457-464.

Schroter, M., Peitsch, M.C., Tschopp, J. 1996. Increased p34cdc2-dependent kinase activity during apoptosis: a possible activation mechanism of DNase I leading to DNA breakdown. *Eur. J. Cell Biol.* 69, 143-150.

Schurmann, A., Mooney, A.F., Sanders, L.C., Sells, M.A., Wang, H.G., Reed, J.C., Bokoch, G.M. 2000. p21-activated kinase 1 phosphorylates the death agonist bad and protects cells from apoptosis. *Mol. Cell Biol.* 20, 453-461.

Schweizer, A., Fransen, J.A., Matter, K., Kreis, T.E., Ginsel, L., Hauri, H.P. 1990. Identification of an intermediate compartment involved in protein transport from endoplasmic reticulum to Golgi apparatus. *Eur. J. Cell Biol.* 53, 185-196.

Seemann, J., Jokitalo, E.J., Warren, G. 2000. The role of the tethering proteins p115 and GM130 in transport through the Golgi apparatus in vivo. *Mol. Biol. Cell* 11, 635-645.

Sengelov, H., Follin, P., Kjeldsen, L., Lollike, K., Dahlgren, C., Borregaard, N. 1995. Mobilization of granules and secretory vesicles during in vivo exudation of human neutrophils. *J. Immunol.* 154, 4157-4165.

Sengelov, H., Kjeldsen, L., Borregaard, N. 1993a. Control of exocytosis in early neutrophil activation. *J. Immunol.* 150, 1535-1543.

Sengelov, H., Kjeldsen, L., Diamond, M.S., Springer, T.A., Borregaard, N. 1993b. Subcellular localization and dynamics of Mac-1 (alpha m beta 2) in human neutrophils. *J. Clin. Invest.* 92, 1467-1476.

Sengelov, H., Kjeldsen, L., Kroeze, W., Berger, M., Borregaard, N. 1994. Secretory vesicles are the intracellular reservoir of complement receptor 1 in human neutrophils. *J. Immunol.* 153, 804-810.

Sesso, A., Fujiwara, D.T., Jaeger, M., Jaeger, R., Li, T.C., Monteiro, M.M., Correa, H., Ferreira, M.A., Schumacher, R.I., Belisario, J., Kachar, B., Chen, E.J. 1999. Structural elements common to mitosis and apoptosis. *Tissue Cell* 31, 357-371.

Sheehan, J.P., Palmer, P.E., Helm, G.A., Tuttle, J.B. 1997. MPP+ induced apoptotic cell death in SH-SY5Y neuroblastoma cells: an electron microscope study. *J. Neurosci. Res.* 48, 226-237.

Shi, L., Nishioka, W.K., Th'ng, J., Bradbury, E.M., Litchfield, D.W., Greenberg, A.H. 1994. Premature p34cdc2 activation required for apoptosis. *Science* 263, 1143-1145.

Shorter, J., Warren, G. 1999. A role for the vesicle tethering protein, p115, in the post-mitotic stacking of reassembling Golgi cisternae in a cell-free system. *J. Cell Biol.* 146, 57-70.

Shorter, J., Watson, R., Giannakou, M.E., Clarke, M., Warren, G., Barr, F.A. 1999. GRASP55, a second mammalian GRASP protein involved in the stacking of Golgi cisternae in a cell-free system. *EMBO J.* 18, 4949-4960.

Silberstein, S., Gilmore, R. 1996. Biochemistry, molecular biology, and genetics of the oligosaccharyltransferase. *FASEB J.* 10, 849-858.

Slee, E.A., Adrain, C., Martin, S.J. 1999a. Serial killers: ordering caspase activation events in apoptosis. *Cell Death. Differ.* 6, 1067-1074.

Slee, E.A., Adrain, C., Martin, S.J. 2001. Executioner caspase-3, -6, and -7 perform distinct, non-redundant roles during the demolition phase of apoptosis. *J. Biol. Chem.* 276, 7320-7326.

Slee, E.A., Harte, M.T., Kluck, R.M., Wolf, B.B., Casiano, C.A., Newmeyer, D.D., Wang, H.G., Reed, J.C., Nicholson, D.W., Alnemri, E.S., Green, D.R., Martin, S.J. 1999b. Ordering the cytochrome c-initiated caspase cascade: hierarchical activation of caspases-2, -3, -6, -7, -8, and -10 in a caspase-9- dependent manner. *J. Cell Biol.* 144, 281-292.

Smith, C.A., Farrah, T., Goodwin, R.G. 1994. The TNF receptor superfamily of cellular and viral proteins: activation, costimulation, and death . *Cell* 76, 959-962.

Sohda, M., Misumi, Y., Yano, A., Takami, N., Ikehara, Y. 1998. Phosphorylation of the vesicle docking protein p115 regulates its association with the Golgi membrane. *J. Biol. Chem.* 273, 5385-5388.

Sollner, T., Bennett, M.K., Whiteheart, S.W., Scheller, R.H., Rothman, J.E. 1993. A protein assembly-disassembly pathway in vitro that may correspond to sequential steps of synaptic vesicle docking, activation, and fusion. *Cell* 75, 409-418.

Sonnichsen, B., Lowe, M., Levine, T., Jamsa, E., Dirac-Svejstrup, B., Warren, G. 1998. A role for giantin in docking COPI vesicles to Golgi membranes. *J. Cell Biol.* 140, 1013-1021.

Sossin, W.S., Fisher, J.M., Scheller, R.H. 1990. Sorting within the regulated secretory pathway occurs in the trans- Golgi network. *J. Cell Biol.* 110, 1-12.

Sprague, J., Condra, J.H., Arnheiter, H., Lazzarini, R.A. 1983. Expression of a recombinant DNA gene coding for the vesicular stomatitis virus nucleocapsid protein. *J. Virol.* 45, 773-781.

Srinivasula, S.M., Ahmad, M., Fernandes-Alnemri, T., Alnemri, E.S. 1998. Autoactivation of procaspase-9 by Apaf-1-mediated oligomerization. *Mol. Cell* 1, 949-957.

Srinivasula, S.M., Hegde, R., Saleh, A., Datta, P., Shiozaki, E., Chai, J., Lee, R.A., Robbins, P.D., Fernandes-Alnemri, T., Shi, Y., Alnemri, E.S. 2001. A conserved XIAP-interaction motif in caspase-9 and Smac/DIABLO regulates caspase activity and apoptosis. *Nature* 410, 112-116.

Stennicke, H.R., Jurgensmeier, J.M., Shin, H., Deveraux, Q., Wolf, B.B., Yang, X., Zhou, Q., Ellerby, H.M., Ellerby, L.M., Bredesen, D., Green, D.R., Reed, J.C., Froelich, C.J., Salvesen, G.S. 1998. Pro-caspase-3 is a major physiologic target of caspase-8. *J. Biol. Chem.* 273, 27084-27090.

Strasser, A., O'Connor, L., Dixit, V.M. 2000. Apoptosis signaling. *Annu. Rev. Biochem.* 69, 217-245.

Stuart, R.A., Mackay, D., Adamczewski, J., Warren, G. 1993. Inhibition of intra-Golgi transport in vitro by mitotic kinase. *J. Biol. Chem.* 268, 4050-4054.

Subramaniam, V.N., Peter, F., Philp, R., Wong, S.H., Hong, W. 1996. GS28, a 28-kilodalton Golgi SNARE that participates in ER-Golgi transport. *Science* 272, 1161-1163.

Susin, S.A., Zamzami, N., Castedo, M., Hirsch, T., Marchetti, P., Macho, A., Daugas, E., Geuskens, M., Kroemer, G. 1996. Bcl-2 inhibits the mitochondrial release of an apoptogenic protease. *J. Exp. Med.* 184, 1331-1341.

Sutterlin, C., Lin, C.Y., Feng, Y., Ferris, D.K., Erikson, R.L., Malhotra, V. 2001. Polo-like kinase is required for the fragmentation of pericentriolar Golgi stacks during mitosis. *Proc. Natl. Acad. Sci. U.S.A.* 98, 9128-9132.

Tabas, I., Kornfeld, S. 1978. The synthesis of complex-type oligosaccharides. III. Identification of an alpha-D-mannosidase activity involved in a late stage of processing of complex-type oligosaccharides. *J. Biol. Chem.* 253, 7779-7786.

Takizawa, C.G., Morgan, D.O. 2000. Control of mitosis by changes in the subcellular location of cyclin-B1- Cdk1 and Cdc25C. *Curr. Opin. Cell Biol.* 12, 658-665.

Tartaglia, L.A., Ayres, T.M., Wong, G.H., Goeddel, D.V. 1993. A novel domain within the 55 kd TNF receptor signals cell death. *Cell* 74, 845-853.

Thomas, W.D., Zhang, X.D., Franco, A.V., Nguyen, T., Hersey, P. 2000. TNF-related apoptosis-inducing ligand-induced apoptosis of melanoma is associated with changes in mitochondrial membrane potential and perinuclear clustering of mitochondria. *J. Immunol.* 165, 5612-5620.

Thornberry, N.A. 1999. Caspases: A decade of death research. Cell Death Diff. 6, 1023-1027.

Towbin, H., Staehelin, T., Gordon, J. 1979. Electrophoretic transfer of proteins from polyacrylamide gels to nitrocellulose sheets: procedure and some applications. *Proc. Natl. Acad. Sci. U.S.A.* 76, 4350-4354.

Urano, F., Wang, X., Bertolotti, A., Zhang, Y., Chung, P., Harding, H.P., Ron, D. 2000. Coupling of stress in the ER to activation of JNK protein kinases by transmembrane protein kinase IRE1. *Science* 287, 664-666.

Valentinis, B., Porcu, P.L., Quinn, K., Baserga, R. 1994. The role of the insulin-like growth factor I receptor in the transformation by simian virus 40 T antigen. *Oncogene* 9, 825-831.

Van de, C.M., Van Loo, G., Pype, S., Van Criekinge, W., Van, d.b., I, Molemans, F., Fiers, W., Declercq, W., Vandenabeele, P. 1998. Identification of a new caspase homologue: caspase-14. *Cell Death Differ.* 5, 838-846.

Varfolomeev, E.E., Schuchmann, M., Luria, V., Chiannilkulchai, N., Beckmann, J.S., Mett, I.L., Rebrikov, D., Brodianski, V.M., Kemper, O.C., Kollet, O., Lapidot, T., Soffer, D., Sobe, T., Avraham, K.B., Goncharov, T., Holtmann, H., Lonai, P., Wallach, D. 1998. Targeted disruption of the mouse Caspase 8 gene ablates cell death induction by the TNF receptors, Fas/Apo1, and DR3 and is lethal prenatally. *Immunity.* 9, 267-276.

von Mollard, G.F., Nothwehr, S.F., Stevens, T.H. 1997. The yeast v-SNARE Vti1p mediates two vesicle transport pathways through interactions with the t-SNAREs Sed5p and Pep12p. *J. Cell Biol.* 137, 1511-1524.

Wagner, J.G., Roth, R.A. 2000. Neutrophil migration mechanisms, with an emphasis on the pulmonary vasculature. *Pharmacol. Rev.* 52, 349-374.

Walker, A., Sheldrake, T., Haslett, C., Pryde, J.G. 2002. Exocytic transport between the endoplasmic reticulum and the Golgi complex is arrested during apoptosis. *In preparation.*

Wang, L., Miura, M., Bergeron, L., Zhu, H., Yuan, J. 1994. Ich-1, an Ice/ced-3-related gene, encodes both positive and negative regulators of programmed cell death. *Cell* 78, 739 -750.

Ward, C., Chilvers, E.R., Lawson, M.F., Pryde, J.G., Fujihara, S., Farrow, S.N., Haslett, C., Rossi, A.G. 1999a. NF-kappaB activation is a critical regulator of human granulocyte apoptosis in vitro. *J. Biol. Chem.* 274, 4309-4318.

Ward, C., Dransfield, I., Chilvers, E.R., Haslett, I., Rossi, A.G. 1999b. Pharmacological manipulation of granulocyte apoptosis: potential therapeutic targets. *Trends Pharmacol. Sci.* 20, 503-509.

Warren, G., Levine, T., Misteli, T. 1995. Mitotic disassembly of the mammalian Golgi apparatus. *trends in CELL BIOLOGY* 5, 413-416.

Warren, G. 1989. Cell biology: mitosis and membranes [news]. *Nature* 342, 857-858.

Warren, G., Featherstone, C., Griffiths, G., Burke, B. 1983. Newly synthesized G protein of vesicular stomatitis virus is not transported to the cell surface during mitosis. *J. Cell Biol.* 97, 1623-1628.

Waters, M.G., Clary, D.O., Rothman, J.E. 1992. A novel 115-kD peripheral membrane protein is required for intercisternal transport in the Golgi stack. *J. Cell Biol* 118, 1015-1026.

Watt, J.A., Pike, C.J., Walencewicz-Wasserman, A.J., Cotman, C.W. 1994. Ultrastructural analysis of beta-amyloid-induced apoptosis in cultured hippocampal neurons. *Brain Res.* 661, 147- 156.

Wei, M.C., Zong, W.X., Cheng, E.H., Lindsten, T., Panoutsakopoulou, V., Ross, A.J., Roth, K.A., MacGregor, G.R., Thompson, C.B., Korsmeyer, S.J. 2001. Proapoptotic BAX and BAK: a requisite gateway to mitochondrial dysfunction and death. *Science* 292, 727-730.

Weide, T., Bayer, M., Koster, M., Siebrasse, J.P., Peters, R., Barnekow, A. 2001. The Golgi matrix protein GM130: a specific interacting partner of the small GTPase rab1b. *EMBO Rep.* 2, 336-341.

Westendorf, J.M., Rao, P.N., Gerace, L. 1994. Cloning of cDNAs for M-phase phosphoproteins recognized by the MPM2 monoclonal antibody and determination of the phosphorylated epitope. *Proc. Natl. Acad. Sci. U. S. A* 91, 714-718.

Whyte, M.K., Meagher, L.C., MacDermot, J., Haslett, C. 1993. Impairment of function in aging neutrophils is associated with apoptosis. *J. Immunol.* 150, 5124-5134.

Whyte, M.K., Savill, J., Meagher, L.C., Lee, A., Haslett, C. 1997. Coupling of neutrophil apoptosis to recognition by macrophages: coordinated acceleration by protein synthesis inhibitors. *J. Leukoc. Biol.* 62, 195-202.

Williams, M.A., Solomkin, J.S. 1999. Integrin-mediated signaling in human neutrophil functioning. *J. Leukoc. Biol.* 65, 725-736.

Wilson, B.S., Nuoffer, C., Meinkoth, J.L., McCaffery, M., Feramisco, J.R., Balch, W.E., Farquhar, M.G. 1994. A Rab1 mutant affecting guanine nucleotide exchange promotes disassembly of the Golgi apparatus. *J. Cell Biol* 125, 557-571.

Wolter, K.G., Hsu, Y.T., Smith, C.L., Nechushtan, A., Xi, X.G., Youle, R.J. 1997. Movement of Bax from the cytosol to mitochondria during apoptosis. *J. Cell Biol.* 139, 1281-1292.

Wyllie, A.H., Kerr, J.F., Currie, A.R. 1980. Cell death: the significance of apoptosis. *Int. Rev. Cytol.* 68, 251-306.

Yamashita, K., Takahashi, A., Kobayashi, S., Hirata, H., Mesner, P.W., Jr., Kaufmann, S.H., Yonehara, S., Yamamoto, K., Uchiyama, T., Sasada, M. 1999.

Caspases mediate tumor necrosis factor-alpha-induced neutrophil apoptosis and downregulation of reactive oxygen production. *Blood* 93, 674-685.

Ye, J., Rawson, R.B., Komuro, R., Chen, X., Dave, U.P., Prywes, R., Brown, M.S., Goldstein, J.L. 2000. ER stress induces cleavage of membrane-bound ATF6 by the same proteases that process SREBPs. *Mol. Cell* 6, 1355-1364.

Yoneda, T., Imaizumi, K., Oono, K., Yui, D., Gomi, F., Katayama, T., Tohyama, M. 2001. Activation of caspase-12, an endoplastic reticulum (ER) resident caspase, through tumor necrosis factor receptor-associated factor 2- dependent mechanism in response to the ER stress. *J. Biol. Chem.* 276, 13935-13940.

Yoshida, H., Okada, T., Haze, K., Yanagi, H., Yura, T., Negishi, M., Mori, K. 2000. ATF6 activated by proteolysis binds in the presence of NF-Y (CBF) directly to the *cis*-acting element responsible for the mammalian unfolded protein response. *Mol. Cell Biol.* 20, 6755-6767.

Yuan, J., Shaham, S., Ledoux, S., Ellis, H.M., Horvitz, H.R. 1993. The *C.elegans* cell death genes ced-3 encodes a protein similar to mammalian interleukin-1β converting enzyme. *Cell* 75, 641-652.

Zajicek, G., Shohat, M., Polliack, A. 1984. On the maturation rate of the neutrophil. *Anat. Rec.* 209, 85-94.

Zamzami, N., Kroemer, G. 2001. The mitochondrion in apoptosis: how Pandora's box opens. *Nat. Rev. Mol. Cell Biol.* 2, 67-71.

Zerial, M., McBride, H. 2001. Rab proteins as membrane organizers. *Nat. Rev. Mol. Cell Biol.* 2, 107-117.

Zhou, B.B., Li, H., Yuan, J., Kirschner, M.W. 1998. Caspase-dependent activation of cyclin-dependent kinases during Fas- induced apoptosis in Jurkat cells. *Proc. Natl. Acad. Sci. U. S. A* 95, 6785-6790.

Zhou, Z., Richard, C., Menard, H.A. 2000. De novo synthesis of proteinase 3 by cytokine primed circulating human polymorphonuclear neutrophils and mononuclear cells. *J. Rheumatol.* 27, 2406-2411.

Zimmermann, K.C., Green, D.R. 2001. How cells die: apoptosis pathways. *J. Allergy Clin. Immunol.* 108, S99-103.

Zuppini, A., Groenendyk, J., Cormack, L.A., Shore, G., Opas, M., Bleackley, R.C., Michalak, M. 2002. Calnexin deficiency and endoplasmic reticulum stress-induced apoptosis. *Biochemistry* 41, 2850- 2858.

THE JOURNAL OF BIOLOGICAL CHEMISTRY
Vol. 275, No. 43, Issue of October 27, pp. 33574–33584, 2000
Printed in U.S.A.

Temperature-dependent Arrest of Neutrophil Apoptosis

FAILURE OF Bax INSERTION INTO MITOCHONDRIA AT 15 °C PREVENTS THE RELEASE OF CYTOCHROME *c**

Received for publication, February 8, 2000, and in revised form, July 12, 2000
Published, JBC Papers in Press, July 13, 2000, DOI 10.1074/jbc.M001008200

James G. Pryde‡, Annemieke Walker§, Adriano G. Rossi, Sharon Hannah, and Christopher Haslett

From the Rayne Laboratory, University of Edinburgh Medical School, Teviot Place, Edinburgh EH8 9AG, United Kingdom

Apoptosis is essential for the resolution of neutrophilic inflammation. To define the mechanisms triggering the execution phase of apoptosis we developed and utilized a model in which culture of human neutrophils at 15 °C for 20 h arrested apoptosis and subsequent warming to 37 °C triggered a synchronous burst of apoptosis. Treatment of 15 °C cultured neutrophils with the pan-caspase inhibitor zVAD-fmk just before warming to 37 °C inhibited the morphological changes associated with apoptosis, but did not prevent the insertion of the proapoptotic protein Bax into mitochondria nor the inhibition of secretion and the externalization of phosphatidylserine, indices of neutrophil apoptosis. In both intact neutrophils and a cell-free extract, cytochrome *c* released from mitochondria induced proteolytic cleavage of procaspase-3. At 15 °C the binding of Bax to mitochondria was uncoupled from Bax insertion into the mitochondrial membrane required for the release of cytochrome *c*. Apoptosis was also inhibited by low pH during warming to 37 °C, suggesting that changes to the conformation of Bax, necessary for membrane insertion, were being inhibited. Bax insertion was only sensitive to zVAD-fmk when added at the start of the 15 °C culture period, suggesting that a cytoplasmic substrate of the effector caspases may mediate in the mechanism of Bax insertion into mitochondria.

Successful resolution of the inflammatory response requires that granulocytes, neutrophils and eosinophils, trigger an intracellular program for "silent" self-destruction called apoptosis (1, 2). If cell-death occurs by necrosis the cytotoxic cargo of granulocyte molecules is released, inducing tissue damage and chronic inflammation and stimulating the release of proinflammatory macrophage products to promote inflammation by other routes. The apoptotic program induces the morphological hallmarks of apoptosis, nuclear condensation and cell shrinkage, and shuts down the secretory potential of granulocytes (3). Changes to the molecular profile of the surface of apoptotic neutrophils target them for phagocytosis by macrophages (4, 5), without release of proinflammatory mediators from macrophages (6). Proinflammatory mediators and cytokines, such as granulocyte-macrophage colony-stimulating factor, lipopolysaccharide, C5a, or an hypoxic environment at the site of inflammation can prolong the functional life span of granulocytes by delaying apoptosis (7, 8) through increased expression of the anti-apoptotic proteins Bcl-X_L (9) and Mcl-1 (10). The molecular mechanism triggering the execution phase of apoptosis in granulocytes is unknown but activation of tumor necrosis factor α and Fas (CD95) cell surface receptors increase expression of the proapoptotic proteins Bax and procaspase-3 (9–14). Both the p38 mitogen-activated protein kinase and p42/p44 mitogen-activated protein kinase, and the transcription factor nuclear factor-κB, regulate the granulocyte apoptotic program (15, 16), the signals transduced by these pathways converging to induce activation of procaspase-3 (17–20).

In mammalian cells the execution phase of apoptosis involves either the direct activation of procaspase-3 by caspase-8 (21), or indirect activation of procaspase-3 through the release of apoptosis-inducing factors, such as cytochrome *c*, from mitochondria (22–30). The proapoptotic Bcl-2 family member Bax is a soluble, monomeric, cytoplasmic protein (31) that inserts an hydrophobic C-terminal membrane-spanning domain into mitochondria (32, 33), inducing release of cytochrome *c* (31–35), triggering the activation of caspase-3 (36–38) and the execution phase of apoptosis. Bax dimerization (39), the addition of recombinant Bax to isolated mitochondria (36) or overexpression of Bax (40) has also been shown to induce the release of cytochrome *c*. The mechanism by which cytochrome *c* is translocated from mitochondria into the cytoplasm is controversial (41). However, once in the cytoplasm cytochrome *c* complexes with apoptosis-protease-activating factor-1 (Apaf-1) and procaspase-9 (26) to form a protein complex the "apoptosome" (42). In the presence of dATP this complex induces the proteolytic cleavage and activation of procaspase-3 that triggers a downstream cascade of caspase activity (43). It has been reported that after differentiation and maturation neutrophils have a reduced number of phenotypically atypical mitochondria, obtaining ATP predominantly by glycolysis (10). Thus, whether mitochondria play a role in triggering neutrophil apoptosis remains to be established.

Here we show that peripheral blood neutrophils cultured *in vitro* at 15 °C for 20 h failed to induce the execution phase of apoptosis until warmed to 37 °C, when they showed a synchronous burst of apoptosis. In temperature-arrested neutrophils endogenous Bax showed peripheral binding to mitochondria but failed to induce activation of caspase-3 and apoptosis. On warming to 37 °C Bax inserted into the neutrophil membranes with concomitant proteolytic cleavage of procaspase-3 and induction of apoptosis. In both intact neutrophils and cell-free

* This work is supported by Program Grant G9016491 from the Medical Research Council, United Kingdom. The costs of publication of this article were defrayed in part by the payment of page charges. This article must therefore be hereby marked "*advertisement*" in accordance with 18 U.S.C. Section 1734 solely to indicate this fact.

‡ To whom correspondence should be addressed: Respiratory Medicine Unit, Dept. of Medicine (RIE), Rayne Laboratory, University of Edinburgh Medical School, Teviot Place, Edinburgh, EH8 9AG. Scotland, UK. Tel.: 44-131-650-6949; Fax: 44-131-650-4384; E-mail: j.pryde@ed.ac.uk.

§ Supported by University of Edinburgh Faculty of Medicine, Vans Dunlop, and Shaw McFie Lang Postgraduate Research Scholarships.

neutrophil extracts we show that the proteolytic cleavage of procaspase-3 is induced by translocation of cytochrome *c* into the cytoplasm. Analysis of plasma membrane events showed that externalization of phosphatidylserine and the inhibition of secretion were uncoupled from the activation of caspase-3, when the pan-caspase inhibitor benzyloxycarbonyl-Val-Ala-Asp-fluoromethyl ketone (zVAD-fmk)[1] was added to 15 °C cultured neutrophils before warming them to 37 °C. Under these conditions the caspase inhibitor did not prevent Bax insertion into mitochondria when the cells were warmed from 15 to 37 °C. However, surprisingly, Bax insertion was inhibited if zVAD-fmk was added to neutrophils at the start of their incubation at 15 °C. This experimental model of apoptosis has provided insights into the molecular mechanisms that trigger the execution phase of neutrophil apoptosis.

EXPERIMENTAL PROCEDURES

Granulocyte Isolation and Culture—Neutrophils were purified on gradients of Percoll® from Amersham Pharmacia Biotech (Bucks, United Kingdom) (44). They were cultured in Tuf-Tainer® Teflon® pots from Pierce & Warriner Ltd. (Chester, UK) at 5×10^6 cells/ml in growth medium containing: Iscove's modified Dulbecco's medium supplemented with 2 mM glutamine, 100 units/ml penicillin, 100 μg/ml streptomycin, and 10% (v/v) autologous serum. Culture at 15 °C was in growth medium containing: 25 mM Hepes-NaOH, pH 7, 0.2% (w/v) endotoxin-free bovine serum albumin (BSA), and 20 μg/ml cycloheximide. BSA and all other chemicals were from Sigma. Neutrophil preparations were 98% pure with <2% eosinophil contamination (16). Granulocytes from atopic donors were used to purify eosinophils by a negative selection procedure (16). Incubations with zVAD-fmk from BACHEM Ltd. (Essex, UK), staurosporine from CN Biosciences (Nottingham, UK), and bongkrekic acid from BIOMOL Research Laboratories Inc. (Plymouth Meeting, PA) were in Iscove's medium with 0.2% (w/v) BSA and 20 μg/ml cycloheximide.

Assessment of Granulocyte Apoptosis—Nuclear morphology was assessed on cytocentrifuged slides stained with Diff-Quik® Gamidor Ltd. (Abingdon, Oxon, UK) (16). Annexin V-FITC, from BenderMed Systems (Vienna, Austria), was used at 1:200 dilution (5×10^5 cells/ml) to assay phosphatidylserine externalization and propidium iodide (10 μg/ml in Ca^{2+}/Mg^{2+}-free phosphate-buffered saline) was used to monitor membrane integrity by flow cytometry on an EPICS Profile II from Coulter Electronics (Luton, UK) (16). DNA fragmentation was detected by the TUNEL® *in situ* cell death detection kit from Roche Molecular Biochemicals (East Sussex, UK) and by sizing of DNA fragments on agarose gels, capturing images using a GS 1600m gel documentation system Ultra-Violet Products Ltd. (Cambridge, UK) (16, 45). The data is representative of at least three experiments unless indicated.

Measurement of Intracellular pH—Neutrophils (5×10^4 cells) in 100 μl of Hank's buffered saline, supplemented with 20 mM Hepes-NaOH, pH 7.4, 5 mM glucose, 0.2% (w/v) BSA, and 10 μM SNARF-1/AM from Molecular Probes (Eugene, OR) were incubated for 10 min at 37 °C. Intracellular SNARF-1 was excited at 488 nm and emission was measured at 575 and 670 nm using linear amplifiers and data plotted as forward scatter *versus* fluorescence ratio (FL2/FL3). The intracellular pH (pH_i) was determined by comparing mean 575/670 nm fluorescence ratio values of histograms, to a calibration curve of histograms from fresh neutrophils. The pH was clamped between 5.6 and 7.8, with overlapping 0.2 pH unit intervals, in 20 mM Mes, Pipes, and Hepes buffers and 2 μg/ml nigericin, in a high-potassium medium containing: 110 mM KCl, 20 mM NaCl, 5 mM glucose, 1 mM $MgCl_2$, 1.5 mM $CaCl_2$, 0.2% (w/v) BSA.

Preparation of Cytosol from 15 °C Neutrophils—Neutrophils (5×10^8; <5% apoptotic after 20 h at 15 °C) were sedimented at $1,500 \times g_{av}$ at 4 °C. They were washed twice in 50 ml of homogenization buffer: 15 mM Pipes-NaOH, pH 7.4, 80 mM KCl, 20 mM NaCl, 0.25 M sucrose, 1 mM dithiothreitol, and a 1:1000 dilution of protease inhibitor mixture: 87 mg of phenylmethylsulfonyl fluoride, 160 mg benzamidine, and 10 mg of leupeptin and aprotinin, and 5 mg each of bestatin, antipain, chymostatin, and pepstatin A solubilized in 1 ml of Me_2SO. Neutrophils were resuspended in 1 ml of homogenization buffer then broken with 20–30 strokes of a tight-fitting pestle in a glass Dounce homogenizer from Wheaton (Millville, NJ), until 80% of the nuclei stained with trypan blue. Intact cells and nuclei were removed by centrifugation at $350 \times g_{av}$ for 5 min at 4 °C. Post-nuclear supernatants were centrifuged at $17,000 \times g_{av}$ in a TLA 100.3 rotor from Beckman (High Wycombe, Bucks, UK) for 10 min to remove secretory granules and mitochondria and the supernatant centrifuged at $541,000 \times g_{max}$ for 15 min in a TLA 100.3 rotor to yield a membrane-free cytosol. Cytosol (200 μl) was frozen and stored in liquid nitrogen. Protein concentrations were assayed by the bicinchonic acid protocol from Pierce & Warriner Ltd. The immunoprecipitation procedure, with a monoclonal antibody to a native cytochrome *c* epitope (6H2.B4, PharMingen), was as described previously (46).

Cell-free Proteolytic Cleavage of Procaspase-3—Cell-free mixtures for the proteolytic cleavage of procaspase-3 contained: 10 μl of 15 °C cytosol (50 mg of protein/ml) and 10 μl of an assay dilution buffer containing: 10 mM Hepes-NaOH, pH 7.4, 40 mM β-glycerophosphate, 50 mM NaCl, 2 mM $MgCl_2$, 5 mM EGTA, 1 mM dithiothreitol, supplemented with dATP (20 μM) and inhibitors where appropriate. Incubations were stopped by transferring samples to ice and adding 20 μl of 50 mM Tris-HCl, pH 8, 0.4 M NaCl, 1% (w/v) deoxycholate, 1% (w/v) Nonidet P-40, 5 mM EDTA, containing protease inhibitor mixture (lysis buffer) for 0.5 h.

Isolation of Mitochondria—Rat liver was washed in 10 mM Pipes-NaOH, pH 7.2, 0.25 M sucrose, 2 mM EDTA and protease inhibitor mixture then forced through a stainless steel sieve (150 μm aperture; Endecotes Ltd., London) to break cells (46). The mitochondria were isolated from a post-nuclear supernatant as described previously and washed in the assay dilution buffer described above (47).

SDS-PAGE and Immunoblotting—Assay samples (40 μl), treated with ice-cold lysis buffer for 0.5 h (40 μl) were solubilized with 80 μl of 2 × SDS-PAGE sample buffer (46) at 95 °C for 10 min, then treated with 1 mM dithiothreitol, cooled, and treated with 10 mM iodoacetamide. The proteins were separated on 12% (w/v) polyacrylamide gels and electrophoretically transferred to nitrocellulose (46). The blots were probed with monoclonal antibodies to procaspase-3 (clone 19) and procaspase-7 (clone 51) from Transduction Laboratories (Lexington, KY) and monoclonal antibodies to procaspase-8 (clone B9-2), procaspase-9 (clone B40), cytochrome *c* (clone 7H8.2C12), and polyclonal human Bax (13666E) all from PharMingen (San Diego, CA), at dilutions of 1:500–1:1000. A hybridoma supernatant to poly(ADP-ribose)polymerase (PARP), used at 1:500 dilution, was a gift from Said Aoufuchi (Laboratory of Molecular Biology, Cambridge, UK). The horseradish peroxidase-conjugated anti-mouse and anti-rabbit IgGs from Kirkegaard & Perry Labs (Gaithersburg, MA) were used at 1:4000 dilution for 0.5 h and detected by enhanced chemiluminescence (46). The level of protein loading and nonspecific proteolysis were monitored by Ponceau S staining (46). Tubulin and actin were assayed with anti-bovine α-tubulin monoclonal antibody (236-10501) from Molecular Probes and a monoclonal antibody to actin; a gift from Simon Brown (Center for Inflammation Research, University of Edinburgh).

Confocal Microscopy—Neutrophils (10^5 cells in 100 μl of medium) were cytocentrifuged (300 rpm for 3 min) onto $1.5 \times 22 \times 22$-mm glass coverslips and fixed in methanol-free 3% (w/v) *p*-formaldehyde/phosphate-buffered saline and processed for immunofluorescence microscopy as described previously (46). The fixed cells were permeabilized with 0.1% (w/v) Triton X-100 and nonspecific binding sites blocked for 1 h with 0.2% (w/v) fish skin gelatin and 20% (v/v) sheep serum in phosphate-buffered saline. A monoclonal antibody to mitochondrial heat shock protein 70 (mtHSP70) from Affinity Bioreagents Inc. (Golden, CO) and a rabbit polyclonal antibody to ubiquinol-cytochrome *c* oxidoreductase (complex III) produced by Herman Schagger (University of Frankfurt-am-Main), were used at 1:200 dilution to stain mitochondria. The polyclonal antibody to human Bax was used at 1:200 dilution. The secondary antibodies used at 1:400 dilution were Alexa® 488 (green) goat anti-mouse IgG (highly cross-adsorbed) and Alexa® 568 (red) goat anti-rabbit (highly cross-adsorbed) and the nucleic acid stain TOPO-3® (8 μM), from Molecular Probes. Cells were observed using a ×63 water immersion objective lens with a numerical aperture of 1.2 on a Leica TCS NT confocal laser scanning microscope system (Heidelberg, GMBH). Single optical sections of the images captured with Leica TCS software were digitally processed using Adobe Photoshop 5.02 and Paint Shop Pro 4.

[1] The abbreviations used are: zVAD-fmk, benzyloxycarbonyl-Val-Ala-Asp-fluoromethylketone; Apaf-1, apoptosis protease activating factor; PARP, poly(ADP-ribose) polymerase; FITC, fluorescein isothiocyanate; PAGE, polyacrylamide gel electrophoresis; Pipes, 1,4-piperazinediethane sulfonic acid; Mes, 2-(*N*-morpholino)ethanesulfonic acid; TUNEL, terminal deoxynucleotydyl transferase (tdt)-mediated dUTP-FITC nick end labeling; BSA, bovine serum albumin; mtHSP, mitochondrial heat shock protein 70; SNARF-1, seminaphthorhodafluor-1.

RESULTS

Neutrophil Apoptosis Is Arrested at 15 °C—Neutrophils from peripheral blood can be maintained in culture at 37 °C for several hours in autologous serum before asynchronously undergoing apoptosis (Fig. 1*A*, *closed squares*). Apoptosis was quantified using annexin V-FITC binding to externalized phosphatidylserine and morphological counting of pyknotic nuclei (16). A synchronous commitment to apoptosis has previously been induced in cells by using cell-free systems (28, 47–49). Dividing cells, for example, blocked at cell cycle checkpoints provide an homogeneous cytosol (49). Although neutrophils are terminally differentiated (post-replicative) cells, we synchronized their commitment to the execution phase of apoptosis by exposure to low temperature.

Low temperature blocks intracellular pathways that rely on membrane fission and fusion, as exemplified by vesicular transport (50, 51). In neutrophils (Fig. 1*A*, *open circles*) or eosinophils (data not shown) cultured at 15 °C, apoptosis was arrested suggesting that a membrane-associated event required for apoptosis was inhibited. In contrast, culture of HL-60 promyelocytic leukemia cells at 15 °C induced apoptosis (data not shown) as described previously for these and many other dividing mammalian cells (52), suggesting that there may be cell-type or differentiation state-dependent pathways for apoptosis. The rate of neutrophil apoptosis at 37 °C was accelerated by treatment with cycloheximide (Fig. 1*A*, *closed circles*). In addition to preventing the translation of new proteins in the cytoplasm, cycloheximide can induce apoptosis through FADD-dependent mechanisms downstream of cell-surface Fas death receptors (53). However, when we cultured neutrophils at 15 °C with cycloheximide there was no increase in the rate of apoptosis (Fig. 1*A*, *open circles*). Treatment of 15 °C cultured neutrophils with tumor necrosis factor α (16) did not induce apoptosis (data not shown), suggesting that the block to the induction of the execution phase of apoptosis was downstream of these plasma membrane-associated events.

Temperature Shift to 37 °C Triggers Synchronous Apoptosis—The low temperature arrest of neutrophil apoptosis was reversed by re-warming neutrophils, cultured for 20 h at 15 °C, to 37 °C. There was reorganization of the cytoskeleton associated with cell polarization (shape-change), monitored by flow cytometry, that showed cytoskeletal integrity had been maintained at 15 °C (data not shown). This polarization of the neutrophils was followed by a burst of synchronous apoptosis (Fig. 1*B*, *closed circles*). The initial rate of apoptosis was 10-fold greater than the rate of constitutive apoptosis in neutrophils maintained at 37 °C (Fig. 1*A*, *closed squares*), and by 2 h after warming 80–90% of the cells were apoptotic (Fig. 1*B*, *closed circles*). Neutrophils maintained for a further 2 h at 15 °C showed no shape change and no increase in their rate of apoptosis (Fig. 1*B*, *open circles*). By culturing neutrophils in medium containing BSA and cycloheximide we removed experimental variables induced by serum factors and translation of mRNA into new protein.

The accelerated rate of neutrophil apoptosis at 37 °C, following preincubation at 15 °C, depended on the period of time neutrophils had been cultured at 15 °C. It was not a cold-shock response, as previously shown for lymphocytes (54). We demonstrated this by maintaining cells at 15 °C for increasing periods of time before warming them to 37 °C and estimating the initial rate of apoptosis over a 1.5-h period as shown in Fig. 1*B* (*closed circles*). For the first 6 h in culture there was no increase in the initial rate of apoptosis (Fig. 1*C*). However, as the cells were cultured for longer periods at 15 °C there was an increase in the initial rate of apoptosis on warming (Fig. 1*C*). These data suggested that there was a time- and temperature-

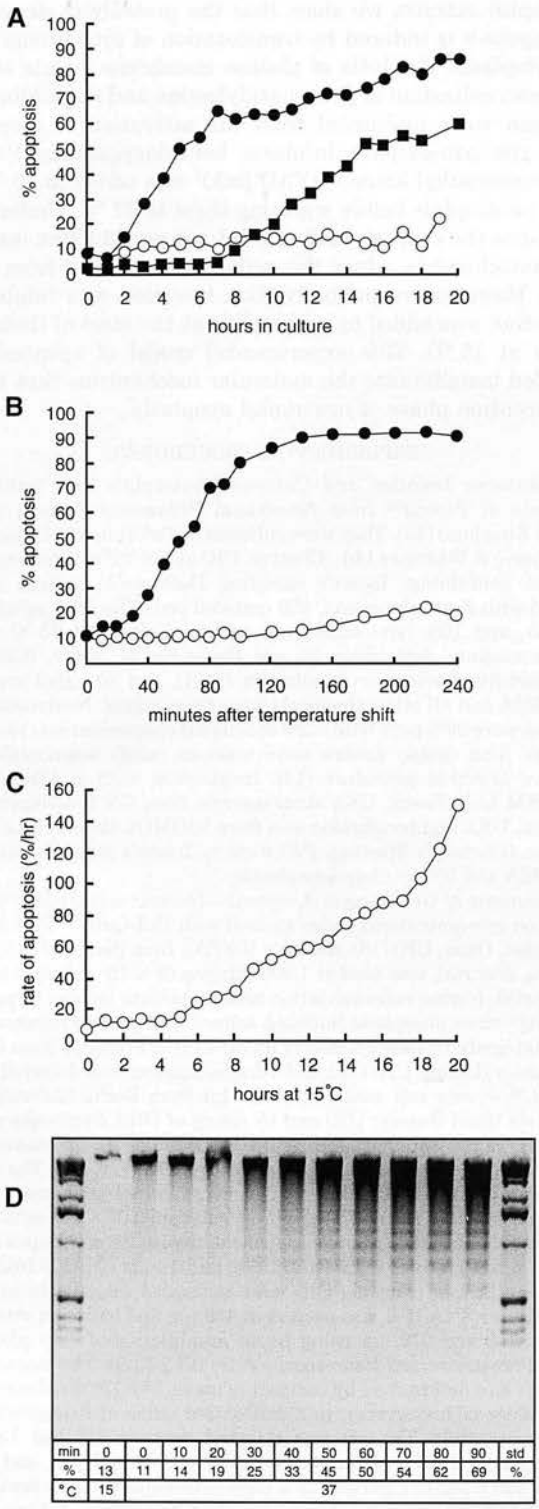

FIG. 1. **Human neutrophil apoptosis was arrested at 15 °C and warming to 37 °C induced a rapid and synchronous apoptosis.** Neutrophils were cultured in medium supplemented with: *A*, 0.2% BSA and 20 μg/ml cycloheximide at 15 °C (○) and 37 °C (●), an incubation with 10% (v/v) autologous serum, without cycloheximide at 37 °C is also shown (■). Apoptosis was assessed by annexin V-FITC binding analyzed by flow cytometry. *B*, neutrophils cultured and analyzed as described in *A* were held at 15 °C for 20 h (○), and subsequently warmed to 37 °C, ●. *C*, neutrophils were cultured at 15 °C as described in *A* and at 1-h intervals harvested and warmed to 37 °C for 1.5 h as described in *B* to assess the initial rate of apoptosis (single experiment). *D*, DNA, extracted from 5×10^6 neutrophils cultured at 15 °C for 20 h and warmed to 37 °C as described in *B*, was separated in agarose gels and stained with ethidium bromide. A 1-kilobase ladder of DNA standards (Std) is shown. Annexin V-FITC binding was used to assess apoptosis and the percentage (%) apoptosis for each sample is shown.

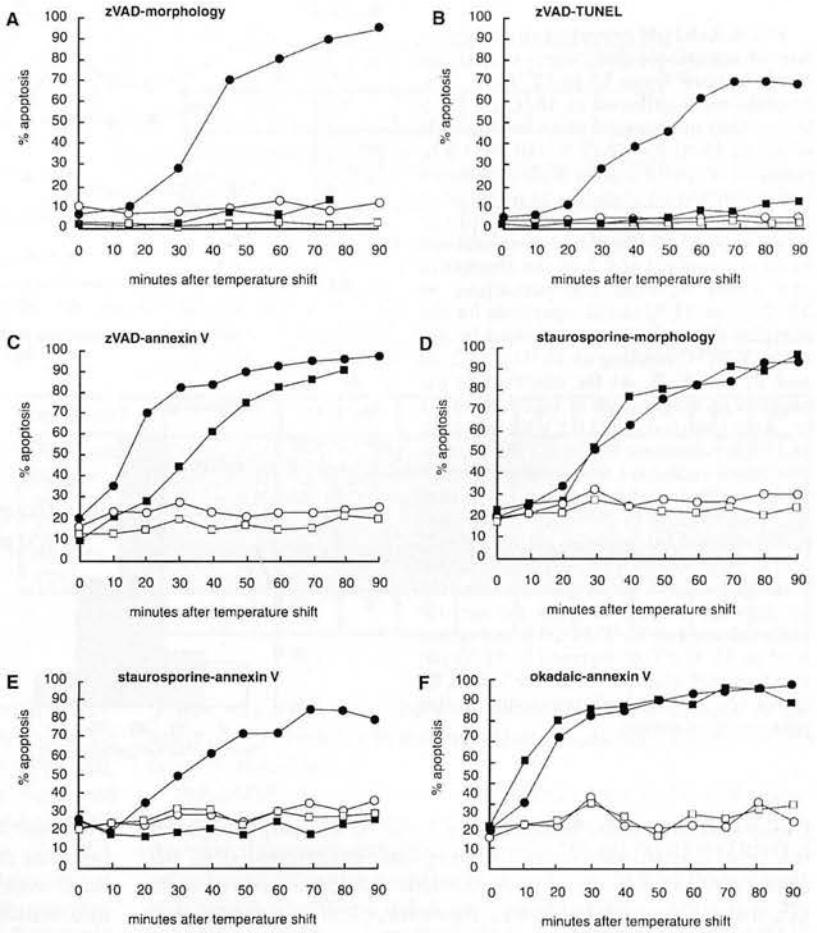

FIG. 2. **zVAD-fmk inhibited morphological apoptosis but not the externalization of phosphatidylserine that is inhibited by staurosporine but not okadaic acid.** Effects of the global caspase inhibitor zVAD-fmk on the triggering of neutrophil apoptosis. *A*, neutrophils were cultured, as described in the legend to Fig. 1*A*, at 15 °C for 20 h (○, □) and warmed to 37 °C (●, ■) and apoptosis estimated by morphological counting. The neutrophils were treated with 100 μM zVAD-fmk for 15 min (□, ■) prior to warming to 37 °C and control neutrophils were mock treated with Me_2SO (○, ●). *B*, DNA fragmentation in the 15 and 37 °C neutrophils shown in *A* was analyzed by TUNEL™ and flow cytometry. *C*, the externalization of phosphatidylserine at the surface of the neutrophil plasma membrane at 15 °C (○, □) and 37 °C (●, ■) was estimated by annexin V-FITC binding for the samples shown in *A* above. *D*, staurosporine inhibited phosphatidylserine externalization. Apoptosis, assessed by morphological counting for neutrophils warmed from 15 °C (○) to 37 °C (●) was not inhibited by 2 μM staurosporine treatment of 15 °C cultured neutrophils (□) for 1 h prior to warming to 37 °C (■). *E*, however, the externalization of phosphatidylserine, assessed by annexin V-FITC-binding, at 15 °C (○), and after warming to 37 °C (●) was inhibited by treatment with staurosporine (□, ■). *F*, neutrophils were cultured at 15 °C for 20 h (○) and before warming to 37 °C (●) they were treated at 15 °C (□) for 1 h with the 1 μM okadaic acid then warmed to 37 °C (■) and showed no inhibition of the triggering of apoptosis assessed by annexin V-FITC binding.

dependent accumulation of a proapoptotic factor at the site of the temperature arrest that led to a synchronization of apoptosis when the cells were subsequently warmed to 37 °C. DNA laddering (Fig. 1*D*), a downstream hallmark of activation of the execution phase of apoptosis, showed kinetics similar to the morphological and annexin V-FITC estimates of apoptosis when 15 °C cultured neutrophils were warmed to 37 °C.

15 °C Arrest Is Proximal to Procaspase-3 Activation—To establish whether inhibition of neutrophil apoptosis at 15 °C (Fig. 2*A*, *open circles*) was upstream of caspase-3 activation and apoptosis at 37 °C (Fig. 2*A*, *closed circles*), 15 °C cultured neutrophils were treated with 100 μM zVAD-fmk (18) (Fig. 2*A*, *open squares*) for 15 min before warming to 37 °C. zVAD-fmk inhibited chromatin condensation and the formation of pyknotic nuclei when neutrophils were warmed from 15 to 37 °C (Fig. 2*A*, *closed squares*). DNA fragmentation at 37 °C (Fig. 2*B*, *closed circles*), indicative of caspase-3 activation, was also inhibited (Fig. 2*B*, *closed squares*) by zVAD-fmk. Phosphatidylserine was still translocated to the cell surface in the presence of zVAD-fmk (Fig. 2*C*, *closed squares*), although the kinetics of translocation were significantly different from the untreated neutrophils (Fig. 2*C*, *closed circles*). Phosphatidylserine externalization has been linked to caspase-3 activity (19, 55–57) so their uncoupling was surprising. However, two other plasma membrane hallmarks of apoptosis phagocytosis (57) and regulated secretion[2] were also uncoupled from caspase-3 by zVAD-fmk. The protein kinase inhibitor staurosporine together with cycloheximide induces apoptosis in many cells (58). However, staurosporine did not stimulate apoptosis at 15 °C (Fig. 2*D*, *open squares*) nor did it accelerate the induction of morphological apoptosis when neutrophils were warmed to 37 °C (Fig. 2*D*, *closed squares*). Phosphatidylserine, detected on the cell surface by annexin-V-FITC after warming to 37 °C (Fig. 2*E*, *closed circles*), was not detected in the presence of staurosporine (Fig. 2*E*, *closed squares*), suggesting that translocation of this phospholipid to the cell surface may rely on a critical phosphorylation event. The inhibition of mitochondrial respiration also blocks phosphatidylserine externalization in apoptotic U937 and THP.1 cells, suggesting that this may be an energy-dependent event (57). Okadaic acid, an inhibitor of phosphatases 1 and 2A (46) had no effect on the induction of apoptosis in 15 °C cultured neutrophils warmed to 37 °C (Fig. 2*F*, *closed squares*). This suggested that caspase activation might not be modulated by phosphorylation events in this experimental model. A number of other agents that induce neutrophil apoptosis, such as the nuclear factor-κB inhibitor gliotoxin (16) and the phosphatidylinositol kinase inhibitor wortmannin, had no effect on the rate of apoptosis in 15 °C cultured neutrophils (data not shown). Our results suggest that the temperature-dependent arrest of apoptosis in neutrophils was not due to signal transduction nor gene transcription events.

A Low Intracellular pH Inhibits the Triggering of Apoptosis—Acid conditions at sites of inflammation inhibit neutrophil apoptosis (59), but conversely, low pH has also been implicated in triggering apoptosis in many cells (60, 61). The pH_i of freshly isolated neutrophils was 7.1, equivalent to the "set point" for resting cells in culture when measured by accumulation of carboxy-seminaphthorhodafluor-1 (SNARF-1), a fluorescent probe whose emission changes with pH (61–63). The pH_i of neutrophils incubated at 15 °C for 20 h was 6.8–7.0 (Fig. 3*A*, *open circles*). However, following the induction of apoptosis (assayed by annexin-V-binding and morphology, Fig. 3, *B* and

[2] J. Pryde unpublished results.

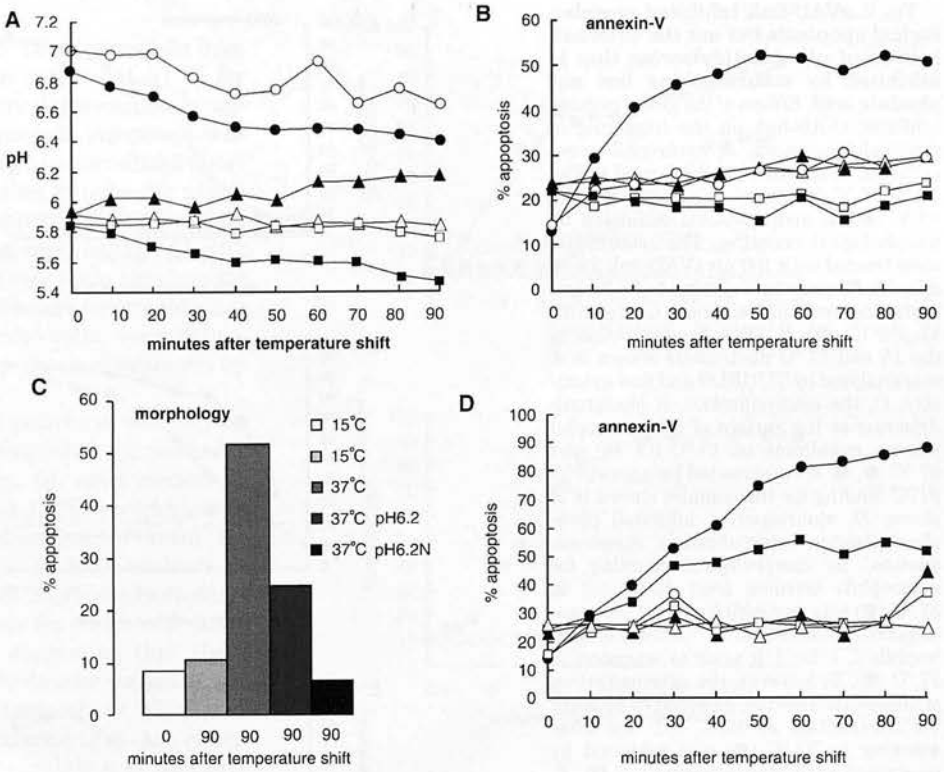

FIG. 3. **Acid pH arrested the triggering of apoptosis following a shift in temperature from 15 to 37 °C.** *A*, neutrophils were cultured at 15 °C for 20 h then either maintained at an external pH of 7.2 at 15 °C (○) or 37 °C (●) for 1.5 h, clamped at pH 6.2 in a high-potassium buffer containing nigericin to maintain a pH_i of 6.2 when cultured at 15 °C (□) or warmed to 37 °C (■) for 1.5 h or exposed to an external pH of 6.2, in the absence of any added nigericin and potassium, at 15 °C (△) or 37 °C (▲). *B*, apoptosis for the samples shown in *A* was assessed by annexin V-FITC-binding at 15 °C (○, □, △) and 37 °C (●, ■, ▲) for neutrophils exposed to an external pH of 7.2 (○, ●) or 6.2 (△, ▲) or clamped at pH 6.2 with nigericin in a high potassium buffer (□, ■). *C*, morphological estimates for neutrophil apoptosis of samples in *B* above at 1.5 h after warming from 15 to 37 °C and for neutrophils exposed to external pH of 6.2 (pH 6.2) or clamped with nigericin and potassium (pH 6.2 N). *D*, apoptosis estimated by annexin-V-FITC binding for neutrophils cultured at 15 °C for 20 h and either held at 15 °C (○) or warmed to 37 °C (●) and their pH_i clamped at either 7.2 (□, ■) or 6.2 (△, ▲) in a high potassium buffer containing nigericin.

C), by increasing the temperature to 37 °C the pH_i dropped to 6.4 (Fig. 3*A*, *closed circles*) as apoptosis progressed (Fig. 3*B*, *closed circles*), consistent with previous measurements of acidic pH_i during apoptosis (60, 61). However, clamping neutrophils at pH 6.2, with nigericin and high K^+ (Fig. 3*A*, *squares*) did not trigger apoptosis at 15 °C (Fig. 3, *B*, *open squares,* and *C*) or at 37 °C (Fig. 3, *B*, *closed squares,* and *C*). This suggested that acid pH alone was not a sufficient trigger for apoptosis as previously suggested (60, 61). Neutrophils cultured in growth-medium buffered at pH 6.2, in the absence of nigericin (Fig. 3*A*, *triangles*), did not induce apoptosis at 15 °C (Fig. 3,*B*, *open triangles,* and *C*) nor on warming to 37 °C (Fig. 3, *B*, *closed triangles,* and *C*). This *in vitro* response to low pH appears to mimic the arrest of neutrophil apoptosis at inflammatory foci where the pH has dropped below 7 (59). When the pH_i of 15 °C cultured neutrophils was clamped at 7.2, the rate of apoptosis was significantly greater when the cells were warmed to 37 °C (Fig. 3*D*, *squares*) than in cells clamped at pH 6.2 (Fig. 3*D*, *closed triangles*). However, apoptosis was still not as efficient as in the untreated cells (Fig. 3*D*, *closed circles*). This result is, however, consistent with reports that suggest an alkaline pH transient is necessary to trigger the execution phase of apoptosis (64).

Neutrophil Apoptosis Is Correlated with Procaspase-3 Cleavage—Procaspase-3 cleavage is required for neutrophil apoptosis (65), but was not detected by immunoblotting in freshly isolated human neutrophils (Fig. 4*A*, *lane 2*). However, treatment of neutrophils with diisopropyl fluorophosphate, a serine protease inhibitor, before solubilization at 0 °C in a nondenaturing lysis buffer and SDS sample buffer for PAGE, prevented nonspecific proteolysis of procaspase-3 (Fig. 4*A*, *lane 3*). Neutrophils were treated with diisopropyl fluorophosphate before isolating cytosols, but while this was not absolutely necessary for 15 °C cultured neutrophils (Fig. 4*A*, *lanes 4* and *5*), diisopropyl fluorophosphate treatment did allow detection of endogenous procaspase-7 and procaspase-8 by immunoblotting. We have been unable to detect procaspase-9 (data not shown).

Neutrophils cultured at 15 °C for 20 h, when warmed to 37 °C for 2 h, proteolytically cleaved procaspase-3 in a time-dependent manner (Fig. 4*B*, *upper panel, lanes 1–11*) that correlated with estimates of apoptosis by counting of pyknotic nuclei and annexin V-FITC binding (Fig. 2, *A* and *C*). Neutrophils held for a further 2 h at 15 °C showed no proteolytic processing of procaspase-3 (Fig. 4*B*, *lower panel, lanes 1–11*).

Proapoptotic Events Can be Detected in Neutrophil Cytosols—To identify the molecular events leading to the proteolytic cleavage and activation of neutrophil procaspase-3, cytosols were prepared from cultures of neutrophils maintained at 15 °C for 20 h. The neutrophils were homogenized in buffered sucrose and fractionated using a two-step ultracentrifugation procedure (see "Experimental Procedures") to minimize damage to organelles, particularly secretory granules. Elastase, a secretory granule marker, sedimented with membrane fractions (data not shown), while procaspase-3 remained in the cytosol (Fig. 5*A*, *lane 1*). Neutrophils cultured at 15 °C and warmed to 37 °C for 1.5 h before preparing the cytosols did not contain procaspase-3 (Fig. 5*A*, *lane 2*). The proteolytic cleavage of procaspase-3, observed in unbroken 15 °C cultured neutrophils warmed to 37 °C (Fig. 4*B*, *lanes 5–11*), had presumably been triggered by apoptosis-inducing factors released from the membranes into the cytoplasm before the cells had been homogenized. Significantly, when cytosols from 15 °C cultured neutrophils were warmed to 37 °C in the presence of dATP, a cofactor involved in the activation of the apoptosome (42), procaspase-3 was not proteolytically cleaved (Fig. 5*A*, *lane 5*) and was present in an amount comparable to the zVAD-fmk-treated controls (Fig. 5*A*, *lane 6*). These data suggested that apoptosis-inducing factors were missing from the cytosol and had been removed with the membrane fraction. The fraction of cytosol from the small number of contaminating apoptotic cells did not catalyze a significant rate of proteolytic cleavage of procaspase-3.

Mitochondria have been shown to play a key role in the control and amplification of apoptotic signals (23, 42). Cytosols from *Xenopus laevis* eggs only trigger apoptosis when membrane fractions enriched in mitochondria are added (25, 27, 48). When rat liver mitochondria were added to cytosols isolated

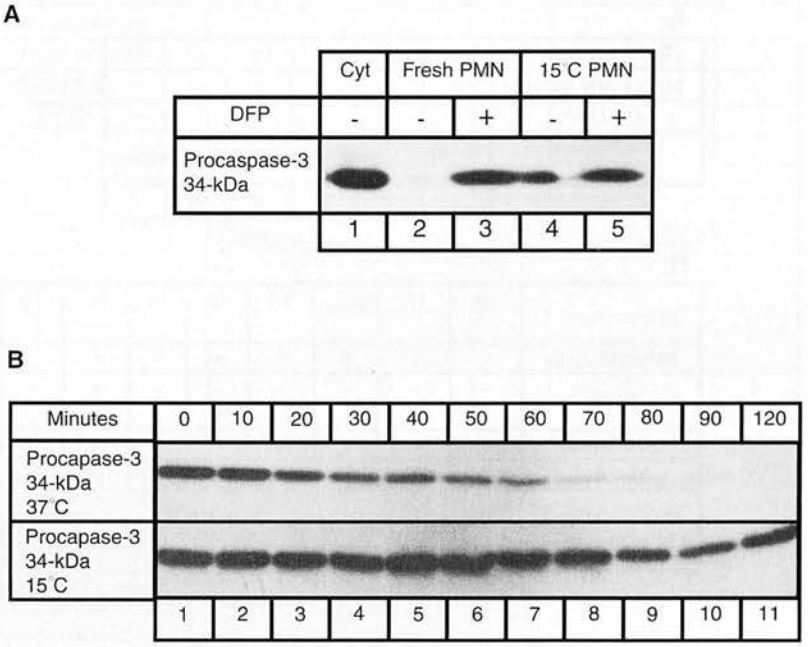

FIG. 4. **Temperature-dependent proteolytic cleavage of endogenous procaspase-3 in intact neutrophils.** *A*, freshly isolated human neutrophils (*PMN*) (*lanes 2* and *3*) and neutrophils cultured at 15 °C for 20 h (*lanes 4* and *5*) were either treated with 2.3 mM diisopropyl fluorophosphate for 15 min on ice (*lanes 3* and *5*) or left untreated (*lanes 2* and *4*). Each lane contains 80 μg of protein solubilized in lysis buffer on ice then in SDS sample buffer before separation on a 12% (w/v) polyacrylamide gel and electrophoretic transfer to nitrocellulose sheets and probing with a monoclonal antibody to procaspase-3. *Lane 1* shows cytosol from 15 °C cultured neutrophils. *B*, neutrophils cultured at 15 °C, as described in the legend to Fig. 1, and cell pellets (5×10^6 cells) were solubilized and analyzed as described in *A*. The 15 °C cultured neutrophils were either warmed to 37 °C (*upper panel, lanes 1–11*) or held at 15 °C (*lower panel, lanes 1–11*) for the times indicated and proteolytic cleavage of procaspase-3 assessed by immunoblotting. Re-probing the blots with antibodies to tubulin or actin (not shown) assessed protein loading and nonspecific proteolysis.

from 15 °C cultured neutrophils, supplemented with dATP then incubated at 15 °C for 2 h, immunoblotting revealed no significant proteolytic processing of procaspase-3 (Fig. 5*B*, *lanes 1–5*). The degree of proteolytic processing was compared with 15 °C cytosols pretreated with zVAD-fmk (Fig. 5*B*, *lane 6*) and with 15 °C cytosols without added mitochondria (Fig. 5*B*, *lane 8*). In cytosols containing dATP and mitochondria permeabilized with Triton X-100, to release apoptosis-inducing factors, an efficient proteolytic cleavage of procaspase-3 was observed by 2 h at either 15 or 37 °C (Fig. 5*B*, *lanes 7* and *14*). Cytosol from 15 °C neutrophils warmed to 37 °C with rat liver mitochondria, and dATP induced proteolytic cleavage of procaspase-3 in a time-dependent manner (Fig. 5*B*, *lanes 9–12*). The protease activity was inhibited by zVAD-fmk (Fig. 5*B*, *lane 13*) and was dependent upon the addition of mitochondria at 37 °C (Fig. 5*B*, *lane 15*).

The involvement of membrane-associated events in the triggering of neutrophil apoptosis was also suggested by analysis of the rate of apoptosis as a function of temperature (Fig. 5*C*). There was a sharp decline in the rate of apoptosis below 20 °C and an Arrhenius plot of this data (not shown) (66) showed that the temperature dependence was biphasic. As the temperature drops to 15 °C reduction in the fluidity of the membrane lipid may affect the behavior of membrane-associated proteins (50, 51, 66). Mitochondrial anion channels have also been shown to respond to lowered temperature by changing their probability of being open, a parameter that is also affected by changes in pH (67). Thus, in our cell-free assay low temperature maintained the segregation of apoptosis-inducing factors within mitochondria, preventing apoptosome activation.

Cytochrome c Induces Procaspase-3 Cleavage—When horse heart cytochrome *c* and dATP were added to cytosol from 15 °C cultured neutrophils and incubated at 15 or 37 °C for 1 h, proteolytic cleavage of procaspase-3 was induced (Fig. 5*D*, *lanes 2* and *4*). The kinetics of procaspase-3 proteolytic cleavage were dependent on the concentration of cytochrome *c*, being complete between 10 and 100 ng of cytochrome *c*/80 μg of cytosol protein after 1 h at 37 °C. Treatment of the neutrophil cytosol with 100 μM zVAD-fmk prior to the addition of cytochrome *c* prevented proteolytic cleavage of procaspase-3 at 15 and 37 °C (Fig. 5*D*, *lanes 3* and *5*). Since an efficient proteolytic cleavage of procaspase-3 occurred at 15 °C the arrest of apoptosis was unlikely to be a consequence of the failure of the apoptosome proteins to undergo conformational changes at low temperature (68).

Poly(ADP-ribose)polymerase Is Cleaved by 15 °C Cytosols—Neutrophil cytosols containing cytochrome *c* and dATP produced active caspase-3 that processed HL-60 PARP (116 kDa), not present in mature neutrophils (17), to an 85-kDa polypeptide fragment after a 1.5-h incubation at 15 °C (Fig. 6, *lower panel, lane 3*). This proteolytic cleavage was inhibited by zVAD-fmk (Fig. 6, *lower panel, lane 4*). There was no apparent proteolysis of procaspase-3 under these conditions (Fig. 6, *upper panel, lane 3*). There was variability between cytosol preparations, and under similar conditions procaspase-3 was fully processed (see Fig. 5*D*, *lane 2*). At 37 °C there was complete proteolytic cleavage of procaspase-3 (Fig. 6, *upper panel, lane 5*) with concomitant proteolytic cleavage of PARP (Fig. 6, *lower panel, lane 5*); again this was inhibited by zVAD-fmk (Fig. 6, *lower panel, lane 6*). No proteolytic processing of neutrophil procaspase-3 or HL-60-PARP by endogenous proteases was detected in the absence of cytochrome *c* (Fig. 6, *upper panel, lane 1,* and *lower panel, lane 7,* respectively).

Release of Cytochrome c from Neutrophil Mitochondria Occurs at 37 but not 15 °C—Cytochrome *c* induced the proteolytic cleavage of endogenous neutrophil procaspase-3 but there was the possibility that this was only a property of the cell-free assay, particularly since we were unable to detect procaspase-9 a component of the apoptosome (42). To monitor translocation of cytochrome *c* from mitochondria into the cytoplasm of intact neutrophils, warmed from 15 to 37 °C, we separated postnuclear supernatants into membrane and cytosol fractions. Cytochrome *c* was immunoprecipitated from the fractions with a monoclonal antibody to a native cytochrome *c* epitope and identified by immunoblotting with an anti-cytochrome *c* antibody that recognized SDS-denatured cytochrome *c*. Neutrophil cytochrome *c* (Fig. 7, *lane 3*) co-migrated with cytochrome *c* from both horse heart and HeLa cells (Fig. 7, *lanes 1* and *2*). In neutrophils held at 15 °C, cytochrome *c* remained with the membrane fraction (Fig. 7, *lanes 4* and *5*), but on warming to 37 °C cytochrome *c* was translocated to the cytosol (Fig. 7, *lanes 7* and *8*). Thus neutrophils released endogenous cytochrome *c* from mitochondria into the cytoplasm, an event that correlated with the onset of apoptosis.

A

Temperature °C	0	0	15	15	37	37
15°C PMN cytosol	+	-	+	+	+	+
zVAD-fmk	-	-	-	+	-	+
Procaspase-3 34-kDa						
	1	2	3	4	5	6

B

Temperature °C	15	15	15	15	15	15	15	15	37	37	37	37	37	37	37
Mitochondria	+	+	+	+	+	+	+	-	+	+	+	+	+	+	-
Triton	-	-	-	-	-	-	+	-	-	-	-	-	-	+	-
zVAD-fmk	-	-	-	-	-	+	-	-	-	-	-	-	+	-	-
Minutes	0	30	60	90	120	120	120	120	30	60	90	120	120	120	120
Procaspase-3 34-kDa															
	1	2	3	4	5	6	7	8	9	10	11	12	13	14	15

C

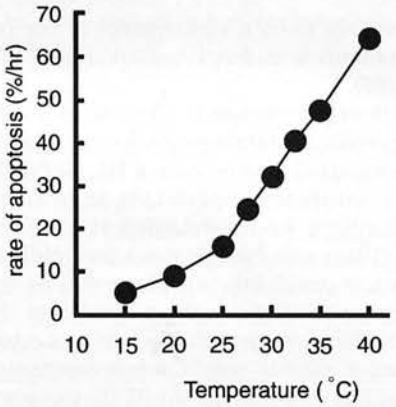

D

Temperature °C	37	15	15	37	37	0
15°C PMN cytosol	+	+	+	+	+	+
zVAD-fmk	+	-	+	-	+	-
Cytochrome c	-	+	+	+	+	-
Procaspase-3 34-kDa						
	1	2	3	4	5	6

FIG. 5. **Cell-free proteolytic cleavage of procaspase-3.** *A*, the proteolytic cleavage of endogenous neutrophil procaspase-3 was analyzed in cytosol supplemented with 20 μM dATP (*lanes 1, 3–6*), and in 15 °C cultured neutrophil cytosol warmed to 37 °C (*lane 2*) by immunoblotting. Samples of the 15 °C cytosol (*lane 1*) and cytosol from 15 °C cultured cells warmed to 37 °C (*lane 2*) were held at 0 °C. The 15 °C cytosol was also held at 15 °C (*lane 3*) or warmed to 37 °C (*lane 5*) in the presence (*lanes 4* and *6*) or absence (*lanes 3* and *5*) of 100 μM zVAD-fmk. *B*, cell-free assays containing cytosol from 15 °C cultured neutrophils were supplemented with 5 μl of rat liver mitochondria fraction (47) and incubated at 15 °C for the times indicated (*lanes 1–5*, respectively). Control incubations at 15 °C contained: 100 μM zVAD-fmk (*lane 6*), mitochondria plus 0.1% (w/v) Triton X-100 (*lane 7*), or no mitochondria (*lane 8*). *Lanes 9–12* show incubations at 37 °C for the times indicated, a zVAD-fmk 2 h control (*lane 13*), a mitochondria plus 0.1% (w/v) Triton X-100 control (*lane 14*), and a control lane with no added mitochondria (*lane 15*). *C*, the rate of neutrophil apoptosis is temperature dependent. Neutrophils were incubated for 22 h at 15 °C and then warmed to the given temperatures (between 15 and 40 °C). The rate of apoptosis was estimated by annexin V-FITC binding as described in the legend for Fig. 1*B*. *D*, induction of the proteolytic cleavage of procaspase-3 by horse heart cytochrome *c*. Incubations and analysis were as described above in *A* and were for 1 h at the temperatures shown. *Lane 1*, 37 °C cytosol control. In *lanes 2–6* the assays were supplemented with 200 ng of cytochrome *c*. Incubations were at 15 °C (*lanes 2* and *3*), 37 °C (*lanes 4* and *5*), and 0 °C (*lane 6*). Controls containing 100 μM zVAD-fmk are shown in *lanes 1, 3,* and *5*.

The Translocation of Bax to Membrane Fractions—How the mitochondrial membrane is permeabilized to release cytochrome *c* during apoptosis is not known (68, 69). However, while the opening or formation of the putative membrane channels may be temperature-sensitive, movement of cytochrome *c* through the channels may not be sensitive to reduced temperature (30). Bax is highly expressed in neutrophils (9–14) and can form membrane pores (39) so we examined the subcellular distribution of Bax during neutrophil apoptosis. Immunoblotting showed that Bax was present in the postnuclear supernatants of 15 °C cultured neutrophils (Fig. 8, *upper panel, lane 1*). Sedimentation of the membranes by ultracentrifugation (Fig. 8, *upper panel, lane 2*) showed that Bax partitioned into the cytosol (Fig. 8, *upper panel, lane 3*) with procaspase-3 (Fig. 8, *lower panel, lane 3*). This is consistent with their localization in freshly isolated neutrophils (data not shown), murine thymocytes, splenocytes, and HL-60 cells (33, 35). In 15 °C cultured neutrophils warmed to 37 °C for 3 h, procaspase-3 was proteolytically cleaved (Fig. 8, *lower panel, lanes 4–6*) and Bax had translocated to the washed membrane fraction (Fig. 8, *upper panel, lane 5*) from the cytosol (Fig. 8, *upper panel, lane 6*). This location suggested that Bax had inserted its hydrophobic membrane-spanning domain into mitochondria (40). In some experiments membrane-associated Bax was processed to an 18-kDa fragment (data not shown), a cleavage product identified in a number of other apoptotic cells (70, 71).

Bax insertion into mitochondria and the release of cytochrome *c* in many experimental models is insensitive to zVAD-fmk (28). In subcellular fractions from neutrophils cultured for 18 h at 15 °C and treated with 100 μM zVAD-fmk for 2 h, before warming to 37 °C, Bax had translocated to the membrane fraction (Fig. 8, *upper panel, lane 11*). Under these conditions

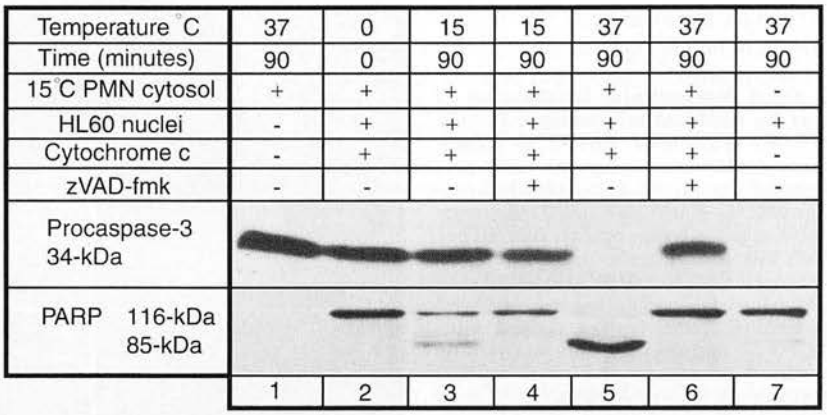

FIG. 6. **Proteolytic processing of HL-60 PARP in heterologous cell-free assays.** HL-60 nuclei were incubated with 15 °C neutrophil cytosol and dATP and proteolytic cleavage of procaspase-3 triggered by the addition of cytochrome *c* (200 ng). Samples were taken at 0 h (*lane 2*) and at 1.5 h after incubation at 15 °C (*lanes 3* and *4*), without zVAD-fmk treatment (*lanes 1–3*, *5* and *7*), with 100 μM zVAD-fmk treatment (*lanes 4* and *6*), and after incubation at 37 °C (*lanes 1* and *5–7*). Samples were solubilized as described in the legend to Fig. 5*B* and the immunoblots probed with monoclonal antibodies to procaspase-3 (*upper panel*) and PARP (*lower panel*).

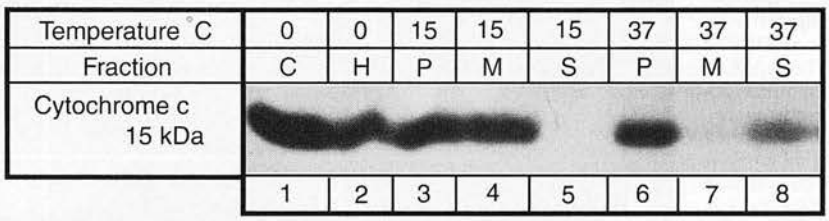

FIG. 7. **The release of endogenous neutrophil cytochrome *c* from membrane fractions into the cytosol.** Neutrophils were cultured at 15 °C as described in the legend to Fig. 1*A*. Samples were solubilized in a nondenaturing lysis buffer for immunoprecipitation (46) with monoclonal antibodies to a native epitope on cytochrome *c*. After SDS-PAGE and electroblotting to nitrocellulose, cytochrome *c* was identified with a monoclonal antibody to the SDS-denatured form of cytochrome *c*. *Lane 1* contains 50 ng of horse heart cytochrome *c* (*C*). *Lane 2* shows an immunoprecipitation of cytochrome *c* from 0.5×10^6 HeLa cells (*H*). *Lanes 3–8* show cytochrome *c* immunoprecipitated from: in *lane 3*, a post-nuclear supernatants (*P*) of 15 °C cultured neutrophils (7.5×10^7 cells); *lane 4*, 15 °C cultured neutrophil membrane fraction (*M*); *lane 5*, 15 °C cultured neutrophil supernatant (*S*) fraction; *lane 6*, post-nuclear supernatants (*S*) of 15 °C cultured neutrophils warmed to 37 °C for 2 h (apoptosis by annexin V-FITC 85%); *lane 7*, 37 °C membrane fraction (M); *lane 8*, 37 °C supernatant (*S*) fraction.

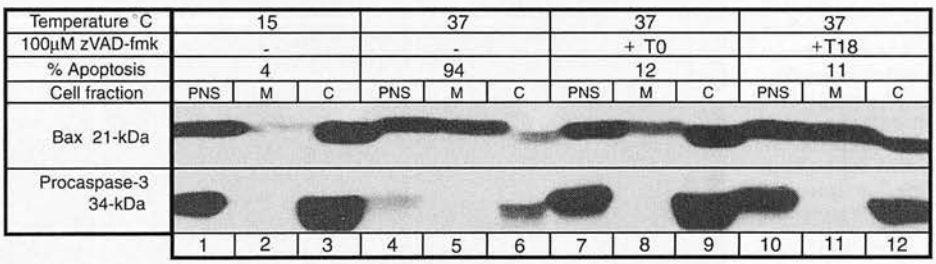

FIG. 8. **Subcellular localization of Bax.** Neutrophils (3×10^8 cells) were held at 15 °C for 18 h. 10^8 cells were incubated at 15 °C for 5 h (*lanes 1–3*); 10^8 cells were cultured for a further 2 h at 15 °C before warming to 37 °C for 3 h (*lanes 4–6*) and 10^8 cells were treated for 2 h at 15 °C with 100 μM zVAD-fmk before warming to 37 °C for 3 h (T18: *lanes 10–12*). One sample of 10^8 freshly isolated neutrophils was treated with 100 μM zVAD-fmk at 15 °C for 20 h and then warmed to 37 °C for 3 h (*lanes 7–9*). Post-nuclear supernatants (post-nuclear supernatants: *lanes 1, 4, 7*, and *10*) were fractionated into membrane (*M: lanes 2, 5, 8*, and *11*) and cytosol (*C: lanes 3, 6, 9*, and *12*) by ultracentrifugation, the membrane fractions being re-homogenized to their original volume in buffer. The fractions were immunoblotted with antibodies to Bax (*upper panel*) and procaspase-3 (*lower panel*).

procaspase-3 was still present in the cytosol (Fig. 8, *lower panel, lane 12*). However, when freshly isolated neutrophils were treated with 100 μM zVAD-fmk at 15 °C for 20 h prior to warming to 37 °C, Bax remained in the cytosol fraction (Fig. 8, *upper panel, lane 9*) with procaspase-3 (Fig. 8, *lower panel, lane 9*). The Bax present in the membrane fraction (Fig. 8, *upper panel, lane 8*) can be accounted for by the apoptotic cells (12%) present. These results suggest that during incubation at 15 °C, caspase activity may prepare Bax for translocation from the cytosol to mitochondria and insertion into the mitochondrial membrane on warming to 37 °C. Caspase-8, a potential candidate for the indirect activation of Bax, can be detected in neutrophil cytosols. However, procaspase-8 was not proteolytically cleaved during either incubations at 15 °C or during the warming of 15 °C cultured neutrophils to 37 °C in the presence of zVAD-fmk (data not shown).

The Translocation of Bax to Neutrophil Mitochondria—We followed the translocation of Bax from the cytoplasm to mitochondria in apoptotic neutrophils by confocal microscopy. Immunofluorescence staining of neutrophils with rabbit preimmune sera and Alexa dye-tagged secondary antibodies showed nuclear staining in freshly isolated neutrophils (Fig. 9*A*) and no significant cytoplasmic staining. Anti-Bax polyclonal antibodies also showed nuclear staining (Fig. 9*B*), but similar staining in HeLa cells and Bax-deficient tumor cells suggested that this staining was nonspecific (72). In fresh preparations of neutrophils the few constitutively apoptotic neutrophils showed Bax staining of large cytoplasmic structures (Fig. 9*B*, *arrow*). These cytoplasmic structures were also stained with polyclonal antibodies to ubiquinol cytochrome *c* oxidoreductase (complex III) that co-localized with mtHSP70 staining (Fig. 9*C*), whose expression was increased in many preparations of 15 °C cultured neutrophils. Significantly, staining of 15 °C cultured neutrophils with mtHSP70 (Fig. 9*D*) and Bax (Fig. 9*E*) showed co-localization (yellow staining) in merged images (Fig. 9*F*) of

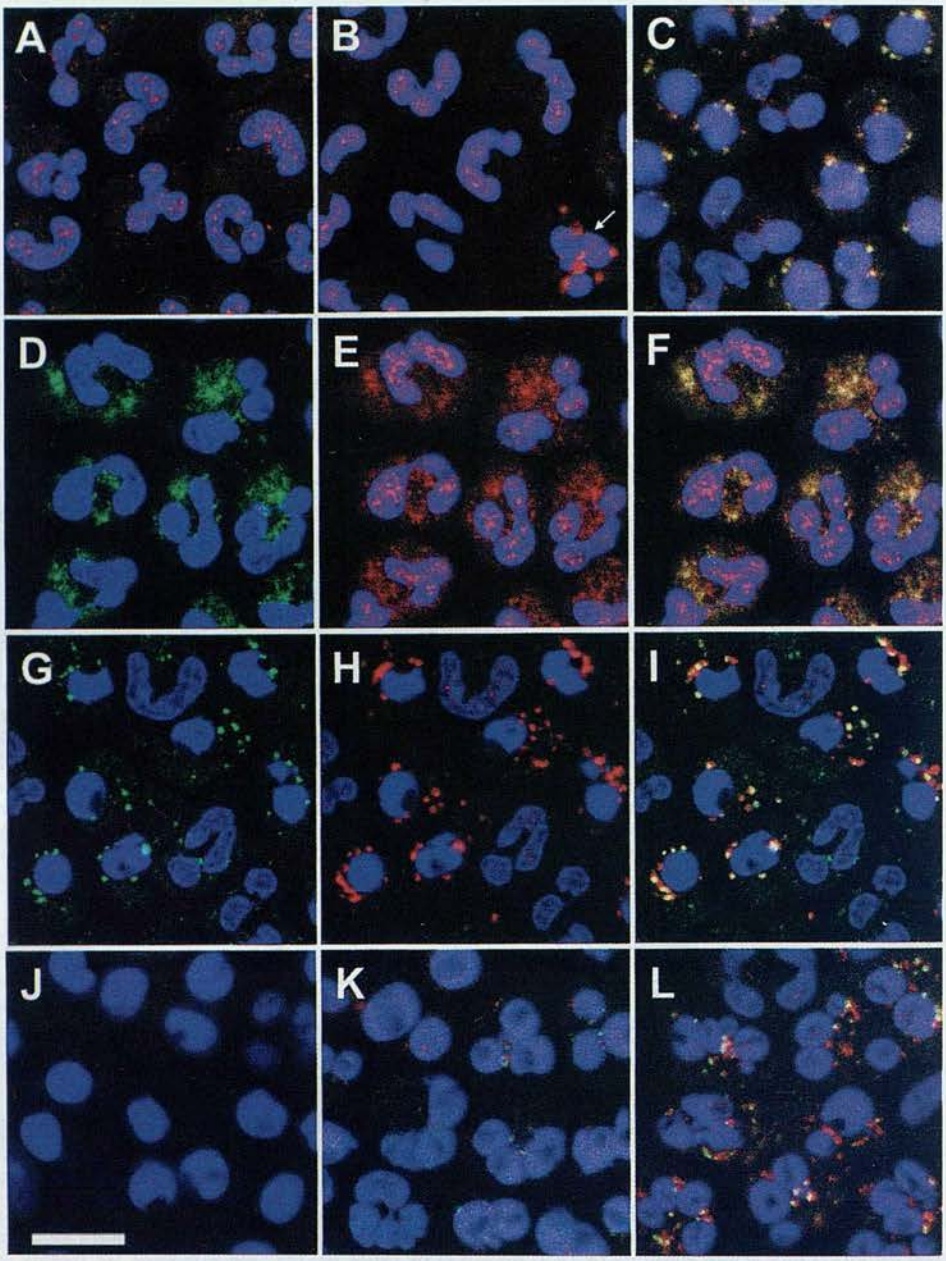

FIG. 9. **Intracellular localization of Bax by confocal microscopy.** Freshly isolated neutrophils showed no significant cytoplasmic staining with rabbit preimmune serum and anti-rabbit IgG-conjugated to Alex™ 568 (*red*) (*A*), with polyclonal antibodies against Bax (*B*) nor with monoclonal antibodies to the mitochondrial marker mtHSP70 detected with anti-mouse IgG-conjugated to Alexa™ 488 (*green*) (*B*). Nuclei were stained with TOPO-3™ and the cells were analyzed by confocal microscopy and single optical sections are shown. Apoptotic cells present in the freshly isolated cells, however, showed Bax staining (*red*) of large cytoplasmic structures (*arrow* in *B*) that co-localized (*yellow*) with staining for both the mitochondrial markers mtHSP70 (*red*) and complex III (*green*) (*C*). After culture for 20 h at 15 °C (*D-F*) neutrophils showed staining for cytoplasmic structures with mtHSP70 (*D*) and Bax (*E*) that co-localized (*yellow* staining) in merged micrographs (*F*). When the 15 °C cultured neutrophils were warmed to 37 °C for 3 h (*G-I*), they showed staining of several discrete cytoplasmic structures. These were also stained for mtHSP70 (*G*) and Bax (*H*) and when the micrographs were merged (*I*) the Bax and mtHSP70 staining was mainly co-localized, although there were some structures that stained for only one or another of the antibodies. A control 15 °C culture was warmed to 37 °C for 3 h and stained with rabbit preimmune (*J*). Freshly isolated neutrophils were treated for 20 h with 100 μM zVAD-fmk and then warmed to 37 °C for 3 h. The micrograph (*K*) shows the merged staining for Bax and mtHSP70. Neutrophils were cultured at 15 °C for 18 h and then treated at 15 °C for 2 h with 100 μM zVAD-fmk before warming to 37 °C for 3 h. The micrograph (*L*) again shows the merged staining for Bax and mtHSP70. The *bar* represents 5 μM.

cytoplasmic structures that were present in cells that showed none of the pyknotic nuclear morphology associated with neutrophil apoptosis. Co-localization analysis, on single optical sections using Leica TCS software, confirmed the subcellular co-localization of Bax and mtHSP70 seen in the merged fluorescent micrographs (data not shown). Bax appeared therefore to translocate to mitochondria at 15 °C, without triggering apoptosis. The binding of Bax to mitochondria without insertion of its hydrophobic membrane-spanning domain would be consistent with Bax being peripherally associated with the mitochondrial membrane and redistributing to the cytosol fraction during homogenization and washing of the membrane fraction (Fig. 8, *lane 3*). After warming the 15 °C cultured neutrophils to 37 °C for 3 h, mtHSP70 staining (Fig. 9*G*) and Bax staining (Fig. 9*H*) were co-localized in the merged micrograph (Fig. 9*I*) with a small number of large, but discrete, cytoplasmic structures. Similar cytoplasmic structures have been identified in HeLa cells treated with staurosporine to induce apoptosis (72) and in cells overexpressing Bax (37, 38) as aggregates of mitochondria. Not all mitochondria stained for Bax and some Bax-stained structures did not stain with mtHSP70. There was therefore a differential response by mitochondria to apoptotic signals and Bax may also translocate to other membrane compartments. Neutrophils cultured at 15 °C for 20 h then warmed to 37 °C for 3 h showed no staining with rabbit preimmune sera (Fig. 9*J*).

After culture of neutrophils at 15 °C for 20 h with zVAD-fmk and warming to 37 °C for 3 h there was no significant Bax staining of neutrophil mitochondria that showed non-apoptotic nuclear morphology (Fig. 9*K*). This was consistent with the immunoblotting data (Fig. 8, *upper panel, lanes 7–9*) that showed no insertion of Bax into mitochondria. However, neutrophils cultured at 15 °C for 18 h, then treated for 2 h with zVAD-fmk before warming to 37 °C for 3 h, did show significant Bax and mtHSP70 staining (Fig. 9*L*). This was consistent with immunoblotting data that showed that Bax had translocated to the membrane fraction (Fig. 8, *upper panel, lanes 10–12*). While the nuclear morphology was significantly different from the nuclei of freshly isolated neutrophils under these conditions, the pyknotic nuclear morphology characteristic of apoptotic neutrophils was not detected and there was no fragmentation of DNA under these conditions (see Fig. 2, *A-C*).

DISCUSSION

We have shown for the first time that culturing neutrophils at 15 °C reversibly arrests the induction of apoptosis, with subsequent warming to 37 °C triggering a burst of synchronous apoptosis. The molecular consequences of temperature reduction on cells are poorly understood. However, between 10 and 20 °C there is a reduction in membrane lipid fluidity, a decrease in the rate of protein translation, and an inhibition of vesicular trafficking and neutrophil respiratory burst activity (67, 50, 51). Our results suggest that the arrest of apoptosis in neutrophils cultured at 15 °C may be due to the failure of the proapoptotic protein Bax to undergo the conformational changes necessary for it to insert into mitochondria. Once in the membrane Bax triggers the release of cytochrome *c* and the subsequent activation of caspase-3 that induces the execution phase of neutrophil apoptosis.

Bax is a soluble protein located in the cytoplasm of freshly isolated neutrophils (10–12). Our immunofluorescence studies on Bax localization in neutrophils cultured at 15 °C have shown that in addition to its cytoplasmic localization, Bax was also associated with mitochondria that showed signs of aggregation; both observations reported for many cell lines cultured at 37 °C (73). However, in neutrophils cultured at 15 °C Bax failed to undergo the conformational changes necessary for insertion of its C-terminal membrane-spanning domain into mitochondria (33). Bax was readily washed from membranes isolated from neutrophils cultured at 15 °C suggesting a peripheral association with the membrane fraction. The N-terminal region of the Bax molecule may bind to and mask its C-terminal domain in the cytoplasm and the removal of the N-terminal domain leads to an autoactivation and constitutive insertion of the mutant protein into mitochondria (72). The cytoplasmic components that normally facilitate this unmasking of the C-terminal membrane-spanning domain and the conformational changes to neutrophil Bax are unknown. However, in HeLa cells, for example, the proapoptotic protein Bid, can induce the insertion of Bax into membranes (22, 72) and may be one of a number of cytoplasmic factors that play a role in the release of cytochrome *c* from mitochondria (29).

In many models of apoptosis the insertion of Bax into mitochondria and the subsequent release of cytochrome *c* are not inhibited by the pan-caspase inhibitor zVAD-fmk, while proteolytic cleavage of procaspase-3 is inhibited (28). Treatment of neutrophils, cultured at 15 °C for 18 h, with zVAD-fmk prior to triggering apoptosis by warming to 37 °C, also failed to inhibit Bax translocation to neutrophil membranes under conditions where procaspase-3 was not proteolytically cleaved, consistent with other models of apoptosis. However, when freshly isolated neutrophils were treated with zVAD-fmk at the beginning of the culture period at 15 °C, Bax failed to insert into mitochondria when the cells were warmed to 37 °C. Assuming the fidelity of zVAD-fmk for its caspase targets, these experiments suggested that caspase-mediated events were necessary for Bax insertion (74) but were not in themselves a sufficient trigger for the induction of Bax insertion into mitochondria at 15 °C. Whatever the role the caspases play in preparing Bax, or in activating a putative effector protein necessary for the activation of Bax binding and insertion once the neutrophils are warmed to 37 °C, we saw no evidence that Bax was proteolytically cleaved at 15 °C. Activation of an effector protein and Bax binding at 15 °C would provide an explanation for the synchronization of apoptosis we observe on warming the cells to 37 °C after culture at 15 °C. Direct proteolytic cleavage of p21 Bax does not appear to be involved in the translocation of Bax to mitochondria (70, 71). However, caspases have been shown to activate the calcium-activated cysteine protease, calpain, that cleaves p21 Bax to p18 Bax at the mitochondrial membrane (70, 71). While this proteolytic processing by calpain augments the homodimerization of Bax and the release of cytochrome *c* it is a relatively late apoptotic event concomitant temporally with the cleavage of many other caspase-3 substrates and with DNA fragmentation (75, 76).

The conformational changes necessary for neutrophil Bax to insert into the mitochondrial membrane were not only inhibited by low temperature, but also by clamping neutrophils at an acidic pH_i during warming to 37 °C, a treatment that was dominant over the effect of temperature reduction. In FL5.12 cells and D1 thymocyte cell lines transient increases in cytoplasmic pH_i have been correlated with pH-dependent conformational change in Bax, an effect that is also inhibited by acid pH (39, 64, 73). This observation may provide an explanation for the inhibition of neutrophil apoptosis observed at inflammatory foci where an acid environment has developed (59). Our data are also consistent with the observation that tumor necrosis factor/cycloheximide-induced cytochrome *c* release is inhibited by zVAD-fmk (30) and that caspase-8 may trigger the release of cytochrome *c* (77). However, our preliminary data (not shown) have suggested that procaspase-8, like procaspase-3 is not proteolytically cleaved at 15 or at 37 °C in the presence of zVAD-fmk, under conditions where Bax insertion occurs.

How cytochrome *c* is translocated across the outer membrane of mitochondria is not known (41, 68, 78, 79). Bax insertion may affect membrane channels by inducing permeability changes that result in the release of cytochrome *c* (78, 80–82). Many cells that obtain their ATP by oxidative phosphorylation can still release cytochrome *c* from mitochondria at low temperature (30, 81). It was possible that extended culture at low temperature would lead to collapse of the inner mitochondrial membrane potential ($\Delta\Psi_m$) and trigger the opening of the mitochondrial permeability transition pore in neutrophils, an event that correlates with the insertion of Bax and the induction of apoptosis (27, 41, 68). In granulocytes, however, ATP is obtained predominantly by glycolysis and this may allow their mitochondria to use pyruvate to maintain their $\Delta\Psi_m$ at low temperature. Apoptosis triggered by warming 15 °C cultured neutrophils to 37 °C was not inhibited by preincubation with 50 μM bongkrekic acid (data not shown), an inhibitor that blocks the permeability transition pore (37, 77). This experiment suggested that the collapse of the membrane potential might be an event triggered downstream of caspase-3 activation (28).

The Bax-dependent release of cytochrome *c* from mitochondria in 15 °C cultured neutrophils, treated with zVAD-fmk just before warming to 37 °C to inhibit caspase-3, triggered the activation of apoptosis inducing activities that led to the arrest of both secretion and phagocytosis (57). The externalization of phosphatidylserine on the cell surface was also induced and this may trigger recognition and phagocytosis of granulocytes by macrophages (55). We have established that mitochondria play a role in triggering neutrophil apoptosis. Our 15 °C cytosols will now enable us to investigate not only the zVAD-fmk sensitive activity that is required for Bax insertion into mitochondria, but also the zVAD-fmk insensitive activities triggered during cytochrome *c* release, that lead to the apoptotic changes associated with the neutrophil plasma membrane. Finally, the differential response of granulocytes and proliferating cells to temperature reduction suggests that therapeutic targets specific for triggering of neutrophil apoptosis may possibly be identified in this clinically relevant cellular model of apoptosis.

Acknowledgments—We thank Ian Dransfield for help with flow cytometry and Linda Sharp for help with confocal microscopy. Said

Aoufuchi, Simon Brown, and David Apps are thanked for gifts of antibodies. We are grateful to Tim Allsopp, David Apps, Ian Dransfield-,Jonathan Lamb, Mary McElroy, and Deborah Pryde for critical reading of the manuscript and discussions during the course of this work.

REFERENCES

1. Wyllie, A. H., Kerr, J. F. R., and Currie, A. R. (1980) *Int. Rev. Cytol.* **68,** 251–306
2. Savill, J. S., Wyllie, A. H., Henson, J. E., Walport, M. J., Henson, P. M., and Haslett, C. (1989) *J. Clin. Invest.* **83,** 865–875
3. Whyte, M. K. B. Meagher, L. C., MacDermot, J., and Haslett, C. (1993) *J. Immunol.* **150,** 5124–5134
4. Savill, J., Dransfield, I., Hogg, N., and Haslett, C. (1990) *Nature* **343,** 170–173
5. Savill, J., Hogg, N., Ren, Y., and Haslett, C. (1992) *J. Clin. Invest.* **90,** 1513–1522
6. Meagher, L. C. Savill, J. S., Baker, A., Fuller, R. W., and Haslett, C. (1992) *J. Leukocyte Biol.* **52,** 269–273
7. Lee, A., Whyte, M. K. B., and Haslett, C. (1993) *J. Leukocyte Biol.* **54,** 283–288
8. Hannah, S., Mecklenburgh, K., Rahman, I., Bellingan, G. J., Greening, A., Haslett, C., and Chilvers, E. R. (1995) *FEBS Lett.* **372,** 233–237
9. Weinmann, P., Gaehtgens, P., and Walzog, B. (1999) *Blood* **93,** 3106–3115
10. Moulding, D. A., Quayle, J. A., Hart, C. A., and Edwards, S. W. (1998) *Blood* **92,** 2495–2502
11. Lagasse, E., and Weissman, I. L. (1994) *J. Exp. Med.* **179,** 1047–1052
12. Ohta, H., Yatomi, Y., Sweeney, E. A., Hakomori, S., and Igarashi, Y. (1994) *FEBS Lett.* **355,** 267–270
13. Liles, W. C., Kiener, P. A., Ledbetter, J. A., Aruffo, A., and Klebanoff, S. J. (1996) *J. Exp. Med.* **184,** 429–440
14. Matsumoto, K., Schleimer, R. P., Saito, H., Iikura, Y., and Bochner, B. S. (1995) *Blood* **86,** 1437–1443
15. Frasch, S. C., Nick, J. A., Fadok, V. A., Bratton, D. L., Worthen, G. S., and Henson, P. M. (1998) *J. Biol. Chem.* **273,** 8389–8397
16. Ward, C., Chilvers, E. R., Lawson, M. F., Pryde, J. G., Fujihara, S., Farrow, S. N., Haslett, C., and Rossi, A. G. (1999) *J. Biol. Chem.* **274,** 4309–4318
17. Sanghavi, D. M., Thelen, M., Thornberry, N. A., Casciola-Rosen, L., and Rosen, A. (1998) *FEBS Lett.* **422,** 179–184
18. Korsmeyer, S. J. (1995) *Trends Genet.* **11,** 101–105
19. Yamashita, K., Takahashi, A., Kobayashi, S., Hirata, H., Mesner, P. W., Kaufmann, S. H., Yonehara, S., Yamamoto, K., Uchiyama, T., and Sasada, M. (1999) *Blood* **93,** 674–685
20. Yuan, J., and Horvitz, H. R. (1990) *Dev. Biol.* **138,** 33–41
21. Stennicke, H. R., Jürgensmeier, J. M., Shin, H., Deveraux, Q., Wolf, B. B., Yang, X., Zhou, Q., Ellerby, H. M., Ellerby, L. M., Bredesen, D., Green, D. R., Reed, J. C., Froelich, C. J., and Salvesen, G. S. (1998) *J. Biol. Chem.* **273,** 27084–27090
22. Kuwana, T., Smith, J. J., Muzio, M., Dixit, V., Newmeyer, D. D., and Kornbluth, S. (1998) *J. Biol. Chem.* **273,** 16589–16594
23. Susin, S. A., Zamzami, N., Castedo, M., Hirsch, T., Marchetti, P., Macho, A., Daugas, E., Geuskens, M., and Kroemer, G. (1996) *J. Exp. Med.* **184,** 1331–1341
24. Li, F., Srinivasan, A., Wang, Y., Armstrong, R. C., Tomaselli, K. J., and Fritz, L. C. (1997) *J. Biol. Chem.* **272,** 30299–30305
25. Kluck, R. M., Martin, S. J., Hoffman, B. M., Zhou, J. S., Green, D. R., and Newmeyer, D. D. (1997) *EMBO J.* **16,** 4639–4649
26. Zou, H., Henzel, W. J., Liu, X., Lutschg, A., and Wang, X. (1997) *Cell* **90,** 405–413
27. Kluck, R. M., Bossy-Wetzel, E., Green, D. R., and Newmeyer, D. D. (1997) *Science* **275,** 1132–1136
28. Bossy-Wetzel, E., Newmeyer, D. D., and Green D. R. (1998) *EMBO J.* **17,** 37–49
29. Bossy-Wetzel, E., and Green, D. R. (1999) *J. Biol. Chem.* **274,** 17484–17490
30. Goldstein, J. C., Waterhouse, N. J., Juin, P., Evan, G. I., and Green, D. R. (2000) *Nat. Cell Biol.* **2,** 156–162
31. Oltvai, Z. N., Milliman, C. L., and Korsmeyer, S. J. (1993) *Cell* **74,** 609–619
32. Wolter, K. G., Hsu, Y-T., Smith, C. L., Nechushtan, A., Xi, X-G., and Youle, R. J. (1997) *J. Cell Biol.* **139,** 1281–1292
33. Nechushtan, A., Smith, C. L., Hsu, Y-T., and Youle, R. J. (1999) *EMBO J.* **18,** 2330–2341
34. Hsu, Y-T., Wolter, K. G., and Youle, R. J. (1997) *Proc. Natl. Acad. Sci. U. S. A.* **94,** 3668–3672
35. Hsu, Y-T., and Youle, R. J. (1997) *J. Biol. Chem.* **272,** 13829–13834
36. Jürgensmeier, J. M., Xie, Z., Deveraux, Q., Ellerby, L., Bredesen, D., and Reed, J. C. (1998) *Proc. Natl. Acad. Sci. U. S. A.* **95,** 4997–5002
37. Eskes, R., Antonsson, B., Osen-Sand, A., Montessuit, S., Richter, C., Sadoul, R., Mazzei, G., Nichols, A., and Martinou, J-C. (1998) *J. Cell Biol.* **143,** 217–224
38. Narita, M., Shimizu, S., Ito, T., Chittenden, T., Lutz, R. J., Matsuda, H., and Tsujimoto, Y. (1998) *Proc. Natl. Acad. Sci. U. S. A.* **95,** 14681–14686
39. Gross, A., Jockel, J., Wei, M. C., and Korsmeyer, S. J. (1998) *EMBO J.* **17,** 3878–3885
40. Rosse, T., Olivier, R., Monney, L., Rager, M., Conus, S., Fellay, I., Jansen, B., and Borner, C. (1998) *Nature* **391,** 496–499
41. Shimizu, S., Narita, M., and Tsujimoto, Y. (1999) *Nature* **399,** 483–487
42. Li, P., Nijhawan, D., Budihardjo, I., Srinivasula, S. M., Ahmad, M., Alnemri, E. S., and Wang, X. (1997) *Cell* **91,** 479–489
43. Slee, E. A., Harte, M. T., Kluck, R. M., Wolf, B. B., Casiano, C. A., Newmeyer, D. D., Wang, H-G., Reed, J. C., Nicholson, D. W., Alnemri, E. S., Green, D. R., and Martin, S. J. (1999) *J. Cell Biol.* **144,** 281–292
44. Haslett, C., Guthrie, L. A., Kopaniak, M. M., Johnston, R. B., and Henson, P. M. (1985) *Am. J. Pathol.* **119,** 101–110
45. Eldadah, B. A., Yakovlev, A. G., and Faden, A. I. (1996) *Nucleic Acids Res.* **24,** 4092–4093
46. Pryde, J. G. (1994) *J. Cell Sci.* **107,** 3425–3436
47. Nicholson, D. W., and McMurray, W. C. (1984) *Can. J. Biochem. Cell Biol.* **62,** 1205–1216
48. Newmeyer, D. D., Farschon, D. M., and Reed, J. C. (1994) *Cell* **79,** 353–364
49. Earnshaw, W. C. (1995) *Curr. Opin. Cell Biol.* **7,** 337–343
50. Tartakoff, A. M. (1986) *EMBO J.* **5,** 1477–1482
51. Manara, F. S., and Schneider, D. L. (1985) *Biochem. Biophys. Res. Commun.* **132,** 696–701
52. Shimura, M., Ishizaka, Y., Yuo, A., Hatake, K., Oshima, M., Sasaki, T., and Takaku, F. (1997) *FEBS Lett.* **417,** 379–384
53. Tang, D., Lahti, J. M., Grenet, J., and Kidd, V. J. (1999) *J. Biol. Chem.* **274,** 7245–7252
54. Gregory, C. D., and Milner, A. E. (1994) *Int. J. Cancer.* **57,** 419–426
55. Martin, S. J., Finucane, D. M., Amarante-Mendes, G. P., O'Brien, G. A., and Green, D. R. (1996) *J. Biol. Chem.* **271,** 28753–28756
56. Vanags, D. M., Pörn-Ares, M. I., Coppola, S., Burgess, D. H., and Orrenius, S. (1996) *J. Biol. Chem.* **271,** 31075–31085
57. Zhuang, J., Ren, Y., Snowden, R. T., Zhu, H., Gogvadze, V., Savill, J. S., and Cohen, G. M. (1998) *J. Biol. Chem.* **273,** 15628–15632
58. Jacobson, M. D., Weil, M., and Raff, M. C. (1997) *Cell* **88,** 347–354
59. Trevani, A. S., Andonegui, G., Giordano, M., López, D. H., Gamberale, R., Minucci, F., and Geffner, J. R. (1999) *J. Immunol.* **162,** 4849–4857
60. Li, J., and Eastman, A. (1995) *J. Biol. Chem.* **270,** 3203–3211
61. Furlong, I. J., Ascaso, R., Rivas, A. L., and Collins, M. K. (1997) *J. Cell Sci.* **110,** 653–661
62. Musgrove, E. A., and Hedley, D. W. (1990) *Methods Cell Biol.* **33,** 59–69
63. Benson, R. S. P., Dive, C., and Watson, A. J. M. (1999) *J. Cell Sci.* **112,** 1755–1760
64. Khaled, A. R., Kim, K., Hofmeister, R., Muegge, K., and Durum, S. K. (1999) *Proc. Natl. Acad. Sci. U. S. A.* **96,** 14476–14481
65. Woo, M., Hakem, R., Soengas, M. S., Duncan, G. S., Shahinian, A., Kägi, D., Hakem, A., McCurrach, M., Khoo, W., Kaufman, S. A., Senaldi, G., Howard, T., Lowe, S. W., and Mak, T. W. (1998) *Genes Dev.* **12,** 806–819
66. Kumamoto, J., Raison, J. K., and Lyons, J. M. (1971) *J. Theor. Biol.* **31,** 47–51
67. Liu, G., Hinch, B., Davatol-Hag, H., Lu, Y., Powers, M., and Beavis, A. D. (1996) *J. Biol. Chem.* **271,** 19717–19723
68. Green, D. R., and Reed, J. C. (1998) *Science* **281,** 1309–1312
69. Schlesinger, P. H., Gross, A., Yin, X-M., Yamamoto, K., Saito, M., Waksman, G., and Korsmeyer, S. J. (1997) *Proc. Natl. Acad. Sci. U. S. A.* **94,** 11357–11362
70. Wood, D. E., Thomas, A., Devi, L. A., Berman, Y., Beavis, R. C., Reed, J. C., and Newcomb, E. W. (1998) *Oncogene* **17,** 1069–1078
71. Kirsch, D. G., Doseff, A., Chau, B. N., Lim, D-S., De Souza-Pinto, N. C., Hansford, R., Kastan, M. B., Lazebnik, Y. A., and Hardwick, J. M. (1999) *J. Biol. Chem.* **274,** 21155–21161
72. Desagher, S., Osen-Sand, A., Nichols, A., Eskes, R., Montessuit, S., Lauper, S., Maundrell, K., Antonsson, B., and Martinou, J-C. (1999) *J. Cell Biol.* **144,** 891–901
73. Goping, I. S., Gross, A., Lavoie, J. N., Nguyen, M., Jemmerson, R., Roth, K., Korsmeyer, S. J., and Shore, G. C. (1998) *J. Cell Biol.* **143,** 207–215
74. Murphy, K. M., Streips, U. N., and Lock, R. B. (1999) *Oncogene* **18,** 5991–5999
75. Wood, D. E., and Newcomb, E. W. (1999) *J. Biol. Chem.* **274,** 8309–8315
76. Wood, D. E., and Newcomb, E. W. (2000) *Exp. Cell Res.* **256,** 375–382
77. Srinivasan, A., Li, F., Wong, A., Kodandapani, L., Smidt, R., Krebs, J. F., Fritz, L. C., Wu, J. C., and Tomaselli, K. J. (1998) *J. Biol. Chem.* **273,** 4523–4529
78. Heidin, M. G., Chandel, N. S., Schumacker, P. T., and Thompson, C. B. (1999) *Mol. Cell* **3,** 159–167
79. Marzo, I., Brenner, C., Zamzami, N., Susin, S. A., Beutner, G., Brdiczka, D., Remy, R., Xie, Z. H., Reed, J. C., and Kroemer, G. (1998) *J. Exp. Med.* **187,** 1261–1271
80. Marchetti, P., Castedo, M., Susin, S. A., Zamzami, N., Hirsch, T., Macho, A., Haeffner, A., Hirsch, F., Geuskens, M., and Kroemer, G. (1996) *J. Exp. Med.* **184,** 1155–1160
81. Heiskanen, K. M., Bhat, M. B., Wang, H. W., Ma, J., and Nieminen, A. L. (1999) *J. Biol. Chem.* **274,** 5654–5658
82. Basanez, G., Nechushtan, A., Drozhinin, O., Chanturitya, A., Choe, E., Tutt, S., Wood, K. A., Hsu, Y-T., Zimmerberg, J., and Youle, R. J. (1999) *Proc. Natl. Acad. Sci. U. S. A.* **96,** 5492–5497